

PROTEIN FOLDING HOMEOSTASIS MAINTAINS RENAL FUNCTION

INHIBITING ENDOPLASMIC RETICULUM STRESS PREVENTS THE
DEVELOPMENT OF HYPERTENSIVE NEPHROSCLEROSIS

By RACHEL E. CARLISLE, Hon. B.Sc.

A Thesis Submitted to the School of Graduate Studies in Partial Fulfilment of the
Requirements for the Degree Doctorate of Philosophy

McMaster University

© Copyright by Rachel E. Carlisle, August 2017

McMaster University DOCTOR OF PHILOSOPHY (2017)

Hamilton, Ontario (Medical Sciences)

TITLE: Inhibiting endoplasmic reticulum stress prevents the development of hypertensive nephrosclerosis

AUTHOR: Rachel E. Carlisle, B.Sc. (University of Guelph)

SUPERVISOR: Jeffrey G. Dickhout, Ph.D.

NUMBER OF PAGES: xxv, 268

LAY ABSTRACT

Chronic kidney disease is characterized by progressive loss of kidney function, and is a major public health problem. Kidney cells make proteins that help the kidney function properly. However, if the proteins are made improperly, the kidney does not function as well. This can lead to poor filtration and protein in the urine, damage to important kidney structures, and kidney scarring. High blood pressure, a risk factor for kidney disease, is often accused of causing kidney damage. This thesis shows that malfunctioning blood vessels can cause kidney injury, and lowering blood pressure may not prevent this. However, there are pharmacological molecules that can protect the kidney from damage. These molecules help the cells make proteins properly, preventing blood vessel malfunction and kidney damage. Our findings suggest that helping blood vessels and kidney cells create properly functioning proteins is more protective for the kidney than lowering blood pressure alone.

ABSTRACT

Endoplasmic reticulum (ER) stress, which results from the aggregation of misfolded proteins in the ER, has been implicated in many forms of kidney injury, including hypertensive nephrosclerosis. ER stress induction increases levels of active TGF β 1, a pro-fibrotic cytokine, which can lead to epithelial-to-mesenchymal transition (EMT) in renal proximal tubular cells. EMT occurs when epithelial cells undergo phenotypic changes, which can be prevented by inhibiting ER stress. Further, the ER stress protein TDAG51 is essential for the development of TGF β 1-mediated fibrosis. The low molecular weight chemical chaperone 4-phenylbutyrate (4-PBA) can protect against ER stress-mediated kidney injury. It acts directly on the kidney, and can prevent ER stress, renal tubular damage, and acute tubular necrosis. In a tunicamycin-mediated model of kidney injury, this damage is prevented primarily through repression of the pro-apoptotic ER stress protein CHOP. Along with providing renoprotective effects, 4-PBA can inhibit endothelial dysfunction and elevated blood pressure in a rat model of essential hypertension. In addition to lowering blood pressure, 4-PBA reduces contractility, augments endothelial-dependent vasodilation, and normalizes media-to-lumen ratio in mesenteric arteries from spontaneously hypertensive rats. Further, ER stress leads to reactive oxygen species generation, which is reduced with 4-PBA. Dahl salt-sensitive rats given 4-PBA are protected from hypertension, proteinuria, albuminuria, and renal pathology. Rats provided with vasodilatory medications demonstrate that lowering blood pressure alone is not renoprotective. In fact, endothelial dysfunction, as demonstrated by an impaired myogenic response, is culpable in the breakdown of the glomerular filtration barrier and subsequent renal damage. As such, alleviating ER stress using 4-PBA serves

as a viable therapeutic strategy to preserve renal function and prevent ER stress-mediated endothelial dysfunction, renal fibrosis, glomerular filtration barrier destruction, and progression of hypertensive nephrosclerosis.

ACKNOWLEDGEMENTS

I would first like to express my sincere gratitude to my supervisor, Dr. Jeffrey G. Dickhout, for providing me with on-going support and guidance, as well as the opportunity to work in his laboratory. I am also especially grateful to my committee members Drs. Richard C. Austin and Peter J. Margetts. Dr. Austin first introduced me to research, and over the years, both he and Dr. Margetts have provided me with exceptional input and encouragement. Thank you, Jeff, Rick, and Peter, I could not have asked for a more *nephenomenal* committee.

Special thanks goes out to Elise Brimble and Dr. Celeste Collins. I was very fortunate to meet such wonderful collaborators, but also to make two amazing friends. You have been a great source of discussion, support, help, humour, and friendship. Many appreciations also go out to past and current HCKR researchers, including, but not limited to (in alphabetical order): Dr. Ali Al-Hashimi, Chao Lu, Dr. Zahraa Mohammed-Ali, Dr. Adrian Rybak, Victoria Yum, and countless undergraduate students. You have made my life so much easier through friendship, the work you contributed, and in many cases, both.

Thank you to my friends and family, who still have no idea what I do. To the Hamilton scum (MP, GB, LC, HR, BD, SK, LR, MZ, CB, BK, EK, AW), who know I research ‘kidneys and molecules’, and my sisters (Jenn/Ween, Andie/Doonce, Sarah/Deebs), who know I ‘do science’, you have helped me maintain my mental health through laughter, mental and physical activities, so much food, and your individual perspectives. An additional thank you to anyone who edited my work for spelling and grammar; despite having no idea what they were reading.

Finally, I wish to express my deepest gratitude to my parents, Jane and Euan, who have unconditionally supported me and cared for me throughout my life. With your help, I was able to make it this far and I am truly grateful, and without your exceptional guidance I might have accidentally studied phrenology. You are genuinely amazing people, and I am proud to be your dotter.

TABLE OF CONTENTS

	Page number
Lay abstract	iii
Abstract	iv
Acknowledgements	vi
Table of contents	viii
List of figures	xiii
List of tables	xvii
List of abbreviations	xviii
Declaration of academic achievement	xxiii
CHAPTER 1	
Introduction	1
1.1 Chronic kidney disease and its complications	2
1.1.1 Chronic kidney disease	2
1.1.2 Hypertension	3
1.1.3 Proteinuria	4
1.1.4 Myogenic response	8
1.2 Endoplasmic reticulum stress	9
1.2.1 Synthesis of proteins through the endoplasmic reticulum	9
1.2.2 Endoplasmic reticulum stress proteins, CHOP and T-cell death-associated gene 51	13
1.2.3 Inhibiting endoplasmic reticulum stress	14
<i>1.2.3.1 Low molecular weight chemical chaperones</i>	<i>14</i>
<i>1.2.3.2 4-phenylbutyrate</i>	<i>20</i>
	viii

1.2.3.3 <i>Specific inhibitors of the unfolded protein response pathways</i>	21
1.2.4 Progression of chronic kidney disease through endoplasmic reticulum stress	22
1.2.5 Endoplasmic reticulum stress and epithelial-to-mesenchymal transition	24
1.3 Animal models of kidney disease	26
1.3.1 Tunicamycin: an acquired model of intrinsic acute kidney injury induced by endoplasmic reticulum stress	26
1.3.2 The spontaneously hypertensive rat: a genetic model of essential hypertension	27
1.3.3 The Dahl salt-sensitive rat: a genetic model of hypertensive proteinuric chronic kidney disease	28
1.4 Project rationale, hypothesis, objectives, and thesis outline	29
1.4.1 Project rationale and hypothesis	29
1.4.2 Objectives and experimental approach	30
1.4.3 Thesis outline	33
CHAPTER 2	
TDAG51 mediates epithelial-to-mesenchymal transition in human proximal tubular epithelium	35
Chapter link	36
Author's contributions	36
Abstract	38
Introduction	39
Methods	42
Results	48
Discussion	54

References	61
Figures	66
CHAPTER 3	
4-phenylbutyrate inhibits tunicamycin-induced acute kidney injury via CHOP/GADD153 repression	84
Chapter link	85
Author's contributions	85
Abstract	87
Introduction	88
Methods	90
Results	97
Discussion	102
References	107
Figures	111
CHAPTER 4	
Endoplasmic reticulum stress inhibition reduces hypertension through the preservation of resistance blood vessel structure and function	127
Chapter link	128
Author's contributions	128
Abstract	131
Introduction	132
Methods	134

Results	141
Discussion	147
References	152
Figures	157
CHAPTER 5	
Endoplasmic reticulum stress inhibition limits the progression of chronic kidney disease in the Dahl salt-sensitive rat	171
Chapter link	172
Author's contributions	173
Abstract	175
Introduction	176
Methods	178
Results	183
Discussion	187
References	194
Figures	200
Table	218
CHAPTER 6	
Discussion and future directions	219
6.1 Discussion	220
6.1.1 ER stress initiates EMT and the development of renal interstitial fibrosis	220

6.1.2 4-PBA is renoprotective through direct ER stress inhibiting effects in the kidney	223
6.1.3 Inhibiting ER stress prevents endothelial dysfunction and subsequent hypertension	226
6.1.4 Preserving the myogenic response through ER stress inhibition, and not simply lowering blood pressure, can protect against glomerular hyperfiltration	228
6.2 Future directions	231
6.2.1 Determination of the role TDAG51 plays in the development of EMT and fibrosis	231
6.2.2 Investigation of ER stress-mediated effects in podocytes in a model of glomerular hyperfiltration	231
6.2.3 Examination of renal function in a model of hypertensive nephrosclerosis	233
6.3 Conclusions	233
CHAPTER 7	
References	235
APPENDICES	254
Appendix 1 – Copyright permissions	255
Appendix 2 – Supplementary figure 1	264
Appendix 2 – Supplementary figure 2	267

LIST OF FIGURES

	Page number
CHAPTER 1	
Introduction	1
Figure 1 Relative risk of chronic kidney disease (CKD) by glomerular filtration rate (GFR) and albuminuria	 6
Figure 2 The unfolded protein response	 12
Figure 3 Effect of inhibitors on thapsigargin-induced endoplasmic reticulum stress	 18
CHAPTER 2	
TDAG51 mediates epithelial-to-mesenchymal transition in human proximal tubular epithelium	35
Figure 1 Unfolded protein response activation and TDAG51 expression in response to endoplasmic reticulum stress	 66
Figure 2 GRP78 and TDAG51 expression in response to endoplasmic reticulum stress	 68
Figure 3 Effect of salubrinal on TDAG51 expression and the unfolded protein response	 70
Figure 4 Induction of β -catenin nuclear translocation by thapsigargin	 72
Figure 5 Ca^{2+} chelator prevents thapsigargin-mediated effects	 74
Figure 6 Thapsigargin treatment reduces epithelial cell phenotype, while inducing the expression of myofibroblast markers	 76
Figure 7 Effects of TDAG51 protein overexpression on cell shape and β -catenin translocation	 78

Figure 8 TDAG51 deficiency prevents TGF- β -mediated peritoneal fibrosis	80
Figure 9 Two-hit model of TDAG51-induced epithelial-to-mesenchymal transition	82
CHAPTER 3 4-Phenylbutyrate inhibits tunicamycin-induced acute kidney injury via CHOP/GADD153 repression	84
Figure 1 Anatomical structures affected by tunicamycin-induced acute kidney injury	111
Figure 2 Damage to the outer stripe of the outer medulla is induced by tunicamycin	113
Figure 3 4-PBA significantly inhibits tunicamycin-induced CHOP expression	114
Figure 4 4-PBA protects against tunicamycin-induced apoptosis, which is mediated by CHOP expression	116
Figure 5 4-PBA inhibits tunicamycin-induced CHOP expression in the medulla	118
Figure 6 4-PBA inhibits tunicamycin-induced apoptosis in the medulla	120
Figure 7 4-PBA inhibits tunicamycin-induced GRP78 expression in the medulla	122
Figure 8 CHOP deficiency protects against tunicamycin-induced acute kidney injury	123
Figure 9 4-PBA protects ultrastructure of pars recta against tunicamycin-induced acute kidney injury	125
CHAPTER 4 Endoplasmic reticulum stress inhibition reduces hypertension through the preservation of resistance blood vessel structure and function	127

Figure 1	
4-PBA treatment lowers hypertensive rat systolic and diastolic blood pressure	157
Figure 2	
4-PBA treatment reduces phenylephrine-mediated vasoconstriction and increases carbachol-mediated vasodilation in hypertensive rat resistance vessels	159
Figure 3	
4-PBA treatment inhibits endoplasmic reticulum stress-mediated, superoxide-induced reduction of nitric oxide vasodilation in hypertensive rat resistance vessels	161
Figure 4	
4-PBA treatment reduces media-to-lumen ratio of mesenteric resistance arteries	163
Figure 5	
4-PBA treatment reduced the media-to-lumen ratio in hypertensive rat arcuate arteries	165
Figure 6	
Tunicamycin-mediated endoplasmic reticulum stress decreases carbachol-induced vasodilation in Wistar Kyoto rat mesenteric arteries	167
Figure 7	
Endoplasmic reticulum stress stimulates reactive oxygen species generation in blood vessels	168
Figure 8	
Proposed mechanism of endoplasmic reticulum stress-induced hypertension in the hypertensive rat	170
CHAPTER 5	
Endoplasmic reticulum stress inhibition limits the progression of chronic kidney disease in the Dahl salt-sensitive rat	171
Figure 1	
4-PBA treatment inhibits thapsigargin-induced accumulation of misfolded proteins in HK-2 cells	200
Figure 2	
4-PBA prevents increased proteinuria and albuminuria	202

Figure 3 4-PBA treatment preserves myogenic constriction in the arcuate artery through modulation of ER stress	204
Figure 4 4-PBA treatment inhibits ER stress and protects the glomerular filtration barrier	206
Figure 5 4-PBA prevents intratubular protein cast formation	210
Figure 6 4-PBA prevents salt-induced renal interstitial fibrosis	212
Figure 7 4-PBA prevents salt-induced renal collagen deposition	214
Figure 8 4-PBA treatment prevents proteinuria, albuminuria, and renal pathology, independent of blood pressure effects	216
APPENDICES	254
Appendix 2 – Supplementary figure 1 TDAG51 is upregulated in the PERK and IRE1 pathways of the unfolded protein response, but not the ATF6 pathway	264
Appendix 2 – Supplementary figure 2 TDAG51 knockout reduces renal interstitial fibrosis in a model of chronic kidney disease.	267

LIST OF TABLES

	Page number
CHAPTER 5	
Endoplasmic reticulum stress inhibition limits the progression of chronic kidney disease in the Dahl salt-sensitive rat	171
Table 1	
Blood pressure, blood urea nitrogen, and plasma creatinine levels before and after salt feeding with 4-PBA treatment	218

LIST OF ABBREVIATIONS

α -SMA or SMA	α -smooth muscle actin
3-NT	3-nitrotyrosine
4-PBA	4-phenylbutyrate or 4-phenylbutyric acid
20-HETE	20-hydroxyeicosatetraenoic acid
ACE	Angiotensin-converting enzyme
AdDL	Control adenovirus
AdTGF β	TGF β 1 adenovirus
AEBSF	4-(2-aminoethyl)benzenesulfonyl fluoride hydrochloride
AKI	Acute kidney injury
Ang II	Angiotensin II
ANOVA	Analysis of variance
ARB	Angiotensin II receptor blocker
AT1-receptor	Angiotensin II receptor, type 1
ATF4	Activating transcription factor 4
ATF6	Activating transcription factor 6
ATN	Acute tubular necrosis
ATP	Adenosine triphosphate
BAPTA-AM	1,2-bis(<i>o</i> -aminophenoxy)ethane- <i>N,N,N',N'</i> -tetraacetic acid acetoxymethyl ester
BP	Blood pressure
BUN	Blood urea nitrogen
Ca ²⁺	Calcium
CCh	Carbachol
CHOP	CCAAT enhancer-binding protein homologous protein
CHOP ^{-/-}	CHOP knockout
CKD	Chronic kidney disease
CsA	Cyclosporine A
DAPI	4',6-diamidino-2-phenylindole
DBP	Diastolic blood pressure

DHA	Docosahexanoic acid
DHE	Dihydroethidium
DMEM	Dulbecco's modified eagle medium
DMSO	Dimethyl sulfoxide
DNA	Deoxyribonucleic acid
DOCA	Deoxycorticosterone acetate
DSS or SS	Dahl salt-sensitive
ECL	Electrochemiluminescence
eGFP	Enhanced green fluorescent protein
EGTA	Ethylene glycol-bis(β -aminoethyl ether)-N,N,N',N'-tetraacetic acid
eIF2 α	Eukaryotic initiation factor 2 α
ELISA	Enzyme-linked immunosorbent assay
EMT	Epithelial-to-mesenchymal transition
eNOS	Endothelial nitric oxide synthase
ER	Endoplasmic reticulum
ERK	Extracellular signal-regulated kinase
ESRD	End-stage renal disease
FBS	Fetal bovine serum
FDA	Food and Drug Administration
FITC	Fluorescein isothiocyanate
GADD34	Growth arrest and DNA damage-inducible protein 34
GADD153	Growth arrest and DNA damage-inducible protein 153
GFB	Glomerular filtration barrier
GFP	Green fluorescent protein
GFR	Glomerular filtration rate
GRP78	Glucose-regulated protein 78
GRP94	Glucose-regulated protein 94
GSK	GSK-2606414
GTP	Guanosine triphosphate
h or hrs	Hour(s)
HBSS	Hank's balanced saline solution

HDAC	Histone deacetylation
HDACi	Histone deacetylation inhibitor
hEGF	Human epidermal growth factor
HEPES	Hydroxyethyl piperazineethanesulfonic acid
HK-2	Human kidney immortalized proximal tubular cell
HPF	High powered field
HRP	Horseradish peroxidase
hRPTEC	Human renal proximal tubular epithelial cell
HS	High salt (8% NaCl)
HS+4-PBA	High salt (8% NaCl) with 4-phenylbutyrate (1 g/kg/day)
HS+H	High salt (8% NaCl) with hydralazine (15 mg/kg/day)
HS+N	High salt (8% NaCl) with nifedipine (25 mg/kg/day)
IHC	Immunohistochemical
I.P.	Intraperitoneal
IRE1	Inositol-requiring enzyme 1
IS	Indoxyl sulfate
KCl	Potassium chloride
KDEL	Target peptide sequence that prevents a protein from being secreted from the endoplasmic reticulum
LacZ	Gene that encodes for the β -galactosidase enzyme
LB	Lysogeny broth
L-NNA	Nitroarginine
LWCC	Low molecular weight chemical chaperone
MAPK	Mitogen-activated protein kinase
MEK	Mitogen-activated protein kinase kinase
MKK3	Mitogen-activated protein kinase kinase 3
NaCl	Sodium chloride
NO	Nitric oxide
NOS	Nitric oxide synthase
NS	Normal salt (0.4% NaCl)
NT	No treatment

O ₂ ⁻	Superoxide
ORP150	Oxygen-regulated protein 150
OsO ₄	Osmium tetroxide
PAS	Periodic acid-Schiff
PBS	Phosphate-buffered saline
PCR	Polymerase chain reaction
PERK	Protein kinase R-like endoplasmic reticulum kinase
PHE	Phenylephrine
PHLDA1	Pleckstrin homology-like domain A family 1
PP1	Protein phosphatase 1
PSR	Picrosirius red
PVDF	Polyvinylidene fluoride
REBM	Renal epithelial cell basal medium
RNA	Ribonucleic acid
S ₁ P	Site 1 protease
S ₂ P	Site 2 protease
Sal	Salubrinal
SBP	Systolic blood pressure
SD	Sprague Dawley
SDS	Sodium dodecyl sulfate
SDS-PAGE	Sodium dodecyl sulfate-polyacrylamide gel electrophoresis
SEM	Standard error of the mean
SERCA	Sarco/endoplasmic reticulum Ca ²⁺ -ATPase
SHR	Spontaneously hypertensive rat
SMA or α-SMA	α-smooth muscle actin
SNP	Sodium nitroprusside
SS or DSS	Dahl salt-sensitive
SS.BN13 or SS-BN13	Brown norway rat with Dahl salt-sensitive rat chromosome 13
STF	STF-083010
TDAG51	T-cell death-associated gene 51

TDAG51 ^{-/-} or TDKO	TDAG51 knockout
TEM	Transmission electron microscopy
TEMPOL	4-hydroxy-2,2,6,6-tetramethylpiperidin-1-oxyl
Tg or TG	Thapsigargin
TGF- β or TGF β	Transforming growth factor- β
Tm or TM	Tunicamycin
TMB	Tetramethylbenzidine
TNF- α	Tumor necrosis factor- α
TNF- α -R1	Tumor necrosis factor- α receptor 1
TUDCA	Tauroursodeoxycholic acid
TUNEL	Terminal deoxynucleotidyl transferase dUTP nick end labelling
UFP	Unfolded proteins
UN	Untreated
UPR	Unfolded protein response
UUO	Unilateral ureteral obstruction
Veh or VEH	Vehicle
VSMC	Vascular smooth muscle cell
WKY	Wistar Kyoto
WT	Wild type
XBP1	X-box binding protein 1

DECLARATION OF ACADEMIC ACHIEVEMENT

This thesis is presented as a sandwich thesis, and is composed of seven chapters. Chapter 1, an introductory chapter, provides background to the material in chapters 2 through 5, and outlines the overall basis for this thesis. Excerpts from authored and co-authored works were used in chapter 1. Chapters 2 through 5 are empirical articles, all of which have been published at the time this thesis was prepared. I am the primary author of the articles in chapters 2, 3, and 4, and a co-author of the article in chapter 5. The author's contribution section preceding each chapter describes the contributions of all authors of a given manuscript. Chapter 6, a concluding chapter, discusses the contributions of the work in chapters 2 through 5, as well as limitations and proposed future directions of this research. References cited in chapters 1 and 6 can be found in chapter 7, a reference chapter. References cited within each manuscript are independent and are consistent with the style of the journal in which the work is published. Appendices are also included, which provide copyright permissions for each article or excerpt used, as well as unpublished data.

This thesis is primarily comprised of four manuscripts, all of which have been published.

Rachel E. Carlisle, Alana Heffernan, Elise Brimble, Limin Liu, Danielle E. Jerome, Celeste A. Collins, Zahraa Mohammed-Ali, Peter J. Margetts, Richard C. Austin, Jeffrey G. Dickhout. (2012). TDAG51 mediates epithelial-to-mesenchymal transition in human proximal tubular epithelium. *Am J Physiol Renal Physiol* 303, F467-481, doi:10.1152/ajprenal.00481.2011.

Rachel E. Carlisle, Elise Brimble, Kaitlyn E. Werner, Gaile Cruz, Kjetil Ask, Alistair J. Ingram, Jeffrey G. Dickhout. (2014). 4-Phenylbutyrate inhibits tunicamycin-induced acute kidney injury via CHOP/GADD153 repression. *PLoS One* 9, e84663, doi:10.1371/journal.pone.0084663.

Rachel E. Carlisle, Kaitlyn E. Werner, Victoria Yum, Chao Lu, Muzammil Memon, Yejin No, Kjetil Ask, Jeffrey G. Dickhout. (2016). Endoplasmic reticulum stress inhibition reduces hypertension through the preservation of resistance blood vessel structure and function. *J Hypertens* 34, 1556-1569, doi:10.1097/HJH.0000000000000943.

Victoria Yum, **Rachel E. Carlisle**, Chao Lu, Elise Brimble, Jasmine Chahal, Chandak Upagupta, Kjetil Ask, Jeffrey G. Dickhout. (2017). Endoplasmic reticulum stress inhibition limits the progression of chronic kidney disease in the Dahl salt-sensitive rat. *Am J Physiol Renal Physiol* 312, F230-F244, doi:10.1152/ajprenal.00119.2016.

This thesis also contains excerpts from two additional manuscripts, both published, and a book chapter, in press.

Jeffrey G. Dickhout, **Rachel E. Carlisle**, Richard C. Austin. (2011). Interrelationship between cardiac hypertrophy, heart failure, and chronic kidney disease: endoplasmic reticulum stress as a mediator of pathogenesis. *Circ Res* 108, 629-642, doi:10.1161/CIRCRESAHA.110.226803.

Chandak Upagupta, **Rachel E. Carlisle**, Jeffrey G. Dickhout. (2017). Analysis of the potency of various low molecular weight chemical chaperones to prevent protein aggregation. *BBRC* 486, 163-170, doi: 10.1016/j.bbrc.2017.03.019.

Zahraa Mohammed-Ali*, **Rachel E. Carlisle***, Samera Nademi, Jeffrey G. Dickhout. (In press; 2017). Animal models of kidney disease. Animal models for the study of human disease. 2nd edition, Michael Conn. Elsevier Publishing Group, Academic Press (2017).

*Both authors contributed equally to this work.

In addition to the works used to produce this thesis, I contributed to the following manuscripts.

Zahraa Mohammed-Ali, Chao Lu, Mandeep K. Marway, **Rachel E. Carlisle**, Kjetil Ask, Dusan Lukic, Joan C. Krepinsky, Jeffrey G. Dickhout. (2017). Endoplasmic reticulum stress inhibition attenuates hypertensive chronic kidney disease through reduction in proteinuria. *Sci Rep* 7, 41572, doi:10.1038/srep41572.

Jasmine Chahal, Ashish Matthews, **Rachel E. Carlisle**, Victor Tat, Safaa N. Abawi, Jeffrey G. Dickhout. (2016). Endoplasmic reticulum stress causes epithelial cell disjunction. *J Pharma Reports* 1, 5.

Zahraa Mohammed-Ali, Gaile L. Cruz, Chao Lu, **Rachel E. Carlisle**, Kaitlyn E. Werner, Kjetil Ask, Jeffrey G. Dickhout. (2015). Development of a model of chronic kidney disease in the C57BL/6 mouse with properties of progressive human chronic kidney disease. *Biomed Res Int* 2015, 172302, doi:10.1155/2015/172302.

Šárka Lhoták, Sudesh K. Sood, Elise Brimble, **Rachel E. Carlisle**, Stephen M. Colgan, Adam Mazzetti, Jeffrey G. Dickhout, Alistair J. Ingram, Richard C. Austin. (2012). ER stress contributes to renal proximal tubule injury by increasing SREBP-2-mediated lipid accumulation and apoptotic cell death. *Am J Physiol Renal Physiol* 303, F266-278, doi:10.1152/ajprenal.00482.2011.

Jeffrey G. Dickhout, **Rachel E. Carlisle**, Danielle E. Jerome, Hua Jiang, Guangdong Yang, Sarathi Mani, Sanjay K. Garg, Ruma Banerjee, Randal J. Kaufman, Kenneth N. Maclean, Rui Wang, Richard C. Austin. (2012). Integrated stress response modulates cellular redox state via induction of cystathionine gamma-lyase: cross-talk between integrated stress response and thiol metabolism. *J Biol Chem* 287, 7603-7614, doi:10.1074/jbc.M111.304576.

Jeffrey G. Dickhout, Šárka Lhoták, Brooke A. Hilditch, Sana Basseri, Stephen M. Colgan, Edward G. Lynn, **Rachel E. Carlisle**, Ji Zhou, Sudesh K. Sood, Alistair J. Ingram, Richard C. Austin. (2011). Induction of the unfolded protein response after monocyte to macrophage differentiation augments cell survival in early atherosclerotic lesions. *FASEB J* 25, 576-589, doi:10.1096/fj.10-159319.

CHAPTER 1

Introduction

1.1 CHRONIC KIDNEY DISEASE AND ITS COMPLICATIONS

1.1.1 Chronic kidney disease

Chronic kidney disease (CKD) is a global health concern that is becoming increasingly prevalent in North America, with an incidence of 15.45% in Canada and the United States (Hill et al., 2016). In 2006, 19 million adults in the United States suffered from early stages of CKD, with an estimated minimum of 2 million adults needing renal replacement therapy by 2030 (Stevens et al., 2006). Thus, focusing effort on alleviating the economic burden caused by CKD is an important public health initiative. Measuring blood and urine samples for specific compounds, such as creatinine, allows for an accurate depiction of how well the kidneys are functioning, and provides data to calculate an estimated glomerular filtration rate (GFR) (Levey et al., 1999).

GFR is the volume of fluid filtered from the glomerular capillaries to the Bowman's space per unit time, normalized to body surface area ($\text{ml}/\text{min}/\text{m}^2$) (Levey et al., 1999). GFR is dependent on the pressure difference between the glomerular afferent and efferent arterioles. Constriction of the afferent arteriole slows blood flow into the glomerulus, thus decreasing GFR, while constriction of the efferent arteriole prevents blood from leaving the glomerulus, which raises glomerular hydrostatic pressure and increases GFR. Optimally, GFR would be calculated in humans using exogenous filtration markers, such as inulin; however, this procedure is complex, expensive, and difficult to perform. Instead, GFR is estimated by measuring endogenous filtration markers, usually serum creatinine levels (Stevens et al., 2006). Other markers of renal function and damage,

including blood urea nitrogen levels, proteinuria, and albuminuria, can be used to quantify development and progression of CKD (Levey & Coresh, 2012).

CKD progresses from stage 1 normal function (>60% kidney function; GFR >90 ml/min/m²) to stage 5 kidney failure (<15% kidney function; GFR <15 ml/min/m²) (Levey & Coresh, 2012). The progressive decline in renal function culminates in end-stage renal disease, requiring renal replacement therapy, either hemodialysis or renal transplantation. Despite the numerous risk factors that predispose individuals to CKD, the disease tends to progress in a predictable manner. Affected individuals develop renal interstitial fibrosis, nephron loss, tubular atrophy, and reduced filtration (Metcalf, 2007). Although the etiology of CKD can vary, hypertension is often considered the most significant risk factor for CKD (Metcalf, 2007).

1.1.2 Hypertension

Hypertension is the leading risk factor for premature death in the world, and is associated with a number of illnesses, including cardiovascular disease and renal failure (Simonds & Cowley, 2013). There are two forms of hypertension: 1) essential hypertension – high blood pressure with an unknown cause, and 2) secondary hypertension – high blood pressure with a known direct cause (Carretero & Oparil, 2000; Oparil et al., 2003). In 2009, an estimated 1 billion people worldwide suffered from hypertension (Bakris & Ritz, 2009), with approximately 95% of hypertensives suffering from essential hypertension (Carretero & Oparil, 2000). While the origins of essential hypertension are unknown and possibly varied, it is typically treated similarly between individuals. The goal to lower blood pressure is attempted using lifestyle changes

(following the Dietary Approaches to Stop Hypertension low salt diet (Sacks et al., 2001), regularly exercising (Pescatello et al., 2004), quitting smoking (Bowman et al., 2007; Jatoi et al., 2007), reducing alcohol consumption (Beilin & Puddey, 2006), and achieving a healthy body weight (Nguyen et al., 2008)), as well as antihypertensive medications (Wu et al., 2005). Essential hypertension is associated with reduced blood vessel luminal size, and subsequent increase in peripheral vascular resistance. Vascular hypertrophy (eutrophic or hypertrophic), vascular wall stiffness, and vascular dysfunction can all contribute to the development of essential hypertension (Intengan & Schiffrin, 2000).

1.1.3 Proteinuria

While hypertension might be considered the most significant risk factor for CKD, proteinuria is recognized as the most accurate predictor of CKD progression (Fraser et al., 2016). In humans, proteinuria is defined as urinary protein excretion of more than 150 mg/day (Carroll & Temte, 2000), most of which is made up of albumin (Levey & Coresh, 2012). Increases in proteinuric levels are associated with corresponding elevations in risk of progression of CKD, with even small changes to baseline proteinuria levels impacting the severity of CKD progression (Figure 1) (Fraser et al., 2016). The presence of protein in the urine is an indicator of reduced renal function, as damaged kidneys are unable to properly filter blood. Typically, proteins are retained in the blood, but renal damage can allow proteins to filter through the glomerulus and infiltrate the urine (Palatini, 2012). Glomerular hyperfiltration is observed in proteinuric kidney disease, suggesting podocyte dysfunction and injury in individuals with proteinuria (Helal et al., 2012; Palatini, 2012).

Glomerular hyperfiltration, essentially increased single nephron GFR, can occur due to afferent arteriolar vasodilation or efferent arteriolar vasoconstriction. Low nephron number, caused by genetics, surgical ablation, or acquired renal disease, stimulates compensatory hyperfiltration by the remaining nephrons, in an attempt to maintain adequate renal function (Helal et al., 2012). However, it is believed that this compensatory mechanism is a precursor for intraglomerular hypertension and podocyte injury, and subsequently causes proteinuria (Helal et al., 2012; Palatini, 2012).

Prognosis of CKD by GFR and albuminuria categories: KDIGO 2012

				Persistent albuminuria categories Description and range		
				A1	A2	A3
				Normal to mildly increased	Moderately increased	Severely increased
				<30 mg/g <3 mg/mmol	30–300 mg/g 3–30 mg/mmol	>300 mg/g >30 mg/mmol
GFR categories (ml/min/1.73m ²) Description and range	G1	Normal or high	≥90			
	G2	Mildly decreased	60–89			
	G3a	Mildly to moderately decreased	45–59			
	G3b	Moderately to severely decreased	30–44			
	G4	Severely decreased	15–29			
	G5	Kidney failure	<15			

Figure 1. Relative risk of chronic kidney disease (CKD) by glomerular filtration rate (GFR) and albuminuria. Low levels of albuminuria (A1) are associated with no/low risk of developing end stage renal disease, while higher levels (A3) increase risk. High GFR (G1) is associated with no/low risk of CKD, while low GFR (G5) increases risk of end stage renal disease. Permission granted for reuse of table (Appendix 1) (Fraser et al., 2016).

Podocytic injury is a common hallmark of glomerular injury, and is found in a number of chronic proteinuric kidney diseases, including minimal change disease, focal segmental glomerulosclerosis, membranous glomerulopathy, diabetic nephropathy, and lupus nephritis (Greka & Mundel, 2012). The glomerular filtration barrier is comprised of three components: 1) the capillary fenestrae, glomerular endothelial cells that contain large pores allowing the passage of macromolecules but preventing the passage of blood cells and platelets, 2) the glomerular basement membrane or basal lamina, a negatively charged layer of glycoproteins found outside the capillary endothelium, and 3) the podocyte cell layer, which is made up of specialized epithelial cells that use foot processes, or pedicels, to wrap around glomerular capillaries to create the slit diaphragm (Greka & Mundel, 2012). Plasma solutes pass easily through all three filtration components, while plasma proteins are typically too big or negatively charged to pass through. The slit diaphragm, as the barrier with the smallest diameter spaces, is the primary filter to exclude plasma proteins from filtrate, and is dependent on parallel actin filament bundles to function properly (Greka & Mundel, 2012). Podocyte foot processes are made up of three membrane domains, and disruption to any of these can alter the actin cytoskeleton. Disruption causes the coordinated parallel actin filament bundles to be reorganized into a dense network of disordered cytoskeletal components. Subsequently, the interdigitating pattern of the foot processes is lost, resulting in foot process effacement and proteinuria (Greka & Mundel, 2012).

As mentioned, medication is commonly used to reverse hypertension; however, blood pressure medications can have varying effects on proteinuria. Angiotensin-converting enzyme (ACE) inhibitors reduce both blood pressure and proteinuria (Maschio

et al., 1996), while calcium channel blockers reduce blood pressure but can increase proteinuria (Dhaun et al., 2009). These differences are likely due to the mechanism by which blood pressure is reduced, as well as the effect each medication has on podocyte function. In support, angiotensin II type 1 surface receptors are increased in podocytes undergoing mechanical stress (Durvasula et al., 2004), indicating that angiotensin II may have a direct effect on these cells (Hoffmann et al., 2004). This may explain why ACE inhibitors and angiotensin receptor blockers reduce podocyte injury and death (Matsusaka et al., 2010). Conversely, calcium channel blockers are unable to prevent detrimental changes in podocyte phenotype after subtotal nephrectomy in rats, which can lead to the development of glomerulosclerosis (Amann et al., 1996). Despite differences in renal protection, antihypertensive medications appear to have similar effects on lowering systemic blood pressure (Amann et al., 1996).

1.1.4 Myogenic response

Two mechanisms are used to protect the kidneys from changes in systemic blood pressure and thereby maintain renal blood flow autoregulation: tubuloglomerular feedback and the myogenic response. Tubuloglomerular feedback occurs when the macula densa signals the glomerular afferent arteriole to vasoconstrict in response to elevations in sodium chloride concentration in the distal tubule, thus reducing GFR (Peti-Peterdi & Harris, 2010). The myogenic response occurs when stretching, caused by increased intraluminal pressure, generates contraction of arteriole smooth muscle cells. This vasoconstriction reduces lumen diameter, which decreases renal blood flow, and thus, GFR (Helal et al., 2012; Palatini, 2012). These mechanisms work in concert to allow

a constant pressure to enter the kidneys; if one or both of these mechanisms become dysfunctional, the kidney is no longer properly protected from high arterial pressure. The Brenner hypothesis stipulates that renal damage can be caused by glomerular hyperfiltration and increased intraglomerular capillary pressure (Brenner et al., 1996; Brenner et al., 1982). Loss of myogenic response results in afferent arteriolar vasodilation, and thus glomerular hyperfiltration.

1.2 ENDOPLASMIC RETICULUM STRESS

1.2.1 Synthesis of proteins through the endoplasmic reticulum¹

The rough endoplasmic reticulum (ER) is the cellular organelle where the synthesis of transmembrane and secretory proteins occur (Lee, 2001). ER stress represents a disturbance in the homeostasis of the ER that interferes with proper protein folding. Protein folding is a complex process by which the nascent polypeptide chain is converted into a thermodynamically stable tertiary structure that corresponds to the proper functional conformation of the protein (Schröder & Kaufman, 2005). Quality control of protein folding is an important component of ER function in the secretory pathway, so that incorrectly folded proteins are recognized before their movement to the Golgi complex and degraded via the proteasome (Schröder & Kaufman, 2005). Protein

¹ This section has been adapted from: Dickhout, J. G., Carlisle, R. E., & Austin, R. C. (2011). Interrelationship between cardiac hypertrophy, heart failure, and chronic kidney disease: endoplasmic reticulum stress as a mediator of pathogenesis. *Circ Res*, *108*(5), 629-642.

misfolding may lead to the aggregation of misfolded proteins in the rough ER, resulting in organelle and cellular dysfunction.

The rough ER is a membrane-bound organelle that creates a distinct environment from the cytosolic space specialized for protein folding. Glutathione in the cytosol acts as a major redox buffer and predominately exists in its reduced form, whereas in the ER reduced glutathione to oxidized glutathione levels are equal, creating a more oxidizing environment that facilitates disulfide bond formation (Schröder & Kaufman, 2005). The ER also functions as an important storage site for calcium (Brostrom et al., 2001; Schröder & Kaufman, 2005), and as such regulates contractility in both smooth and cardiac muscle. Furthermore, many of the ER-resident molecular chaperones are calcium-binding proteins (Schröder & Kaufman, 2005), including glucose-regulated protein 78 (GRP78), calnexin and calreticulin.

Agents and/or conditions that cause ER stress induce the unfolded protein response (UPR) (Figure 2), an integrated intracellular signalling pathway that consists of three resident ER membrane-bound transducers; inositol-requiring enzyme (IRE)1, activating transcription factor (ATF)6, and protein kinase R-like endoplasmic reticulum kinase (PERK). GRP78 regulates the activation of these transducers through its interaction with them or its interaction with unfolded proteins within the lumen of the ER. Once GRP78 dissociates from these transducers, the UPR is activated, resulting in IRE1 and PERK autophosphorylation, as well as ATF6₉₀ release from the ER and cleavage by site 1 (S₁P) and site 2 proteases (S₂P) in the Golgi. The signalling from PERK leads to the phosphorylation of eukaryotic initiation factor 2 α (eIF2 α), which reduces the translation of many proteins through inhibition of GTP, eIF2, tRNA complex formation (Kimball,

1999). However, under these conditions some proteins are preferentially translated, including ATF4. ATF4 acts in the nucleus as a transcription factor to induce C/EBP homologous protein (CHOP), which then acts to upregulate growth arrest and DNA damage-inducible protein (GADD)34-protein phosphatase (PP)1 complex formation to dephosphorylate the α subunit of eIF2 (Boyce et al., 2005). IRE1 activation leads to the splicing of X-box binding protein (XBP)1 mRNA generating an active XBP1 transcription factor that translocates to the nucleus to upregulate the expression of protein folding chaperones (Minamino & Kitakaze, 2010). The UPR also plays a role in unstressed cells. Specifically it appears to be important in the differentiation of certain cell types including the plasma cell (Schröder & Kaufman, 2005), adipocytes (Basseri et al., 2009a), and in epithelial-to-mesenchymal transition (EMT) (Dickhout et al., 2011b; Pallet et al., 2008a).

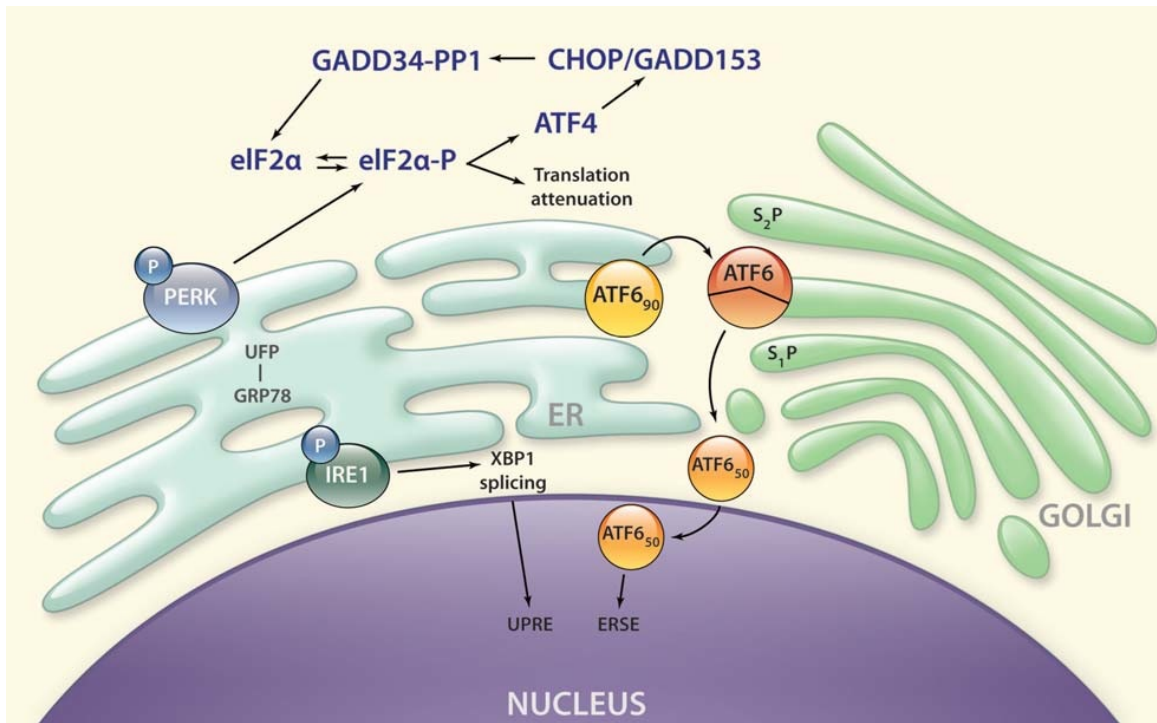


Figure 2. The unfolded protein response. When unfolded proteins (UFP) accumulate in the endoplasmic reticulum (ER), GRP78 dissociates from PERK, IRE1, and ATF6₉₀, activating the three arms of the unfolded protein response. These pathways work to maintain proteostasis through general reduced protein translation and increased transcription of molecular chaperones. Prolonged activation of the unfolded protein response can lead to apoptosis. Permission granted for reuse of figure (Appendix 1) (Dickhout et al., 2011b).

1.2.2 Endoplasmic reticulum stress proteins, CHOP and T-cell death-associated gene

51

CHOP, also known as GADD153, is a small nuclear protein (30 kDa) that is activated by ER stress. Initially, CHOP was believed to be expressed in response to DNA damage, as its expression was increased in cells in response to ultraviolet light. However, it is now known that CHOP expression is significantly induced by other factors, including inhibition of N-linked protein glycosylation (nutrient depletion or tunicamycin treatment) and calcium disequilibrium (A23187 or thapsigargin treatment) (Wang et al., 1996). Normally, CHOP is absent or expressed at very low levels in the cell, and cells that lack CHOP are typically protected from ER stress-induced death, while cells that express CHOP are not (Marciniak et al., 2004). CHOP is comprised of two functional domains, the N-terminal transactivation domain and the C-terminal basic-leucine zipper domain. The transactivation domain contains two neighbouring serine residues, which act as substrates in the p38 mitogen-activated protein kinase (MAPK) pathway to alter gene transcription and induce apoptosis. The basic-leucine zipper domain contains a basic amino acid-rich DNA-binding region and a leucine zipper dimerization domain comprised of conserved glycine and proline residues (Oyadomari & Mori, 2004).

T-cell death-associated gene 51 (TDAG51), also known as the pleckstrin homology-like domain, family A member 1 (PHLDA1) protein, can be upregulated by various ER stress inducers, including thapsigargin and peroxynitrite, both of which inhibit the sarco/endoplasmic reticulum calcium ATPase (Dickhout et al., 2005; Hossain et al., 2003a). ER stress-mediated TDAG51 induction can lead to cell shape change, and decreased cell adhesion resulting in anoikis (detachment-mediated apoptosis), in human

vascular endothelial cells (Hossain et al., 2003a). TDAG51 expression results in cell shape change through a mechanism that may be related to co-localization with focal adhesion kinase (Hossain et al., 2003a). Further, The Human Protein Atlas has confirmed that human renal proximal tubule epithelial cells express a moderate amount of the TDAG51 protein ("Tissue Expression of PHDLA1," 2017), indicating it may play a role in ER stress-induced renal tubular damage.

1.2.3 Inhibiting endoplasmic reticulum stress

1.2.3.1 Low molecular weight chemical chaperones²

Proteins are responsible for the molecular processes within the body and are vital for its survival. The function of any protein is dependent on its structure, which is divided into four major domains: primary, secondary, tertiary, and quaternary. The primary structure is the amino acid makeup of the protein and is outlined in nucleic acids. This is what most significantly determines the ultimate structure of all proteins and therefore their function. The structure is further developed through unique and precise foldings that allow for proper and optimal functionality. Hydrogen bonding between amino acids determines the secondary structure of a protein, as sections fold into α -helices or β -sheets. The side-chain groups of amino acids determine the tertiary structure, folding the molecule to produce maximum stability, and securing the protein structure with disulphide bridges. The quaternary structure is produced when multiple protein subunits

² This section has been adapted from: Upagupta, C., Carlisle, R. E., & Dickhout, J. G. (2017). Analysis of the potency of various low molecular weight chemical chaperones to prevent protein aggregation. *Biochem Biophys Res Commun*, 486(1), 163-170.

bond together to form an aggregate protein complex. Following synthesis of a relatively small amino acid sequence, strong interactions within the sequence and between its surroundings cause it to quickly fold to reach a low thermodynamic state, and therefore a stable conformation (Yao et al., 2015). In long sequences, however, different regions are not close enough to experience such strong forces, and instead fold in certain ways to reach a reduced thermodynamic state. This conformation is not usually the most stable structure, which is required for proper function. In unstable structures the sequences reside in local thermodynamic minimum, which make it difficult for the sequences to later unfold and then refold into the proper structure.

Molecular chaperones overcome this problem by providing long amino acid sequences with a suitable environment and enough energy in the form of ATP to fold into the proper structure (Gething & Sambrook, 1992). Chaperones were first detected in yeast, in which their ability to aid in protein folding and reduce protein aggregation was observed (Quan & Bardwell, 2012). Misfolded proteins are detrimental to the cell, both through dysfunction and susceptibility to form aggregates (Bucciantini et al., 2002). When amino acid sequences are in an incorrect conformation, certain hydrophobic regions, which are usually enclosed in the interior of the protein after proper folding, are exposed to the aqueous environment. In an attempt to further reach a lower thermodynamic state, these misfolded proteins bind to other exposed hydrophobic regions on other misfolded proteins. This allows the hydrophobic regions of these sequences to reduce their interaction with the aqueous environment; however, in the process they form protein aggregates. This misfolding and subsequent aggregation frequently occurs and is natural for a cell, and the amount of aggregation is maintained to a relatively low amount

by chaperones. Under certain physiological and pathological conditions however, this aggregation can become too great and can cause severe stress within certain regions of the cell, specifically the ER. This ER stress leads to the activation of the UPR through which the cells undergo apoptosis when ER stress is too high (Dickhout & Krepinsky, 2009). Over time, this cell death can have physiologically notable effects due to the loss of suitable function of the organ the cells make up. This process is implicated in the pathogenesis of many degenerative diseases, including Huntington's disease, inflammatory bowel disease, and CKD (Dickhout & Krepinsky, 2009; Niederreiter & Kaser, 2011; Tanaka et al., 2004).

There are two major classes of low molecular weight chemical chaperones (LWCCs): 1) hydrophobic chaperones (4-PBA, TUDCA), and 2) osmolyte chaperones, which include carbohydrates (glycerol, sorbitol), amino acids and derivatives (glycine, proline), and methylamines (betaine, trimethylamine *N*-oxide) (Engin & Hotamisligil, 2010). As their name suggests, LWCCs are small compounds that aid in proper folding and reduce aggregation of proteins (Figure 3) (Perlmutter, 2002). The specific method through which this is done is unclear and may be unique for every molecule; however, it is believed that they stabilize improperly folded proteins and prevent non-productive interactions with other resident proteins. These molecules have proven effective at alleviating ER stress in many different *in vivo* and *in vitro* models, including neural and respiratory models (Kim et al., 2013; Tanaka et al., 2004). Additionally, most LWCCs can pass through the blood-brain barrier, which allows them to be an effective treatment for neurodegenerative diseases, such as Parkinson's disease and Huntington's disease, where ER stress is considered one of the mechanisms of disease pathology (Engin & Hotamisligil, 2010).

These compounds, however, need to be administered at high concentrations to allow for noticeable reduction of ER stress; therefore, they may lead to non-specific effects and become toxic. Hence, it is important to understand the association between the structure of these LWCCs and the effects they cause, so that a more selective and effective ER stress-reducing molecule can be developed (Upagupta et al., 2017).

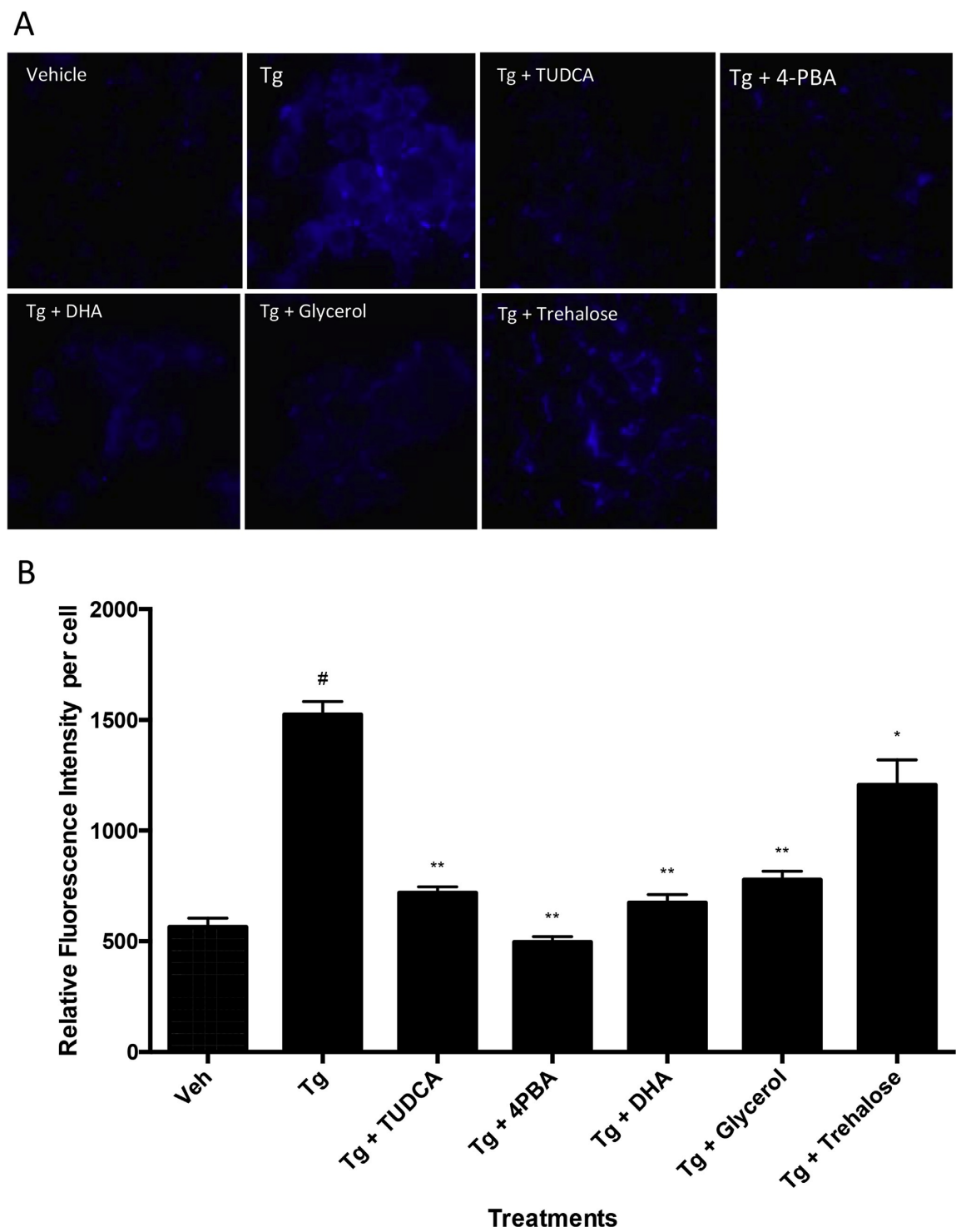
Figure 3.

Figure 3. Effect of inhibitors on thapsigargin-induced endoplasmic reticulum stress.

(A) Human proximal tubular (HK-2) cells were treated with DMSO (vehicle; Veh), thapsigargin (Tg; 1 μ M) or Tg co-treated with tauroursodeoxycholic acid (TUDCA; 500 μ M), 4-phenylbutyrate (PBA; 1 mM), docosahexanoic acid (DHA; 10 μ M), glycerol (1%), or trehalose (1 mM) for 24 hrs. Protein aggregation was stained with thioflavin T (5 μ M) and imaged using fluorescence microscopy at 40X magnification. (B) Quantitative analysis was performed to determine relative endoplasmic reticulum stress between treatments. #, $P < 0.0001$ vs Veh; *, $P < 0.05$ vs Tg; **, $P < 0.0001$ vs Tg; n = 30. This figure was adapted from (Upagupta et al., 2017).

1.2.3.2 4-phenylbutyrate

4-phenylbutyrate (4-PBA) is an effective LWCC that has been approved by the Food and Drug Administration for clinical use in urea cycle disorders. 4-PBA functions as an ammonia scavenger (Wright et al., 2011), a weak histone deacetylase inhibitor (HDACi) (Miller et al., 2011), and an ER stress inhibitor (Basseri et al., 2009a; Xiao et al., 2011; Yam et al., 2007a). As an ammonia scavenger, 4-PBA decreases free ammonia levels through the production of glutamine. Glutamine is a substrate for ammoniogenesis, which can lead to hyperammonaemia. In short, 4-PBA is converted to phenylacetate, which covalently binds with circulating glutamine, forming phenylacetylglutamine. Phenylacetylglutamine is then excreted by the kidneys (Wright et al., 2011). Histone acetylation regulates gene expression by modulating chromatin structure. HDACis prevent the removal of acetyl groups from histones, resulting in histone hyperacetylation, and altered gene expression (Yoshikawa et al., 2007). This can result in antifibrogenic effects in organs such as the liver, skin, lungs, and kidneys (Kinugasa et al., 2010; Niki et al., 1999; Rishikof et al., 2004; Rombouts et al., 2002). However, the mechanisms behind these actions are incompletely understood. Interestingly, HDACis acetylate spliced XBP1, increasing stability and transcriptional activity of the protein (Wang et al., 2011). Spliced XBP1 is a key transcriptional inducer of the IRE1 arm of the UPR and may protect against apoptosis by upregulating the expression of protein folding chaperones, including GRP78 (Hosoi et al., 2012). 4-PBA functions as an ER stress inhibitor via its LWCC properties, preventing protein mislocalization and aggregation (Mimori et al., 2013). The hydrophobic regions of 4-PBA interact with the exposed hydrophobic regions of misfolded proteins, forcing proper folding (Cortez & Sim, 2014; Mimori et al., 2013).

However, it is possible that the HDACi effects of 4-PBA complement the ER stress inhibitor effects, as HDAC inhibition can regulate genes involved in the UPR (Cortez & Sim, 2014). 4-PBA is currently in clinical trials for treatment of a number of diseases, including cystic fibrosis (Loffing et al., 1999), sickle cell disease (Collins et al., 1995), neurodegenerative diseases (Mimori et al., 2012), and certain cancers (Carducci et al., 1996; Dyer et al., 2002; Phuphanich et al., 2005). These trials take advantage of both the ER stress inhibitor effects and HDACi effects of 4-PBA.

1.2.3.3 Specific inhibitors of the unfolded protein response pathways

In addition to chemical chaperone ER stress inhibitors, there are a number of UPR inhibitors. Unlike LWCCs, which work to prevent protein aggregation and misfolding, UPR inhibitors do not prevent ER stress, but simply inhibit the response that leads to cellular proteostasis. UPR inhibitors target and inhibit specific pathways of the UPR: STF-083010 blocks the IRE1 pathway (Papandreou et al., 2011), GSK-2606414 is a PERK phosphorylation inhibitor (Moreno et al., 2013), salubrinal inhibits the dephosphorylation of phosphorylated eIF2 α (Boyce et al., 2005), and AEBSF blocks the ATF6 pathway (Saw et al., 2012). Unlike LWCC, these molecules can be used to examine if inhibition of a specific UPR pathway will have advantageous or damaging results. For example, STF-083010 has demonstrated antimyeloma activity in human plasma cells and a mouse model of multiple myeloma (Papandreou et al., 2011), GSK-2606414 was able to prevent neurodegeneration in prion-infected mice (Moreno et al., 2013), salubrinal has been shown to protect against ischemic neuronal cell death in animals and has prevented viral replication in cultured cells (Bryant et al., 2008;

Umareddy et al., 2007), and AEBSF has been shown to prevent airway inflammation in a mouse model of airway allergy (Saw et al., 2012). Recognizing which pathway of the UPR provides protection or causes damage can lead to a more complete understanding of ER stress-mediated pathological mechanisms, including in CKD.

1.2.4 Progression of chronic kidney disease through endoplasmic reticulum stress³

CKD is often progressive and can result in a steady decline in the filtration capacity of the kidney. One result of severe CKD is uremia, which can be defined as the accumulation of waste products in the blood due to reduced renal filtration capacity or estimated GFR by at least 50% (Meyer & Hostetter, 2007). One nitrogenous waste product that has been found to accumulate in the blood of both human patients experiencing CKD and animal models of the disease is indoxyl sulfate (IS). IS is a nitrogen-containing organic anion that has been shown to interfere with organic anion transporters 1 and 3 in proximal and distal tubules, accumulate in the tubular epithelium, and hasten the progression of CKD in the 5/6-nephrectomized rat model (Enomoto et al., 2002). Further study into the mechanism by which IS accumulation in proximal tubules leads to the progression of CKD has shown that IS induces the ER stress markers CHOP and ATF4 in the HK-2 proximal tubular cell model system, leading to a reduction in the proliferation of these cells (Kawakami et al., 2010). Although the doses of IS (2 to 5 mmol/L) are high in comparison with what would be expected in the plasma of uremic

³ This section has been adapted from: Dickhout, J. G., Carlisle, R. E., & Austin, R. C. (2011). Interrelationship between cardiac hypertrophy, heart failure, and chronic kidney disease: endoplasmic reticulum stress as a mediator of pathogenesis. *Circ Res*, *108*(5), 629-642.

patients (250 $\mu\text{mol/L}$), they also demonstrate that IS treatment in HK-2 human proximal tubular cells had additive effects when combined with another uremic toxin, indoleacetic acid, to induce ER stress (Kawakami et al., 2010). Thus, the effects of an array of uremic toxins may act additively to induce ER stress and reduce the ability of the proximal tubule to regenerate, contributing to the progressive decline found in severe CKD associated with uremia.

Proteinuria is also a frequent complication of CKD and may result from a breakdown of the glomerular filtration barrier. Proteinuria itself, or in combination with high glucose as a model of diabetic nephropathy, induced ER stress in the HK-2 cell line (Lindenmeyer et al., 2008). In an animal model of streptozotocin-induced diabetes in C57BL/6 mice, ER stress developed and was associated with severe nephropathy at 22 months and CHOP upregulation (Wu et al., 2010b). Furthermore, in patients with nephrotic syndrome, including those with a diagnosis of minimal change disease, IgA nephropathy, primary mesangial proliferative glomerulonephritis, and membranous nephropathy, immunohistochemical staining showed an increase in staining for the molecular chaperones GRP78 and ORP150 in comparison to controls (Wu et al., 2010c). CHOP expression was also increased and showed nuclear localization in the proximal tubule epithelium of nephrotic patients. Human kidney cells exposed to human serum albumin overload showed ER stress induction and CHOP-mediated apoptosis (Wu et al., 2010c). These findings show the importance of ER stress in CKD induced by a number of primary pathologies (Dickhout et al., 2011b).

1.2.5 Endoplasmic reticulum stress and epithelial-to-mesenchymal transition

In recent years, the term EMT has been criticized as being a flawed concept, with much debate over whether this phenomenon has a significant effect *in vivo* or even if it actually occurs. There is substantial literature demonstrating EMT *in vitro*, but opinions and results differ when discussing the possibility of EMT causing fibrosis *in vivo*. This is particularly true for the pathogenesis of renal fibrosis, with some researchers hypothesizing that, in the kidney, myofibroblasts are derived from perivascular pericytes (Humphreys et al., 2010) and fibrocytes (Sakai et al., 2006), and not epithelial cells. However, recent lineage tracing studies have provided direct evidence confirming epithelial origin of at least part of the myofibroblast population in renal fibrosis (Higgins et al., 2007a; Iwano et al., 2002a; Zeisberg et al., 2008a). EMT has been demonstrated in mice, using unilateral ureteral obstruction (UUO) as a model of renal interstitial fibrosis (Iwano et al., 2002a). By genetically tagging the renal epithelium with LacZ, fibroblasts expressing type I collagen were derived from both the bone marrow and tubular epithelium of mice (Iwano et al., 2002a). While phenotypic changes have been observed in humans, migration of epithelial cells into the interstitium has not been found. Despite the lack of migration in humans, the epithelial cells do undergo a phenotypic change, which can, in itself, induce signals to initiate interstitial fibrosis (Farris & Colvin, 2012).

ER stress can lead to fibrosis; by preventing proteins from reaching their correct tertiary structure, they are unable to properly function within the cell, which may induce the transition from an epithelial cell phenotype to a fibroblast-like phenotype, through EMT (Pallet et al., 2008a; Prunotto et al., 2010). This procedure is typified by the displacement of F-actin filaments from the periphery of the cell to the cytoplasm, reduced

cell-cell junctions, increased cellular mobility, and a change in cell shape, from the cuboidal shape of an epithelial cell to the elongated shape of a fibroblast (Cannito et al., 2010). Consequently, important epithelial junctional proteins are reduced (such as E-cadherin (Liu, 2010a)), or translocated (such as β -catenin (Dickhout et al., 2016)), while expression of myofibroblast proteins is increased (such as α -smooth muscle actin (El-Nahas, 2003)). Adherens junctions between epithelial cells are formed by E-cadherin and β -catenin interactions with the actin cytoskeleton. β -catenin chauffeurs E-cadherin from the ER to the plasma membrane (Chen et al., 1999), suggesting that ER stress may impede this junctional complex, leading to epithelial cell disjunction and subsequent phenotypic change. Therefore, ER stress-mediated kidney injury may lead to EMT in renal proximal tubule cells through retention of junctional proteins in the ER (Dickhout et al., 2016).

It should be noted that chapter 2 and chapter 6 use the term ‘EMT’ extensively. In this case, EMT refers to the phenotypic change that occurs, and not necessarily to the cell-type transition from epithelial cell to fibroblast and subsequent migration of the cell.

1.3 ANIMAL MODELS OF KIDNEY DISEASE

1.3.1 Tunicamycin: an acquired model of intrinsic acute kidney injury induced by endoplasmic reticulum stress⁴

Tunicamycin is the most common agent used to study the effects of nucleoside antibiotics on the kidney. It is also commonly used *in vitro* to study the effects of ER stress in various cell types (Bassik & Kampmann, 2011). Tunicamycin inhibits protein glycosylation, resulting in vacuolization of the renal tubular epithelium and acute tubular necrosis (Carlisle et al., 2014). Tunicamycin is typically administered intraperitoneally at a dose of 0.5-1 mg/kg for 3 days (Carlisle et al., 2014; Marciniak et al., 2004). The principal area of renal damage caused by tunicamycin occurs in the corticomedullary region of the kidney (Carlisle et al., 2014).

By inhibiting N-linked glycosylation, tunicamycin induces ER stress, including increased GRP78, and the pro-apoptotic protein CHOP. CHOP is upregulated specifically in proximal tubular cells (Carlisle et al., 2014). CHOP knockout mice and mice with mutant GADD34 are resistant to tunicamycin-mediated renal damage (Carlisle et al., 2014; Marciniak et al., 2004), suggesting ER stress-mediated apoptosis is the primary mechanism of renal damage. Male and female mice have different responses to tunicamycin; female mice are more susceptible to damage in the S3 segment of the proximal tubule, while male mice, and female mice pre-treated with testosterone, are

⁴ This section has been adapted from the following book chapter, with permission from Elsevier Publishing Group: Mohammed-Ali Z*, Carlisle RE*, Nademi S, Dickhout JG. (2017) Animal models of kidney disease. In “*Animal models for the study of human disease.*” 2nd edition, Michael Conn. Elsevier Publishing Group, Academic Press.

*, Both authors contributed equally to this work.

more susceptible to damage in the outer cortex (S1 and S2 segments). Female mice also demonstrate reduced expression of ER stress markers and pro-apoptotic markers (Hodeify et al., 2013). While limited studies have been performed on tunicamycin and renal inflammation, it has been noted that knockout of the inflammatory cytokine TNF- α or its receptor TNF- α -R1 results in increased sensitivity to tunicamycin-mediated ER stress and renal injury (Huang et al., 2011). While it is unknown if tunicamycin induces a fibrotic response, it is a likely outcome, as ER stress tends to facilitate the development of fibrosis (Tanjore et al., 2013).

The tunicamycin model is useful in studying the direct effects of ER stress on the kidney; however, the effects in this model may differ significantly from major causes of acute kidney injury in the patient population, such as warm ischemia/reperfusion or sepsis.

1.3.2 The spontaneously hypertensive rat: a genetic model of essential hypertension

The spontaneously hypertensive rat (SHR) is the most widely used rat model to study hypertension and cardiovascular disease. Okamoto and colleagues developed this strain in the 1960s by selectively breeding Wistar Kyoto (WKY) rats with high blood pressure (Okamoto & Aoki, 1963). Thus, WKY rats are the accepted normotensive controls in studies using SHRs. SHRs develop hypertension at 5-6 weeks of age, with blood pressure stabilizing around 180-200 mmHg at 17-19 weeks (Bianchi et al., 1974; Dickhout & Lee, 1997b). While SHRs are largely salt resistant, renal pathology can be exacerbated by high salt diet (Yu et al., 1998). Cardiovascular disease and renal disease develop as the SHR ages, usually presenting around 40-50 weeks (Conrad et al., 1995; Feld et al., 1981;

Ofstad & Iversen, 2005), though GFR begins to decrease around 30 weeks (Reckelhoff et al., 1997). SHRs typically develop vascular and cardiac hypertrophy, as well as glomerulosclerosis, renal interstitial fibrosis, intratubular protein cast formation, and proteinuria (Ofstad & Iversen, 2005; Reckelhoff et al., 1997). While SHRs suffer from mild renal disease, severe damage is prevented due to greater preglomerular vasoconstriction, which impedes potential excessive blood flow and subsequent glomerular hyperfiltration (Arendshorst & Beierwaltes, 1979; Kimura & Brenner, 1997).

1.3.3 The Dahl salt-sensitive rat: a genetic model of hypertensive proteinuric chronic kidney disease

The Dahl salt-sensitive (DSS) rat is an animal model that mimics salt sensitivity in humans. Hypertension and renal injury in this model develop in a similar manner as in patients with diabetic nephropathy, as well as hypertensive black Americans (a population susceptible to kidney failure) (Campese, 1994; Cowley & Roman, 1996; O'Bryan & Hostetter, 1997; Ritz & Orth, 1999). DSS rats develop hypertensive CKD when fed a high salt diet (4-8% NaCl). However, even when fed a normal salt diet (0.1-0.4% NaCl), these rats tend to have higher blood pressure and more renal damage than control rats (De Miguel et al., 2010; Hayakawa et al., 2010; Rapp & Dene, 1985; Yu et al., 1998). Renal damage consists of mesangial expansion, glomerulosclerosis, cortical and medullary intratubular protein cast formation, interstitial fibrosis, and inflammation. Further, urinary excretion of protein, albumin, and nephrin is higher in DSS rats fed a high salt diet (Hye Khan et al., 2013). Interestingly, kidneys of high salt diet-fed DSS rats demonstrate increased expression of ER stress genes (Hye Khan et al., 2013). Consomic DSS rats, in

which chromosome 13 is introgressed from normotensive Brown Norway rats, are typically used as control animals (SS.BN13) (Cowley et al., 2001b).

1.4 PROJECT RATIONALE, HYPOTHESIS, OBJECTIVES, AND THESIS OUTLINE

1.4.1 Project rationale and hypothesis

The overall objective of this thesis is to determine if inhibiting ER stress prevents hypertensive CKD, and through what mechanism(s) this is achieved.

Fibrosis is a major factor in the progression of CKD, and ER stress can play a role in the development of fibrosis (Tanjore et al., 2013). In support, the development of fibrosis and the expression of fibrotic markers are prevented by inhibiting ER stress (Pallet et al., 2008a). TDAG51 is a translational regulator that is induced with ER stress (Dickhout et al., 2005; Hossain et al., 2003a); its expression results in cell shape change and decreased cell adhesion, resulting in anoikis (Hossain et al., 2003a). Thus, we hypothesized that the ER stress protein TDAG51 induces renal proximal tubular epithelial cell plasticity, resulting in a mesenchymal phenotype *in vitro*, leading to fibrosis.

Tunicamycin is frequently used as a nephrotoxic model of ER stress-induced intrinsic acute kidney injury (Marciniak et al., 2004). The nephrotoxic effects of tunicamycin are reduced in CHOP knockout and GADD34 mutant mice (Marciniak et al., 2004), suggesting a role for ER stress in this model of kidney injury. We therefore hypothesized that pharmacologically inhibiting ER stress in the kidney, using 4- PBA delivered at a dose of 1 g/kg/day orally, prevents structural damage to the kidney.

LWCCs, including 4-PBA, have been shown to reduce blood pressure in hypertensive mice (Kassan et al., 2012) and rats (Spitler & Webb, 2014). It is apparent that ER stress plays a role in the development of hypertension, however, a mechanism elucidating the blood pressure reduction effects of LWCCs is lacking. Given these data, we hypothesized that orally available 4-PBA can prevent structural vessel alterations and inhibit ER stress in resistance vessels in animal models of essential hypertension.

ER stress can lead to activation of the UPR, and is activated in nephrons of animals and humans with proteinuric nephropathy (Lindenmeyer et al., 2008). Treatment with the LWCC 4-PBA can prevent ER stress-mediated renal damage by inhibiting the UPR, and contractility studies indicate that inhibiting ER stress with 4-PBA can improve endothelial-dependent relaxation in mesenteric resistance arteries. Based on this knowledge, we further hypothesized that inhibiting ER stress with 4-PBA can reduce hypertensive nephrosclerosis more effectively than lowering blood pressure alone.

In summary, the hypothesis of my PhD research consists of four layers: 1) renal fibrosis is mediated by ER stress-induced TADG51, 2) 4-PBA is capable of inhibiting ER stress in the kidney when delivered orally, 3) ER stress inhibition reduces hypertension and prevents blood vessel dysfunction, and 4) preserving the myogenic response through ER stress inhibition, and not simply lowering blood pressure, is essential in preventing hypertensive CKD.

1.4.2 Objectives and experimental approach

To investigate this hypothesis, research was focused on the examination of the following objectives:

1. Examine the role of the ER stress protein TDAG51 in the development of renal fibrosis and tubular epithelial cell apoptosis.
2. Determine if inhibiting protein aggregation will prevent ER stress-mediated kidney damage.
3. Define mechanisms by which ER stress induces hypertension.
4. Compare the effects of ER stress inhibition and blood pressure lowering alone on end organ damage and blood pressure reduction.

In order to investigate the hypothesis of this thesis, *in vitro*, *in vivo*, and *ex vivo* experiments were performed.

Human proximal tubular cells (both primary and immortalized) and primary vascular smooth muscle cells were used when appropriate. Immortalized human proximal tubular (HK-2) cells were primarily used throughout experimentation. These cells were produced by transduction of HPV 16 E6/E7 genes into primary proximal tubular cells from a normal adult human renal cortex (Ryan et al., 1994). Primary human proximal tubular cells are believed to be more biologically relevant than immortalized HK-2 cells, as they are isolated directly from tissue. However, they have a finite lifespan and are thus less practical for extended use. While experiments were primarily performed in HK-2 cells, results were corroborated in primary proximal tubular cells or *in vivo* models. Primary

vascular smooth muscle cells were derived from Sprague Dawley rat aortas. Sprague Dawley rats appear clinically normal, with no cardiovascular or renal disease ("Sprague Dawley outbred rat," 2017). Thus, vascular smooth muscle cells derived from these animals are unlikely to exhibit any unfavourable phenotypic traits.

C57BL/6 wild type mice were used, as were CHOP knockout and TDAG51 knockout mice. C57BL/6 wild type mice were used, as CHOP knockout and TDAG51 knockout mice are bred on the C57BL/6 background and, as such, they are considered an adequate control animal. SHR and DSS rats were used, along with their respective controls, WKY and SS.BN13 rats. SHRs were used as a model of essential hypertension without renal injury. As SHRs were bred from WKY rats with high blood pressure (Okamoto & Aoki, 1963), WKY rats were used as controls. DSS rats were used due to the phenotypic traits observed with salt ingestion, including hypertension, decreased renal function, proteinuria, and albuminuria (De Miguel et al., 2010; Hayakawa et al., 2010; Hye Khan et al., 2013; Rapp & Dene, 1985; Yu et al., 1998). These traits mimic effects seen in humans with salt sensitivity. SS.BN13 rat strain is a consomic strain that is 98% identical to DSS rats; a subset of genes on chromosome 13, including the renin gene, differ (Cowley et al., 2001b). All animals were purchased from Charles River or bred in-house at McMaster University, and all animal work was performed according to the McMaster University Animal Research Ethics Board guidelines.

Resistance arteries regulate blood pressure by contracting, thereby creating resistance to flow (Intengan & Schiffrin, 2000). Thus, resistance arteries were used to examine vascular functionality and ER stress marker expression in animals with hypertension and/or renal damage. Resistance arteries were extracted from animals of interest;

mesenteric resistance arteries were used from WKY rats and SHRs, while renal arcuate resistance arteries were used from Sprague Dawley and DSS rats.

1.4.3 Thesis outline

The thesis objectives are explored in four manuscripts (chapters 2, 3, 4, and 5), and are presented as follows:

Chapter 2: TDAG51 mediates epithelial-to-mesenchymal transition in human proximal tubular epithelium.

This journal article, published in *American Journal of Physiology Renal Physiology* (2012), was accepted for publication on May 8, 2012. This journal article demonstrates that the ER stress and pro-apoptotic protein TDAG51 mediates EMT in human proximal tubular epithelium.

Chapter 3: 4-phenylbutyrate inhibits tunicamycin-induced acute kidney injury via CHOP/GADD153 repression.

This journal article, published in *PLoS One* (2014), was accepted for publication on November 18, 2013. This journal article demonstrates that the LWCC 4-PBA is able to effectively inhibit ER stress in the kidney.

Chapter 4: Endoplasmic reticulum stress inhibition reduces hypertension through the preservation of resistance blood vessel structure and function.

This journal article, published in *Journal of Hypertension* (2016), was accepted for publication on April 1, 2016. This journal article describes how ER stress inhibition reduces blood pressure and prevents blood vessel dysfunction.

Chapter 5: Endoplasmic reticulum stress inhibition limits the progression of chronic kidney disease in the Dahl salt-sensitive rat.

This journal article, published in *American Journal of Physiology Renal Physiology* (2017), was accepted for publication on November 7, 2016. This journal article provides evidence that inhibiting ER stress with 4-PBA can protect the kidney from damage more effectively than lowering blood pressure alone.

CHAPTER 2

TDAG51 mediates epithelial-to-mesenchymal transition in human proximal tubular epithelium

Rachel E. Carlisle, Alana Heffernan, Elise Brimble, Limin Liu, Danielle Jerome, Celeste A. Collins, Zahraa Mohammed-Ali, Peter J. Margetts, Richard C. Austin, Jeffrey G. Dickhout

American Journal of Physiology Renal Physiology (2012). 303(3):F467-481. Doi: 10.1152/ajprenal.00481.2011.

© Copyright by *The American Physiological Society*

Chapter link:

The ER stress protein TDAG51 mediates EMT in proximal tubular cells and plays a role in TGF- β 1-induced peritoneal fibrosis. Fibrosis is a major factor in the progression of CKD, and ER stress can play a role in the development of fibrosis (Tanjore et al., 2013). In fact, the development of fibrosis and the expression of fibrotic markers are prevented by inhibiting ER stress (Pallet et al., 2008). TDAG51 is a translational regulator that is induced with ER stress (Dickhout et al., 2005; Hossain et al., 2003); its expression results in cell shape change and decreased cell adhesion, resulting in anoikis (detachment-mediated apoptosis) (Hossain et al., 2003). This paper demonstrates that ER stress induces renal proximal tubular epithelial cell plasticity, resulting in a mesenchymal phenotype *in vitro*. Further, absence of the TDAG51 protein can prevent TGF- β 1-mediated peritoneal fibrosis.

Author's contribution:

R.E. Carlisle and J.G. Dickhout designed the study. R.E. Carlisle performed cell culture experiments, western blotting, fluorescent staining, and related analyses with help from E. Brimble. D. Jerome performed cytosolic Ca²⁺ experiments. A. Heffernan and C.A. Collins performed cellular transfection experiments. L. Liu conducted the animal studies, and collected and analysed tissues. R.E. Carlisle wrote and revised the manuscript. Z. Mohammed-Ali helped revise the manuscript. R.E. Carlisle, P.J. Margetts, R.C. Austin, and J.G. Dickhout reviewed and edited the manuscript. All authors approved of the final submission.

Running title: TDAG51-mediated EMT

TDAG51 mediates epithelial-to-mesenchymal transition in human proximal tubular epithelium.

Rachel E. Carlisle¹, Alana Heffernan¹, Elise Brimble¹, Limin Liu¹, Danielle Jerome¹, Celeste A. Collins¹, Zahraa Mohammed-Ali¹, Peter J. Margetts¹, Richard C. Austin¹ and Jeffrey G. Dickhout¹.

¹Department of Medicine, Division of Nephrology, McMaster University and St. Joseph's Healthcare Hamilton, Hamilton, Ontario, Canada.

Address correspondence to:

Jeffrey G. Dickhout, PhD
Department of Medicine, Division of Nephrology
McMaster University and St. Joseph's Healthcare Hamilton
50 Charlton Avenue East
Hamilton, Ontario, Canada, L8N 4A6
Phone: 905-522-1155 ext. 35334
Fax: 905-540-6589
Email: jdickhou@stjosham.on.ca

Key words: chronic kidney disease, fibrosis, TGF β 1, endoplasmic reticulum stress, β -catenin

ABSTRACT

Epithelial-to-mesenchymal transition (EMT) contributes to renal fibrosis in chronic kidney disease. Endoplasmic reticulum (ER) stress, a feature of many forms of kidney disease, results from the accumulation of misfolded proteins in the ER and leads to the unfolded protein response (UPR). We hypothesized that ER stress mediates EMT in human renal proximal tubules. ER stress is induced by a variety of stressors differing in their mechanism of action, including tunicamycin, thapsigargin and the calcineurin inhibitor, cyclosporine A. These ER stressors increased the UPR markers GRP78, GRP94, and phospho-eIF2 α in human proximal tubular cells. Thapsigargin and cyclosporine A also increased cytosolic [Ca²⁺] and T-cell death associated gene 51 (TDAG51) expression, whereas tunicamycin did not. Thapsigargin was also shown to increase levels of active TGF β 1 in the media of cultured human proximal tubular cells. Thapsigargin induced cytoskeletal rearrangement, β -catenin nuclear translocation, and α -smooth muscle actin and vinculin expression in proximal tubular cells, indicating an EMT response. Subconfluent primary human proximal tubular cells were induced to undergo EMT by TGF β 1 treatment. In contrast, tunicamycin treatment did not produce an EMT response. Plasmid-mediated overexpression of TDAG51 resulted in cell shape change and β -catenin nuclear translocation. These results allowed us to develop a two-hit model of ER stress-induced EMT, where Ca²⁺ dysregulation-mediated TDAG51 upregulation primes the cell for mesenchymal transformation via Wnt signalling and then TGF β 1 activation leads to a complete EMT response. Thus, the release of Ca²⁺ from ER stores mediates EMT in human proximal tubular epithelium via the induction of TDAG51.

INTRODUCTION

Chronic kidney disease (CKD) is a major contributor to morbidity and mortality with an estimated prevalence of 11% in the United States (9). However, many individuals who have early stage CKD are asymptomatic. There are many risk factors for the progression of CKD, including hypertension (18), proteinuria (8, 34), and poor glucose control in diabetes (35). Features of CKD progression remain consistent regardless of cause, including declining glomerular filtration rate, peritubular capillary loss resulting in tubular ischemia, and interstitial fibrosis (42). It has been suggested that epithelial to mesenchymal transition (EMT) is not a source of fibroblasts in renal fibrosis (55), however, recent lineage studies have provided direct evidence proving epithelial cell involvement in producing the fibroblasts found in renal interstitial fibrosis (29, 33, 54). EMT can cause interstitial fibrosis by transition of the tubular epithelium to collagen-producing fibroblasts (33). When the basement membrane is altered or damaged, the epithelium expresses cytokines, such as TGF β , that promote EMT (33). TGF β 1 is an important mediator of EMT (37), however, it is becoming clear that epithelial adherens junction detachment primes the cell for the TGF β 1 effect (39). The transformation from an epithelial to mesenchymal phenotype results in local formation of fibroblasts. When this occurs, epithelial cells decrease the expression of typical epithelial cell proteins such as E-cadherin, show β -catenin cytoplasmic to nuclear translocation, and express mesenchymal proteins, such as type I collagen, and vimentin (7, 37). This can occur via Wnt/ β -catenin signalling. Wnt/ β -catenin signalling is activated when β -catenin is released from its E-cadherin anchor in epithelial cell adherens junctions, and accumulates in the

cytoplasm. The β -catenin/TCF/LEF complex is then formed, and translocated to the nucleus, resulting in the upregulation of specific genes, such as fibronectin, vimentin, matrilysin, and SNAI2 (7).

Recent studies have shown that endoplasmic reticulum (ER) stress is a common feature of CKD of diverse etiology (12, 15). When there is a disruption in the protein folding process, ER stress occurs (49). Transmembrane, ER luminal resident, and secretory proteins are synthesized in the ER, including proximal tubular cell transporter proteins such as the Na^+/K^+ ATPase that are critical for the reabsorption of ultrafiltrate components (1, 15). ER stress activates the unfolded protein response (UPR), thereby leading to the phosphorylation of eIF2 α and inhibition of general translation (12). The drug salubrinal (Sal) is a selective inhibitor of the dephosphorylation of eIF2 α that protects from ER stress. Its mode of action involves the reduced formation of the PP1/GADD34 dephosphatase complex. This has been demonstrated by the inhibition of ER stress-mediated apoptosis induced by tunicamycin (Tm) in PC12 cells (6). Sal has also been shown to protect against cyclosporine A (CsA)-induced nephrotoxicity, which may involve ER stress (44).

We have previously reported that T-cell death associated gene 51 (TDAG51), also known as the pleckstrin homology-like domain (PHLD), family A member 1 protein, is induced by certain ER stressors, including peroxynitrite, which inhibits the sarco/endoplasmic reticulum Ca^{2+} ATPase (SERCA) (14, 31). Others have shown that the ER stress inducer farnesol causes TDAG51 upregulation through the MEK/ERK/MAPK pathway (36). Initially, it was determined that TDAG51 is necessary for Fas-induced apoptotic cell death in T-cells (45). However, TDAG51 knockout in the whole animal did

not prevent the induction of T-cell apoptosis (47). Subsequently, it was demonstrated that TDAG51 has significant homology to a tumour suppressor gene, *Ipl/Tssc3* (21). We previously demonstrated that overexpression of TDAG51 leads to cell shape change and decreased cell adhesion, resulting in anoikis (detachment-mediated apoptosis), in human vascular endothelium (31). The mechanism by which TDAG51 generates cell shape change may be related to its colocalization with focal adhesion kinase in focal adhesions (31). Additionally, TDAG51 contains proline-histidine and proline-glutamine repeat sequences similar to apoptotic promoting genes (25), transcriptional activators (45), and a pleckstrin homology-like domain similar to proteins regulating cytoskeletal function (27, 32). Further, it has been confirmed by the human protein atlas that human renal proximal tubular epithelial cells (hRPTEC) express a moderate amount of the TDAG51 protein (4).

Since EMT and ER stress are both important in the pathology of CKD, we hypothesized that EMT can result from Ca^{2+} dysregulation-induced ER stress, and is mediated by TDAG51 upregulation. Different ER stress inducers were utilized to determine if ER stress results in hRPTEC EMT. Treatment with ER stress inducers, Tg and CsA, which generated Ca^{2+} dysregulation-induced ER stress and TDAG51 overexpression, resulted in EMT. Sal, an inhibitor of TDAG51 overexpression during Tg-mediated ER stress, inhibited the EMT response. This response was also inhibited by buffering Ca^{2+} with the intracellular Ca^{2+} chelator BAPTA-AM. Further, TDAG51 overexpression was found to induce proximal tubular cell shape change and the disruption of epithelial cell junctions, priming the proximal tubular cells for EMT. Moreover, TDAG51 knockout in the whole animal inhibited TGF β 1-induced peritoneal fibrosis, a

response involving mesothelial cell EMT. Taken together, our findings provide evidence that TDAG51 is a novel mediator of EMT.

METHODS

Cell culture

hRPTECs (passage 2 – 5; Lonza; Walkersville, MD) were cultured on cover slips in REBM containing 0.5 ml hEGF, 0.5 ml hydrocortisone, 0.5 ml epinephrine, 0.5 ml insulin, 0.5 ml triiodothyronine, 0.5 ml transferrin, 0.5 ml GA-1000, 2.5 ml fetal bovine serum SingleQuots per 500 ml of medium (Lonza), as indicated by the manufacturer. HK-2 cells were cultured in a 1:1 ratio of DMEM 1 g/L glucose media (Invitrogen; Carlsbad, CA) and F12 GlutaMAX nutrient mix (Invitrogen). Twenty-four hours prior to experiments, HK-2 cells were transferred into DMEM medium containing 4.5 g/L glucose (Invitrogen), unless otherwise stated.

Reagents

Tm, Tg, CsA and DAPI were purchased from Sigma-Aldrich (St. Louis, MO). Sal was purchased from CalBioChem (EMD; Gibbstown, NJ). Recombinant human TGF β 1 was purchased from R&D systems (Minneapolis, MN), and activated according to the manufacturer's instructions. Non-water soluble reagents were dissolved in DMSO (Sigma-Aldrich) as a transitional solvent and DMSO was used as a vehicle control. Rhodamine phalloidin, Fura-2-AM and BAPTA-AM were purchased from Invitrogen. Paraformaldehyde was obtained as a 4% solution in PBS (BioLynx Inc; Brockville, Canada).

Gel electrophoresis

Total cell lysates were generated in 4X SDS lysis buffer with protease inhibitor cocktail added (complete Mini; Roche; Laval, Canada). Protein levels were determined using BioRad DC Protein Assay for control of protein loading. Cell lysates were subjected to electrophoretic separation in a 10% SDS-PAGE reducing gel (BioRad).

Quantitative analysis of protein expression

Primary antibodies were detected using appropriate horseradish peroxidase-conjugated secondary antibodies and ECL Western Blotting Detection Reagents (GE Healthcare; Mississauga, Canada), as previously (31). Results were densitometrically quantified using ImageJ software (NIH, Bethesda, MD, ver. 1.43) and expressed as a ratio of β -actin loading control, unless otherwise stated, for blots developed on X-ray film.

Protein expression was quantified using quantum dots for fluorescence detection. To achieve this, low fluorescence PVDF membranes (Immobilon-FL, Millipore; Billerica, MA) were blocked in WesternDot blocking buffer (Invitrogen). Membranes were incubated with primary antibodies for β -actin (A-5316, 1:5000; Sigma), TDAG51 (sc-23866, 1:200; Santa Cruz, CA), phospho-eIF2 α (97215, 1:1000; Cell Signaling, Danvers, MA), eIF2 α (sc-11386, 1:200; Santa Cruz) or KDEL, which detects both GRP78 and GRP94 (SPA-827, 1:1000; Stressgen, Enzo Life Sciences; Plymouth Meeting, PA). Subsequently, membranes were incubated with biotinylated secondary antibodies (Biotin-XX-Goat anti-mouse, 1:2000) and then Qdot 625 streptavidin conjugate (1:2000). Qdot

conjugates were used no more than three times. Membranes were imaged using a BioRad ChemiDoc XRS+ through a specific filter 630BP30 and results were densitometrically quantified using Image Lab software version 2.0 (BioRad), where the signal for the primary antibody was expressed as a ratio of the β -actin loading control, as previously (12).

Fluorescence microscopy

An Olympus IX81 Nipkow scanning disc confocal microscope was used for fluorescence microscopy. Living cells were imaged in white light using differential interference contrast. HK-2 or hRPTECs were stained using anti-GRP78 antibodies (1:100, sc-1050; Santa Cruz), anti-TDAG51 antibodies (1:100, sc-23866; Santa Cruz), anti- β -catenin antibodies (1:200, #2677; Cell Signaling), anti- α -smooth muscle actin (α -SMA) antibodies (1:200, 1A4 clone; Thermo Scientific, Nepean, Canada) or anti-vinculin antibodies (1:100, V4505; Sigma). This was followed by the addition of a species-specific secondary antibody conjugated to an Alexa dye at 488 nm or 594 nm excitation (1:200; Invitrogen, Molecular Probes). The DNA specific dye, 4',6-diamidino-2-phenylindole (DAPI) was used to label the nuclei of cells. Permafluor (Thermo Scientific) was used to mount the cover slips on microscope slides. Individual wavelengths for fluorophore excitation were as follows: DAPI: 377 nm/50 nm bandpass; Alexa488: 482 nm/35 nm bandpass; Alexa594: 562 nm/40 nm bandpass.

Cytosolic Ca²⁺ measurements

Cytosolic Ca²⁺ measurements were performed as previously described (16). Briefly, the Fura-2-AM Ca²⁺-sensitive dye was used to measure cytosolic Ca²⁺ concentrations as a ratio of the fluorescent signal stimulated by 340 (dye bound to Ca²⁺) or 380 (free dye) nm excitation with emission collected at 510 nm on a SpectraMax Gemini spectrofluorometer (Molecular Devices). This was accomplished in cell populations of HK-2 cells cultured in 96-well plates (BD-Falcon, Black/Clear bottom, Optilux), maintained at 37°C in Hanks' balanced salt solution (Invitrogen) containing 20 mM HEPES buffer at pH 7.4.

Construction and transfection of expression plasmids

TDAG51 cDNA was amplified via PCR and subsequently digested using the restriction enzymes *HindIII* and *XbaI*. Following digestion, the cDNA was then cloned into an eGFP (Clontech, Mountain View, CA) vector creating a plasmid where the green fluorescent protein was linked to TDAG51 protein (termed eGFP-TDAG51), as previously described (31). The PHLD-GFP fusion protein was generated using an eGFP-C1 plasmid (Clontech). TDAG51 cDNA encoding the PHLD amino acid (aa) sequence (10- LKEGVLEKRS DGLLQLWKKK CCILTEEGLL LIPPKQLQHQ QQQQQQQQQQ QQPGQGPAE PSQPSGPAVA SLEPPVKLKE LHFSNMKTVD CVERKGGKMYMY FTVVMAEGKE IDFRCPQDQG WNAEITLQMV QY-132 aa) was amplified by PCR prior to subcloning into a T-overhang pGEM-T vector (Promega). Primers were designed with *BglIII* and *KpnI* terminal restriction sites (*Fwd* 5' AGATCTCTGAAGGAGGGCGTG; *Rev* 5' GGTACCGTACTGCACCATCTGC AGC) and synthesized by Integrated DNA Technologies (Skokie, IL). The pGEM-T

transition vector containing the PHLD was digested with *BglII* and *KpnI*, and the PHLD fragment was purified by gel extraction prior to cloning into the *BglII/KpnI* sites of pEGFP-C1. Construct identity was confirmed by DNA sequencing (MOBIX, Hamilton, Canada). To replicate the plasmids, competent DH5 α bacteria were transformed and grown overnight on kanamycin-resistant agar plates. Single colonies were selected and placed into kanamycin selective LB broth and grown to the logarithmic growth phase. Plasmid-expressing bacteria were isolated using the EndoFree Plasmid Maxi Kit (Qiagen), as per the manufacturer's instructions. The amount and purity of plasmid recovered (which ranged between 1.8 and 1.9, as a 260/280 nm ratio) was determined by the SmartSpec 3000 (BioRad). HK-2 cells or hRPTECs were transfected with eGFP plasmid alone, as a control, or with the eGFP-TDAG51 plasmid using FuGENE 6 transfection reagent (Roche) at a 6:1 ratio. The transfection efficiency between eGFP and eGFP-TDAG51 ($29.7\% \pm 4.7$ vs. $25.3\% \pm 2.2$, respectively) did not differ significantly.

Treatment and staining of transfected cells

HK-2 cells and hRPTECs were fixed using 4% paraformaldehyde, permeabilized with 0.1% Triton-X (BioRad) in PBS and blocked for 30 minutes in 1% BSA. F-actin in the cytoskeleton was stained using rhodamine phalloidin (Invitrogen, Molecular Probes) and nuclei were counterstained using DAPI (100 ng/ml) for 30 minutes.

Measurement of TDAG51 effect on cell shape change

ImageJ software was used to measure the area and perimeter of eGFP- and eGFP-TDAG51-transfected HK-2 cells. These measurements were accomplished by selecting

the perimeter of eGFP- or eGFP-TDAG51-transfected HK-2 cells using ImageJ software, which then calculated the perimeter and area of each individual cell. Graphical and statistical analysis was performed using Microsoft Excel software.

Measurement of TGF β 1 by sandwich ELISA

The TGF β ELISA (R&D systems) was used to measure active TGF β levels in the conditioned media of HK-2 cells, as per the manufacturer's instructions. Cells were grown to confluence in 1:1 DMEM (Invitrogen) and F12 GlutaMAX nutrient mix (Invitrogen) (7.75 mM D-glucose) and were treated with drug vehicle DMSO or Tg (200 nM) for 24 h. The reaction for active TGF β 1 was developed with tetramethyl benzidine (Sigma-Aldrich). Absorbance was measured at 450 nm and the non-specific absorbance at 540 nm was used as a control on a VERSAmax microplate reader (Molecular Devices).

Animal studies

TDAG51^{-/-} mice on a C57BL/6 background were maintained in an in-house breeding colony at McMaster University and originally derived from mice obtained from the TDAG51^{-/-} colony developed by Rho et al (47). Six-week-old female TDAG51^{-/-} animals or C57BL/6 wild type control animals were injected in the peritoneum with an adenovirus containing the coding region for active TGF β 1 or AdDL control (empty/null) adenovirus (38), with five animals in each group. Previously, our group used a LacZ adenovirus to demonstrate that expression of β -galactosidase was limited to the mesothelial cells of the peritoneum, and was not observable in liver, spleen, skeletal muscle, or the

submesothelial interstitium (39). Ten days after injection, mice were euthanized and abdominal tissue was immediately fixed with 10% buffered formalin. Animals were maintained on a normal chow diet with free access to food and drinking water for the duration of the study. All procedures were in accordance with the guidelines of the McMaster University Animal Research Board.

Statistical analysis

Values are expressed as mean \pm the standard error of the mean. Statistical comparison between the means was accomplished in MiniTab software (Ver. 16, Microsoft). For multiple comparisons amongst means, analysis of variance was utilized with Tukey's correction for multiple comparisons. Significance was accepted at the 95% level.

RESULTS

Classical ER stressors and cyclosporine A induce the UPR and differentially affect TDAG51 protein expression.

Western blot analysis demonstrated a significant increase in the UPR marker GRP78 at 18 h in response to all ER stress inducers (Figure 1). TDAG51 protein levels were increased in response to the SERCA inhibitor, Tg, and the calcineurin inhibitor, CsA, but not the N-linked glycosylation inhibitor, Tm, in HK-2 cells at both 7 and 18 h (Figure 1) and primary hRPTECs at 18 h (data not shown). Treatment of cells with Tg or Tm was combined with Sal to determine whether dephosphorylation of eIF2 α alters the levels of

ER stress markers in HK-2 cells. However, Sal treatment did not reduce the expression of GRP78 or TDAG51 in HK-2 cells. To determine the effect of ER stress on cell shape change, HK-2 cells were treated with DMSO (vehicle), Tm or Tg. GRP78 (green) upregulation was observed for both Tm and Tg (Figure 2A), however, TDAG51 (green) levels were increased in response to Tg, but not Tm by indirect immunofluorescence (Figure 2B). This confirms the Western blotting results showing no change in Tm-treated cells and increased TDAG51 expression in Tg-treated cells (Figure 1). Unlike vehicle- and Tm-treated cells, Tg-treated cells showed a lack of F-actin (red) in the periphery as well as cellular elongation, indicative of EMT. CsA treatment also produced F-actin rearrangement and shape change indicative of EMT (Figure 2C), as shown in other studies (41, 44, 47, 51).

ER stress induction and inhibition of thapsigargin-induced TDAG51 up-regulation by salubrinal in HK-2 cells.

At 4 h, HK-2 cells showed an increase in phospho-eIF2 α in response to Tm, Sal, Tm plus Sal, Tg, and Tg plus Sal (Figure 3A). To determine the effect of Sal alone on TDAG51 expression, HK-2 cells were treated with Sal for 18 h. Treatment with Sal alone exhibited a significant decrease in TDAG51 levels (Figure 3B). Combined treatment with Tg plus Sal inhibited Tg-induced increases in TDAG51 expression at 48 h (Figure 3C). Thus, we used Sal to determine if it would inhibit EMT. Additionally, GRP78 expression was significantly increased in response to treatment with Sal alone for 18 h (Figure 3D).

Cytosolic β -catenin accumulation and nuclear translocation induced by thapsigargin leads to EMT.

To demonstrate the localization of β -catenin in response to ER stressors and Sal, proximal tubular cells were treated for 24 h and stained for β -catenin (Figure 4A). Primary hRPTECs show β -catenin staining around the periphery of the cell in response to vehicle, Tm, and Sal treatments. Cells treated with Tg showed an accumulation of β -catenin in the perinuclear and nuclear regions, with reduced β -catenin in the periphery of the cell. β -catenin staining was quantified, and shows that, unlike the other treatments, Tg-treated cells contained significantly more β -catenin in the nuclear and perinuclear area, and less β -catenin in the periphery of the cell (Figure 4A). This is indicated by a significant increase in the cytoplasmic-to-peripheral ratio of Tg treatment (2.37 ± 0.39) over vehicle (0.55 ± 0.08). Neither Sal (0.66 ± 0.06) nor Tm (0.67 ± 0.07) caused a significant change in this ratio, when compared with the vehicle. HK-2 cells were treated and stained as in (A), and similar results were obtained (data not shown; see supplemental video for 3-dimensional re-construction). To determine the effect of cadherin junction disruption on β -catenin staining, HK-2 cells were treated with the Ca^{2+} chelator EGTA for 18 h. EGTA treatment resulted in translocation of β -catenin (red) to the perinuclear and nuclear region, indicating Ca^{2+} -mediated cadherin disruption leads to β -catenin cytoplasmic to nuclear translocation. Tg-treated cells show β -catenin cytoplasmic to nuclear translocation as well, however, they developed a distinct fibroblast-like morphology (Figure 4B).

Ca²⁺ chelator prevents thapsigargin-mediated effects.

Cytosolic [Ca²⁺] was measured ratiometrically, to determine if treatment with various ER stressors resulted in Ca²⁺ disequilibrium, which is associated with epithelial junction disruption (39). Epithelial junction disruption, particularly the breaking of cadherin junctions, releases β-catenin from its anchorage on the plasma membrane, allowing it to accumulate in the cytoplasm and translocate to the nucleus (43). Tm treatment showed no change in cytosolic [Ca²⁺], while both Tg and CsA demonstrated significant increases in cytosolic [Ca²⁺] (Figure 5A). Since only ER stressors associated with Ca²⁺ disequilibrium resulted in TDAG51 upregulation, the intracellular Ca²⁺ chelator BAPTA-AM was used to inhibit cytosolic [Ca²⁺] increase and determine the effect on TDAG51 induction. HK-2 cells were treated with DMSO (vehicle), Tg (200 nM) or Tg with BAPTA-AM (100 μM). Cytosolic [Ca²⁺] was measured ratiometrically, to determine if co-treatment with BAPTA-AM would suppress Tg-mediated Ca²⁺ dysregulation. As expected, Tg treatment resulted in increased [Ca²⁺]. Co-treatment with BAPTA-AM prevented the Tg-mediated increase in cytosolic [Ca²⁺] (Figure 5B). HK-2 cells were treated with DMSO, Tg, or Tg with BAPTA-AM, for 18 h. Western blot analysis demonstrated that treatment with BAPTA-AM inhibited the Tg-mediated increase in GRP78 and TDAG51 expression (Figure 5C).

Mesenchymal marker up-regulation in response to thapsigargin- and TGFβ1-induced EMT.

Increased expression of α -SMA and vinculin are markers of EMT, and are induced by factors such as TGF β 1 (3, 37). After HK-2 cells were treated with DMSO (vehicle) or Tg (200 nM) for 24 h, active TGF β 1 was measured from the supernatant. Tg was found to cause a significant increase in the activation of TGF β 1 (Figure 6A). HK-2 cells were then treated for 48 h with vehicle, Tg or Tg plus Sal, and subsequently stained for F-actin and α -SMA (Figure 6B) or vinculin (Figure 6C). Most Tg-treated cells demonstrated an increase in α -SMA, decreased peripheral F-actin staining, and the formation of stress fibres, indicative of a fibroblastic phenotype (Figure 6B). HK-2 cells treated with Tg plus Sal showed less α -SMA expression and maintained an epithelial morphology, compared with Tg alone-treated cells. This indicates the eIF2 α dephosphorylation inhibitor Sal partially prevents the progression of Tg-induced EMT (Figure 6B), as well as TDAG51 expression at 48 h (Figure 3C). Tg-treated cells show vinculin induction, another marker of EMT (7), which is inhibited by Sal (Figure 6C). To establish that TGF β 1 induces EMT in subconfluent primary hRPTECs, cells were treated with 1 or 5 ng/mL of human recombinant TGF β 1. Immunofluorescent staining determined both doses of TGF β 1 induced an EMT response in these cells, as shown by changes in cell phenotype and increased expression of α -SMA (Figure 6D).

TDAG51 overexpression associated with epithelial phenotypic changes.

To assess the phenotypic changes associated with TDAG51 expression, TDAG51 was overexpressed in HK-2 cells (Figure 7). HK-2 cells were transfected with the expression plasmids for eGFP (Figure 7A) or eGFP-TDAG51 fusion protein expression

(Figure 7B) for 48 h. Rounded up and detached cells were observed after eGFP-TDAG51 transfection, but not eGFP transfection. eGFP-TDAG51-transfected cells had a significantly lower area (Figure 7C) and perimeter (Figure 7D), indicative of shape change. To determine if eGFP-TDAG51 resulted in apoptotic cell death, eGFP- (Figure 7E) and eGFP-TDAG51-transfected cells (Figure 7F) were stained with TUNEL. Statistical analysis determined that eGFP-TDAG51 transfection resulted in significantly more apoptosis than eGFP transfection (Figure 7G). It was demonstrated using F-actin and GFP staining that cells transfected with eGFP did not undergo shape change or F-actin rearrangement (Figure 7H), while eGFP-TDAG51 transfected cells appeared rounded up (Figure 7I) or elongated (Figure 7J), breaking epithelial adherens junctions. Cells transfected with the PHLD of TDAG51 underwent shape change and β -catenin disruption. This indicates that the PHLD of TDAG51 may be the structural motif of the protein that causes cellular shape change, adherens junction dissolution, β -catenin nuclear translocation, and EMT induction.

TDAG51 deficiency inhibits TGF β 1-mediated peritoneal fibrosis *in vivo*.

To determine if TDAG51 mediates EMT in the whole animal, the TGF β 1 adenovirus-induced model of EMT was utilized (38) (Figure 8). In order to determine the effect of TDAG51 on peritoneal fibrosis, C57BL/6 wild type and TDAG51^{-/-} mice were treated with a control vector (AdDL) or TGF β 1 adenovirus (AdTGF β 1). Untreated C57BL/6 wild type mouse parietal peritoneum is illustrated as a comparison to viral treated mice. After treatment with the AdTGF β 1, submesothelial thickness of the parietal

peritoneum from the anterior abdominal wall was measured. Results indicate that wild type mice were significantly more fibrotic than TDAG51^{-/-} mice, suggesting that TDAG51 plays a role in EMT-mediated fibrosis in the whole animal.

DISCUSSION

Tubulointerstitial fibrosis is a common factor in the progression of CKD, caused by a variety of renal pathologies (40, 55). Fibroblast accumulation leading to tubulointerstitial fibrosis is partly derived from epithelial cells comprising the proximal tubule modified through a process of EMT. There are three types of EMT: type 1, EMT in embryogenesis; type 2, EMT in organ fibrosis; and type 3, EMT in cancer progression and metastasis. Type 2 EMT, under conditions of chronic organ injury, contributes to organ fibrosis (7). Organ fibrosis is mediated by fibroblasts and myofibroblasts. Although some debate exists whether EMT is a source of fibroblasts in renal fibrosis (55), recent lineage tracing studies have provided direct evidence (29, 33, 54). EMT involves the cells losing epithelial adhesions, expressing stress fibres and α -SMA, and producing extracellular matrix components, including type I collagen (17). Additionally, focal adhesion proteins, such as vinculin, are expressed in human renal tubular epithelial cells in response to CsA-induced EMT (44). Vinculin facilitates cell spreading and lamellipodia formation (24). ER stress appears to be an important feature of CKD (10, 12, 15), including as a response to proteinuria (11). Loss of the epithelial cell phenotype involves cytoskeletal rearrangement and changes in cell adhesion, both of which are effects mediated by TDAG51. Thus, we tested whether ER stress induces EMT through TDAG51 expression.

We found that Tm, Tg, and CsA induced a UPR response, indicative of ER stress, in hRPTECs. Tm prevents the synthesis of N-linked glycoproteins, Tg blocks the SERCA pump, and CsA inhibits calcineurin, a Ca^{2+} -activated phosphatase; each of these different actions causes ER stress. However, only Tg and CsA elicited an increase in the expression of TDAG51, a protein previously shown to be induced by Ca^{2+} disequilibrium-mediated ER stress (14, 30). This suggests a Ca^{2+} -mediated mechanism, as treatment with Tg and CsA (but not Tm) resulted in increased intracellular $[\text{Ca}^{2+}]$. Additionally, in cells co-treated with Tg and the Ca^{2+} chelator BAPTA-AM, BAPTA-AM prevented ER stress, as shown by the inhibition of GRP78 upregulation and TDAG51 overexpression. Taken together, these data indicate that Ca^{2+} -mediated ER stress results in TDAG51 overexpression in HK-2 cells. Tg-induced TDAG51 expression was associated with hRPTEC shape change, indicative of EMT, whereas Tm did not induce TDAG51 expression or result in shape change. Treatment with the ER stress inhibitor Sal reduced TDAG51 expression at 18 h in non-stressed cells and inhibited Tg-induced TDAG51 expression and EMT at 48 h. It should be noted, however, that Sal did not inhibit Tg-induced TDAG51 expression at 18 h. This effect may be related to the ability of Sal to increase GRP78 expression at 18 h and the action of GRP78 as a Ca^{2+} -binding ER luminal protein. We have demonstrated that TDAG51 expression is dependent on ER Ca^{2+} disruption, as shown by our BAPTA-AM results. Further, GRP78 overexpression has been shown to retain ER Ca^{2+} (16). This may have caused Sal to act much like BAPTA-AM to buffer the ER Ca^{2+} disruption induced by Tg and thus TDAG51 overexpression. However, this effect shows time dependence due to the time required for Sal to induce new GRP78 protein synthesis.

Tg also caused disruption of epithelial junctions, shown by β -catenin cytoplasmic to nuclear translocation. Transient overexpression of TDAG51 directly caused hRPTEC shape change and β -catenin translocation in HK-2 cells. TDAG51 contains a PHLD, which is found in proteins that are targeted to the membrane and interact with the cytoskeleton (27). This is the structural motif in the TDAG51 protein that may cause hRPTEC shape change and β -catenin signalling. To test this hypothesis, we constructed an expression plasmid containing the PHLD of TDAG51 in a GFP fusion protein to track its subcellular localization and its effect on hRPTEC shape change. It appears that the PHLD domain of TDAG51 interacts with the cytoskeleton and induces hRPTEC shape change. Thus, this seems the region in the TDAG51 protein that induces cell shape change and initiates the canonical Wnt/ β -catenin signalling pathway.

One important form of kidney disease associated with tubulointerstitial fibrosis is CsA-induced nephropathy. CsA-induced nephropathy consists of an early and a late phase. The acute phase is mediated by increased levels of endothelin and angiotensin II and reduced nitric oxide bio-availability (19). This leads to increased vascular resistance, and decreased renal blood flow and glomerular filtration rate. The chronic phase is mediated by TGF β , platelet derived growth factor, fibroblast growth factor and tumour necrosis factor alpha (19), and can be diagnosed by typical histological findings such as striped fibrosis (20, 46) and arteriolar hyalinosis (46). Previously, it has been demonstrated that CsA causes ER stress while concurrently inducing phenotypic changes in human renal epithelial cells, indicative of EMT (44). Other ER stress inducers, such as Tg, were shown to produce human renal epithelial cell shape change (12, 44).

Additionally, the eIF2 α dephosphorylation inhibitor, Sal, inhibited the CsA-induced epithelial cell shape change *in vitro*, and tubulointerstitial fibrosis associated with CsA-induced nephrotoxicity in rats, *in vivo* (44). We found a similar effect of Sal on epithelial cell shape change *in vitro*, and also demonstrate that Sal alone increases GRP78 expression. This is a potential mechanism for the action of Sal, since GRP78 overexpression can inhibit UPR activation by binding to the ER transmembrane UPR transducers, IRE1 and PERK and preventing their activation (5). Further, GRP78 is an ER luminal Ca²⁺ binding protein (12), whose overexpression has been found to inhibit ER Ca²⁺ disequilibrium (14, 16). Thus, Sal may have acted to inhibit TDAG51 expression through its effects on GRP78 expression.

Other studies, using the HK-2 cell model of hRPTECs, have also shown that CsA induces an EMT response characterized by F-actin stress fibre formation, β -catenin cytoplasmic and nuclear translocation, and extracellular matrix component production (41). These effects appear to have been mediated by TGF β 1, as they were inhibited by an anti-TGF β 1 neutralizing antibody (41). CsA-treated renal epithelial cells showed the induction of α -SMA mRNA and protein (41, 51). This induction was associated with an increase in TGF β 1 release, inhibited by the protein kinase C- β inhibitor, hispidin (51). Protein kinase C- β requires cytosolic Ca²⁺ upregulation for activation, which we have demonstrated is induced by CsA (Figure 5A). One previous report has indicated that ER stress leads to an EMT-like phenotype in epithelial cells. In PC C13 thyroid cells, this EMT response was accompanied by changes in the epithelial monolayer, downregulation of E-cadherin, and upregulation of vimentin, α -SMA, type I collagen and SNAI1/SIP1

(52). However, it is unknown whether ER stress induction in this cell type results in TDAG51 expression.

ER stress-induced EMT appears to be mediated by changes in cytosolic Ca^{2+} , since both CsA and Tg resulted in these changes whereas the N-linked glycosylation inhibitor, Tm, showed no changes in cytosolic Ca^{2+} and did not induce EMT. These data are in agreement with previous reports that showed Tm did not change cytosolic Ca^{2+} (2, 13). It has been demonstrated that contact disassembly of proximal tubular cells mediated by Ca^{2+} removal primes cells for TGF β 1-induced EMT (39). These experiments suggested a two-hit mechanism where contact disassembly primes the cells for TGF β 1-induced EMT via β -catenin signalling (39). Further, the Wnt/ β -catenin signalling pathway is important in tubular EMT (37). Using the unilateral ureter obstruction model of interstitial renal fibrosis, it has been demonstrated that β -catenin target genes, including Twist, lymphoid enhancer-binding factor 1, and fibronectin, were induced, correlating with renal β -catenin abundance (28). Wnt signalling induces the expression of Snail, a transcription factor that is sufficient to initiate EMT through the downregulation of E-cadherin (7, 53). β -catenin, when transported to the nucleus, interacts with lymphoid enhancer binding factor T-cell factor to induce gene transcription required for EMT (26). This shows the importance of β -catenin signalling through the canonical Wnt pathway in renal interstitial fibrosis. A number of studies have shown an increase in TDAG51 (PHLDA1) expression when Wnt signalling is activated (23, 50), however, it has been demonstrated that TDAG51 is not a direct downstream target of canonical Wnt signalling (48). Our results suggest that increased TDAG51 expression activates Wnt signalling, priming the cells for an EMT

response. We have shown that ER stress inducers that alter cytosolic $[Ca^{2+}]$ cause TDAG51 overexpression, disrupt epithelial junctions, and cause β -catenin cytoplasmic to nuclear translocation leading to proximal tubular cell EMT. This appears to be the first hit in our ER stress-induced model of EMT, sensitizing the cells for the action of TGF β 1. Our results demonstrate that TDAG51 is required for the progression of peritoneal fibrosis *in vivo*, indicating it plays an important role in this process. The model utilized an adenovirus-mediated TGF β 1 induced mesothelial cell EMT and peritoneal fibrosis model (38), allowed the direct testing of our hypothesis since it does not rely on a non-specific induction of EMT through inflammation or injury. This model is dependent solely on the direct action of TGF β 1 to induce EMT. TDAG51 is a potential molecular mediator of ER stress-induced Wnt/ β -catenin signalling, since overexpression of the TDAG51 protein causes proximal tubular cell shape change, leading to junctional breakage and β -catenin cytoplasmic and nuclear translocation, and TDAG51 deficiency prevents the development of TGF β 1-induced peritoneal fibrosis.

In proximal tubular epithelial cells, a decrease in ER Ca^{2+} , which leads to the disruption of ER Ca^{2+} homeostasis, causes ER stress. Unresolved Ca^{2+} dysregulation-mediated ER stress appears to lead to an increase in TDAG51 protein expression. Increased TDAG51 expression causes cytoskeletal reorganization, characterized by rounding up or elongation of the cells. Cytoskeletal reorganization results in loss of cell-cell adhesions, thereby causing disruption of the monolayer. After loss of epithelial cell adhesion and monolayer disruption, β -catenin is translocated to the nucleus where it upregulates transcription of EMT-related genes. This is one effector in the “two-hit”

model, the other being TGF β 1 signalling. Together, β -catenin nuclear translocation and TGF β 1 signalling lead to the final stage of EMT - an increase in EMT-related gene expression and protein synthesis, including α -SMA and vinculin, resulting in a mesenchymal cell (Figure 9).

In summary, our data indicate that TDAG51 is a novel mediator of EMT in hRPTECs. As stated, TDAG51 expression is associated with ER stress caused by Ca²⁺-mediated mechanisms. We demonstrated that Ca²⁺ dysregulation, as induced by select ER stressors, upregulates TDAG51 expression, though this upregulation is not seen in ER stress caused via other mechanisms. It has previously been shown that intracellular Ca²⁺ fluctuations can cause EMT (22); however, Ca²⁺-mediated ER stress-induced TDAG51 expression leading to EMT is a novel finding. Our results indicate that TDAG51 leads to cytoskeletal rearrangement, priming the cells for TGF β 1-induced EMT, and that TDAG51 is essential for the development of TGF β 1-induced peritoneal fibrosis *in vivo*. The elucidation of this novel molecular mediator of hRPTEC EMT holds promise for the development of therapeutic compounds that can reduce the ER stress response and specifically down regulate the expression of TDAG51 preventing the progression of CKD through the inhibition of ER stress-induced renal interstitial fibrosis.

REFERENCES

1. Akayama M, Nakada H, Omori K, Masaki R, Taketani S, and Tashiro Y. The (Na⁺, K⁺)ATPase of rat kidney: purification, biosynthesis, and processing. *Cell Struct Funct* 11: 259-271, 1986.
2. Al-Hashimi AA, Caldwell J, Gonzalez-Gronow M, Pizzo SV, Aboumrad D, Pozza L, Al-Bayati H, Weitz JI, Stafford A, Chan H, Kapoor A, Jacobsen DW, Dickhout JG, and Austin RC. Binding of anti-GRP78 autoantibodies to cell surface GRP78 increases tissue factor procoagulant activity via the release of calcium from endoplasmic reticulum stores. *J Biol Chem* 285: 28912-28923, 2010.
3. Araki S, Eitel JA, Batuello CN, Bijangi-Vishehsaraei K, Xie XJ, Danielpour D, Pollok KE, Boothman DA, and Mayo LD. TGF-beta1-induced expression of human Mdm2 correlates with late-stage metastatic breast cancer. *J Clin Invest* 120: 290-302, 2010.
4. Berglund L, Bjorling E, Oksvold P, Fagerberg L, Asplund A, Szigartyo CA, Persson A, Ottosson J, Wernerus H, Nilsson P, Lundberg E, Sivertsson A, Navani S, Wester K, Kampf C, Hober S, Ponten F, and Uhlen M. A genecentric Human Protein Atlas for expression profiles based on antibodies. *Mol Cell Proteomics* 7: 2019-2027, 2008.
5. Bertolotti A, Zhang Y, Hendershot LM, Harding HP, and Ron D. Dynamic interaction of BiP and ER stress transducers in the unfolded-protein response. *Nat Cell Biol* 2: 326-332, 2000.
6. Boyce M, Bryant KF, Jousse C, Long K, Harding HP, Scheuner D, Kaufman RJ, Ma D, Coen DM, Ron D, and Yuan J. A selective inhibitor of eIF2alpha dephosphorylation protects cells from ER stress. *Science* 307: 935-939, 2005.
7. Cannito S, Novo E, di Bonzo LV, Busletta C, Colombatto S, and Parola M. Epithelial-mesenchymal transition: from molecular mechanisms, redox regulation to implications in human health and disease. *Antioxid Redox Signal* 12: 1383-1430, 2010.
8. Chiurchiu C, Remuzzi G, and Ruggenenti P. Angiotensin-converting enzyme inhibition and renal protection in nondiabetic patients: the data of the meta-analyses. *J Am Soc Nephrol* 16 Suppl 1: S58-63, 2005.
9. Coresh J, Wei GL, McQuillan G, Brancati FL, Levey AS, Jones C, and Klag MJ. Prevalence of high blood pressure and elevated serum creatinine level in the United States: findings from the third National Health and Nutrition Examination Survey (1988-1994). *Arch Intern Med* 161: 1207-1216, 2001.
10. Cunard R, and Sharma K. The endoplasmic reticulum stress response and diabetic kidney disease. *Am J Physiol Renal Physiol* 300: F1054-1061, 2011.

11. Cybulsky AV. Endoplasmic reticulum stress in proteinuric kidney disease. *Kidney Int* 77: 187-193, 2010.
12. Dickhout JG, Carlisle RE, and Austin RC. Inter-Relationship between Cardiac Hypertrophy, Heart Failure and Chronic Kidney Disease – Endoplasmic Reticulum Stress as a Mediator of Pathogenesis. *Circ Res* 108: 629-642, 2011.
13. Dickhout JG, Colgan SM, Lhotak S, and Austin RC. Increased endoplasmic reticulum stress in atherosclerotic plaques associated with acute coronary syndrome - A balancing act between plaque stability and rupture. *Circulation* 116: 1214-1216, 2007.
14. Dickhout JG, Hossain GS, Pozza LM, Zhou J, Lhotak S, and Austin RC. Peroxynitrite causes endoplasmic reticulum stress and apoptosis in human vascular endothelium: implications in atherogenesis. *Arterioscler Thromb Vasc Biol* 25: 2623-2629, 2005.
15. Dickhout JG, and Krepinsky JC. Endoplasmic reticulum stress and renal disease. *Antioxid Redox Signal* 11: 2341-2352, 2009.
16. Dickhout JG, Sood SK, and Austin RC. Role of endoplasmic reticulum calcium disequilibria in the mechanism of homocysteine-induced ER stress. *Antioxid Redox Signal* 9: 1863-1873, 2007.
17. El-Nahas AM. Plasticity of kidney cells: role in kidney remodeling and scarring. *Kidney Int* 64: 1553-1563, 2003.
18. El Kossi M, and El Nahas M. Epidemiology and pathophysiology of chronic kidney disease: natural history, risk factors, and management. In: *Comprehensive Clinical Nephrology*, edited by Feehally J FJ, Johnson RJ. Philadelphia, PA: Elsevier, 2007, p. 813-821.
19. Fellstrom B. Cyclosporine nephrotoxicity. *Transplant Proc* 36: 220S-223S, 2004.
20. Fioretto P, Najafian B, Sutherland DE, and Mauer M. Tacrolimus and cyclosporine nephrotoxicity in native kidneys of pancreas transplant recipients. *Clin J Am Soc Nephrol* 6: 101-106, 2010.
21. Frank D, Mendelsohn CL, Ciccone E, Svensson K, Ohlsson R, and Tycko B. A novel pleckstrin homology-related gene family defined by Ipl/Tssc3, TDAG51, and Tih1: tissue-specific expression, chromosomal location, and parental imprinting. *Mamm Genome* 10: 1150-1159, 1999.
22. Garriock RJ, and Krieg PA. Wnt11-R signaling regulates a calcium sensitive EMT event essential for dorsal fin development of *Xenopus*. *Dev Biol* 304: 127-140, 2007.

23. Gaspar C, Cardoso J, Franken P, Molenaar L, Morreau H, Moslein G, Sampson J, Boer JM, de Menezes RX, and Fodde R. Cross-species comparison of human and mouse intestinal polyps reveals conserved mechanisms in adenomatous polyposis coli (APC)-driven tumorigenesis. *Am J Pathol* 172: 1363-1380, 2008.
24. Goldmann WH, and Ingber DE. Intact vinculin protein is required for control of cell shape, cell mechanics, and rac-dependent lamellipodia formation. *Biochem Biophys Res Commun* 290: 749-755, 2002.
25. Gomes I, Xiong W, Miki T, and Rosner MR. A proline- and glutamine-rich protein promotes apoptosis in neuronal cells. *J Neurochem* 73: 612-622, 1999.
26. Grande MT, and Lopez-Novoa JM. Fibroblast activation and myofibroblast generation in obstructive nephropathy. *Nat Rev Nephrol* 5: 319-328, 2009.
27. Haslam RJ, Koide HB, and Hemmings BA. Pleckstrin domain homology. *Nature* 363: 309-310, 1993.
28. He W, Dai C, Li Y, Zeng G, Monga SP, and Liu Y. Wnt/beta-catenin signaling promotes renal interstitial fibrosis. *J Am Soc Nephrol* 20: 765-776, 2009.
29. Higgins DF, Kimura K, Bernhardt WM, Shrimanker N, Akai Y, Hohenstein B, Saito Y, Johnson RS, Kretzler M, Cohen CD, Eckardt KU, Iwano M, and Haase VH. Hypoxia promotes fibrogenesis in vivo via HIF-1 stimulation of epithelial-to-mesenchymal transition. *J Clin Invest* 117: 3810-3820, 2007.
30. Hinz T, Flindt S, Marx A, Janssen O, and Kabelitz D. Inhibition of protein synthesis by the T cell receptor-inducible human TDAG51 gene product. *Cell Signal* 13: 345-352, 2001.
31. Hossain GS, van Thienen JV, Werstuck GH, Zhou J, Sood SK, Dickhout JG, de Koning AB, Tang D, Wu D, Falk E, Poddar R, Jacobsen DW, Zhang K, Kaufman RJ, and Austin RC. TDAG51 is induced by homocysteine, promotes detachment-mediated programmed cell death, and contributes to the development of atherosclerosis in hyperhomocysteinemia. *J Biol Chem* 278: 30317-30327, 2003.
32. Ingley E, and Hemmings BA. Pleckstrin homology (PH) domains in signal transduction. *J Cell Biochem* 56: 436-443, 1994.
33. Iwano M, Plieth D, Danoff TM, Xue C, Okada H, and Neilson EG. Evidence that fibroblasts derive from epithelium during tissue fibrosis. *J Clin Invest* 110: 341-350, 2002.
34. Jafar TH, Stark PC, Schmid CH, Landa M, Maschio G, Marcantoni C, de Jong PE, de Zeeuw D, Shahinfar S, Ruggenti P, Remuzzi G, and Levey AS. Proteinuria as a

- modifiable risk factor for the progression of non-diabetic renal disease. *Kidney Int* 60: 1131-1140, 2001.
35. James MT, Hemmelgarn BR, and Tonelli M. Early recognition and prevention of chronic kidney disease. *Lancet* 375: 1296-1309, 2010.
 36. Joo JH, Liao G, Collins JB, Grissom SF, and Jetten AM. Farnesol-induced apoptosis in human lung carcinoma cells is coupled to the endoplasmic reticulum stress response. *Cancer Res* 67: 7929-7936, 2007.
 37. Liu Y. New insights into epithelial-mesenchymal transition in kidney fibrosis. *J Am Soc Nephrol* 21: 212-222, 2010.
 38. Margetts PJ, Bonniaud P, Liu L, Hoff CM, Holmes CJ, West-Mays JA, and Kelly MM. Transient overexpression of TGF- β 1 induces epithelial mesenchymal transition in the rodent peritoneum. *J Am Soc Nephrol* 16: 425-436, 2005.
 39. Masszi A, Fan L, Rosivall L, McCulloch CA, Rotstein OD, Mucsi I, and Kapus A. Integrity of cell-cell contacts is a critical regulator of TGF- β 1-induced epithelial-to-myofibroblast transition: role for beta-catenin. *Am J Pathol* 165: 1955-1967, 2004.
 40. Mathew A, Cunard R, and Sharma K. Antifibrotic treatment and other new strategies for improving renal outcomes. *Contrib Nephrol* 170: 217-227, 2011.
 41. McMorro T, Gaffney MM, Slattery C, Campbell E, and Ryan MP. Cyclosporine A induced epithelial-mesenchymal transition in human renal proximal tubular epithelial cells. *Nephrol Dial Transplant* 20: 2215-2225, 2005.
 42. Metcalfe W. How does early chronic kidney disease progress? A background paper prepared for the UK Consensus Conference on early chronic kidney disease. *Nephrol Dial Transplant* 22 Suppl 9: ix26-30, 2007.
 43. Oloumi A, McPhee T, and Dedhar S. Regulation of E-cadherin expression and beta-catenin/Tcf transcriptional activity by the integrin-linked kinase. *Biochim Biophys Acta* 1691: 1-15, 2004.
 44. Pallet N, Bouvier N, Bendjallabah A, Rabant M, Flinois JP, Hertig A, Legendre C, Beaune P, Thervet E, and Anglicheau D. Cyclosporine-induced endoplasmic reticulum stress triggers tubular phenotypic changes and death. *American Journal of Transplantation* 8: 2283-2296, 2008.
 45. Park CG, Lee SY, Kandala G, and Choi Y. A novel gene product that couples TCR signaling to Fas(CD95) expression in activation-induced cell death. *Immunity* 4: 583-591, 1996.
 46. Pichler RH, Franceschini N, Young BA, Hugo C, Andoh TF, Burdmann EA, Shankland SJ, Alpers CE, Bennett WM, Couser WG, and et al. Pathogenesis of

- cyclosporine nephropathy: roles of angiotensin II and osteopontin. *J Am Soc Nephrol* 6: 1186-1196, 1995.
47. Rho J, Gong S, Kim N, and Choi Y. TDAG51 is not essential for Fas/CD95 regulation and apoptosis in vivo. *Mol Cell Biol* 21: 8365-8370, 2001.
 48. Sakthianandeswaren A, Christie M, D'Andreti C, Tsui C, Jorissen RN, Li S, Fleming NI, Gibbs P, Lipton L, Malaterre J, Ramsay RG, Phesse TJ, Ernst M, Jeffery RE, Poulosom R, Leedham SJ, Segditsas S, Tomlinson IP, Bernhard OK, Simpson RJ, Walker F, Faux MC, Church N, Catimel B, Flanagan DJ, Vincan E, and Sieber OM. PHLDA1 expression marks the putative epithelial stem cells and contributes to intestinal tumorigenesis. *Cancer Res* 71: 3709-3719, 2011.
 49. Schroder M, and Kaufman RJ. ER stress and the unfolded protein response. *Mutat Res* 569: 29-63, 2005.
 50. Segditsas S, Sieber O, Deheragoda M, East P, Rowan A, Jeffery R, Nye E, Clark S, Spencer-Dene B, Stamp G, Poulosom R, Suraweera N, Silver A, Ilyas M, and Tomlinson I. Putative direct and indirect Wnt targets identified through consistent gene expression changes in APC-mutant intestinal adenomas from humans and mice. *Hum Mol Genet* 17: 3864-3875, 2008.
 51. Slattery C, Campbell E, McMorro T, and Ryan MP. Cyclosporine A-induced renal fibrosis: a role for epithelial-mesenchymal transition. *Am J Pathol* 167: 395-407, 2005.
 52. Ulianich L, Garbi C, Treglia AS, Punzi D, Miele C, Raciti GA, Beguinot F, Consiglio E, and Di Jeso B. ER stress is associated with dedifferentiation and an epithelial-to-mesenchymal transition-like phenotype in PC C13 thyroid cells. *J Cell Sci* 121: 477-486, 2008.
 53. Vasyutina E, and Treier M. Molecular mechanisms in renal degenerative disease. *Semin Cell Dev Biol* 21: 831-837, 2010.
 54. Zeisberg EM, Potenta SE, Sugimoto H, Zeisberg M, and Kalluri R. Fibroblasts in kidney fibrosis emerge via endothelial-to-mesenchymal transition. *J Am Soc Nephrol* 19: 2282-2287, 2008.
 55. Zeisberg M, and Neilson EG. Mechanisms of tubulointerstitial fibrosis. *J Am Soc Nephrol* 21: 1819-1834, 2010.

Figure 1.

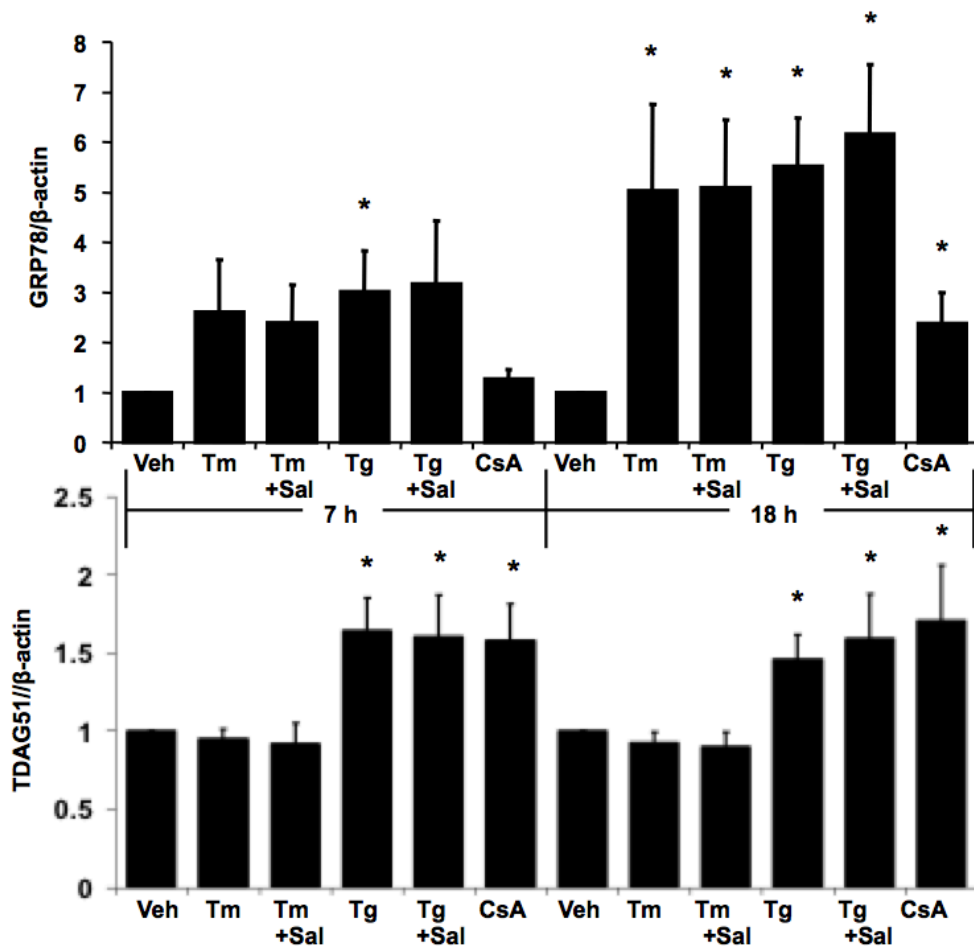
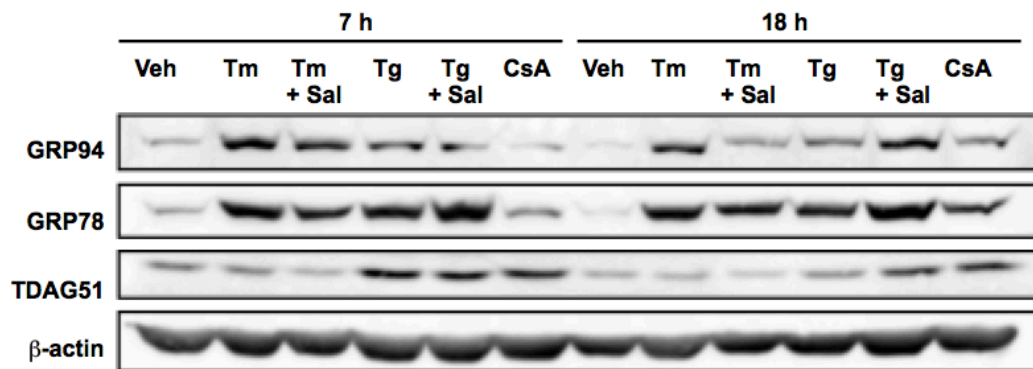


Figure 1. UPR activation and TDAG51 expression in response to ER stress. HK-2 cells were treated with vehicle, thapsigargin (Tg), tunicamycin (Tm), cyclosporine A (CsA) or combined treatments of Tm plus Sal (Tm + Sal) or Tg plus Sal (Tg + Sal), for 7 or 18 h. Cell lysates were assessed by Western blotting and probed for GRP94, GRP78, TDAG51 and β -actin. Densitometry showed a significant up-regulation of GRP78 protein in response to Tg at 7 h. At 18 h, GRP78 protein levels were up-regulated by all treatments, indicating ER stress induction. Densitometry also indicated a significant up-regulation of TDAG51 in response to Tg, Tg + Sal, and CsA treatments at 7 and 18 h ($N = 4$, $P < 0.05$). Tg = 200 nM; Tm = 1 μ g/ml; Sal = 30 μ M; CsA = 5 μ M.

Figure 2.

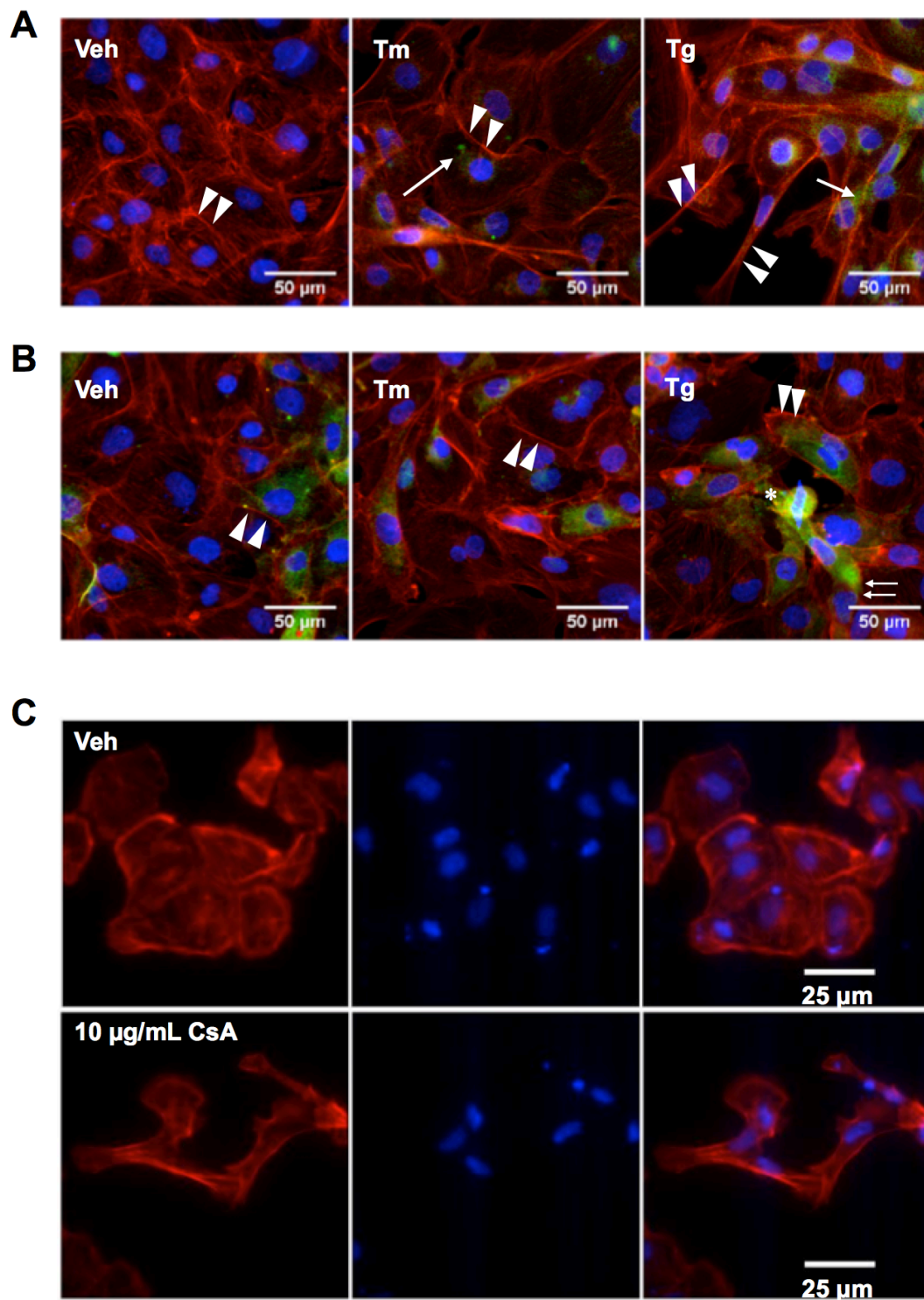


Figure 2. GRP78 and TDAG51 expression in response to ER stress. (A) HK-2 cells were treated for 18 h with vehicle, tunicamycin (Tm), or thapsigargin (Tg), and then stained for F-actin (red, arrowheads), GRP78 (green, arrows) and cell nuclei (blue). Vehicle and Tm-treated cells indicate F-actin fibrils at the periphery of the cells (arrowheads), typical of the epithelial phenotype. Tg-treated cells show F-actin filaments at the periphery of cells undergoing change from an epithelial to mesenchymal phenotype (arrowheads). GRP78 staining appears to be more abundant in the perinuclear region of Tm- and Tg-treated cells, indicating activation of the UPR (arrows). (B) HK-2 cells were stained for F-actin (red, arrowheads), TDAG51 (green) and cell nuclei (blue). F-actin staining showed similar results as (A). Tm treatments show no increase in TDAG51 levels; however, Tg-treated cells demonstrated abundant TDAG51 expression in cells that had undergone shape change (*). (C) Treatment with cyclosporine A (CsA) for 24 h induces translocation of β -catenin (red) from the periphery of the cell to the perinuclear and nuclear area, nuclei stained in blue (DAPI). (A and B) Bar = 50 μ m; (C) Bar = 25 μ m. Tg = 200 nM; Tm = 1 μ g/ml; CsA = 5 μ M.

Figure 3.

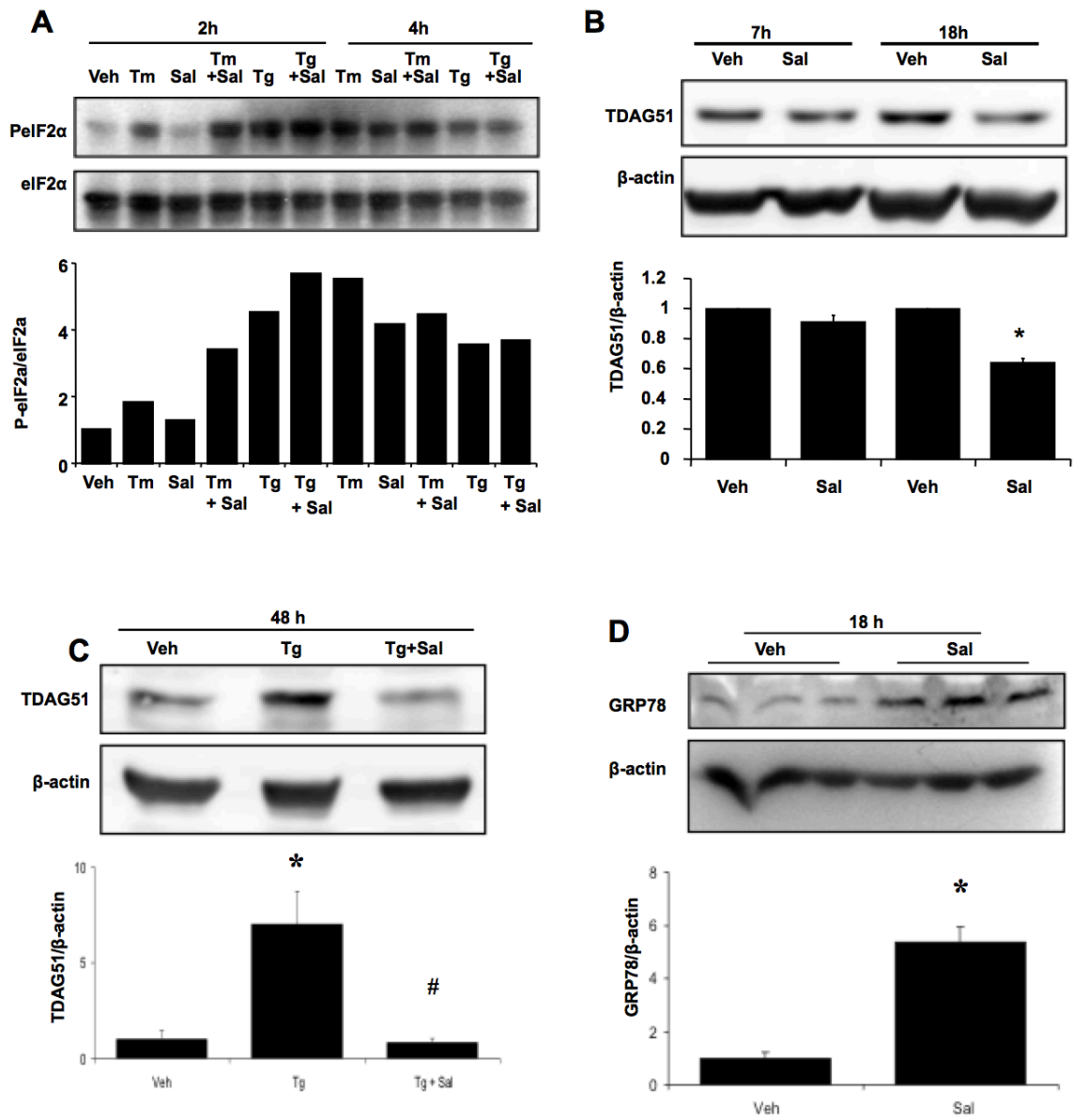


Figure 3. Effect of salubrinal on TDAG51 expression and the UPR. (A) HK-2 cells were treated with vehicle, tunicamycin (Tm), thapsigargin (Tg), salubrinal (Sal), a combination of Tm plus Sal (Tm + Sal), or Tg plus Sal (Tg + Sal) for 2 or 4 h. Results demonstrate an increase in phosphorylated eIF2 α (PeIF2 α) in response to Tm, Tm + Sal, Tg, and Tg + Sal at 2 h, and all treatments at 4 h. (B) HK-2 cells were treated with vehicle or Sal for 7 or 18 h. Sal treatment for 7 h showed a non-significant down regulation of TDAG51; however, there was a significant decrease in TDAG51 levels at 18 h in Sal-treated cells (N = 6; $P < 0.001$). (C) HK-2 cells were treated with vehicle, Tg, or Tg plus Sal (Tg + Sal) for 48 h. Western blotting demonstrates an increase in TDAG51 protein expression in response to Tg, but not Tg + Sal combined (*, $P < 0.05$ vs. Veh; #, $P < 0.05$ vs. Tg). (D) HK-2 cells were treated with vehicle or Sal for 18 h. Sal treatment demonstrated a significant increase in GRP78 expression, when compared with vehicle-treated cells (N = 3; *, $P < 0.05$). Tg = 200 nM; Tm = 1 μ g/ml; Sal = 30 μ M.

Figure 4.

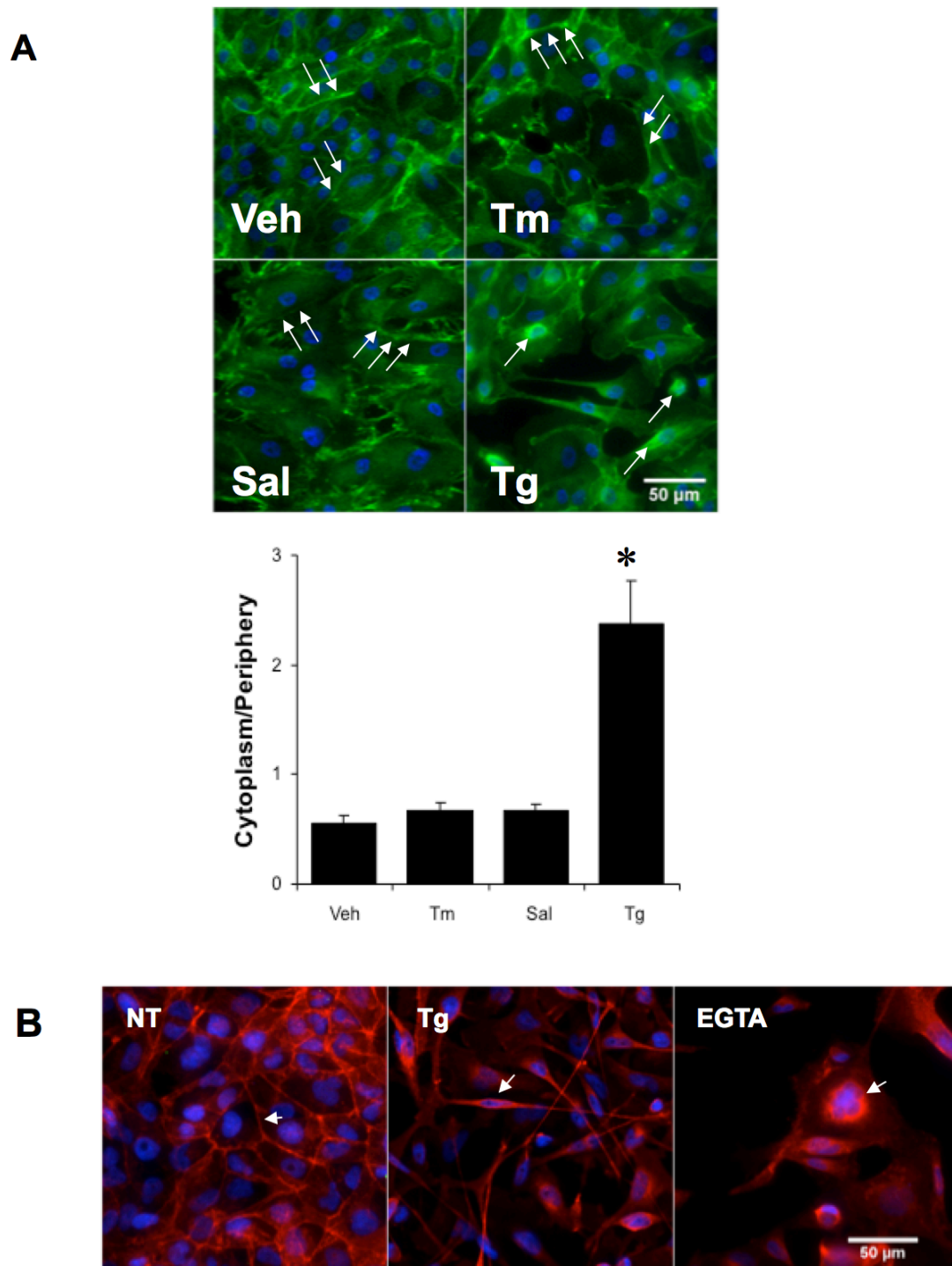


Figure 4. Induction of β -catenin nuclear translocation by thapsigargin. (A) Staining for β -catenin (arrows) was found in the periphery of primary hRPTECs treated for 24 h with vehicle, tunicamycin (Tm), and salubrinal (Sal). Thapsigargin (Tg) treatment showed the translocation of β -catenin from the periphery of the cell to the perinuclear area (arrows) and the cell nucleus. Quantification reveals a significant increase in β -catenin found in the nuclear and perinuclear area. Bar = 50 μ m. (B) HK-2 cells were untreated or treated with Tg or the Ca^{2+} chelator EGTA for 18 h. Both Tg and EGTA treatments resulted in changes in cell shape and translocation of β -catenin (red) to the perinuclear and nuclear area. Tg = 200 nM; Tm = 1 μ g/ml; Sal = 30 μ M.

Figure 5.

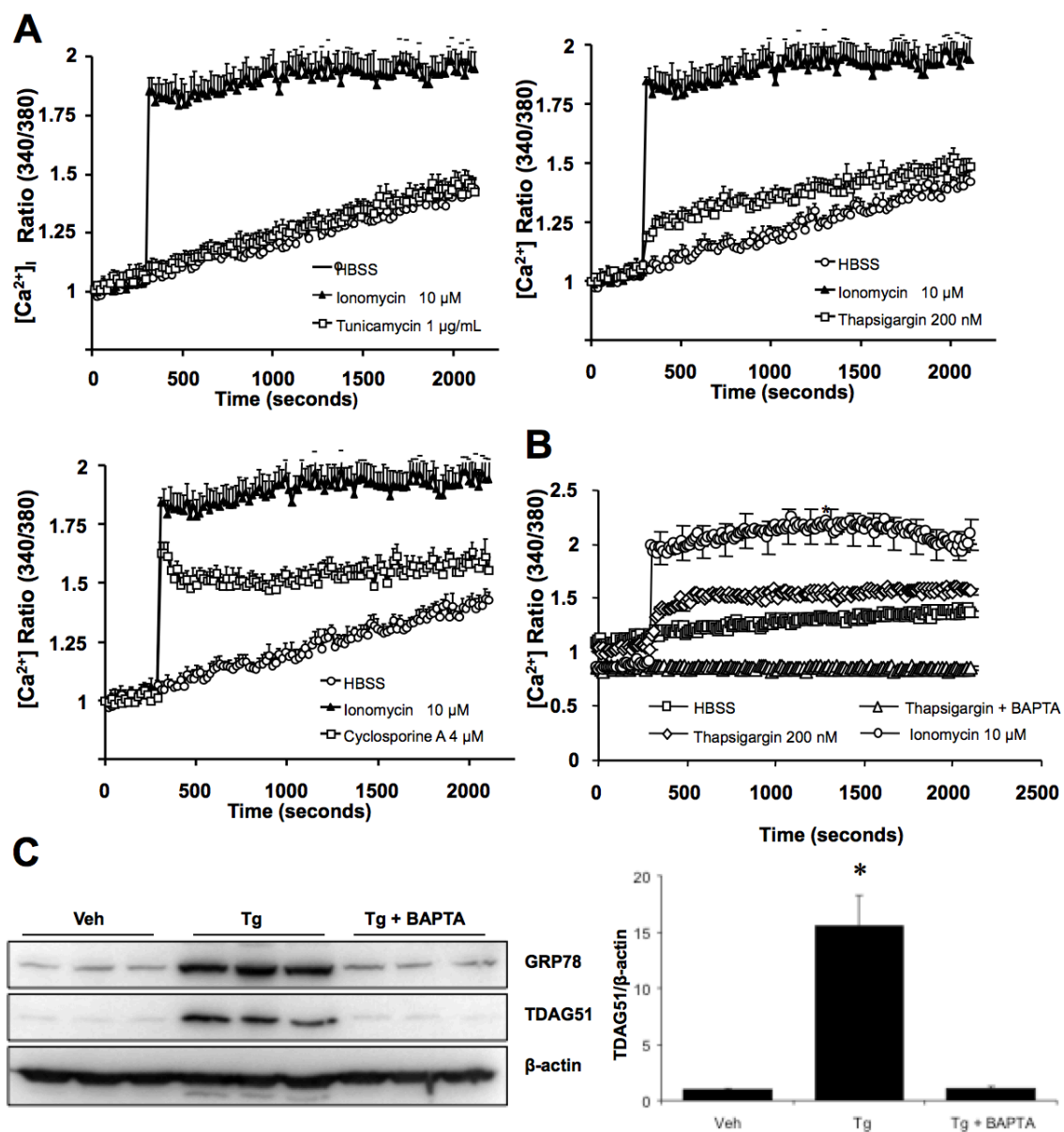


Figure 5. Ca²⁺ chelator prevents thapsigargin-mediated effects. (A) Cytosolic [Ca²⁺] was measured ratiometrically using the Ca²⁺-binding fluorophore Fura-2. Treatment with ER stress inducers show that thapsigargin (Tg) and cyclosporine A caused an increase in cytosolic [Ca²⁺] whereas tunicamycin (TM) did not. Ionomycin (10 mM) was used as a positive control for increased [Ca²⁺]. (B) HK-2 cells were treated with Tg or Tg with the Ca²⁺ chelator BAPTA-AM (Tg + BAPTA). Cytosolic [Ca²⁺] was measured ratiometrically, demonstrating that BAPTA-AM inhibited Tg-mediated Ca²⁺ dysregulation. (C) HK-2 cells were treated with Tg or Tg with the Ca²⁺ chelator BAPTA-AM (Tg + BAPTA) for 18 h. Western blotting demonstrated that Tg treatment resulted in a significant increase in TDAG51 and GRP78 expression. However, this effect was prevented by co-treatment with BAPTA-AM (N = 3; *, *P* < 0.05). Tg = 200 nM; BAPTA-AM = 100 μM.

Figure 6.

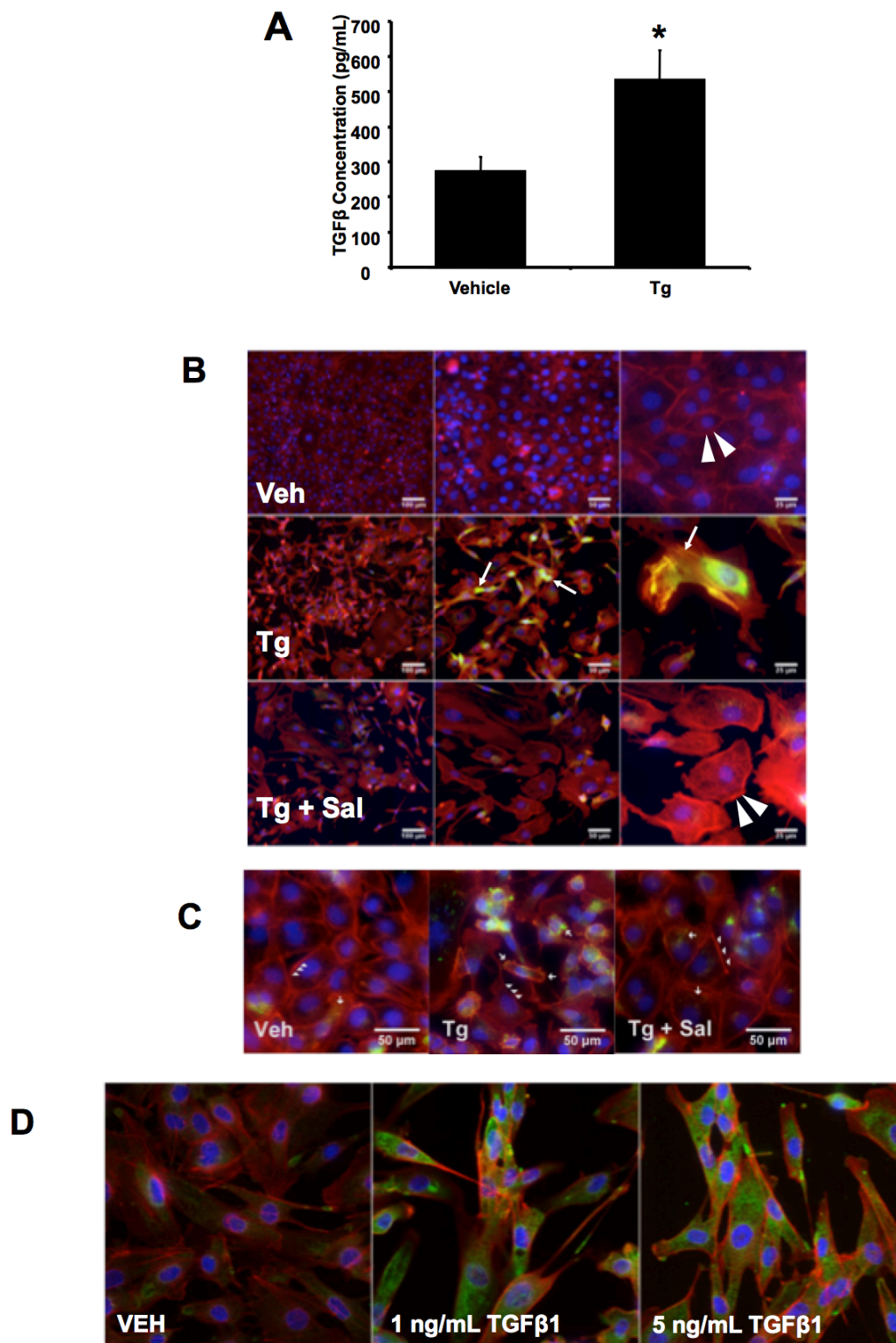


Figure 6. Thapsigargin treatment reduces epithelial cell phenotype, while inducing the expression of myofibroblasts markers. (A) A 24 h treatment with thapsigargin (Tg) was found to significantly increase the levels of active TGF β 1 in the supernatant of cultured HK-2 cells; $p < 0.05$. (B) HK-2 cells were treated for 48 h with vehicle, Tg, or Tg pre-treated with salubrinal (Sal) for 1 h. Cells were stained for F-actin (red), nuclei (blue) and α -smooth muscle actin (α -SMA, green). Vehicle treatment showed typical epithelial cell phenotype, with prominent F-actin filaments at the cell periphery (arrowheads). Tg treatment induced α -SMA expression in cells that had undergone shape change, typical of mesenchymal transformation (arrows). Sal pre-treatment appeared to reduce the Tg-mediated expression of α -SMA. (C) HK-2 cells were treated as in (B). Cells were stained for F-actin (red), nuclei (blue) and vinculin (green). Vehicle treated cells show prominent F-actin filaments in the cell periphery, and few cells expressing vinculin (arrows). Tg treatment showed an increase in vinculin staining (arrows) in cells that underwent shape change. Sal pre-treatment (1 h) appeared to reduce the effect caused by Tg, resulting in reduced vinculin staining at the cell periphery (arrows). F-actin filaments were also visualized in the cell periphery (arrowheads). (D) Immunofluorescent staining demonstrating that low and high doses of human recombinant TGF β 1 induced an epithelial to mesenchymal transition response in primary human renal proximal tubule epithelial cells, as shown by change in cell phenotype (F-actin, red) and increased expression of α -SMA (green). Bar = 50 μ m. Tg = 200 nM; Sal = 30 μ M; low dose TGF β 1 = 1 ng/mL; high dose TGF β 1 = 5 ng/mL.

Figure 7.

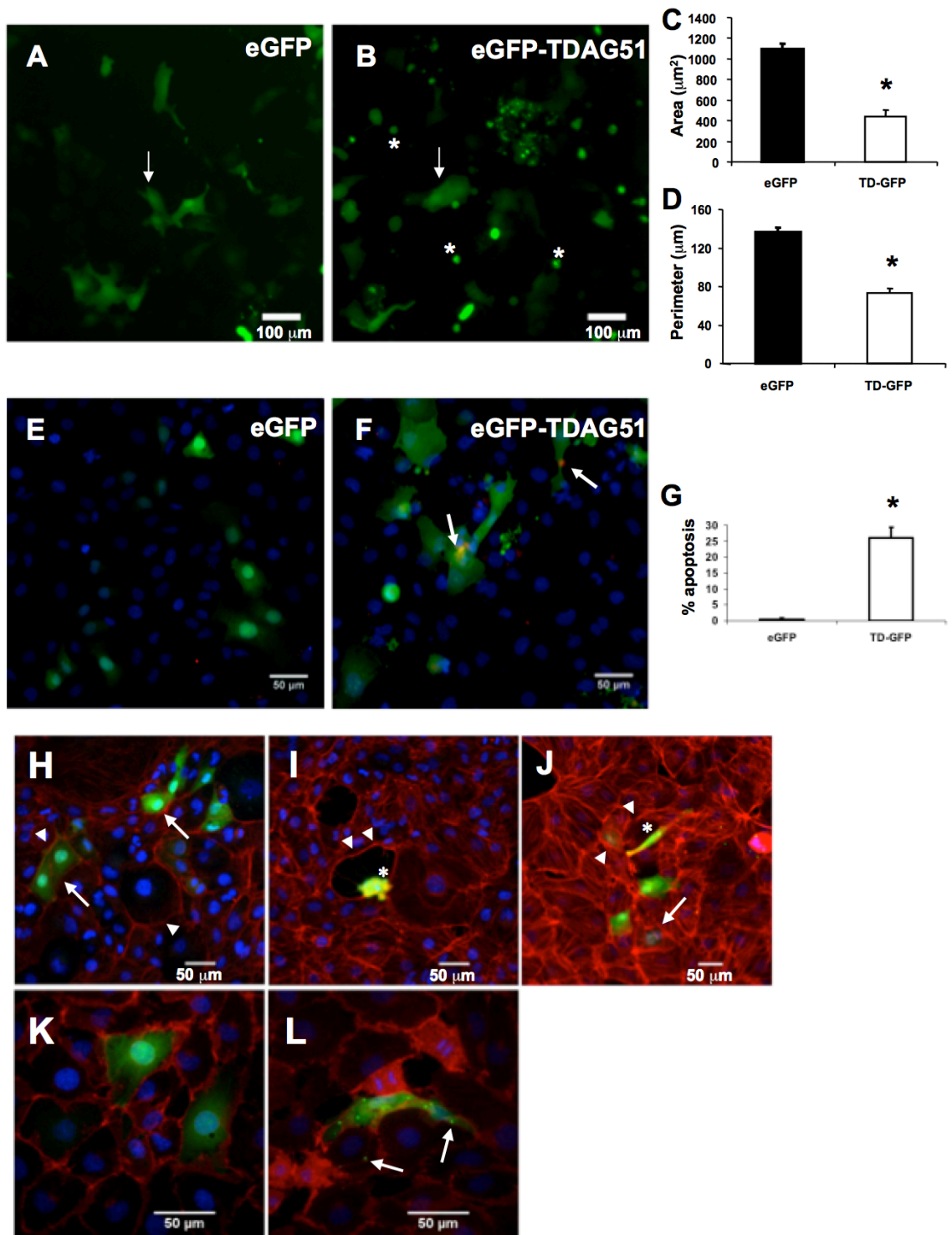


Figure 7. The effects of TDAG51 protein overexpression on cell shape and β -catenin translocation. (A and B) HK-2 cells were transfected with either the expression plasmid for eGFP (A, green) or eGFP-TDAG51 (B, green) fusion protein for 48 h. Adherent cells were observed in both eGFP- and eGFP-TDAG51-transfected cells (arrows), while cells that had rounded and detached were observed mainly in eGFP-TDAG51-transfected cells (*). (C and D) There was a significant decrease in the area (C) (*, $P < 0.05$; 1091.1 ± 56.9 vs 438.6 ± 61.5 , eGFP and eGFP-TDAG51 respectively) and perimeter (D) (*, $P < 0.05$; 136.3 ± 4.4 vs 73.4 ± 4.8 , eGFP and eGFP-TDAG51 respectively) of cells transfected with eGFP-TDAG51. (E and F) HK-2 cells were transfected with eGFP (E) or eGFP-TDAG51 (F) plasmid (green) for 48 h. The cells were TUNEL-stained and imaged to observe apoptosis. (G) Significantly more TUNEL-stained apoptotic cells (red, arrows) were observed in eGFP-TDAG51-transfected cells when compared with eGFP-transfected cells (*, $P < 0.05$; $0.5\% \pm 0.4$ vs $26.0\% \pm 3.4$, eGFP and eGFP-TDAG51, respectively). (H through J) Cells were stained for F-actin (red, arrowheads), eGFP (H) or eGFP-TDAG51 (I and J) (green) and nuclei (blue). eGFP transfected cells did not undergo a shape change (arrows), while eGFP-TDAG51 transfected cells did, as observed by the cell condensing and pulling off the plate (I) or elongating into a fibroblast-like phenotype (J) (*). HK-2 cells were transfected with control eGFP (K, green) or PHLD-GFP (L, green) and stained for β -catenin 24 h after transfection. PHLD-GFP transfected cells underwent shape change (arrows) and β -catenin disruption similar to (J).

Figure 8.

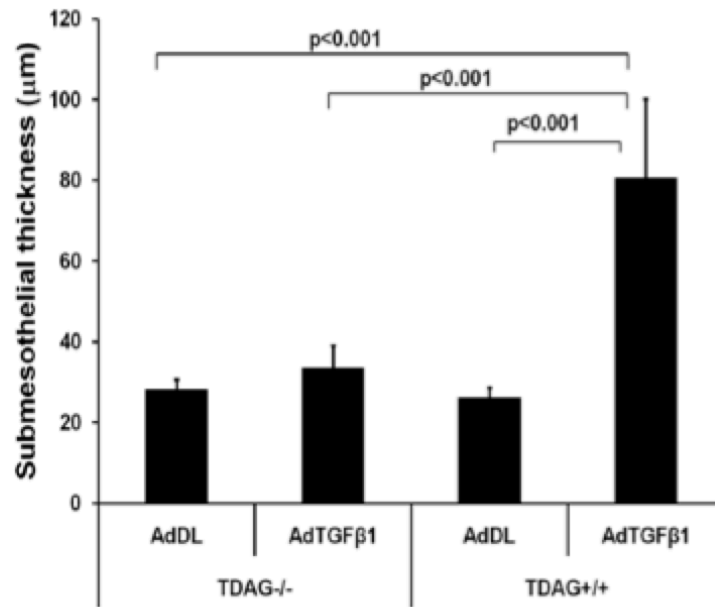
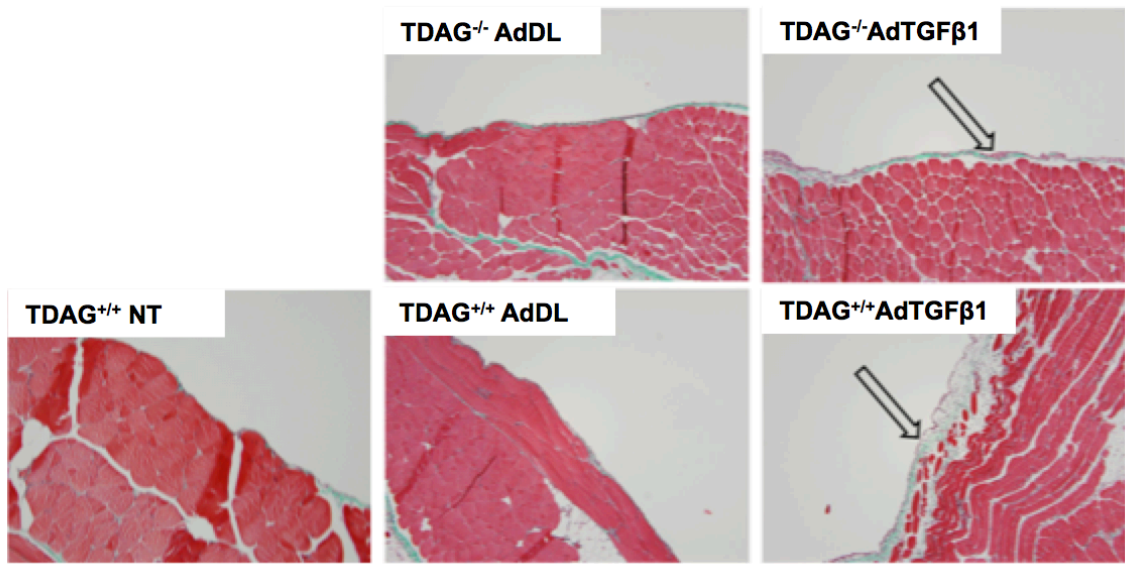


Figure 8. TDAG51 deficiency prevents TGF β 1-mediated peritoneal fibrosis.

C57BL/6 wild type (TDAG^{+/+}) and TDAG^{-/-} mice were injected with a control (AdDL) or TGF β 1 adenovirus (AdTGF β 1) for ten days. Untreated C57BL/6 wild type mouse parietal peritoneum (NT TDAG^{+/+}) is illustrated as a comparison to viral treated mice. Results indicate no difference in submesothelial thickness between AdDL-treated wild type (TDAG^{+/+}) and TDAG^{-/-} mice. However, submesothelial thickness of the parietal peritoneum from the anterior abdominal wall was significantly increased in wild type mice treated with TGF β 1 adenovirus ($p < 0.001$) when compared with TDAG51^{-/-} mice, which appeared to be resistant to AdTGF β 1-mediated peritoneal fibrosis.

Figure 9.

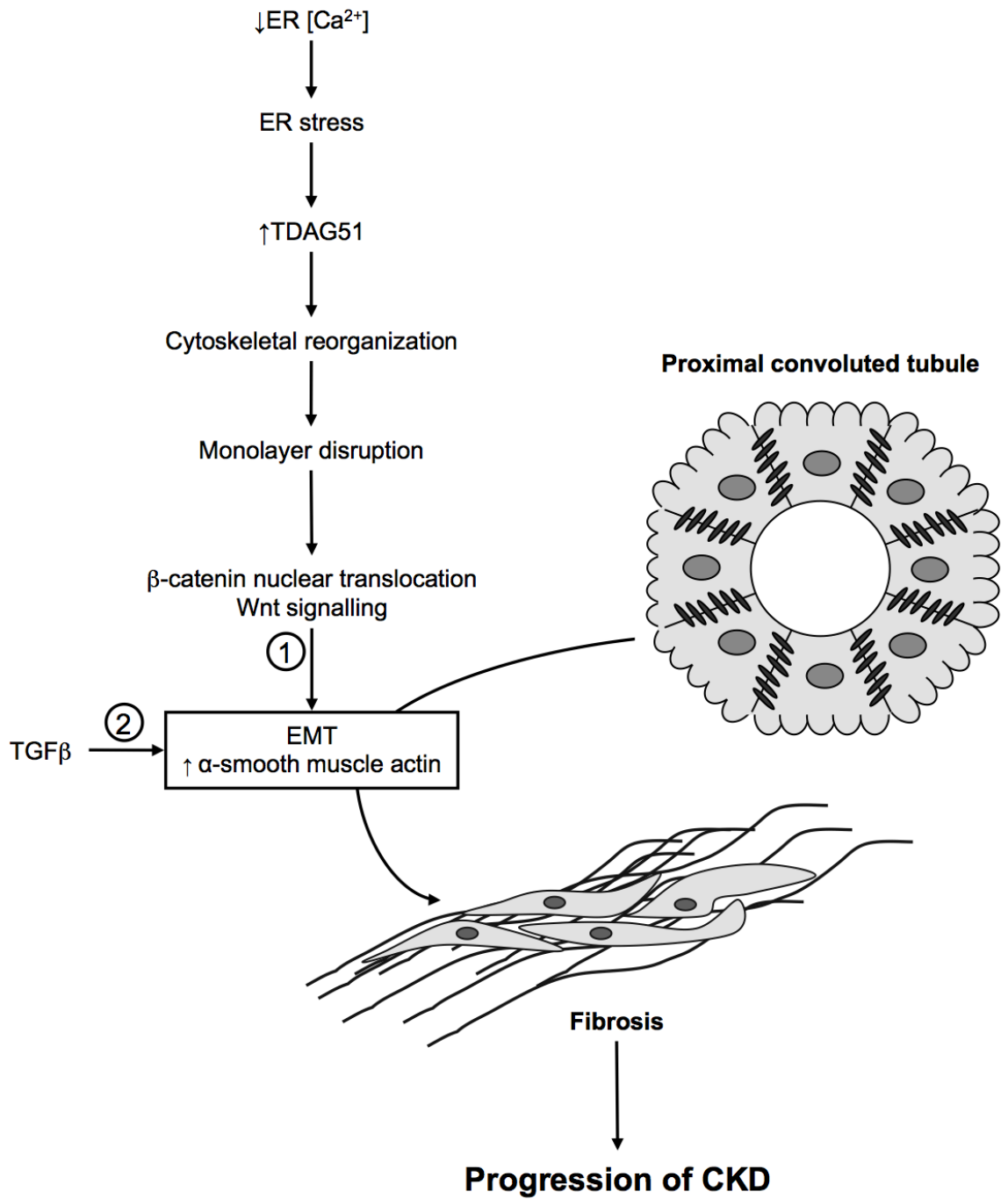


Figure 9. Two-hit model of TDAG51-induced EMT. In human renal epithelial cells, a decrease in ER Ca^{2+} concentration can lead to ER stress and the upregulation of TDAG51 expression. Conditions that cause ER stress without decreasing ER Ca^{2+} fail to induce TDAG51 levels. The increase in TDAG51 expression causes rearrangement of the cytoskeleton, and disruption of the cellular monolayer. β -catenin is then released from epithelial adherens junctions, translocates to the perinuclear and nuclear region of the cell, and Wnt signalling is initiated. Wnt signalling primes the cell for the action of $\text{TGF}\beta_1$, to induce late phase epithelial-to-mesenchymal transition genes, including α -smooth muscle actin.

CHAPTER 3

4-Phenylbutyrate inhibits tunicamycin-induced acute kidney injury via CHOP/GADD153 repression

Rachel E. Carlisle, Elise Brimble, Kaitlyn E. Werner, Gaile L. Cruz, Kjetil Ask, Alistair J. Ingram, and Jeffrey G. Dickhout.

PLoS ONE (2014). 9(1).
Doi: 10.1371/journal.pone.0084663.

© *Copyright by Carlisle et al.*

Chapter link:

Inhibiting protein aggregation with the LWCC 4-PBA reduces ER stress-mediated kidney damage. Tunicamycin is a nucleoside antibiotic that is frequently used as a nephrotoxic model of intrinsic acute kidney injury (Marciniak et al., 2004). Tunicamycin inhibits N-linked glycosylation, which results in the induction of ER stress. The nephrotoxic effects of tunicamycin are reduced in CHOP knockout and GADD34 mutant mice (Marciniak et al., 2004), suggesting a role for ER stress in this model of acute kidney injury. This manuscript establishes that inducing ER stress results in renal injury, with pathological features of acute tubular necrosis. It also demonstrates that inhibiting ER stress, and especially expression of the pro-apoptotic protein CHOP, can reduce this renal damage. 4-PBA treatment reduces CHOP expression, apoptosis, and GRP78 expression, in the tunicamycin-targeted region of the kidney. Finally, complete genetic knock out of CHOP prevents tunicamycin-mediated damage on structural and ultrastructural levels.

Author's contribution:

R.E. Carlisle, E. Brimble, and J.G. Dickhout designed the study. R.E. Carlisle conducted the animal studies and collected tissues with help from E. Brimble. R.E. Carlisle and K.E. Werner stained tissues and performed related analyses. R.E. Carlisle and G.L. Cruz performed cell culture experiments, and related analyses. R.E. Carlisle assembled the results, generated the figures in the manuscript, and wrote and revised the manuscript. R.E. Carlisle, E. Brimble, K. Ask, A.J. Ingram, and J.G. Dickhout reviewed and edited the manuscript. All authors approved of the final submission.

Running title: 4-PBA inhibits acute kidney injury

4-Phenylbutyrate inhibits tunicamycin-induced acute kidney injury via CHOP/GADD153 repression.

Rachel E. Carlisle¹, Elise Brimble¹, Kaitlyn E. Werner¹, Gaile L. Cruz¹, Kjetil Ask²,
Alistair J. Ingram¹ and Jeffrey G. Dickhout¹.

¹Department of Medicine, Division of Nephrology, McMaster University and St. Joseph's Healthcare Hamilton, Hamilton, Ontario, Canada.

²Department of Medicine, Division of Respiriology, McMaster University and St. Joseph's Healthcare Hamilton, Hamilton, Ontario, Canada.

Address correspondence to:

Jeffrey G. Dickhout, PhD
Department of Medicine, Division of Nephrology
McMaster University and St. Joseph's Healthcare Hamilton
50 Charlton Avenue East
Hamilton, Ontario, Canada, L8N 4A6
Phone: 905-522-1155 ext. 35334
Fax: 905-540-6589
Email: jdickhou@stjosham.on.ca

Key words: acute kidney injury, 4-phenylbutyrate, endoplasmic reticulum stress, tunicamycin

ABSTRACT

Different forms of acute kidney injury (AKI) have been associated with endoplasmic reticulum (ER) stress; these include AKI caused by acetaminophen, antibiotics, cisplatin, and radiocontrast. Tunicamycin (TM) is a nucleoside antibiotic known to induce ER stress and is a commonly used inducer of AKI. 4-phenylbutyrate (4-PBA) is an FDA approved substance used in children who suffer from urea cycle disorders. 4-PBA acts as an ER stress inhibitor by aiding in protein folding at the molecular level and preventing misfolded protein aggregation. The main objective of this study was to determine if 4-PBA could protect from AKI induced by ER stress, as typified by the TM-model, and what mechanism(s) of 4-PBA's action were responsible for protection. C57BL/6 mice were treated with saline, TM or TM plus 4-PBA. 4-PBA partially protected the anatomic segment most susceptible to damage, the outer medullary stripe, from TM-induced AKI. *In vitro* work showed that 4-PBA protected human proximal tubular cells from apoptosis and TM-induced CHOP expression, an ER stress inducible proapoptotic gene. Further, immunofluorescent staining in the animal model found similar protection by 4-PBA from CHOP nuclear translocation in the tubular epithelium of the medulla. This was accompanied by a reduction in apoptosis and GRP78 expression. CHOP^{-/-} mice were protected from TM-induced AKI. The protective effects of 4-PBA extended to the ultrastructural integrity of proximal tubule cells in the outer medulla. When taken together, these results indicate that 4-PBA acts as an ER stress inhibitor, to partially protect the kidney from TM-induced AKI through the repression of ER stress-induced CHOP expression.

INTRODUCTION

Endoplasmic reticulum (ER) stress is caused by the accumulation of unfolded or misfolded proteins in the ER (2). The ER chaperone GRP78 binds to the accumulating unfolded proteins after dissociating from ER transmembrane proteins, where it is typically anchored. These anchor proteins then transduce the signals involved in initiating the unfolded protein response (UPR) (3). Initiation leads to the activation of three main UPR pathways, the inositol requiring enzyme-1 (IRE1) pathway, the activating transcription factor 6 (ATF6) pathway, and the protein kinase-like ER kinase (PERK) pathway (4). IRE1 can be found in yeast, and therefore represents the first evolved arm of the UPR. Upon activation, a UPR specific transcription factor (HAC1 in fungi, or XBP1 in animals) is cleaved in two specific positions. This results in a spliced transcript that is translated to the active form of XBP1. It is translocated to the nucleus to act as a transcription factor inducing the expression of UPR genes, including the molecular chaperones GRP78 and GRP94. When ATF6 is activated, it is translocated to the Golgi, where site 1 and site 2 proteases remove the luminal domain and the transmembrane anchor, respectively. This allows the N-terminal cytosolic fragment to translocate to the nucleus, activating UPR target genes (5). PERK is an ER-resident transmembrane kinase, which is autophosphorylated when unfolded or misfolded proteins accumulate in the ER. Phosphorylated PERK phosphorylates eIF2 α , which then leads to general protein translation attenuation and the increased transcription of ATF4. The expression of the ATF4 target CHOP, also known as GADD153, is induced, which increases the formation of the GADD34-PP1 complex. This goes on to dephosphorylate phosphorylated eIF2 α

(5). This re-initiation of protein synthesis through eIF2 α dephosphorylation may be why CHOP exerts proapoptotic effects in cells that have not yet resolved ER stress (1).

GRP78 and CHOP are well-established markers of ER stress and UPR activation. CHOP is a proapoptotic UPR response gene and may play a role in the contribution of ER stress to acute tubular necrosis (ATN) and the resulting acute kidney injury (AKI). AKI, the primary pathology of which is ATN, can be caused by ischemia (6, 7), nephrotoxic drugs (8, 9), or radiocontrast medium (10). The tubular injury in response to many of these insults has been associated with ER stress (8-10). In addition, tunicamycin (TM), a known inducer of ER stress, has previously been used as a model of antibiotic-induced AKI (11). It prevents N-linked glycosylation, and has both antibiotic and antiviral properties. Several other studies have shown its effects on the kidney, including upregulated ER stress response proteins, extensive tubular interstitial damage at the cortico-medullary junction, and increased apoptosis (1, 11-15).

4-phenylbutyrate (4-PBA) is a low molecular weight chemical chaperone that is currently approved for clinical use in urea cycle disorders. 4-PBA has 3 main biologic effects: it is an ammonia scavenger (16), a weak histone deacetylase (HDAC) inhibitor (17), and an ER stress inhibitor (18-20). It has been shown to restore glucose homeostasis in obese mice (21), and has been used in clinical trials for treatment of cystic fibrosis (22), sickle cell disease (23), neurodegenerative diseases (24) and certain cancers (25-27). Many of these intervention trials with 4-PBA have relied on the effect of this drug to reduce ER stress.

We therefore hypothesized that 4-PBA would prevent kidney damage in a TM model of AKI through inhibition of ER stress-induced CHOP expression. To investigate this

hypothesis, we examined a number of ER stress markers, as well as apoptotic markers both *in vitro* and *in vivo*. This is the first *in vivo* study, to our knowledge, detailing a renoprotective effect of 4-PBA in AKI.

METHODS

Ethics statement

All animal work was done in accordance with and approved by the McMaster University Animal Research Ethics Board.

Cell culture

HK-2 cells were used as a cell model system of human renal proximal tubular epithelial cells. These cells are an immortalized human proximal tubule cell line obtained from ATCC (28). HK-2 cells were cultured in a 1:1 ratio of DMEM 1 g/L glucose media (Invitrogen; Carlsbad, CA) and F12 GlutaMAX nutrient mix (Invitrogen) containing 1X penicillin/streptomycin antibiotic (Invitrogen) and 0.5X non-essential amino acids (Invitrogen). For Western blotting experiments, cells were grown to confluence on 6-well tissue culture plates (BD Falcon, Mississauga, Canada) and for apoptosis experiments, confluent cells were treated on borosilicate glass cover slips to allow subsequent microscopic analysis.

Reagents

DMSO (Sigma-Aldrich) was used to dissolve non-water soluble reagents and as a vehicle control. TM was purchased from Sigma-Aldrich (St. Louis, MO). 4-PBA sodium salt was purchased from Scandinavian Formulas (Sellersville, PA). Paraformaldehyde was obtained as a 4% solution in phosphate buffered saline (BioLynx Inc; Brockville, Canada) and used for fixation.

Animal studies

Wild type C57BL/6 mice were purchased from Charles River (Charles River Laboratories International, Inc., Wilmington, MA) and CHOP^{-/-} mice were obtained from Jackson Laboratories (Stock Number: 005530). Mice were maintained at McMaster University with free access to food and drinking water. Animals were housed with a 12-hour light dark cycle. Wild type animals ranging from 21-28 weeks of age were utilized to examine the effects of 4-PBA on AKI. Sham mice (N = 13) had a mean body weight of 33.2 g. TM-treated mice (N = 14) weighed on average 29.0 g. TM with 4-PBA-treated mice (N = 15) had an average weight of 28.9 g. Mice were given regular drinking water or 4-PBA (1 g/kg/day) in the drinking water for 10 days. On the seventh day, mice were intraperitoneally (I.P.) injected with TM (0.5 mg/kg). On the tenth day, mice were sacrificed, and kidneys were harvested. CHOP^{-/-} mice were utilized from 12-30 weeks of age. Sham mice (N = 4) had an average weight of 20.3 g, while TM-treated mice (N = 6) had a mean weight of 23.2 g. Mice were I.P. injected with TM and three days afterwards were sacrificed via exsanguination, and kidneys were harvested.

Assessment of renal pathology

Kidneys were sectioned and stained with Periodic Acid-Schiff reagent (PAS). Briefly, kidney sections were mounted on microscope slides. Sections (4 μm thick) were cut, air-dried, and deparaffinized through a series of xylene and graded ethanol (100%-70%). Slides were oxidized in 1% aqueous periodic acid, treated with Schiff reagent, counterstained with haematoxylin, and then mounted. The kidneys were scored for tubular damage by two independent investigators blinded to the treatment groups as follows: (0) 0% kidney damage, (1) 1-25% kidney damage, (2) 26-50% kidney damage, (3) >50% kidney damage. Damage was defined as vacuolization of the tubular epithelium, as well as its denudation and loss of cellular nuclei. Scores were collected then averaged to produce a single score for each animal. Kidney sections also underwent Masson's Trichrome staining to further evaluate tissue damage and fibrosis. Nine or more animals were scored in each treatment group.

Urine and plasma analysis

Animals were placed in metabolic cages prior to sacrifice. After 24 h, food and water intake were measured, and urine was collected. Urine was then sent to our in-house laboratory (St Joseph's Healthcare Hamilton) for levels of urinary protein to be measured. Animals were sacrificed via exsanguination; blood was collected from the left ventricle in heparinized tubes, and subsequently centrifuged to separate the plasma. Plasma samples were sent to our in-house laboratory for levels of plasma creatinine to be measured.

Gel electrophoresis

Total cell lysates were generated in 4X SDS lysis buffer with protease inhibitor cocktail (complete Mini; Roche; Laval, Canada) and phosphatase inhibitor cocktail added. Protein levels were determined using BioRad DC Protein Assay (BioRad, Mississauga, Canada) for control of protein loading. Cell lysates were subjected to electrophoretic separation in an SDS-PAGE reducing gel (BioRad). Primary antibodies were detected using appropriate horseradish peroxidase-conjugated secondary antibodies and ECL Western Blotting Detection Reagents (GE Healthcare, Mississauga, Canada), as described previously (29-31). CHOP antibody (sc-793, Santa Cruz Biotechnology; Santa Cruz, CA) was diluted 1:200, KDEL antibody (SPA-827, Stressgen) was diluted 1:1000, and β -actin antibody (Sigma) was diluted 1:4000. Results were densitometrically quantified using ImageJ software (NIH, Bethesda, MD, ver. 1.43) and expressed as a ratio of β -actin loading control.

Apoptosis assay

A terminal deoxynucleotidyl transferase dUTP nick end labelling (TUNEL) staining kit (TMR-In situ cell death detection kit, Roche) was utilized to label cells undergoing apoptosis *in vitro*, as previously described (32). Apoptotic cells and total cells were counted and analyzed using ImageJ software. Total cell counts were based on 4',6-diamidino-2-phenylindole (DAPI) nuclear staining. For cells to be considered TUNEL positive the red emission of the TMR-oligo tag was required to overlap with DAPI nuclear staining. This allowed the number of apoptosis-positive cells to be expressed as a percentage of total cells. Tissue sections were stained for apoptosis using the same

TUNEL assay kit according to the manufacturer's instructions. In this case, the level of apoptosis was expressed as the number of apoptotic cells per high-power field.

Transfections

HK-2 cells were transfected with pcDNA3.1 control vector alone or with the pcDNA3.1 vector containing the open reading frame for the human CHOP gene using FuGENE 6 transfection reagent (Roche) at a 6:1 ratio. Cells were then fixed with 4% paraformaldehyde, permeabilized, and stained with TUNEL and anti-CHOP antibodies (sc-575; Santa Cruz). HK-2 cells were transfected with CHOP siRNA (Thermo Scientific, Dharmacon ON-TARGET plus, SMARTpool) as per the manufacturer's instructions. Briefly, cells incubated overnight in a 6-well plate in antibiotic-free complete medium. siRNA and DharmaFECT transfection reagent were diluted in serum-free medium. After a five minute incubation, siRNA and DharmaFECT transfection reagent were combined and incubated for a further 20 mins. The transfection medium was then added to each well. Cells incubated at 37°C for 72 h, and were subsequently treated with TM for 48 h. Cells were then fixed with 4% paraformaldehyde and stained for TUNEL. A scrambled siRNA (Dharmacon, Non-targeting siRNA#1) was used as a siRNA transfection control.

Immunofluorescence

Sections (4 µm thick) were cut, air-dried, and deparaffinized through a series of xylene and graded ethanol (100%-70%). Heat-Induced Epitope Retrieval was performed in Retrieve-All-2 buffer (Signet Laboratories, Dedham, MA) pH 10, for 30 min followed by 0.1% Triton-X for 10 min at room temperature for CHOP staining (12). No antigen

retrieval was used for GRP78 staining (32). Tissues were stained for CHOP to determine if treatment with TM or 4-PBA resulted in modifications in the expression of this transcription factor. Sections were incubated with either a rabbit anti-CHOP antibody (1:40, sc-575; Santa Cruz Biotechnology) or a goat anti-GRP78 antibody (1:40, sc-1050; Santa Cruz Biotechnology). The primary antibody was detected using a species-specific secondary antibody conjugated to an Alexa dye at 647 nm excitation wavelength, producing an emission maximum at 668 nm in the far-red region of the spectrum (1:500; Invitrogen). This emission wavelength was used due to the high levels of autofluorescence in the renal tubular epithelium at the typical emission wavelengths for FITC (520 nm) or tetramethylrhodamine (580 nm). Sections were incubated with 100 ng/ml DAPI to label cell nuclei and mounted with Permafluor (Thermo Scientific).

Fluorescence microscopy

An Olympus IX81 Nipkow scanning disc confocal microscope was used for fluorescence microscopy. Image analysis was performed using Metamorph image analysis software (Molecular Devices, Sunnyvale, CA), as previously (32). CHOP-positive cell nuclei were counted and expressed as a percent of total cell nuclei. Cell nuclei were identified with DAPI DNA-based staining and quantified using the cell scoring application in Metamorph software (ver 7.71). Utilizing this system, cell nuclei were gated to be between 5 and 20 microns in size and positivity for CHOP was assessed by significantly increased fluorescence intensity over tubular epithelial background utilizing Adaptive background correction™. Apoptotic cells were counted and expressed as the number of TUNEL positive nuclei in each high power field. CHOP analysis

consisted of nine animals per group, while TUNEL analysis consisted of six animals per group. Six microscope fields were randomly sampled in both the cortex and the medulla. This allowed the quantification of approximately 5000 cells for CHOP or TUNEL staining per animal per kidney region. GRP78 positive cells were quantified by thresholding for the specific emission of the secondary antibody tag (665 nm), and allowing the software to detect the percent thresholded area for each image, producing the area density of the quantified protein.

Transmission electron microscopy (TEM)

TEM was performed to assess the ultrastructural features of the proximal tubular cells (pars recta) of the outer medulla in wild type sham-, TM-, and TM + 4-PBA-treated mice, as well as CHOP^{-/-} mice with or without TM treatment. Briefly, kidney tissues were fixed in 2% glutaraldehyde in 0.1 M cacodylate buffer, followed by fixation in 1% OsO₄ in 0.1 M cacodylate buffer. The tissue was then dehydrated in a graded series of ethanol and embedded in Spurr's resin for ultra-thin sectioning. Toluidine blue sections were cut to visualize the outer stripe of the medulla and once localized, were marked to allow the blocks to be trimmed for ultra-thin sectioning in this region. Ultra-thin sections were cut to approximately 100 nm in thickness with an ultramicrotome. Sections were then stained with uranyl acetate and lead citrate and observed with a JEOL 1200EX TEMSCAN (Tokyo, Japan) at 80 KV.

Statistical analysis

Quantitative results were expressed as the mean \pm SEM and statistically analyzed using the Student's t-test. The significance of differences in the means was assigned at a level of less than a 5% probability ($P < 0.05$) of the difference occurring by chance.

RESULTS

Wild type C57BL/6 mice were randomized into three groups: (1) control (VEH), treated with saline (I.P.; N = 13), (2) treated with TM (0.5 mg/kg, I.P.; N = 14) or (3) co-treated with TM (0.5 mg/kg, I.P.) and 4-PBA (1 g/kg/day, drinking water; N = 15). Mouse kidney sections stained with PAS were examined for pathology in the major anatomical structures of the kidney to determine the precise location of the TM-induced AKI. The outer stripe of the outer medulla was the major region of damage induced by TM injection at this dose. The pars recta were identified as straight segments of proximal tubule, as shown by the presence of a prominent PAS-positive brush border. Damage was characterized by tubular atrophy, loss of brush border and epithelial cell vacuolization in the proximal tubule cells of the pars recta of the outer stripe of the outer medulla (Figure 1A, arrows). These changes were observed less frequently in animals pre-treated with 4-PBA. TM-injected animals also showed damage to the proximal convoluted tubules of the renal cortex with epithelial cell vacuolization (Figure 1A, arrow), as observed previously (12). Treatment with 4-PBA partially inhibited this injury. The vascular bundles of the renal medulla showed no gross histological change upon TM treatment (Figure 1A). The kidneys were scored as described in the methods. Results show that mice treated with TM

alone displayed significantly more damage when compared with saline-treated mice. Mice co-treated with TM and 4-PBA suffered from less kidney damage than TM alone-treated mice, particularly in the pars recta (arrows; Figure 1B and 1C). Substantive proteinuria was not expected in this model at the 0.5 mg/kg dose of TM, however, proteinuria levels were measured and no statistical significance was found between any of the groups. 24 h protein levels were as follows: VEH, 6.23 ± 2.05 mg; TM, 3.13 ± 1.29 mg; TM \pm 4-PBA, 5.07 ± 0.60 mg.

To assess if the renal damage involved interstitial fibrosis, mouse kidney sections were stained with Masson's Trichrome. Similar to PAS staining, Masson's Trichrome staining demonstrated that most damage in the kidney occurred in the outer stripe of the outer medulla (Figure 2, arrows). A significant amount of damage occurred in TM-treated mice, but not in TM + 4-PBA-treated mice (Figure 2). Trichrome staining also revealed that TM-induced AKI did not elicit a fibrotic response.

To determine if TM-induced AKI at the 0.5 mg/kg dose resulted in detectable functional damage, creatinine levels were measured. Blood was collected from mice immediately prior to sacrifice. Blood plasma was subsequently analyzed, and it was determined that creatinine levels for TM and TM + 4-PBA treatment groups did not statistically differ from controls. Creatinine concentrations were as follows: VEH, 37.3 ± 1.86 $\mu\text{mol/L}$; TM-treated, 34.5 ± 2.23 $\mu\text{mol/L}$; TM + PBA-treated, 40.0 ± 1.25 $\mu\text{mol/L}$.

Since previous work had determined that CHOP^{-/-} mice were protected against TM-induced AKI (1), we attempted to elucidate whether 4-PBA, through its action as an ER stress inhibitor, could repress CHOP expression. In these experiments, HK-2 cells were used as a model of human proximal tubule cells *in vitro*. Cells were treated with VEH,

TM, 4-PBA, or TM with 4-PBA for 24 h, and were analyzed via Western blotting (Figure 3A). Tunicamycin treatment increased GRP78 expression, confirming UPR induction. 4-PBA alone did not increase GRP78 expression nor did it repress GRP78 expression when combined with TM treatment (Figure 3B). Densitometric analysis indicated that TM treatment also upregulated CHOP expression in HK-2 cells, while 4-PBA did not. Further, 4-PBA partially prevented TM-induced CHOP expression in human proximal tubular cells (Figure 3C).

To determine if TM treatment increased apoptotic cell death in human proximal tubule cells and if 4-PBA would inhibit this effect, TUNEL staining was performed in HK-2 cells. Apoptotic cell death was measured in cells treated with VEH, TM, TM with 4-PBA, or 4-PBA alone for 24 h. Results indicate that TM treatment resulted in significantly more apoptotic cell death than VEH-treated cells. Furthermore, co-treatment with 4-PBA prevented the apoptosis (Figure 4A). To determine if CHOP overexpression alone was capable of inducing apoptosis, a pcDNA3.1 plasmid vector containing the coding region for the human CHOP protein was transfected into HK-2 cells. Cells overexpressing CHOP demonstrated significantly more apoptosis than vector control-transfected cells (Figure 4B). To determine if CHOP was responsible for the apoptosis induced by TM treatment, HK-2 cells were subjected to siRNA knockdown of CHOP, and treated with 1 $\mu\text{g}/\text{ml}$ of TM for 48 h. Non-transfected cells treated with TM resulted in a significant increase in apoptosis. Cells transfected with CHOP siRNA and treated with TM showed a reduced level of apoptosis. TM-induced apoptosis was not affected by the scrambled siRNA control (scRNA; Figure 4C).

Kidney sections from the animal treatment groups were stained for CHOP (red) and its expression analyzed in both the cortex and medulla (Figure 5A). Results indicate that TM treatment induced CHOP expression in the cortex to some degree; however, CHOP expression was much greater in the renal medulla. Treatment with 4-PBA significantly inhibited TM-induced medullary CHOP expression (Figure 5B); however, it did not inhibit the lower levels of TM-induced CHOP expression in the renal cortex (Figure 5C). Kidney sections stained for CHOP were viewed in combination with 488 nm stimulated renal autofluorescence as viewed through a FITC band pass filter (green) to show renal anatomy and DAPI staining (blue) to identify nuclei. This demonstrated that the main area of CHOP staining occurred in the nuclei of proximal tubule cells of the pars recta in the outer stripe of the medulla. Confocal imaging spatially located this CHOP-linked immunofluorescent signal to the nuclei of this cell type (Figure 5D).

To determine if TM treatment increased apoptotic cell death in kidney cells *in vivo* and if 4-PBA would inhibit this effect, kidney sections were stained for apoptotic cell death with the TUNEL procedure (Figure 6A). Apoptotic cell death was measured in the renal cortex and medulla of mice treated with VEH, TM, or TM with 4-PBA. Results indicate that TM treatment resulted in significantly more apoptotic cell death than VEH-treated cells in the renal medulla (Figure 6B) but not in the renal cortex (Figure 6C). In addition, co-treatment with 4-PBA prevented the programmed cell death in the renal medulla. Confocal images of kidney sections stained with TUNEL were viewed in combination with renal autofluorescence and DAPI staining as above, demonstrating that the main area of apoptosis occurred where renal damage occurred and the TUNEL signal originated from the nuclei of the pars recta (Figure 6D)

To determine if treatment with 4-PBA affected the expression of other ER stress markers in the cortex or the medulla, kidneys were stained for GRP78 (Figure 7A). Analysis demonstrated that GRP78 expression was significantly increased in the medulla of TM-treated kidneys; this effect was inhibited by 4-PBA (Figure 7B). GRP78 expression was not increased in the cortex (Figure 7C).

To investigate whether increased CHOP expression alone may be responsible for the AKI induced by our TM model and whether inhibiting CHOP expression could explain 4-PBA's protective effect, CHOP^{-/-} mice were subjected to the TM model. PAS staining was used to examine kidney damage in wild type and CHOP^{-/-} mouse kidneys. As previously described, wild type TM-treated mouse kidneys suffered from tubular atrophy, loss of brush border, and epithelial cell vacuolization in the outer stripe of the outer medulla (arrow). However, CHOP^{-/-} mice treated with TM did not suffer from any noticeable kidney damage and showed intact pars recta (*) (Figure 8). Blood plasma was analyzed for serum creatinine, and it was determined that creatinine levels from TM-treated CHOP^{-/-} mice did not differ from levels from wild type mice (wild type, 34.5 ± 2.23 vs CHOP^{-/-}, 34.8 ± 1.19 $\mu\text{mol/L}$), both of which were within the normal range.

To determine if 4-PBA preserved the ultrastructural integrity of proximal tubule cells with TM treatment, we utilized TEM. Care was taken to focus on the outer medullary stripe. Wild type TM-treated mice demonstrated severe ultrastructural injury in proximal tubule cells. Examination of a number of cellular organelles, including nuclei, mitochondria, rough ER, as well as microvilli, revealed that 4-PBA inhibited TM-induced ultrastructural injury. Further, the ultrastructure of TM-treated CHOP^{-/-} mice appeared

similar to that of VEH-treated wild type and CHOP^{-/-} mice and showed less ultrastructural abnormalities than TM-treated wild type mice (Figure 9).

DISCUSSION

TM is a well-known ER stress inducer, and has previously been used as a model of antibiotic-induced AKI (11, 12). Using mouse embryonic fibroblasts, researchers demonstrated that knockout of CHOP inhibits TM-induced effects, including decreased levels of GADD34 expression, and increased phosphorylation of eIF2 α . CHOP knockout also prevents TM-induced AKI in mice. CHOP heterozygous mice treated with TM suffered from pyknotic nuclei (a marker of apoptosis), cellular casts in the urine, and cellular debris in the tubules, unlike CHOP^{-/-} mice. CHOP^{-/-} mice also displayed significantly less apoptosis. Additionally, in mice with mutant GADD34 incompetent to bind to PP1 and dephosphorylate eIF2 α , protection against TM-induced AKI is similarly observed (1). This model of ER stress-induced AKI differed from our model only in the dose of TM applied, where previously 1.0 mg/kg was used, we used a lower dose of 0.5 mg/kg. Our results in regard to the protective effect of CHOP knockout at this lower dose of AKI induction are in agreement with the previous study.

We found that 4-PBA was able to prevent or partially prevent the pathologic changes associated with TM-induced AKI. As previously mentioned, 4-PBA has an effect as an ER stress inhibitor (18-20); however, 4-PBA also acts as a HDAC inhibitor (17). Its effects on protein acetylation may extend beyond those affecting histones. HDAC inhibitors are known to prevent deacetylation of spliced XBP1, increasing stability and

transcriptional activity (33). Spliced XBP1 is a key transcriptional inducer of the IRE1 arm of the UPR and may protect against apoptosis by upregulating the expression of protein folding chaperones, including GRP78 (34). If 4-PBA increased spliced XBP1 stability and transcriptional activity, it may have led to increased GRP78 expression early in TM-induced AKI (18-24 hours). This would have resulted in reduced UPR activation through GRP78-mediated repression of PERK and IRE1 autophosphorylation. Diminished PERK response would then have resulted in the lower TM-induced CHOP expression observed at the 3-day time point. However, we found a repression of GRP78 expression at the 3-day time point in our TM model, coinciding with CHOP repression. This suggests that the primary mode of action for 4-PBA, in the animal model, was to repress ER stress in general and protect against renal epithelial cell death unrelated to its HDAC inhibitor properties. A similar effect of 4-PBA treatment on the inhibition of TM-induced neuronal cell death was attributed to be due to its protein folding chaperone properties, rather than its HDAC inhibitor properties through the derivation of compounds with similar molecular structure but varying protein folding chaperone and HDAC inhibitor properties (35).

4-PBA has previously been shown to repress ER stress. Liver and adipose tissue of *ob/ob* mice treated with 4-PBA displayed significantly lower levels of the ER stress markers, phospho-PERK and phospho-IRE1, when compared with vehicle-treated mice (21). Similar results were found *in vitro*, with reduced levels of GRP78 and phospho-eIF2 α found in rat hepatoma cells treated with 4-PBA (36). In fact, 4-PBA may even alleviate lipid-induced insulin resistance and β -cell dysfunction in obese individuals by inhibiting ER stress (19). The main effect of 4-PBA treatment on human proximal tubular

cells *in vitro* was to repress the pro-apoptotic gene CHOP induced by TM treatment while maintaining cytoprotective levels of GRP78 expression. Further, we demonstrated through plasmid-mediated CHOP expression that CHOP overexpression alone was capable of inducing proximal tubular cell apoptosis and that the siRNA-mediated inhibition of CHOP expression prevented apoptosis.

In the animal model, TM-induced AKI resulted in increased GRP78 and CHOP staining in mouse kidneys, indicating the development of ER stress. As previously noted, GRP78 is a common marker of ER stress, as it binds to unfolded or misfolded proteins in the ER and is transcriptionally upregulated by ER stress through the UPR (2). CHOP is a transcription factor involved in ER stress, and has been characterized as a pro-apoptotic protein (1). Treatment with TM increased levels of ER stress markers, such as CHOP, particularly in the pars recta of the renal medulla. Others have demonstrated intense CHOP nuclear staining in the cortex of kidneys from TM-treated mice (11). We suspect this variation is due to different concentrations of TM treatment, with higher concentrations causing more severe renal damage in the cortex. As previously mentioned, we treated our mice with 0.5 mg/kg TM, while researchers demonstrating cortical CHOP staining utilized a higher dose of 1.0 mg/kg TM (11). Treatment with 4-PBA resulted in significantly lower levels of ER stress marker proteins, demonstrating inhibition of ER stress in the kidney with 4-PBA treatment. These results indicate that the major mechanism by which 4-PBA prevents TM-induced AKI may be through inhibition of ER stress. This inhibition of ER stress in the kidneys also coincided with 4-PBA's inhibition of renal apoptosis in the pars recta.

Through our TEM examination, we found that treatment with 4-PBA prevented TM-mediated ultrastructural damage to the proximal tubule cells in the pars recta of the outer medulla. We found through ultrastructural examination that CHOP knock out had a protective effect against TM, similar to treatment with 4-PBA. We suggested previously that 4-PBA prevents TM-induced kidney damage through the inhibition of ER stress. Since we have demonstrated that 4-PBA inhibits the expression of CHOP induced by TM and that CHOP^{-/-} mice are also protected at the ultrastructural level from TM-induced toxicity, we conclude that 4-PBA prevents TM-induced kidney damage through a CHOP-mediated mechanism.

As such, the ability of 4-PBA to directly aid in the reduction of misfolded proteins in the ER (37, 38) appears to be the molecular mechanism behind its ability to inhibit ER stress, as shown by repressed UPR marker expression of both GRP78 and CHOP *in vivo*. In particular, the reduction in CHOP expression may be responsible for preventing the tubular damage associated with TM-induced nephrotoxicity. This conclusion is corroborated by previous reports demonstrating similar results, in which CHOP^{-/-} and GADD34 mutant mice were protected from TM-induced kidney damage. In these studies, wild type mice suffered from extensive tubular interstitial damage, including apoptosis at the cortico-medullary junction (1), similar to ATN. A further study demonstrated that TRIF-dependent toll-like receptor engagement, brought about by lipopolysaccharide treatment, repressed CHOP expression and renal injury in TM-treated mice (39). As mentioned, these TM-induced insults are comparable to our results, suggesting that ER stress is the main mechanism by which TM causes AKI. This also indicates that it is by inhibiting ER stress, and in particular CHOP expression, that 4-PBA protects the kidney

from the damage caused by TM. To confirm these findings we also subjected CHOP^{-/-} mice to our model of TM-induced AKI and demonstrated that CHOP deletion in the presence of TM treatment prevented ER stress-induced AKI, at both a light level and ultrastructurally. Thus, 4-PBA, being an approved pharmaceutical with demonstrated CHOP repressing action, becomes a practical technique to modulate CHOP expression.

CONCLUSIONS

4-PBA prevents TM-induced AKI in C57BL/6 mice. The main mechanism of 4-PBA's inhibitory effect appears to be the repression of CHOP expression *in vitro* in human proximal tubular cells and *in vivo* in the proximal tubule of the outer stripe of the outer medulla. 4-PBA's inhibition of CHOP expression is correlated with its ability to inhibit TM-induced apoptosis. Thus, our results support the hypothesis that 4-PBA exerts its protective effects on TM-induced AKI by inhibiting CHOP expression through the inhibition of ER stress. Given the fact that 4-PBA is in current clinical use and is well-tolerated, it is an attractive agent for study in situations where AKI might be expected to occur.

REFERENCES

1. Marciniak SJ, Yun CY, Oyadomari S, Novoa I, Zhang Y, Jungreis R, et al. CHOP induces death by promoting protein synthesis and oxidation in the stressed endoplasmic reticulum. *Genes Dev.* 2004;18(24):3066-77.
2. Schroder M, Kaufman RJ. ER stress and the unfolded protein response. *Mutat Res.* 2005;569(1-2):29-63.
3. Dickhout JG, Carlisle RE, Austin RC. Inter-Relationship between Cardiac Hypertrophy, Heart Failure and Chronic Kidney Disease – Endoplasmic Reticulum Stress as a Mediator of Pathogenesis. *Circ Res.* 2011;108(5):629-42.
4. Dickhout JG, Krepinsky JC. Endoplasmic reticulum stress and renal disease. *Antioxid Redox Signal.* 2009;11(9):2341-52.
5. Walter P, Ron D. The unfolded protein response: from stress pathway to homeostatic regulation. *Science.* 2011;334(6059):1081-6.
6. Prachasilchai W, Sonoda H, Yokota-Ikeda N, Ito K, Kudo T, Imaizumi K, et al. The protective effect of a newly developed molecular chaperone-inducer against mouse ischemic acute kidney injury. *J Pharmacol Sci.* 2009;109(2):311-4.
7. Prachasilchai W, Sonoda H, Yokota-Ikeda N, Oshikawa S, Aikawa C, Uchida K, et al. A protective role of unfolded protein response in mouse ischemic acute kidney injury. *Eur J Pharmacol.* 2008;592(1-3):138-45.
8. Peyrou M, Hanna PE, Cribb AE. Calpain inhibition but not reticulum endoplasmic stress preconditioning protects rat kidneys from p-aminophenol toxicity. *Toxicol Sci.* 2007;99(1):338-45.
9. Peyrou M, Cribb AE. Effect of endoplasmic reticulum stress preconditioning on cytotoxicity of clinically relevant nephrotoxins in renal cell lines. *Toxicol In Vitro.* 2007;21(5):878-86.
10. Wu CT, Sheu ML, Tsai KS, Weng TI, Chiang CK, Liu SH. The role of endoplasmic reticulum stress-related unfolded protein response in the radiocontrast medium-induced renal tubular cell injury. *Toxicol Sci.* 2010;114(2):295-301.
11. Zinszner H, Kuroda M, Wang X, Batchvarova N, Lightfoot RT, Remotti H, et al. CHOP is implicated in programmed cell death in response to impaired function of the endoplasmic reticulum. *Genes Dev.* 1998;12(7):982-95.
12. Lhotak S, Sood S, Brimble E, Carlisle RE, Colgan SM, Mazzetti A, et al. ER stress contributes to renal proximal tubule injury by increasing SREBP-2-mediated lipid

- accumulation and apoptotic cell death. *Am J Physiol Renal Physiol*. 2012;303(2):F266-78.
13. Yan K, Khoshnoodi J, Ruotsalainen V, Tryggvason K. N-linked glycosylation is critical for the plasma membrane localization of nephrin. *J Am Soc Nephrol*. 2002;13(5):1385-9.
 14. Nakagawa T, Zhu H, Morishima N, Li E, Xu J, Yankner BA, et al. Caspase-12 mediates endoplasmic-reticulum-specific apoptosis and cytotoxicity by amyloid-beta. *Nature*. 2000;403(6765):98-103.
 15. Huang L, Zhang R, Wu J, Chen J, Grosjean F, Satlin LH, et al. Increased susceptibility to acute kidney injury due to endoplasmic reticulum stress in mice lacking tumor necrosis factor-alpha and its receptor 1. *Kidney Int*. 2011;79(6):613-23.
 16. Lichter-Konecki U, Diaz GA, Merritt JL, 2nd, Feigenbaum A, Jomphe C, Marier JF, et al. Ammonia control in children with urea cycle disorders (UCDs); phase 2 comparison of sodium phenylbutyrate and glycerol phenylbutyrate. *Mol Genet Metab*. 2011;103(4):323-9.
 17. Miller AC, Cohen S, Stewart M, Rivas R, Lison P. Radioprotection by the histone deacetylase inhibitor phenylbutyrate. *Radiat Environ Biophys*. 2011;50(4):585-96.
 18. Basseri S, Lhotak S, Sharma AM, Austin RC. The chemical chaperone 4-phenylbutyrate inhibits adipogenesis by modulating the unfolded protein response. *J Lipid Res*. 2009;50:2486-501.
 19. Xiao C, Giacca A, Lewis GF. Sodium phenylbutyrate, a drug with known capacity to reduce endoplasmic reticulum stress, partially alleviates lipid-induced insulin resistance and beta-cell dysfunction in humans. *Diabetes*. 2011;60(3):918-24.
 20. Yam GH, Gaplovska-Kysela K, Zuber C, Roth J, Yam GH-F, Gaplovska-Kysela K, et al. Sodium 4-phenylbutyrate acts as a chemical chaperone on misfolded myocilin to rescue cells from endoplasmic reticulum stress and apoptosis. *Investigative Ophthalmology & Visual Science*. 2007;48(4):1683-90.
 21. Ozcan U, Yilmaz E, Ozcan L, Furuhashi M, Vaillancourt E, Smith RO, et al. Chemical chaperones reduce ER stress and restore glucose homeostasis in a mouse model of type 2 diabetes. *Science*. 2006;313(5790):1137-40.
 22. Loffing J, Moyer BD, Reynolds D, Stanton BA. PBA increases CFTR expression but at high doses inhibits Cl(-) secretion in Calu-3 airway epithelial cells. *Am J Physiol*. 1999;277(4 Pt 1):L700-8.

23. Collins AF, Pearson HA, Giardina P, McDonagh KT, Brusilow SW, Dover GJ. Oral sodium phenylbutyrate therapy in homozygous beta thalassemia: a clinical trial. *Blood*. 1995;85(1):43-9.
24. Mimori S, Okuma Y, Kaneko M, Kawada K, Hosoi T, Ozawa K, et al. Protective effects of 4-phenylbutyrate derivatives on the neuronal cell death and endoplasmic reticulum stress. *Biol Pharm Bull*. 2012;35(1):84-90.
25. Dyer ES, Paulsen MT, Markwart SM, Goh M, Livant DL, Ljungman M. Phenylbutyrate inhibits the invasive properties of prostate and breast cancer cell lines in the sea urchin embryo basement membrane invasion assay. *Int J Cancer*. 2002;101(5):496-9.
26. Carducci MA, Nelson JB, Chan-Tack KM, Ayyagari SR, Sweatt WH, Campbell PA, et al. Phenylbutyrate induces apoptosis in human prostate cancer and is more potent than phenylacetate. *Clin Cancer Res*. 1996;2(2):379-87.
27. Phuphanich S, Baker SD, Grossman SA, Carson KA, Gilbert MR, Fisher JD, et al. Oral sodium phenylbutyrate in patients with recurrent malignant gliomas: a dose escalation and pharmacologic study. *Neuro Oncol*. 2005;7(2):177-82.
28. Ryan MJ, Johnson G, Kirk J, Fuerstenberg SM, Zager RA, Torok-Storb B. HK-2: an immortalized proximal tubule epithelial cell line from normal adult human kidney. *Kidney Int*. 1994;45(1):48-57.
29. Hossain GS, van Thienen JV, Werstuck GH, Zhou J, Sood SK, Dickhout JG, et al. TDAG51 is induced by homocysteine, promotes detachment-mediated programmed cell death, and contributes to the development of atherosclerosis in hyperhomocysteinemia. *J Biol Chem*. 2003;278(32):30317-27.
30. Dickhout JG, Lhotak S, Hilditch BA, Basseri S, Colgan SM, Lynn EG, et al. Induction of the unfolded protein response after monocyte to macrophage differentiation augments cell survival in early atherosclerotic lesions. *FASEB J*. 2011;25(2):576-89.
31. Dickhout JG, Carlisle RE, Jerome DE, Mohammed-Ali Z, Jiang H, Yang G, et al. Integrated stress response modulates cellular redox state via induction of cystathionine gamma-lyase: cross-talk between integrated stress response and thiol metabolism. *J Biol Chem*. 2012;287(10):7603-14.
32. Carlisle RE, Heffernan A, Brimble E, Liu L, Jerome D, Collins CA, et al. TDAG51 mediates epithelial-to-mesenchymal transition in human proximal tubular epithelium. *Am J Physiol Renal Physiol*. 2012;303(3):F467-81.

33. Wang FM, Chen YJ, Ouyang HJ. Regulation of unfolded protein response modulator XBP1s by acetylation and deacetylation. *Biochem J.* 2011;433(1):245-52.
34. Hosoi T, Korematsu K, Horie N, Suezawa T, Okuma Y, Nomura Y, et al. Inhibition of casein kinase 2 modulates XBP1-GRP78 arm of unfolded protein responses in cultured glial cells. *PLoS One.* 2012;7(6):e40144.
35. Mimori S, Ohtaka H, Koshikawa Y, Kawada K, Kaneko M, Okuma Y, et al. 4-Phenylbutyric acid protects against neuronal cell death by primarily acting as a chemical chaperone rather than histone deacetylase inhibitor. *Bioorg Med Chem Lett.* 2013;23(21):6015-8.
36. Ota T, Gayet C, Ginsberg HN. Inhibition of apolipoprotein B100 secretion by lipid-induced hepatic endoplasmic reticulum stress in rodents. *J Clin Invest.* 2008;118(1):316-32.
37. de Almeida SF, Picarote G, Fleming JV, Carmo-Fonseca M, Azevedo JE, de Sousa M. Chemical chaperones reduce endoplasmic reticulum stress and prevent mutant HFE aggregate formation. *J Biol Chem.* 2007;282(38):27905-12.
38. Wang WJ, Mulugeta S, Russo SJ, Beers MF. Deletion of exon 4 from human surfactant protein C results in aggresome formation and generation of a dominant negative. *J Cell Sci.* 2003;116(Pt 4):683-92.
39. Woo CW, Cui D, Arellano J, Dorweiler B, Harding H, Fitzgerald KA, et al. Adaptive suppression of the ATF4-CHOP branch of the unfolded protein response by toll-like receptor signalling. *Nat Cell Biol.* 2009;11(12):1473-80.

Figure 1.

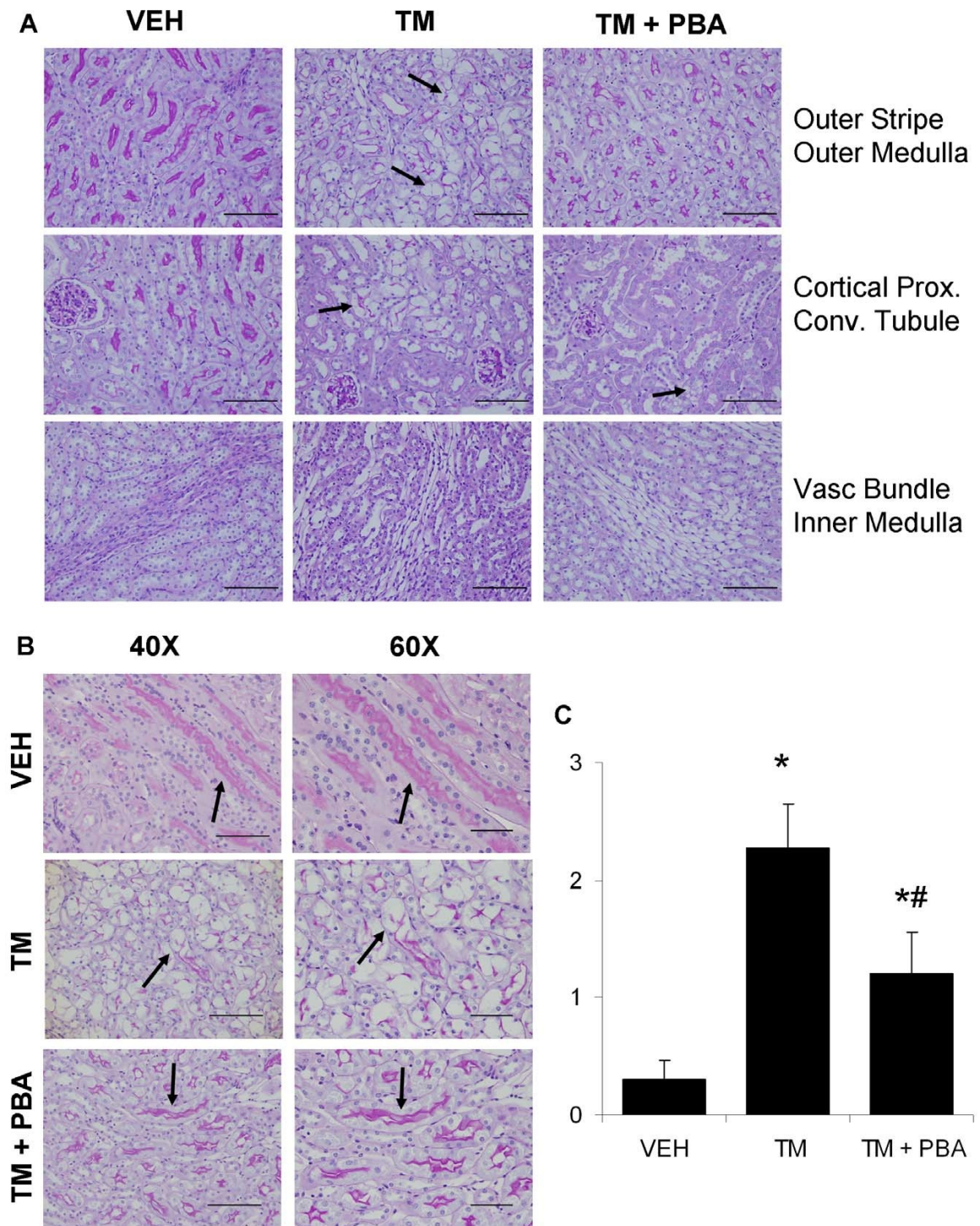


Figure 1. Anatomical structures affected by tunicamycin (TM)-induced acute kidney injury. C57BL/6 wild type mice were treated with saline (VEH), TM for 3 days, or pre-treated with 4-PBA for 7 days followed by 3 days of TM and 4-PBA co-treatment. PAS staining of mouse kidney sections indicate that TM causes acute kidney injury primarily in the outer stripe of the outer medulla (Outer Stripe Outer Medulla, arrows) of the kidney. 4-PBA treatment combined with TM inhibits this effect. TM also induced cortical proximal convoluted tubule (Cortical Prox. Conv. Tubule, arrow) damage; this effect was only partially inhibited by 4-PBA (arrow). Vascular bundles (Vasc Bundle Inner Medulla) were unaffected by TM-induced acute kidney injury at this dose (0.5 mg/kg) or 4-PBA treatment (A; bar = 100 μ m). Higher magnification images show the pars recta of the outer medulla in all treatment groups (arrows) and the damage induced by TM and its inhibition by 4-PBA (B; 40X, bar = 100 μ m; 60X, bar = 50 μ m). The PAS-stained kidneys were scored for tubular damage as follows: (0) 0% kidney damage, (1) 1-25% kidney damage, (2) 26-50% kidney damage, (3) >50% kidney damage. Results indicate that 4-PBA inhibits tubular damage mediated by TM treatment (C). N = 10. *, P<0.05 vs VEH; #, P<0.05 vs TM.

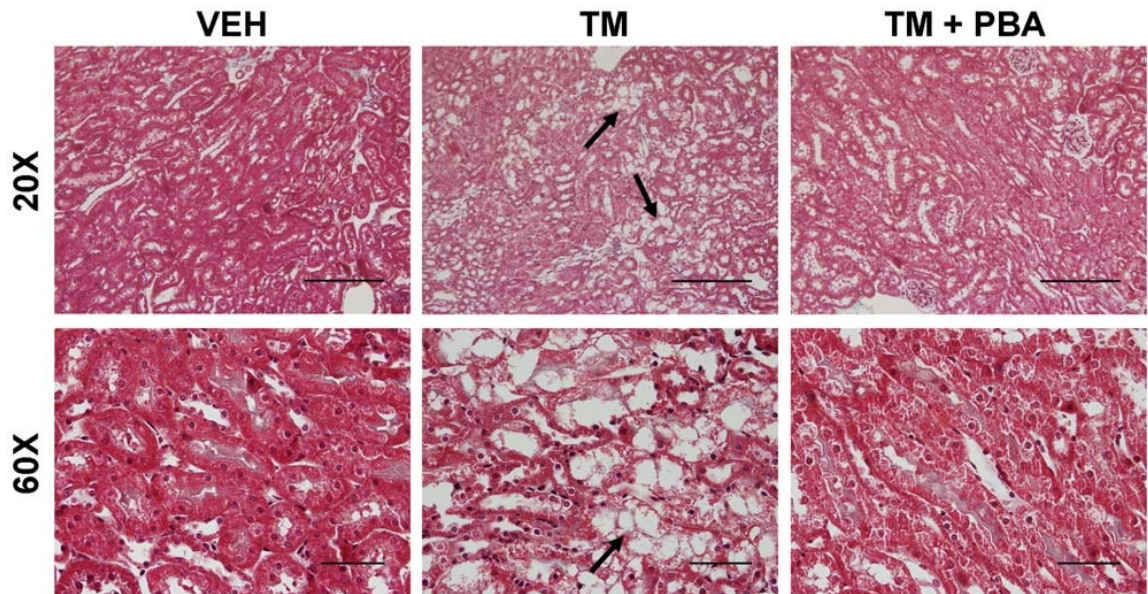


Figure 2. Damage to the outer stripe of the outer medulla is induced by tunicamycin (TM). C57BL/6 wild type mice were treated with saline (VEH), TM for 3 days, or pre-treated with 4-PBA for 7 days followed by 3 days of TM and 4-PBA co-treatment. Masson's Trichrome staining of mouse kidney sections indicate that TM causes acute kidney injury in the outer stripe of the outer medulla (arrows). This damage is prevented by co-treatment with 4-PBA. However, renal interstitial fibrosis was not induced by treatment with TM or 4-PBA (20X, bar = 200 μ m; 60X, bar = 50 μ m).

Figure 3.

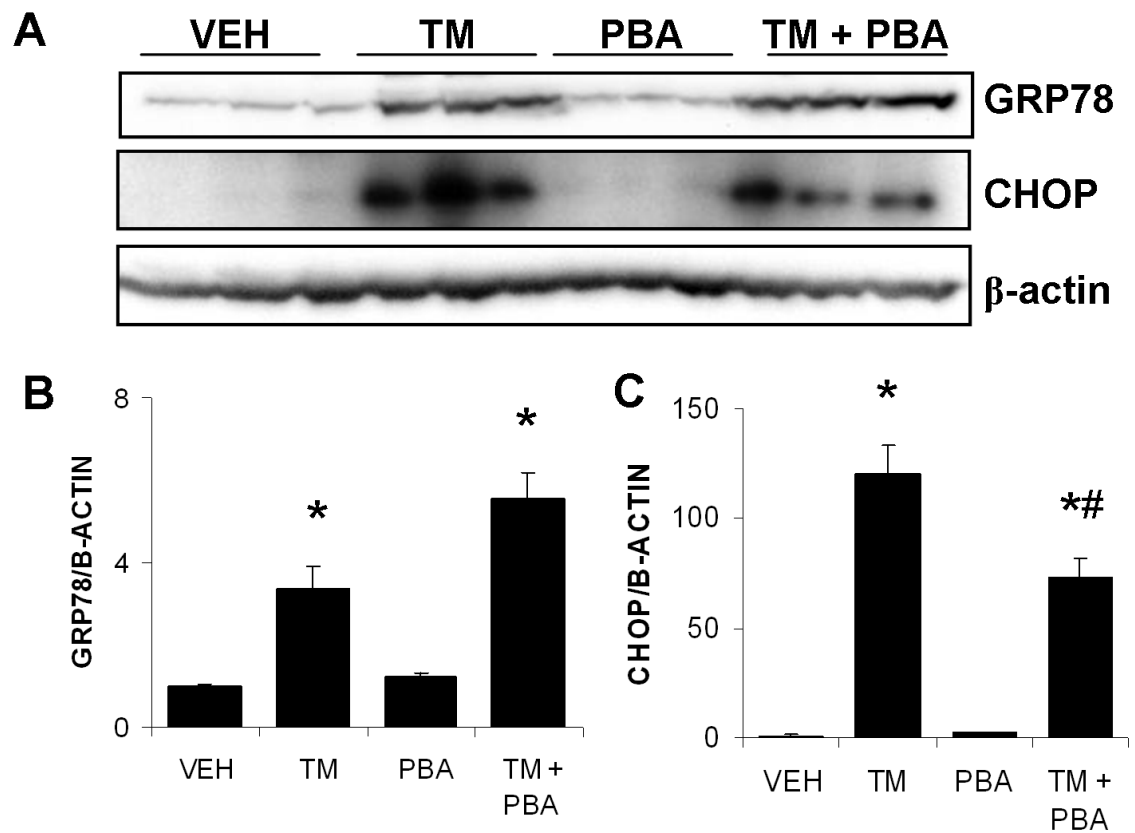


Figure 3. 4-PBA significantly inhibits tunicamycin (TM)-induced CHOP expression.

HK-2 cells were treated with DMSO (VEH), TM (1 µg/ml), 4-PBA alone (1 mM), or TM with 4-PBA for 24 h. Cells were lysed and underwent Western blotting for GRP78, CHOP and β-actin (A). Densitometric analysis indicates that TM treatment significantly upregulated GRP78 expression. A combined treatment of TM with 4-PBA also resulted in increased GRP78 expression over VEH, but did not show increased expression over TM treatment. 4-PBA alone had no effect on GRP78 expression (B). CHOP expression was increased in response to TM treatment. Co-treatment of TM and 4-PBA resulted in increased CHOP expression, which was significantly higher than VEH treatment, but significantly lower than TM alone treatment. 4-PBA alone-treated cells showed no difference in CHOP expression, when compared with VEH (C). *, P<0.05 vs VEH; #, P<0.05 vs TM.

Figure 4.

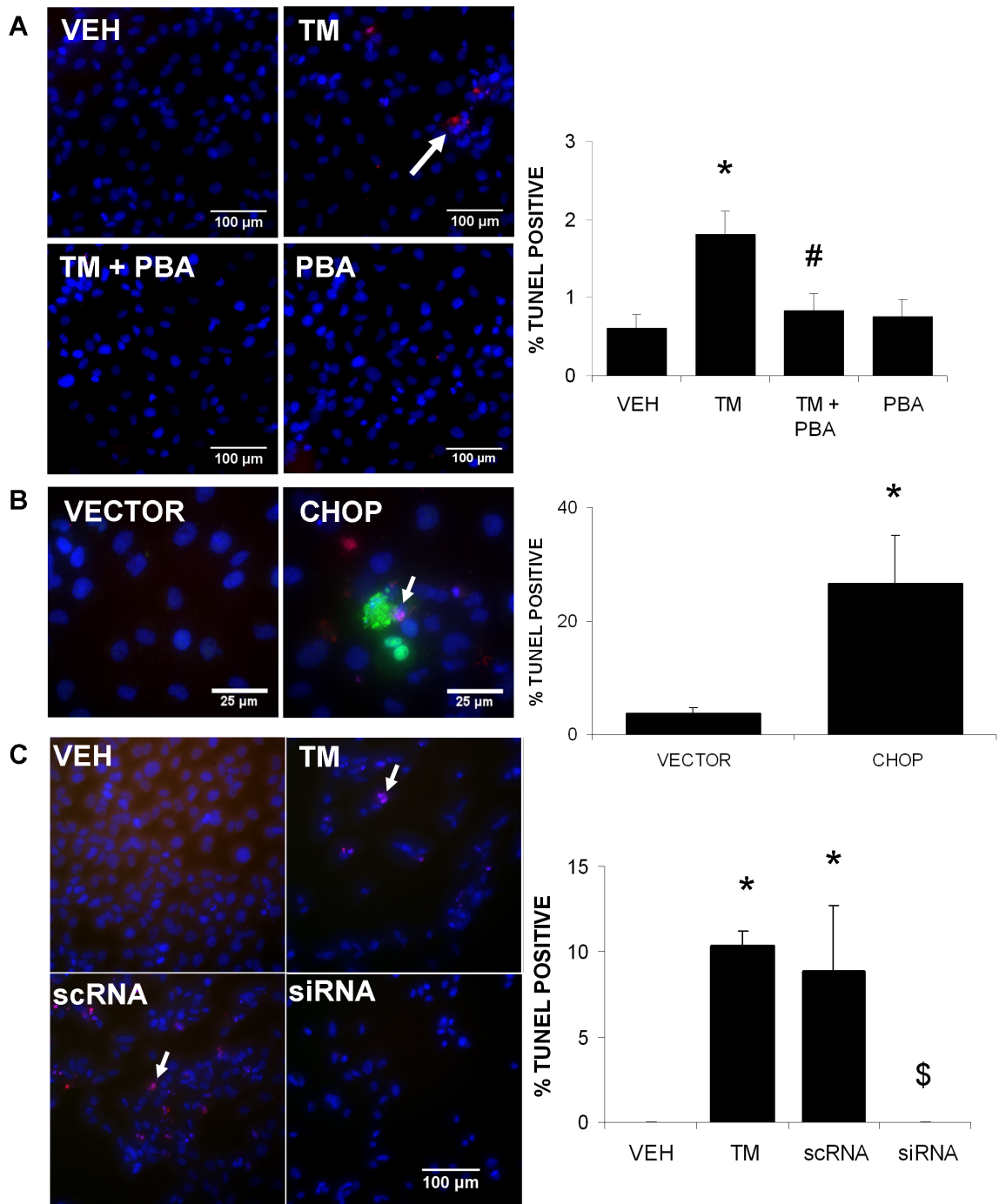


Figure 4. 4-PBA protects against tunicamycin (TM)-induced apoptosis, which is mediated by CHOP expression. HK-2 cells were treated with DMSO (VEH), TM (1 µg/ml), TM with 4-PBA (1 mM) or 4-PBA alone for 24 h. Cells were then stained for apoptosis, using a TUNEL procedure (red). Apoptotic cells and total cells were counted. Results indicate that TM treatment significantly increased apoptosis. Co-treatment of TM with 4-PBA inhibited apoptotic cell death (A). HK-2 cells were transfected with a pcDNA3.1 control (VECTOR) or CHOP in a pcDNA3.1 vector, and immunofluorescently stained for CHOP (green) and TUNEL (red). Results indicate that increased expression of CHOP resulted in significantly more apoptosis than control-transfected cells (B). Cells were transfected with siRNA (Dharmacon ON-TARGET plus SMARTpool) to inhibit CHOP expression and then treated with TM for 48 h. Cells experienced significantly less apoptosis than non-transfected TM-treated or control-scrambled siRNA (scRNA) transfected cells (C). DAPI was used to stain all cell nuclei (blue). *, P<0.05 vs. control; #, P<0.05 vs. TM; \$, P<0.05 vs. scRNA.

Figure 5.

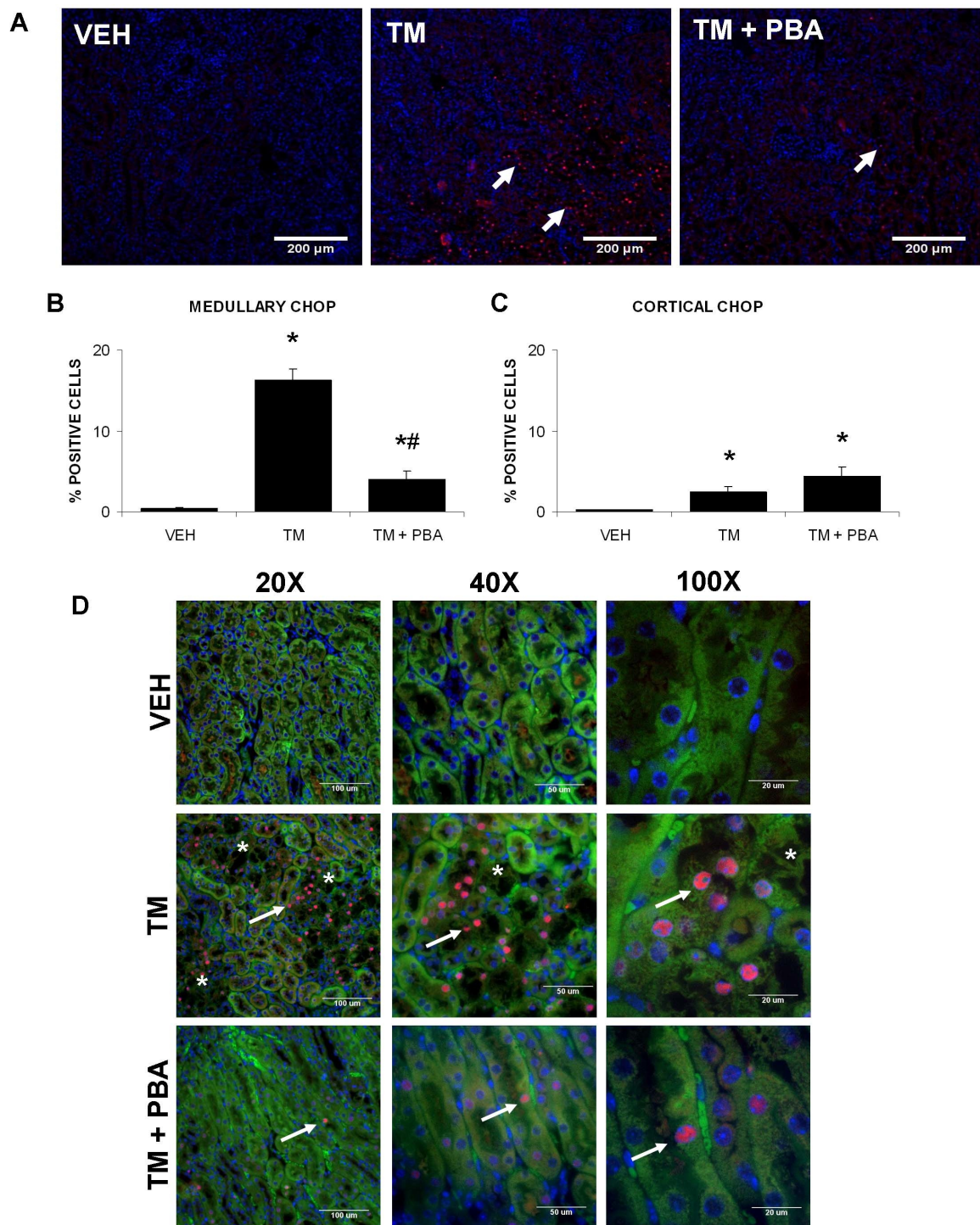


Figure 5. 4-PBA inhibits tunicamycin (TM)-induced CHOP expression in the medulla. Mice were treated with saline (VEH), TM for 3 days, or pre-treated with 4-PBA for 7 days followed by 3 days of TM and 4-PBA co-treatment. Kidney sections from untreated or treated mice were immunofluorescently stained for CHOP (A). CHOP-stained cells and total cells were counted. Results indicate that TM upregulates CHOP expression primarily in the outer stripe of the outer medulla (arrows); TM-induced CHOP expression was lower in the cortex. Further, 4-PBA appears to attenuate the TM-induced CHOP expression in the medulla (arrows) (B), but does not have an effect in the cortex (C). Confocal images demonstrate the localization of CHOP in the nuclei of the proximal tubules (pars recta) of the kidney (arrows). *, region of damage (D). N = 9. *, P<0.05 vs VEH; #, P<0.05 vs TM.

Figure 6.

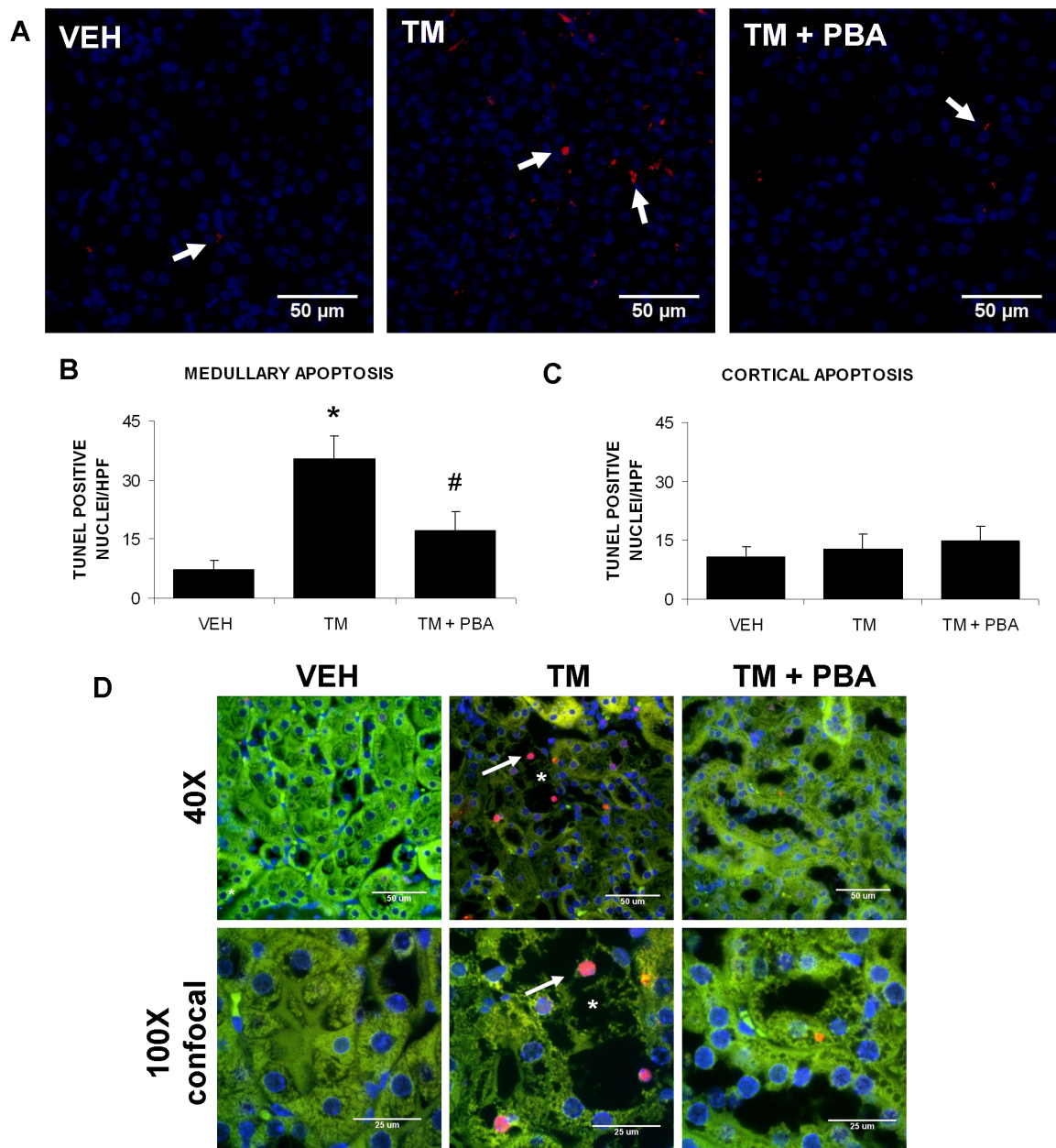


Figure 6. 4-PBA inhibits tunicamycin (TM)-induced apoptosis in the medulla. Mice were treated with saline (VEH), TM for 3 days, or pre-treated with 4-PBA for 7 days followed by 3 days of TM and 4-PBA co-treatment. Kidney sections from untreated or treated mice were TUNEL stained for cells undergoing apoptosis (A). TUNEL-stained cells (red) were counted. Results, expressed as the number of TUNEL positive nuclei per high-powered field (HPF), indicate that TM treatment increases apoptotic cell death in the medulla (arrows). Further, 4-PBA appears to prevent the TM-induced apoptosis in the medulla (B). Apoptosis in the cortex did not significantly differ between groups (C). Confocal images demonstrated that the localization of apoptotic cells in the kidney was confined to regions of renal damage of the proximal tubular cells. *, region of damage; arrow, apoptotic nuclei (D). N = 6. *, P<0.05 vs VEH; #, P<0.05 vs TM).

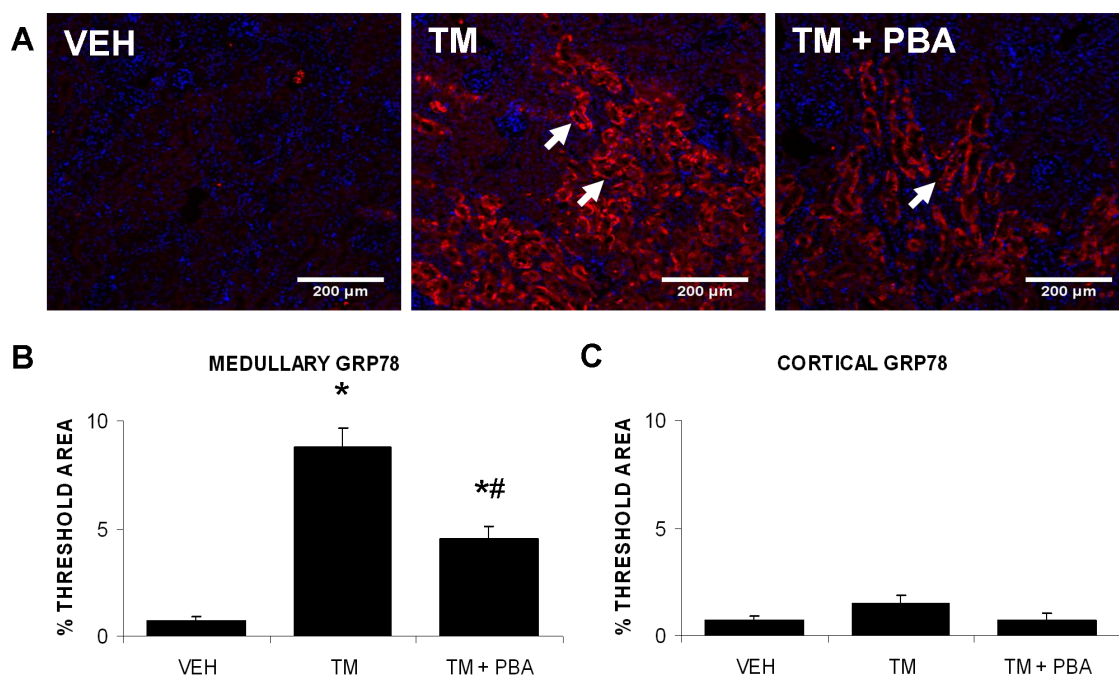


Figure 7. 4-PBA inhibits tunicamycin (TM)-induced GRP78 expression in the medulla. Mice were treated with saline (VEH), TM for 3 days, or pre-treated with 4-PBA for 7 days followed by 3 days of TM and 4-PBA co-treatment. Kidney sections from mice were immunofluorescently stained for GRP78 (arrows) (A). The area of GRP78 staining was determined through wavelength specific thresholding. Results demonstrated that TM treatment led to upregulation of GRP78 expression, mainly in the medullary region of the kidney; this was inhibited by co-treatment with 4-PBA (B). Comparatively less GRP78 staining was found in the cortex of the kidney (C). N = 9. *, P<0.05 vs VEH; #, P<0.05 vs TM.

Figure 8.

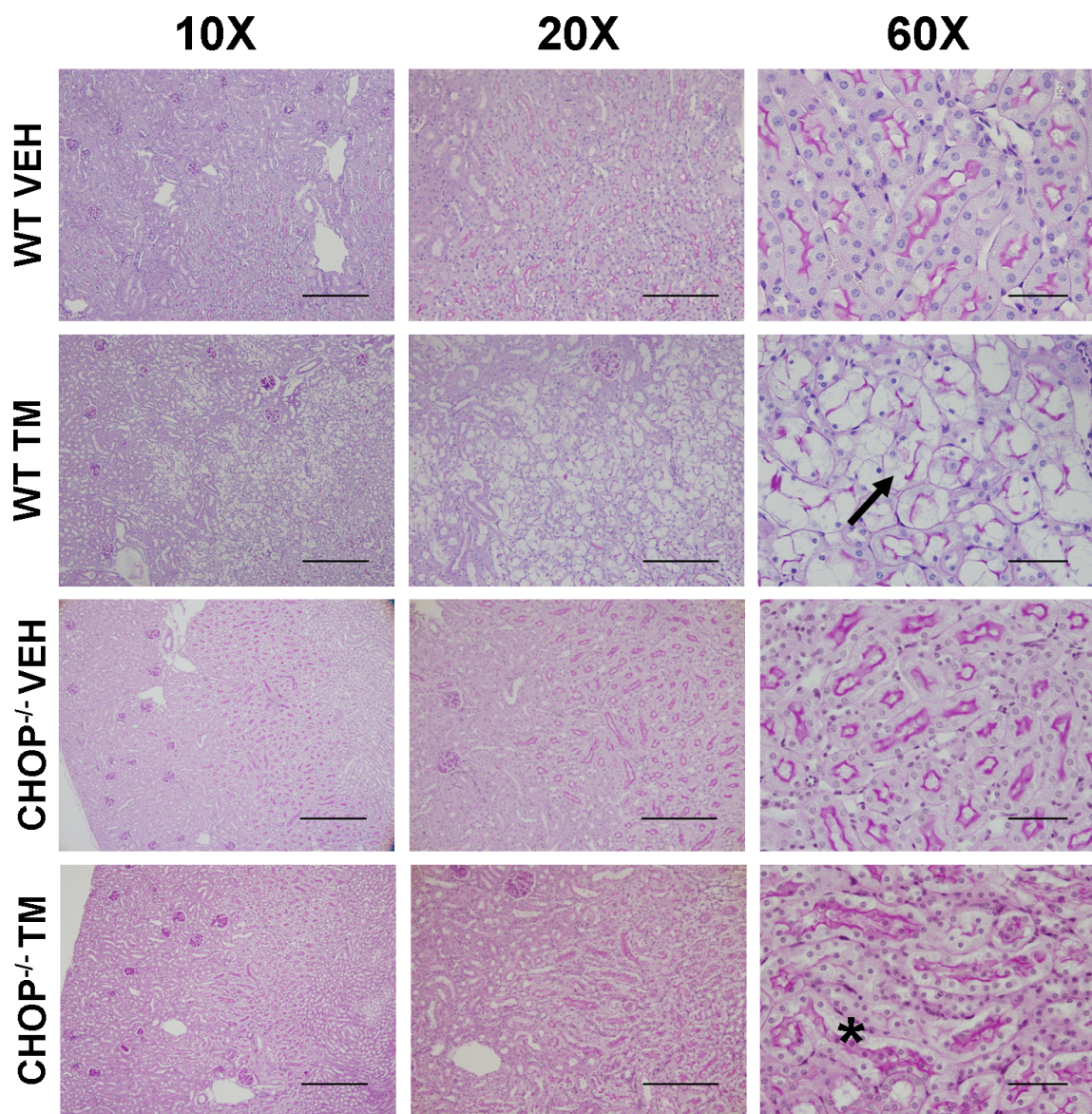


Figure 8. CHOP deficiency protects against tunicamycin (TM)-induced acute kidney injury. Kidney sections from C57BL/6 wild type mice and CHOP^{-/-} mice treated with saline (VEH) or TM for 3 days were PAS stained. Staining demonstrates that CHOP^{-/-} mice treated with TM did not display pathological signs of acute kidney injury like wild type mice, including those found in the pars recta (*). High magnification images are of the outer stripe of the outer medulla, the main area of damage in the wild type mice (arrow). 10X, bar = 350 µm; 20X, bar = 200 µm; 60X, bar = 50 µm.

Figure 9.

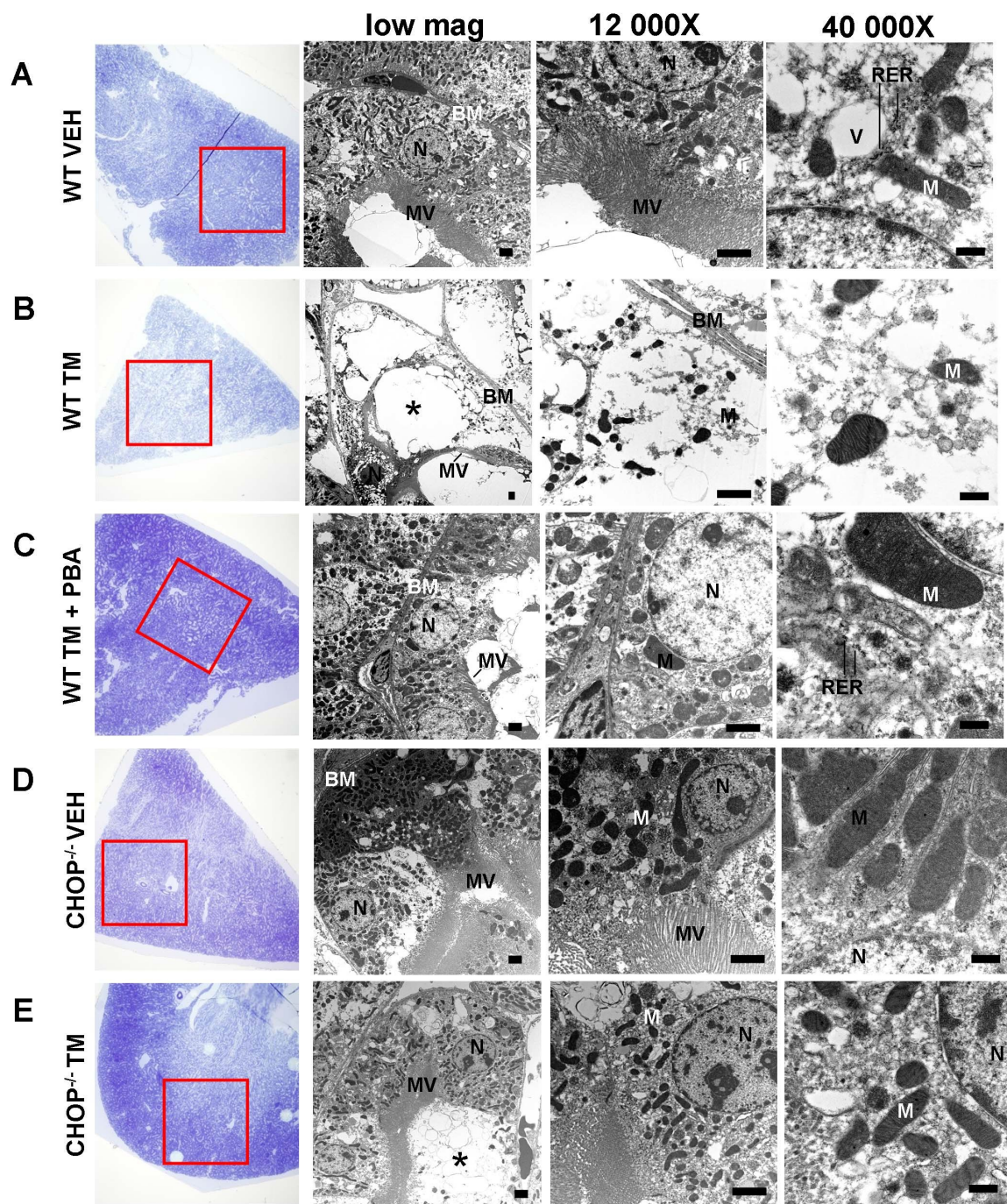


Figure 9. 4-PBA protects ultrastructure of pars recta against tunicamycin (TM)-induced acute kidney injury. Transmission electron microscopy was used to visualize the ultrastructure of proximal tubule epithelial cells in the pars recta of kidneys from wild type and CHOP^{-/-} mice. Low magnification image (blue sections) show regions of outer medulla prepared for ultra-thin sectioning (red box). Proximal tubule cells of wild type sham-treated mice within this region showed prominent brush border with microvilli and nuclei. Detailed images show numerous mitochondria in the perinuclear region, rough endoplasmic reticulum and pinocytotic vesicles (A). Wild type mice treated with TM (0.5 mg/kg) showed severe disruption of proximal tubule cells within the outer medulla where most of the cytoplasm of these cells was lost or degraded (*). However, microvilli on the brush border remained visible, as well as nuclei and mitochondria within the cytoplasm. Further, the basement membrane remained intact (B). In contrast, co-treatment of TM with 4-PBA (1 g/kg/day) preserved the proximal tubule cells of the outer stripe, which displayed intact cytoplasm, undamaged nuclei, mitochondria, and rough endoplasmic reticulum (C). Kidneys of CHOP^{-/-} mice displayed proximal tubule cells in the outer medulla, which did not differ from those of wild type mice (D). CHOP deficiency protected the proximal tubular cells from TM treatment, maintaining undamaged nuclei, mitochondria and rough endoplasmic reticulum in the cytoplasm. Infrequent cells displaying ultrastructural degeneration similar to that found in wild type TM-treated mice remained in TM-treated CHOP^{-/-} mice (*) (E). MV, microvilli; N, nuclei; M, mitochondria; RER, rough endoplasmic reticulum; V, pinocytotic vesicles; BM, basement membrane. Low mag, bar = 2 µm; 12 000X, bar = 2 µm; 40 000X, bar = 500 nm.

CHAPTER 4

Endoplasmic reticulum stress inhibition reduces hypertension through the preservation of resistance blood vessel structure and function

Rachel E. Carlisle, Kaitlyn E. Werner, Victoria Yum, Chao Lu, Victor Tat, Muzammil Memon, Yejin No, Kjetil Ask, and Jeffrey G. Dickhout.

Journal of Hypertension (2016). 34(8); 1556-1569.
Doi: 10.1097/HJH.0000000000000943

© Copyright by Wolters Kluwer Health, Inc

Chapter link:

ER stress inhibition increases vasodilation in hypertensive vessels through a nitric oxide-dependent mechanism. LWCC, 4-PBA and TUDCA, have been shown to reduce blood pressure in hypertensive mice (Kassan et al., 2012) and rats (Spitler & Webb, 2014). Further, Young and colleagues demonstrated that ER stressors delivered directly to the brain induced elevated blood pressure, and brain-specific inhibition of ER stress reduced angiotensin II-mediated hypertension (Young et al., 2012). It is apparent that ER stress plays a role in the development of hypertension, however, a mechanism elucidating the blood pressure reduction effects of LWCCs is lacking. Chapter 3 illustrated that pharmacological inhibition of ER stress, using 4-PBA, can have protective effects in the kidney. This paper demonstrates that orally available 4-PBA can prevent structural vessel alterations and inhibit ER stress in resistance vessels in an animal model of essential hypertension. This manuscript demonstrates that endothelium-dependent relaxation is almost entirely produced by nitric oxide in resistance vessels from hypertensive animals; inhibiting ER stress with 4-PBA reduces superoxide formation, and thus prevents a decrease in nitric oxide bioavailability. Further, inhibiting ER stress in the kidney can normalize renal blood vessel structural change and reduce hypertension.

Author's contribution:

R.E. Carlisle, K.E. Werner, and J.G. Dickhout designed the study. C. Lu and Y. No conducted the animal studies and collected tissues. R.E. Carlisle, K.E. Werner, V. Yum, C. Lu, and Y. No analysed tissues and performed related quantifications. R.E. Carlisle and M. Memon performed cell culture experiments, and related analyses. R.E. Carlisle

assembled the results, and generated the figures in the manuscript. R.E. Carlisle and K.E. Werner wrote the manuscript. R.E. Carlisle revised the manuscript. R.E Carlisle, K. Ask, and J.G. Dickhout reviewed and edited the manuscript. All authors approved of the final submission.

Running title: ER stress inhibition lowers blood pressure

Endoplasmic reticulum stress inhibition reduces hypertension through the preservation of resistance blood vessel structure and function.

Rachel E. Carlisle¹, Kaitlyn E. Werner¹, Victoria Yum¹, Chao Lu¹, Victor Tat¹, Muzammil Memon¹, Yejin No¹, Kjetil Ask² and Jeffrey G. Dickhout¹.

¹Department of Medicine, Division of Nephrology, McMaster University and St. Joseph's Healthcare Hamilton, Hamilton, Ontario, Canada.

²Department of Medicine, Division of Respiriology, McMaster University and St. Joseph's Healthcare Hamilton, Hamilton, Ontario, Canada.

Address Correspondence to:

Jeffrey G. Dickhout, PhD

Department of Medicine, Division of Nephrology

McMaster University and St. Joseph's Healthcare Hamilton

50 Charlton Avenue East

Hamilton, ON, Canada, L8N 4A6

Tel: 905-522-1155 ext. 35334

Fax: 905-540-6589

Email: jdickhou@stjosham.on.ca

Key words: 4-phenylbutyric acid, endoplasmic reticulum stress, essential hypertension, nitric oxide, superoxide

ABSTRACT

Objective: Our purpose was to determine if endoplasmic reticulum (ER) stress inhibition lowers blood pressure (BP) in hypertension by correcting vascular dysfunction.

Methods: The spontaneously hypertensive rat (SHR) was used as a model of human essential hypertension with its normotensive control, the Wistar Kyoto rat (WKY). Animals were subjected to ER stress inhibition with 4-phenylbutyric acid (4-PBA; 1g/kg/day, orally) for 5 weeks from 12 weeks of age. BP was measured weekly non-invasively and at end-point with carotid arterial cannulation. Small mesenteric arteries were removed for vascular studies. Function was assessed with a Mulvany-Halpern style myograph and structure was assessed by measurement of medial-to-lumen ratio in perfusion fixed vessels as well as three-dimensional confocal reconstruction of vessel wall components. ER stress was assessed by qRT-PCR and Western blotting; oxidative stress was assessed by 3-nitrotyrosine and dihydroethidium (DHE) staining.

Results: 4-PBA significantly lowered BP in SHR (vehicle 206.1 ± 4.4 vs. 4-PBA 179.0 ± 3.1 , systolic) but not WKY. 4-PBA diminished contractility and augmented endothelial-dependent vasodilation in SHR small mesenteric arteries as well as reducing media-to-lumen ratio. 4-PBA significantly reduced ER stress in SHR resistance vessels. Normotensive resistance vessels, treated with the ER stress inducing agent, tunicamycin, show decreased endothelial-dependent vasodilation; this was improved with 4-PBA treatment. 3-Nitrotyrosine and DHE staining indicated that ER stress leads to reactive oxygen species generation resolvable by 4-PBA treatment.

Conclusion: ER stress caused endothelial-mediated vascular dysfunction contributing to elevated blood pressure in the SHR model of human essential hypertension.

INTRODUCTION

Hypertension is the leading global risk factor for mortality and the third leading risk factor for disease burden, including cardiovascular, cerebrovascular and renal disease (1). Up to 90% of patients with chronic renal failure develop hypertension. In these patients, inhibitors of the renin angiotensin aldosterone system effectively prevent vascular stiffness, endothelial dysfunction and oxidative stress (2, 3). Numerous lines of evidence have suggested endothelial dysfunction is associated with chronic kidney disease (CKD) (4, 5). Correction of blood vessel structure and/or function is one systematic approach to lower blood pressure (BP) and prevent the end organ damage associated with essential hypertension.

Reduced endothelial vasodilatory response, brought about by decreased nitric oxide (NO) bioavailability, is an important aspect of vascular dysfunction found in both human essential hypertensives (6) and hypertensive animal models (7). Endothelial nitric oxide synthase (eNOS) deficiency can cause hypertension, as demonstrated in the eNOS knockout mouse (8) and in human subjects treated with nitric oxide synthase (NOS) inhibitors (9). Endothelial dysfunction in several studies of human prehypertensives has been shown to be predictive of the eventual development of hypertension (10). Further, interventions to lower BP that produced the best improvement in endothelial dysfunction resulted in lower rates of cardiovascular events (11). In hypertensives, it is lack of NO production or bioavailability in response to stimulus that results in hypertension, as opposed to lack of effectiveness of NO donors (6).

The spontaneously hypertensive rat (SHR) is the most commonly used animal model to study human essential hypertension and displays renal vascular damage (12). Blood

vessels of the SHR have impaired endothelium-dependent relaxation (13), as well as exaggerated contractile responses (14). A recent study revealed that the altered contractile responses seen in the aorta of the SHR may be attributed to endoplasmic reticulum (ER) stress (14).

ER stress occurs when misfolded proteins accumulate in the ER, which can occur in diseased blood vessels (15, 16). Importantly, oxidative processes within the blood vessels may be responsible for reduced NO bioavailability (17) and generate peroxynitrite, an ER stress inducer (16). ER stress results in activation of the unfolded protein response (UPR), an intracellular signaling pathway (18). UPR activation results in the upregulation of ER-resident molecular chaperones such as glucose-regulated protein 78 (GRP78) and glucose-regulated protein 94 (GRP94). ER-resident chaperones increase cellular protein folding capacity and aid in ER-associated protein degradation to dispose of misfolded proteins (19). However, failure to resolve the imbalance in protein folding can lead to oxidative stress since the formation and degradation of disulfide bonds to remove misfolded proteins generates reactive oxygen species (20, 21). If ER stress is severe or prolonged, the cell will undergo apoptosis.

In this study, we examined the ability of 4-phenylbutyric acid (4-PBA), an ER stress inhibitor, to improve vascular function and/or structure and reduce blood pressure in the SHR. We hypothesized that ER stress causes superoxide generation in resistance vessels of the SHR, decreasing NO bioavailability and leading to reduced endothelial-dependent vasodilation. This in turn increases total peripheral resistance contributing to hypertension in the SHR. By reducing protein misfolding in the SHR vessels, 4-PBA should reduce superoxide generation and increase NO bioavailability, leading to improved vasodilation

and decreased BP. This represents a novel pathway to reduce BP in essential hypertension.

METHODS

Animal studies

12-week-old male SHRs with established hypertension were used to examine the effect of 4-PBA on BP; 12-week-old male Wistar Kyoto (WKY) rats were used as a normotensive control. Animals were randomized into either 4-PBA (n=8) or non-treated (n=7) groups. Treatment with 1g/kg/day 4-PBA in the drinking water proceeded for 5 weeks. 4-PBA dosage was adjusted in fresh drinking water every 3 days. This dose of 4-PBA has been used to alleviate ER stress in multiple rodent models (22, 23). All animals were fed a normal-sodium diet (0.4% NaCl, AIN-76A, Research Diets Inc.). BP was measured 1 week before treatment (week 0) and after each week of treatment using tail cuff plethysmography, a method that accurately determines tail blood volume with a volume pressure recording sensor and an occlusion tail-cuff (CODA system, Kent Scientific) (24). Animals were placed in metabolic cages at weeks 0, 1 and 3 of treatment where 24 hour food intake, water intake and urine output was measured. After 5 weeks, animals were sacrificed, organs were harvested and mesenteric resistance vessels were collected for functional and structural analysis. Vessels were perfused with Hank's buffered salt solution containing SNP (10^{-4} M) to place the resistance arteries in a maximally relaxed state (25). Final BP measurement was performed directly through carotid artery cannulation, as previously (26). 20-week-old WKY rats, also fed a normal-

sodium diet, were used to examine the direct effect of ER stress and its inhibition with 4-PBA on resistance blood vessel function. All animal work was performed according to the McMaster University Animal Research Ethics Board guidelines.

Functional analysis

Within 30 minutes of animal sacrifice, mesenteric resistance arteries were collected and placed into Hank's Balanced Salt Solution (HBSS). Vessels were mounted on a small vessel wire style heated myograph (M4 series Myograph System; Radnoti LLC, Monrovia, CA) maintained at 37°C, and bubbled with 100% O₂. Mesenteric resistance arteries were mounted with 0.3 g of tension. Resting tensions were determined after performing length-tension experiments to find optimal resting tension for resistance vessels. Vessels were washed with HBSS and allowed to balance for 30 minutes. To induce smooth muscle-mediated contraction directly, vessels were treated with 60 mM KCl. After the contraction reached a plateau, vessels were washed to restore membrane potential. These procedures were performed prior to all contractility protocols.

To determine the effect of 4-PBA treatment on the contractility of SHR and WKY mesenteric resistance vessels from both non-treated and 4-PBA treated groups, vessels were induced to contract with an α 1 adrenergic receptor agonist, phenylephrine (PHE), in a cumulative manner (10^{-8} - 10^{-5} M). Vessels pre-constricted with PHE to 50% of their maximal response were then treated with varying doses (10^{-8} - 10^{-4} M) of carbachol (CCh) to determine the effect of 4-PBA on endothelium-derived relaxation. After washing, vessels were again constricted with PHE to 50% of their maximal response. Dose

response to the NO donor, sodium nitroprusside (SNP, 10^{-7} - 10^{-4} M), was then performed to determine the effect of 4-PBA on NO-mediated relaxation.

To determine if tunicamycin (TM), an ER stress inducer that inhibits N-linked protein glycosylation (27), affected CCh-dependent relaxation of mesenteric arteries, non-treated WKY mesenteric resistance arteries were incubated for 6 hours with vehicle, 1 μ g/ml TM, or 1 μ g/ml TM with 1 mM 4-PBA. This dose of TM has been used previously to examine the effects of ER stress on vascular smooth muscle (28). After incubation, arteries were pre-constricted with PHE and then treated with 10^{-5} M CCh, similarly to methods above. After washing, arteries were again pre-constricted with PHE followed by SNP-mediated relaxation.

To determine the role of superoxide in endothelium-dependent relaxation of resistance arteries from SHR rats, vessels were incubated alone or with 1 mM TEMPOL, to scavenge superoxide, for 30 minutes. After incubation, arteries were pre-constricted with PHE to 50% of their maximal response followed by varying doses of CCh (10^{-8} - 10^{-4} M) to induce relaxation, similarly to the methods above.

To determine if L-NNA, a NOS inhibitor, had an effect on the CCh-dependent relaxation of resistance arteries, non-treated and 4-PBA-treated vessels were incubated alone or with 10^{-4} M L-NNA for 30 minutes. After incubation, arteries were pre-constricted with PHE to 50% of their maximal response followed by varying doses of CCh (10^{-8} - 10^{-4} M), to determine the effect of L-NNA on CCh-dependent relaxation.

Data from isolated vessel studies were recorded using WINDAQ data acquisition software through a DI-720-USB Series analog to digital converter (DATAQ Instruments, Inc. Akron, OH). Responses induced by PHE are expressed as a percentage of the initial

60 mM KCl response. Responses induced by CCh are expressed as a percentage relaxation of PHE-pre-constricted vessels.

Structural analysis of mesenteric and arcuate arteries

At sacrifice and after removal of tissues for functional analysis, animal organs were perfused with HBSS containing SNP, placing resistance blood vessels in a maximally relaxed state. Mesenteric arteries and kidneys were then perfusion fixed in 4% paraformaldehyde. Arteries and kidneys were subsequently embedded in paraffin, sectioned (4 μm thick) and stained with Masson's Trichrome for assessment of mesenteric artery and renal arcuate artery structure. Cross-sections of the mesenteric and arcuate arteries were imaged using a light microscope at 20x or 40x magnification. A computer-aided tracing method (Metamorph image analysis software) was utilized to determine the area of the adventitia, media, intima, and lumen. The innermost single layer of cells stained with haematoxylin was determined to be the intima. Using this data, % area of each layer of the vessels was determined, as well as the media-to-lumen ratio.

Mesenteric arteries were also fixed and stained with ethidium bromide and structural analysis was performed utilizing confocal microscopy for volume reconstruction, as previously described (25). Image analysis was performed using Metamorph image analysis software (Molecular Devices, Sunnyvale, CA). The ethidium bromide stain allowed for easy identification of medial and adventitial layers of the artery. A computer-aided tracing method was used to determine the area of these layers on each optical section. The Cavalierian estimator of volume was used to calculate medial and adventitial

volumes, as previously (25). This allowed calculation of volume without any assumptions about tissue shape and independent of tissue orientation.

Vascular smooth muscle cell isolation

Vascular smooth muscle cells (VSMC) were isolated from the aortas of Sprague-Dawley rats (Charles River Laboratories) utilizing the explant method (29). Rats were placed under isoflurane /oxygen anesthesia and the thoracic cavity opened to expose the heart. The abdomen was opened surgically to expose the inferior vena cava, where an opening was made to allow an exit for perfusate and the animal was perfused by injection into the left ventricle of the heart with sterile phosphate buffered saline (PBS) containing 5X Antibiotic-Antimycotic solution (Life Technologies). The thoracic aorta was then dissected from the animal and placed in ice-cold 5X Anti-Anti solution under a dissecting microscope. The adventitial layer of the aorta was removed from the media with fine forceps and the aorta opened longitudinally with Vannas Scissors (Fine Scientific Tools). After opening, the endothelial layer was disrupted by gentle scrapping with forceps. The aorta was cut into 3 mm lengths and placed on type I collagen gels in 24-well plates (Falcon) in DMEM medium containing 10% FBS. Explants were incubated in a 5% CO₂ incubator at 37°C for approximately 1-week undisturbed to allow cells to grow out of the explants. Where outgrowth was observed, cells were trypsinized for subculturing and were utilized for experiments after passage 3.

Quantitative rt-PCR analysis

To determine the effect of 4-PBA treatment on ER stress marker expression in blood vessels of SHR and WKY rats, as well as TM-treated WKY resistance arteries and VSMC, quantitative RT-PCR (qRT-PCR) analysis was performed. In the case of blood vessel analysis, the mesentery was excised from the small intestine by blunt dissection and the superior mesenteric artery was cut away at the aortic branch point and perfused with RNAlater® Stabilization (Life Technologies, Ambion), an RNA preservation buffer. The excised mesenteric arcade was placed in ice-cold HBSS and dissection was immediately performed to remove the surrounding tissue. The cleaned second branches of mesenteric artery were stored at -80°C for further RNA extraction. Total RNA was isolated from the frozen vessels using the RNeasy Mini Kit (Qiagen). Briefly, vessels were homogenized using a Sonic Dismembrator (Fisher Scientific) in RLT lysis buffer (Qiagen), RNA bound to spin columns, incubated in RNase-free DNase to eliminate DNA contamination, and eluted in RNase-free DNase-free water, as per manufacturer's instructions. cDNA was synthesized from RNA using a High Capacity cDNA Reverse Transcription Kit (Life Technologies, Applied Biosystems) and reverse transcription performed on a Mastercycler gradient (Eppendorf) thermocycler. Once cDNA was obtained, qRT-PCR was performed to determine relative levels of GRP78 and CHOP message. mRNAs were detected with Fast SYBR Green Master Mix (Life Technologies, Applied Biosystems) and qRT-PCR analysis was performed using 7500 Software (Life Technologies, Applied Biosystems). Primers for GRP78 and CHOP were as follows: GRP78 forward: 5-CTG GGT ACA TTT GAT CTG ACT GG-3; GRP78 reverse, 5-GCA TCC TGG TGG CTT TCC AGC CAT TC-3; CHOP forward, 5-AGC TGG AAG CCT

GGT ATG AG-3; and CHOP reverse, 5-GAC CAC TCT GTT TCC GTT TC-3. 18S was used as an internal standard with forward and reverse primers as follows: 18S forward, 5-GTT GGT TTT CGG AAC TGA GGC-3; and 18S reverse, 5-GTC GGC ATC GTT TAT GGT CG-3.

Fluorescence microscopy

3-NT staining was used to measure peroxynitrite generation in perfusion-fixed mesenteric arteries. Anti-3-NT primary antibody (06-284, EMD Millipore, Etobicoke, Canada) was used at a dilution of 1:200, followed by an AlexaFluor 594 donkey anti-rabbit secondary antibody (A21207, ThermoFisher Scientific, Burlington, Canada) at 1:200. An Olympus IX81 Nipkow scanning disc confocal microscope was used for fluorescence microscopy. A constant EM gain and exposure time was used for all images. The average fluorescence intensity in each vessel was quantified and background intensity was subtracted. Image analysis was performed using Metamorph image analysis software (Molecular Devices, Sunnyvale, CA).

Superoxide generation was measured, as previously, with dihydroethidium (DHE) staining technique (16, 30) in rat VSMC treated for 18 hours with the ER stress inducer TM (1 µg/mL), the ER stress inhibitor 4-PBA (1 mM), or TM in combination with 4-PBA. Images were captured as described above. DHE is oxidized by superoxide in the cell resulting in production of ethidium bromide, which is trapped in the nucleus and emits red fluorescence (31). Superoxide positivity was quantified by measuring the average fluorescent intensities. Images were analyzed as described above.

Gel electrophoresis

Protein levels of cell lysates were determined using BioRad DC Protein Assay (BioRad, Mississauga, Canada) for control of protein loading. Electrophoretic separation was used to separate cell lysates in an SDS-PAGE reducing gel (BioRad). Primary antibodies were detected using appropriate horseradish peroxidase-conjugated secondary antibodies and ECL Western Blotting Detection Reagents (GE Healthcare, Mississauga, Canada), as described previously (27). CHOP antibody (sc-793, Santa Cruz Biotechnology, Santa Cruz, CA) was diluted 1:200 and β -actin antibody (A-2228, Sigma-Aldrich, St. Louis, MO) was diluted 1:4000. KDEL antibody (SPA-827, Stressgen, Victoria, Canada) was diluted 1:1000 and used to probe for GRP94 and GRP78, which both contain the amino acid sequence KDEL. Results were densitometrically quantified using ImageJ software (NIH, Bethesda, MD, ver. 1.43) and expressed as a ratio of β -actin loading control.

RESULTS

ER stress inhibitor, 4-phenylbutyrate, reduces hypertension.

Indirect measurements of systolic BP were similar between non-treated and 4-PBA-treated SHR prior to 4-PBA treatment (week 0). Once 4-PBA treatment began, during week 1, differences between the groups were observed. Systolic BP was significantly lower in SHR treated with 4-PBA at weeks 1, 3, 4 and 5. Final systolic BP was 206.1 ± 4.3 mmHg in non-treated SHR and 178.9 ± 3.1 mmHg in 4-PBA-treated SHR. 4-PBA had no effect on indirect systolic BP measurements in WKY animals (Figure 1A).

BP measured directly through carotid artery cannulation was significantly lower in 4-PBA-treated compared to non-treated SHR at time of sacrifice, week 5. Final non-treated systolic BP was 179.91 ± 23 mmHg and 4-PBA-treated systolic BP was 159.6 ± 3.2 mmHg. Diastolic BP was 151.2 ± 6.6 mmHg in non-treated SHR and 123.5 ± 7.1 in 4-PBA-treated SHR. 4-PBA treatment did not cause any change in direct blood pressure measurements in WKY rats (Figure 1B). Animals were placed in metabolic cages for the measurement of water intake to adjust the oral dosing of 4-PBA throughout the treatment study. 4-PBA treatment resulted in a small, but significant, reduction in body weight in both SHR and WKY rats (Supplemental Figure 1A). Minor variation in food intake occurred independently of 4-PBA treatment status (Supplemental Figure 1B). We found both SHR and WKY rats experienced a significant decrease in drinking water intake (Supplemental Figure 1C) and urine output (Supplemental Figure 1D) with 4-PBA treatment.

4-PBA treatment alters resistance blood vessel function.

To determine if 4-PBA treatment had an effect on contractility, mesenteric resistance vessels were treated with cumulative doses of PHE (10^{-8} – 10^{-5} M). Resulting dose-response curves revealed a significantly attenuated contractile response in mesenteric arteries from 4-PBA-treated SHRs compared with those of the non-treated animals. Statistically significant differences between treatment groups were found at 10^{-6} and 10^{-5} M (Figure 2A). There was no significant difference in WKY mesenteric artery constriction with 4-PBA treatment (Figure 2B). PHE contracted vessels were treated with the stable acetylcholine mimetic, CCh (10^{-8} – 10^{-4} M), to study the effect of 4-PBA on endothelium-derived relaxation. Compared to non-treated SHR mesenteric arteries, 4-

PBA-treated SHR mesenteric arteries displayed a significantly higher relaxation to CCh (Figure 2C). There was no difference in endothelium-dependent relaxation of the mesenteric vessels from non-treated or 4-PBA-treated WKY rats (Figure 2D). The NO donor, SNP (10^{-7} - 10^{-4} M) was used to determine the effect of 4-PBA treatment on direct NO-mediated relaxation in these vessels. There was no difference in the NO-mediated relaxation of non-treated and 4-PBA-treated SHR resistance vessels (Figure 2E) or WKY mesenteric vessels (Figure 2F).

Superoxide scavenging increased SHR endothelial-mediated vasodilation.

Non-treated SHR vessels pre-constricted with PHE were incubated with or without the superoxide scavenger TEMPOL (1 mM) to determine if the reduced endothelial-dependent vasodilation in SHR resistance vessels was due to superoxide generation. TEMPOL incubation significantly increased CCh-induced relaxation in mesenteric arteries (Figure 3A). To determine if NO mediated the increased vasodilatory response in 4-PBA-treated SHR vessels, these vessels were incubated with or without the NO synthase inhibitor L-NNA and subjected to CCh-induced relaxation. L-NNA pre-incubation eliminated CCh-induced vasodilation in both non-treated and 4-PBA-treated SHR vessels (Figure 3B).

ER stress marker expression is increased in SHR resistance vessels.

To examine ER stress marker expression, both non-treated and 4-PBA-treated SHR and WKY resistance vessels were processed for qRT-PCR analysis. RNA was extracted for qRT-PCR analysis of CHOP and GRP78. Both CHOP and GRP78 expression were

significantly increased in non-treated SHR vessels compared to 4-PBA-treated SHR vessels. However, in WKY resistance vessels CHOP and GRP78 expression were not significantly changed between the non-treated and 4-PBA-treated groups (Figure 3C-D).

Effect of 4-PBA treatment on blood vessel structure.

To assess structural features of blood vessels, mesenteric arteries stained with Masson's Trichrome were imaged using a light microscope (40x magnification) (Figure 4A). Non-treated SHR mesenteric arteries demonstrated a significantly higher media-to-lumen ratio in comparison to non-treated WKY arteries. 4-PBA-treated vessels had a significantly reduced ratio when compared with non-treated SHR arteries. No statistical difference was found in the mesenteric artery media-to-lumen ratio between treatment groups in WKY rats (Figure 4B). Mesenteric arteries were stained with ethidium bromide and imaged confocally. 3D-reconstructed images show medial smooth muscle and adventitia layers (Figure 4C). No significant difference was found between non-treated and 4-PBA-treated SHR mesenteric arteries with regard to medial or adventitial volumes. Medial and adventitia volumes of non-treated and 4-PBA-treated WKY animals were also not significantly different. Medial volume was significantly increased in non-treated SHR compared to that of non-treated WKY (Figure 4D, E).

Kidneys were stained with Masson's Trichrome and arcuate arteries were imaged using a light microscope (20x magnification) to determine arcuate artery structure (Figure 5A). Images were analyzed to determine the area of the adventitia, media, intima and lumen, and subsequently, the % area of each layer. No significant changes in structural composition were found between the non-treated and 4-PBA-treated groups in either SHR

(Figure 5B) or WKY rats (Figure 5C). Non-treated SHR vessels showed a significantly higher media-to-lumen ratio in comparison to non-treated WKY vessels and 4-PBA-treated SHR vessels. Further, no significant difference was found in the arcuate artery media-to-lumen ratio between the treatment groups in WKY rats (Figure 5D).

ER stress induction reduces endothelial-mediated vasodilation.

To directly determine the effect of ER stress induction on endothelial-dependent vasodilation in mesenteric resistance vessels, vessels from normotensive WKY rats were treated with TM. Mesenteric resistance arteries were incubated with TM, TM+4-PBA or DMSO (vehicle) for 6 hours before vasodilation studies were carried out. PHE pre-constricted WKY vessels were treated with 10^{-5} M CCh to study the direct effect of TM and TM+4-PBA incubation on endothelial-mediated vasodilation. Compared to vehicle-treated mesenteric arteries, TM-treated vessels displayed significantly reduced vasodilatory responses. Vessels co-incubated with TM and 4-PBA displayed a significantly increased vasodilatory response to CCh in comparison to TM-treated vessels (Figure 6A). Vehicle, TM- and TM+4-PBA-incubated WKY mesenteric vessels all showed similar values of relaxation to SNP (Figure 6A).

RNA was extracted from TM-, TM+4-PBA- and vehicle (DMSO)-treated WKY arteries for qRT-PCR analysis of CHOP and GRP78 expression. TM treatment increased both CHOP (Figure 6B) and GRP78 (Figure 6C) levels compared to control; 4-PBA co-treatment reversed this effect.

4-PBA inhibits 3-nitrotyrosine expression in mesenteric arteries.

To examine oxidative stress in this model, mesenteric arteries were stained for 3-NT, a marker of peroxynitrite generation (Figure 7A). Quantification of fluorescence demonstrated that 4-PBA reduced 3-NT generation in SHR mesenteric arteries. Further, WKY vessels had naturally lower levels of 3-NT than SHR vessels; 4-PBA had no effect on 3-NT generation in WKY vessels (Figure 7B).

ER stress stimulates superoxide generation in rat vascular smooth muscle cells.

Rat VSMC were used to determine if inducing ER stress would lead to the generation of superoxide as sensed by DHE staining, and if 4-PBA would inhibit this effect. VSMC were treated with the ER stress inducer, TM, in the presence or absence of 4-PBA for 18 hours and were stained with DHE (Figure 7C). Quantification of DHE background-corrected fluorescence indicated that TM significantly stimulated superoxide generation and the combination of TM + 4-PBA significantly inhibited ER stress-mediated superoxide generation. 4-PBA alone also significantly reduced superoxide generation in rat VSMC (Figure 7D).

4-PBA inhibits expression of ER stress markers in rat vascular smooth muscle cells.

Rat VSMC were treated with vehicle (DMSO), TM, TM+4-PBA, or 4-PBA alone for 18 hours (Figure 7E). Densitometric analysis of Western blotting demonstrated that treatment with the ER stress inducer, TM, resulted in increased GRP78 and GRP94 expression. 4-PBA combined with TM treatment reduced GRP78 and GRP94 levels. 4-PBA alone had little effect on GRP78 or GRP94 expression (Figure 7F). Vehicle, TM, or

TM+4-PBA 6 hour-treated rat VSMC were also analyzed for ER stress markers, CHOP and GRP78, by qRT-PCR analysis. TM significantly increased both CHOP (Figure 7G) and GRP78 (Figure 7H) levels in VSMC; co-treatment with 4-PBA significantly reversed this effect.

DISCUSSION

The SHR is a model of human essential hypertension that involves an increase in total peripheral resistance (32) with structural and functional modifications in both renal and mesenteric blood vessels (25, 33). ER stress has recently been shown to exert effects on blood vessel function in angiotensin II-mediated hypertension (34). ER stress, through the accumulation of misfolded proteins, may cause superoxide generation (35). Superoxide is known to have a high affinity for NO and reacts to form the product peroxynitrite (16). The interaction of superoxide and NO can decrease the bioavailability of NO in blood vessels (36), resulting in an inhibition of endothelium-dependent vasodilation. We have found that ER stress leads to superoxide generation and reduces NO bioavailability. This process could be responsible for the increased BP found in the SHR. We found that ER stress inhibition with 4-PBA was able to reduce hypertension in the SHR. Additionally, treatment with 4-PBA rescued vasodilatory responses in SHR resistance vessels and scavenging of superoxide with TEMPOL was also able to restore vasodilatory responses. Long-term treatment with 4-PBA reduced α_1 adrenoreceptor-mediated constriction in resistant vessels and significantly reduced the media-to-lumen ratio in maximally relaxed renal arcuate arteries and mesenteric vessels. These effects of

4-PBA treatment on resistance blood vessel structure seem to involve no change in medial volume but instead an increase in lumen diameter.

Several studies have shown a role for ER stress in hypertension (34, 37). However, this study is the first to demonstrate an effect of ER stress inhibition on the restoration of vascular function in essential hypertension and normalization of blood vessel structure. It appears that ER stress inhibition with 4-PBA has a direct effect on resistance blood vessels, since an increase in endothelial-dependent NO-mediated vasodilation and a decrease in adrenergic agonist-mediated vasoconstriction was observed in resistance vessels isolated from the SHR undergoing long-term treatment with 4-PBA. This observation was made concomitantly with 4-PBA treatment-induced reduction in resistance blood vessel ER stress marker expression.

We also observed that the superoxide scavenger, TEMPOL, was able to restore endothelium-dependent vasodilation in *ex vivo* mesenteric vessels of the SHR. This finding is in agreement with a previous study showing that TEMPOL was able to lower BP in the SHR, suggesting a mechanism of NO preservation through superoxide inhibition (38). Further work revealed that the BP lowering effect of TEMPOL in the SHR was in part NO-dependent (39). TEMPOL's action *in vitro* appears to be mainly related to its ability to scavenge superoxide anions (40, 41). However, *in vivo* effects of TEMPOL may extend to prevent the formation of hydroxyl radicals via Fenton reaction inhibition (42) or direct sympathetic nerve inhibition (43). We found that long-term treatment of the SHR with 4-PBA resulted in greater endothelial-dependent vasodilation in resistance vessels compared to no treatment. Further, through the use of the NOS inhibitor L-NNA, we have shown this increase in vasodilation to be NO-dependent. We

also demonstrated that TM, a classic ER stress inducer (44), increased superoxide in a 4-PBA inhibitable manner and that direct application of TM to normotensive control vessels reduced endothelial dependent vasodilation.

4-PBA is a low molecular weight chemical chaperone that is currently approved for clinical use in urea cycle disorders (45) and has been shown to inhibit ER stress (22, 23). The precise action of 4-PBA to dampen UPR marker expression, as shown in these reports, appears to be due to its ability to prevent protein aggregation and aid in the folding of proteins. 4-PBA facilitates protein folding and reduces ER stress both *in vitro* and *in vivo* by stabilizing protein-folding intermediates and preventing protein aggregation (28). A mouse model of chronic angiotensin II-induced hypertension has demonstrated reduced BP when treated with 4-PBA (34). These effects may be due to 4-PBA's ability to augment protein folding and prevent protein degradation-mediated superoxide generation in the resistance blood vessels. Indeed, Kassan *et al.* (34) were able to determine that 4-PBA treatment augmented endothelium-dependent vasodilatory responses, as elicited by acetylcholine, in mesenteric resistance arteries of angiotensin II-infused mice. Our data is in agreement with this finding and suggests that the action of 4-PBA to preserve this dilatory response is mediated through its ability to prevent ER stress-induced superoxide generation. Further, the decrease in α_1 adrenoreceptor-mediated constriction we observed may also have been due to the inhibition of superoxide generation by 4-PBA, as the superoxide anion has been shown to increase vascular tone (46). Differences in resistance blood vessel structure have been shown to precede hypertension development in the SHR (25). BP reduction, particularly with AT1-receptor antagonist irbesartan (47), reduced structural changes. The BP reduction induced by 4-

PBA was found to be associated with a reduced media-to-lumen ratio in the 4-PBA-treated vessels from both the mesentery and kidney. It is possible that longer-term treatment with 4-PBA or initiation of treatment with 4-PBA in the developing hypertensive phase of the SHR may have a greater effect on inhibition of structural change in resistance blood vessels and produce a greater lowering of BP. The significant media-to-lumen ratio reduction may also be reflective of 4-PBA lowering blood pressure, rather than a direct effect of 4-PBA on blood vessel structure.

The main effects of 4-PBA treatment on parameters that could influence BP in the sustained hypertensive phase of the SHR were the reduction of resistant vascular contractility and increased NO-mediated endothelial vasodilatation. Our results are illustrated in an overall model in Figure 8 that depicts how ER stress contributes to hypertension in the SHR. In our study, treatment with 4-PBA resulted in a decrease of blood pressure in hypertensive SHR. We found that 4-PBA reduced ER stress in the SHR resistance vessels as well as VSMCs. The increase in total peripheral resistance associated with essential hypertension may be initiated by ER stress. Various factors in the hypertensive may lead to this ER stress response; however, once initiated, the accumulation of misfolded proteins can lead to oxidative stress. We have shown the direct induction of ER stress causes superoxide generation. 4-PBA treatment was able to reverse this effect. We know superoxide and NO react to form peroxynitrite, which causes a decrease in NO bioavailability. As well, peroxynitrite is a known ER stress inducer, and likely further exacerbates ER stress via the depletion of ER Ca^{2+} (16). Treatment with 4-PBA was able to improve vasodilatory responses in the SHR, though to a level lower than the responses seen in WKY animals. By scavenging superoxide with TEMPOL,

vasodilatory responses in the SHR were rescued and were similar to levels of 4-PBA-treated SHRs. By using L-NNA we were able to eliminate 4-PBA's ability to increase vasodilation, demonstrating the mechanism of 4-PBA to increase SHR resistance vessel vasodilation is NO-dependent. The ability of 4-PBA to reduce BP in hypertensive SHR can be attributed to an increase in vasodilation that occurs in the SHR resistance vessels. The reduced vasodilation in the SHR vessels would increase total peripheral resistance and so increase BP.

REFERENCES

1. Kearney, P. M., Whelton, M., Reynolds, K., Whelton, P. K., and He, J. (2004) Worldwide prevalence of hypertension: a systematic review. *J Hypertens* 22, 11-19
2. Inrig, J. K. (2010) Antihypertensive agents in hemodialysis patients: a current perspective. *Semin Dial* 23, 290-297
3. de Cavanagh, E. M., Ferder, L., Carrasquedo, F., Scrivo, D., Wassermann, A., Fraga, C. G., and Inserra, F. (1999) Higher levels of antioxidant defenses in enalapril-treated versus non-enalapril-treated hemodialysis patients. *Am J Kidney Dis* 34, 445-455
4. Passauer, J., Pistrosch, F., and Bussemaker, E. (2005) Nitric oxide in chronic renal failure. *Kidney Int* 67, 1665-1667
5. Baylis, C. (2008) Nitric oxide deficiency in chronic kidney disease. *Am J Physiol Renal Physiol* 294, F1-9
6. Giles, T. D., Sander, G. E., Nossaman, B. D., and Kadowitz, P. J. (2012) Impaired vasodilation in the pathogenesis of hypertension: focus on nitric oxide, endothelial-derived hyperpolarizing factors, and prostaglandins. *J Clin Hypertens (Greenwich)* 14, 198-205
7. Rajapakse, N. W., and Mattson, D. L. (2013) Role of cellular L-arginine uptake and nitric oxide production on renal blood flow and arterial pressure regulation. *Curr Opin Nephrol Hypertens* 22, 45-50
8. Shesely, E. G., Maeda, N., Kim, H. S., Desai, K. M., Krege, J. H., Laubach, V. E., Sherman, P. A., Sessa, W. C., and Smithies, O. (1996) Elevated blood pressures in mice lacking endothelial nitric oxide synthase. *Proc Natl Acad Sci U S A* 93, 13176-13181
9. Sander, M., Chavoshan, B., and Victor, R. G. (1999) A large blood pressure-raising effect of nitric oxide synthase inhibition in humans. *Hypertension* 33, 937-942
10. Quyyumi, A. A., and Patel, R. S. (2010) Endothelial dysfunction and hypertension: cause or effect? *Hypertension* 55, 1092-1094
11. Kitta, Y., Obata, J. E., Nakamura, T., Hirano, M., Kodama, Y., Fujioka, D., Saito, Y., Kawabata, K., Sano, K., Kobayashi, T., Yano, T., Nakamura, K., and Kugiyama, K. (2009) Persistent impairment of endothelial vasomotor function has a negative impact on outcome in patients with coronary artery disease. *J Am Coll Cardiol* 53, 323-330
12. Hultstrom, M. (2012) Development of structural kidney damage in spontaneously hypertensive rats. *J Hypertens* 30, 1087-1091

13. Bennett, M. A., Hillier, C., and Thurston, H. (1996) Endothelium-dependent relaxation in resistance arteries from spontaneously hypertensive rats: effect of long-term treatment with perindopril, quinapril, hydralazine or amlodipine. *J Hypertens* 14, 389-397
14. Spitler, K. M., Matsumoto, T., and Webb, R. C. (2013) Suppression of endoplasmic reticulum stress improves endothelium-dependent contractile responses in aorta of the spontaneously hypertensive rat. *Am J Physiol Heart Circ Physiol* 305, H344-353
15. Dickhout, J. G., Colgan, S. M., Lhotak, S., and Austin, R. C. (2007) Increased endoplasmic reticulum stress in atherosclerotic plaques associated with acute coronary syndrome - A balancing act between plaque stability and rupture. *Circulation* 116, 1214-1216
16. Dickhout, J. G., Hossain, G. S., Pozza, L. M., Zhou, J., Lhotak, S., and Austin, R. C. (2005) Peroxynitrite causes endoplasmic reticulum stress and apoptosis in human vascular endothelium: implications in atherogenesis. *Arterioscler Thromb Vasc Biol* 25, 2623-2629
17. Hong, H. J., Hsiao, G., Cheng, T. H., and Yen, M. H. (2001) Supplementation with tetrahydrobiopterin suppresses the development of hypertension in spontaneously hypertensive rats. *Hypertension* 38, 1044-1048
18. Dickhout, J. G., and Krepinsky, J. C. (2009) Endoplasmic reticulum stress and renal disease. *Antioxid Redox Signal* 11, 2341-2352
19. Walter, P., and Ron, D. (2012) The unfolded protein response: from stress pathway to homeostatic regulation. *Science* 334, 1081-1086
20. Dickhout, J. G., Carlisle, R. E., and Austin, R. C. (2011) Inter-Relationship between Cardiac Hypertrophy, Heart Failure and Chronic Kidney Disease – Endoplasmic Reticulum Stress as a Mediator of Pathogenesis. *Circ Res* 108, 629-642
21. Malhotra, J. D., and Kaufman, R. J. (2007) Endoplasmic reticulum stress and oxidative stress: a vicious cycle or a double-edged sword?. *Antioxid Redox Signal*. 9, 2277-2293
22. Carlisle, R. E., Brimble, E., Werner, K. E., Cruz, G. L., Ask, K., Ingram, A. J., and Dickhout, J. G. (2014) 4-Phenylbutyrate Inhibits Tunicamycin-Induced Acute Kidney Injury via CHOP/GADD153 Repression. *PLoS One* 9, e84663
23. Basseri, S., Lhotak, S., Sharma, A. M., and Austin, R. C. (2009) The chemical chaperone 4-phenylbutyrate inhibits adipogenesis by modulating the unfolded protein response. *J Lipid Res* 50, 2486-2501

24. Feng, M., Whitesall, S., Zhang, Y., Beibel, M., D'Alecy, L., and DiPetrillo, K. (2008) Validation of volume-pressure recording tail-cuff blood pressure measurements. *Am J Hypertens* 21, 1288-1291
25. Dickhout, J. G., and Lee, R. (1997) Structural and functional analysis of small arteries from young spontaneously hypertensive rats. *Hypertension* 29, 781-789
26. Parasuraman, S., and Raveendran, R. (2012) Measurement of invasive blood pressure in rats. *J Pharmacol Pharmacother* 3, 172-177
27. Dickhout, J. G., Carlisle, R. E., Jerome, D. E., Mohammed-Ali, Z., Jiang, H., Yang, G., Mani, S., Garg, S. K., Banerjee, R., Kaufman, R. J., Maclean, K. N., Wang, R., and Austin, R. C. (2012) Integrated stress response modulates cellular redox state via induction of cystathionine gamma-lyase: cross-talk between integrated stress response and thiol metabolism. *J Biol Chem* 287, 7603-7614
28. Cao, S. S., Zimmermann, E. M., Chuang, B. M., Song, B., Nwokoye, A., Wilkinson, J. E., Eaton, K. A., and Kaufman, R. J. (2013) The unfolded protein response and chemical chaperones reduce protein misfolding and colitis in mice. *Gastroenterology* 144, 989-1000 e1006
29. Hall, K. L., Harding, J. W., and Hosick, H. L. (1991) Isolation and characterization of clonal vascular smooth muscle cell lines from spontaneously hypertensive and normotensive rat aortas. *In Vitro Cell Dev Biol* 27A, 791-798
30. Hossain, G. S., Lynn, E. G., Maclean, K. N., Zhou, J., Dickhout, J. G., Lhotak, S., Trigatti, B., Capone, J., Rho, J., Tang, D., McCulloch, C. A., Al-Bondokji, I., Malloy, M. J., Pullinger, C. R., Kane, J. P., Li, Y., Shiffman, D., and Austin, R. C. (2013) Deficiency of TDAG51 protects against atherosclerosis by modulating apoptosis, cholesterol efflux, and peroxiredoxin-1 expression. *J Am Heart Assoc* 2, e000134
31. Steireif, C., Garcia-Prieto, C. F., Ruiz-Hurtado, G., Pulido-Olmo, H., Aranguéz, I., Gil-Ortega, M., Somoza, B., Schonfelder, G., Schulz, A., Fernandez-Alfonso, M. S., and Kreutz, R. (2013) Dissecting the genetic predisposition to albuminuria and endothelial dysfunction in a genetic rat model. *J Hypertens* 31, 2203-2212; discussion 2212
32. Dornas, W. C., and Silva, M. E. (2011) Animal models for the study of arterial hypertension. *J Biosci* 36, 731-737
33. Dickhout, J. G., and Lee, R. M. (2000) Increased medial smooth muscle cell length is responsible for vascular hypertrophy in young hypertensive rats. *Am J Physiol Heart Circ Physiol* 279, H2085-2094

34. Kassan, M., Galan, M., Partyka, M., Saifudeen, Z., Henrion, D., Trebak, M., and Matrougui, K. (2012) Endoplasmic reticulum stress is involved in cardiac damage and vascular endothelial dysfunction in hypertensive mice. *Arterioscler Thromb Vasc Biol* 32, 1652-1661
35. Tang, C., Koulajian, K., Schuiki, I., Zhang, L., Desai, T., Ivovic, A., Wang, P., Robson-Doucette, C., Wheeler, M. B., Minassian, B., Volchuk, A., and Giacca, A. (2012) Glucose-induced beta cell dysfunction in vivo in rats: link between oxidative stress and endoplasmic reticulum stress. *Diabetologia* 55, 1366-1379
36. Raffai, G., Durand, M. J., and Lombard, J. H. (2011) Acute and chronic angiotensin-(1-7) restores vasodilation and reduces oxidative stress in mesenteric arteries of salt-fed rats. *Am J Physiol Heart Circ Physiol* 301, H1341-1352
37. Young, C. N., Cao, X., Gurujju, M. R., Pierce, J. P., Morgan, D. A., Wang, G., Iadecola, C., Mark, A. L., and Davisson, R. L. (2012) ER stress in the brain subfornical organ mediates angiotensin-dependent hypertension. *J Clin Invest* 122, 3960-3964
38. Schnackenberg, C. G., Welch, W. J., and Wilcox, C. S. (1998) Normalization of blood pressure and renal vascular resistance in SHR with a membrane-permeable superoxide dismutase mimetic: role of nitric oxide. *Hypertension* 32, 59-64
39. Chen, X., Patel, K., Connors, S. G., Mendonca, M., Welch, W. J., and Wilcox, C. S. (2007) Acute antihypertensive action of Tempol in the spontaneously hypertensive rat. *Am J Physiol Heart Circ Physiol* 293, H3246-3253
40. Laight, D. W., Andrews, T. J., Haj-Yehia, A. I., Carrier, M. J., and Anggard, E. E. (1997) Microassay of superoxide anion scavenging activity in vitro. *Environ Toxicol Pharmacol* 3, 65-68
41. Krishna, M. C., Russo, A., Mitchell, J. B., Goldstein, S., Dafni, H., and Samuni, A. (1996) Do nitroxide antioxidants act as scavengers of O₂⁻. or as SOD mimics? *J Biol Chem* 271, 26026-26031
42. Mitchell, J. B., Samuni, A., Krishna, M. C., DeGraff, W. G., Ahn, M. S., Samuni, U., and Russo, A. (1990) Biologically active metal-independent superoxide dismutase mimics. *Biochemistry* 29, 2802-2807
43. Xu, H., Fink, G. D., and Galligan, J. J. (2004) Tempol lowers blood pressure and sympathetic nerve activity but not vascular O₂⁻ in DOCA-salt rats. *Hypertension* 43, 329-334
44. Carlisle, R. E., Heffernan, A., Brimble, E., Liu, L., Jerome, D., Collins, C. A., Mohammed-Ali, Z., Margetts, P. J., Austin, R. C., and Dickhout, J. G. (2012)

TDAG51 mediates epithelial-to-mesenchymal transition in human proximal tubular epithelium. *Am J Physiol Renal Physiol* 303, F467-481

45. Lichter-Konecki, U., Diaz, G. A., Merritt, J. L., 2nd, Feigenbaum, A., Jomphe, C., Marier, J. F., Beliveau, M., Mauney, J., Dickinson, K., Martinez, A., Mokhtarani, M., Scharschmidt, B., and Rhead, W. (2011) Ammonia control in children with urea cycle disorders (UCDs); phase 2 comparison of sodium phenylbutyrate and glycerol phenylbutyrate. *Mol Genet Metab* 103, 323-329
46. Ding, L., Chapman, A., Boyd, R., and Wang, H. D. (2007) ERK activation contributes to regulation of spontaneous contractile tone via superoxide anion in isolated rat aorta of angiotensin II-induced hypertension. *Am J Physiol Heart Circ Physiol* 292, H2997-3005
47. Intengan, H. D., Thibault, G., Li, J. S., and Schiffrin, E. L. (1999) Resistance artery mechanics, structure, and extracellular components in spontaneously hypertensive rats : effects of angiotensin receptor antagonism and converting enzyme inhibition. *Circulation* 100, 2267-2275

Figure 1.

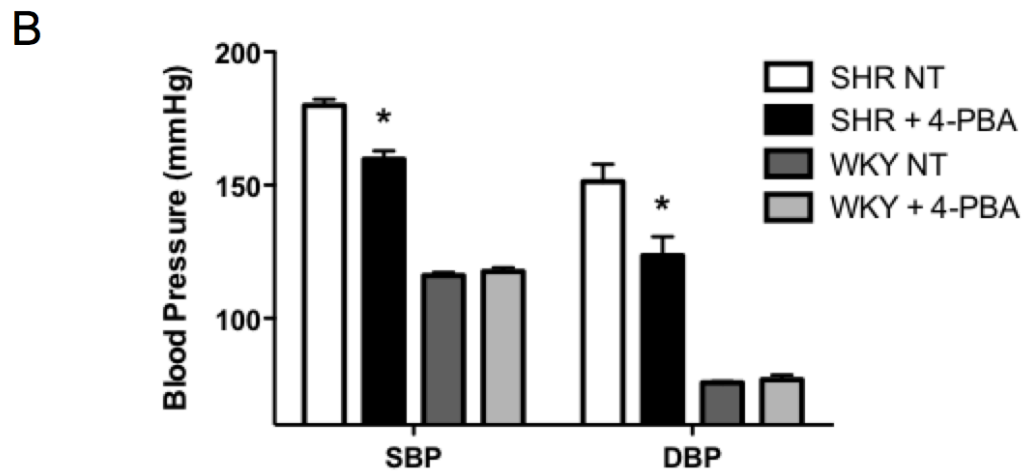
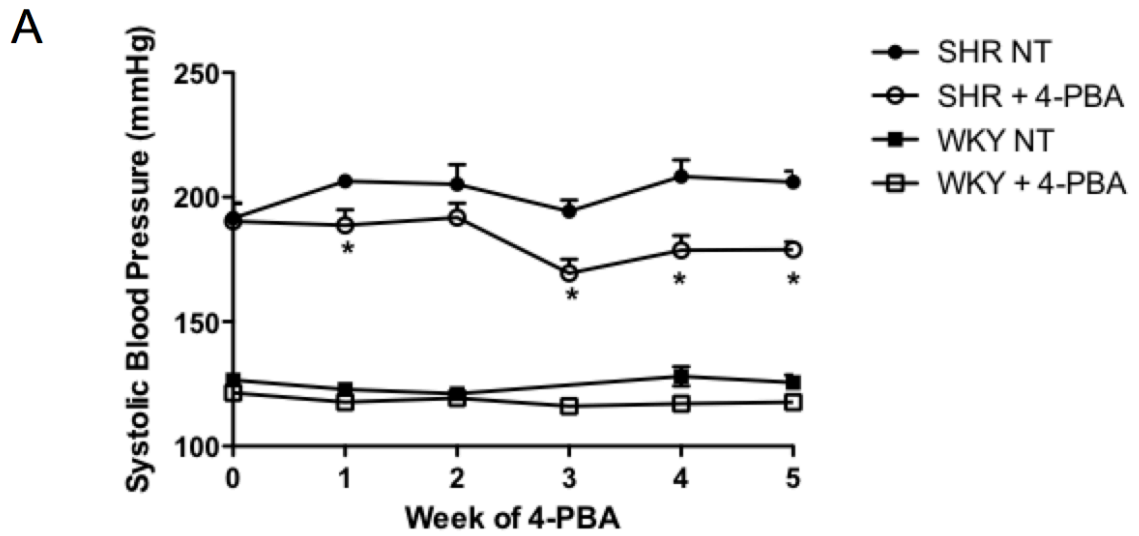


Figure 1. 4-PBA treatment lowers SHR systolic and diastolic blood pressure. (A)

Indirect blood pressure measured via tail cuff plethysmography demonstrated significantly lower SHR systolic blood pressure (SBP) after weeks 1, 3, 4 and 5 of 4-PBA treatment. There was no change in BP in WKY rats. (B) Direct BP measurements recorded through carotid artery cannulation revealed significantly lower SBP and diastolic blood pressure (DBP) with 4-PBA treatment in SHRs after 5 weeks. There was no change in direct blood pressure measurements in WKY rats. *, $P < 0.05$ vs. NT.

Figure 2.

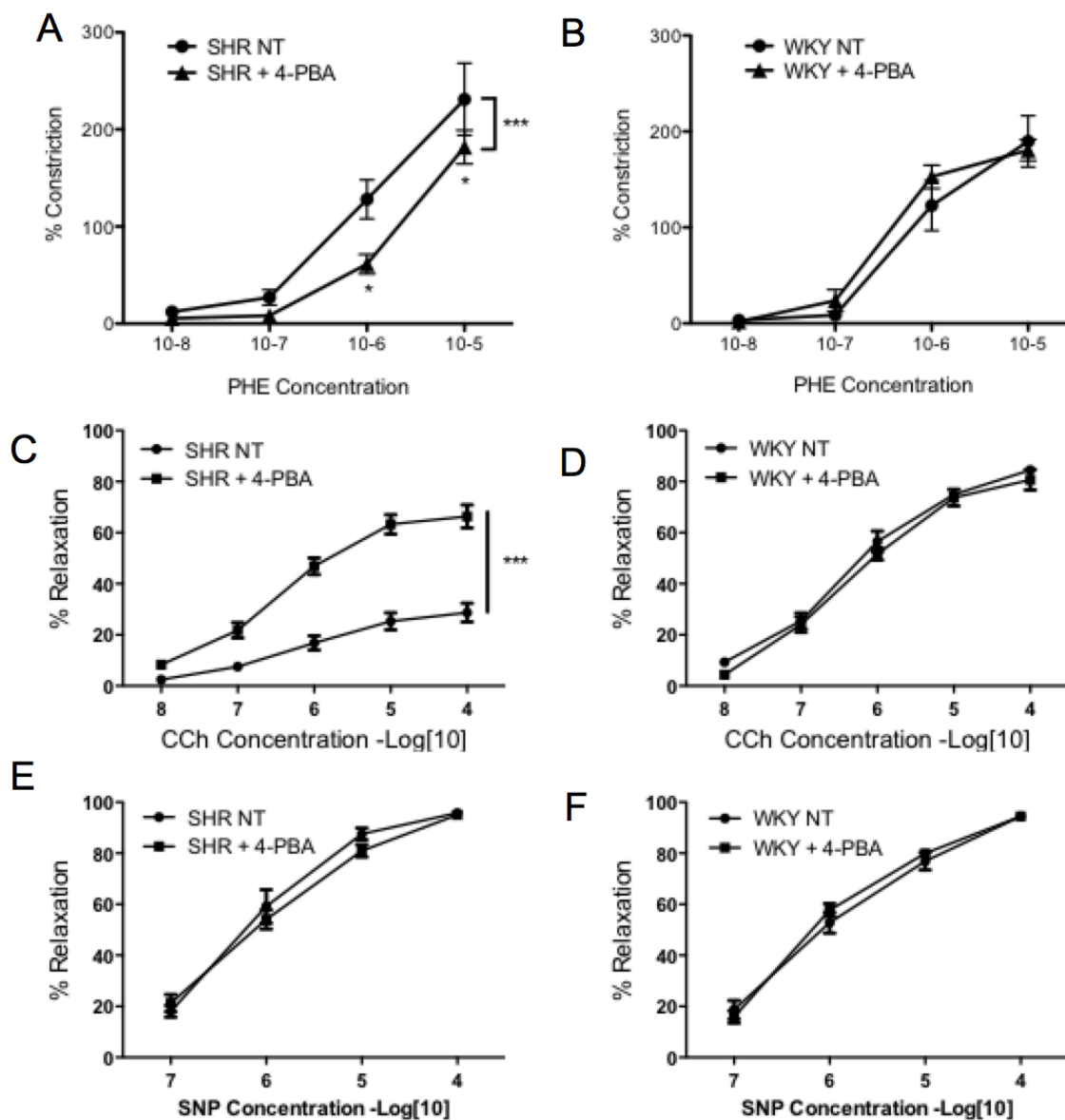


Figure 2. 4-PBA treatment reduces phenylephrine-mediated vasoconstriction and increases carbachol-mediated vasodilation in SHR resistance vessels. (A) Dose-response curves for phenylephrine (PHE)-mediated vasoconstriction revealed a significantly attenuated contractile response in 4-PBA-treated SHR mesenteric arteries. (B) 4-PBA had no effect on PHE-mediated vasoconstriction in WKY mesenteric arteries. (C) 4-PBA treatment significantly increased carbachol (CCh)-induced vasodilation in SHR mesenteric arteries. (D) 4-PBA had no effect on the CCh-mediated dilatory response of WKY mesenteric arteries. (E) Sodium nitroprusside (SNP)-induced vasodilation revealed no difference between non-treated and 4-PBA-treated SHR mesenteric arteries. (F) SNP showed no difference in its ability to vasodilate non-treated and 4-PBA-treated mesenteric arteries from WKY rats. *, $P < 0.05$ vs. NT; ***, $P < 0.01$ vs. NT.

Figure 3.

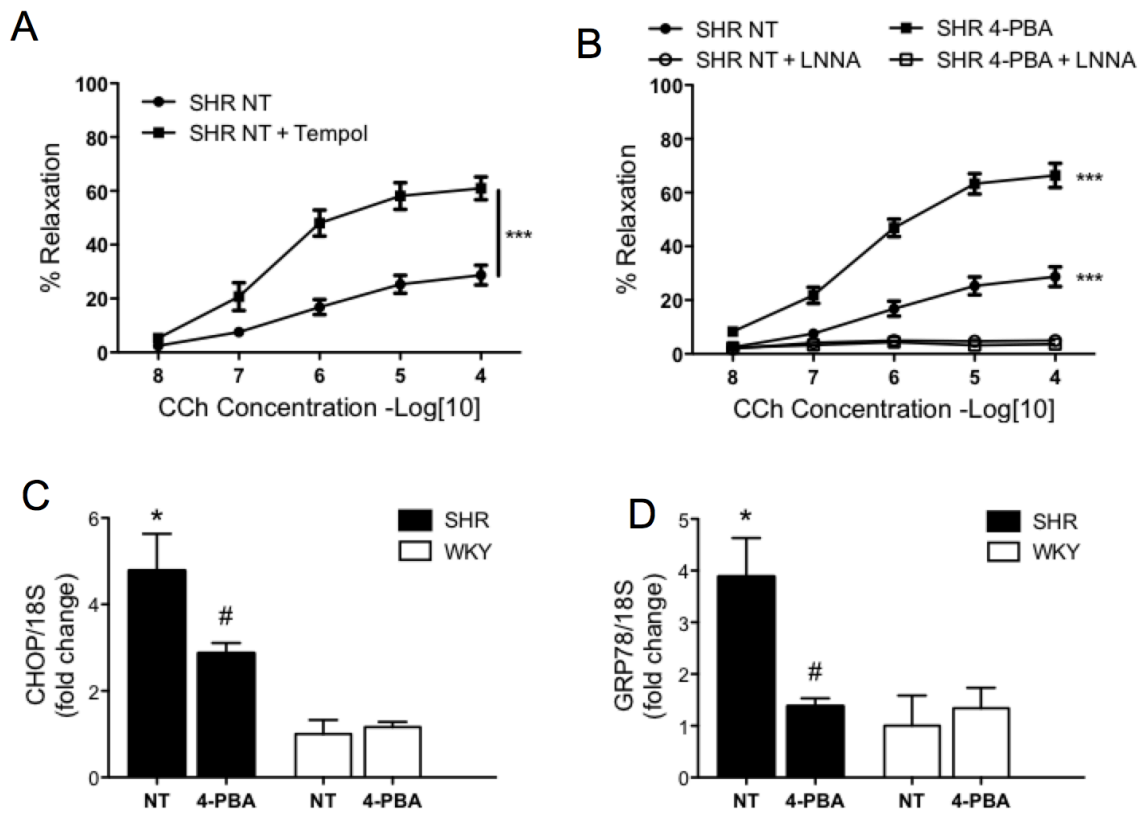


Figure 3. 4-PBA treatment inhibits ER stress-mediated, superoxide-induced reduction of nitric oxide vasodilation in SHR resistance vessels. (A) Carbachol-mediated relaxation of non-treated SHR mesenteric arteries was significantly increased with TEMPOL treatment. (B) Carbachol-induced vasodilation was significantly reduced with nitric oxide synthase inhibitor, L-NNA, treatment in non-treated and 4-PBA-treated SHR mesenteric arteries. (C) rt-PCR analysis demonstrates a significant decrease in CHOP mRNA levels with 4-PBA treatment in SHR resistance vessels. No change was found in resistance vessels from WKY rats. (D) GRP78 mRNA levels were significantly reduced in 4-PBA-treated SHR resistance vessels. WKY resistance vessels demonstrated no change in GRP78 mRNA levels. ***, $P < 0.05$ vs. NT; *, $P < 0.05$ vs. WKY NT; #, $P < 0.05$ vs. NT.

Figure 4.

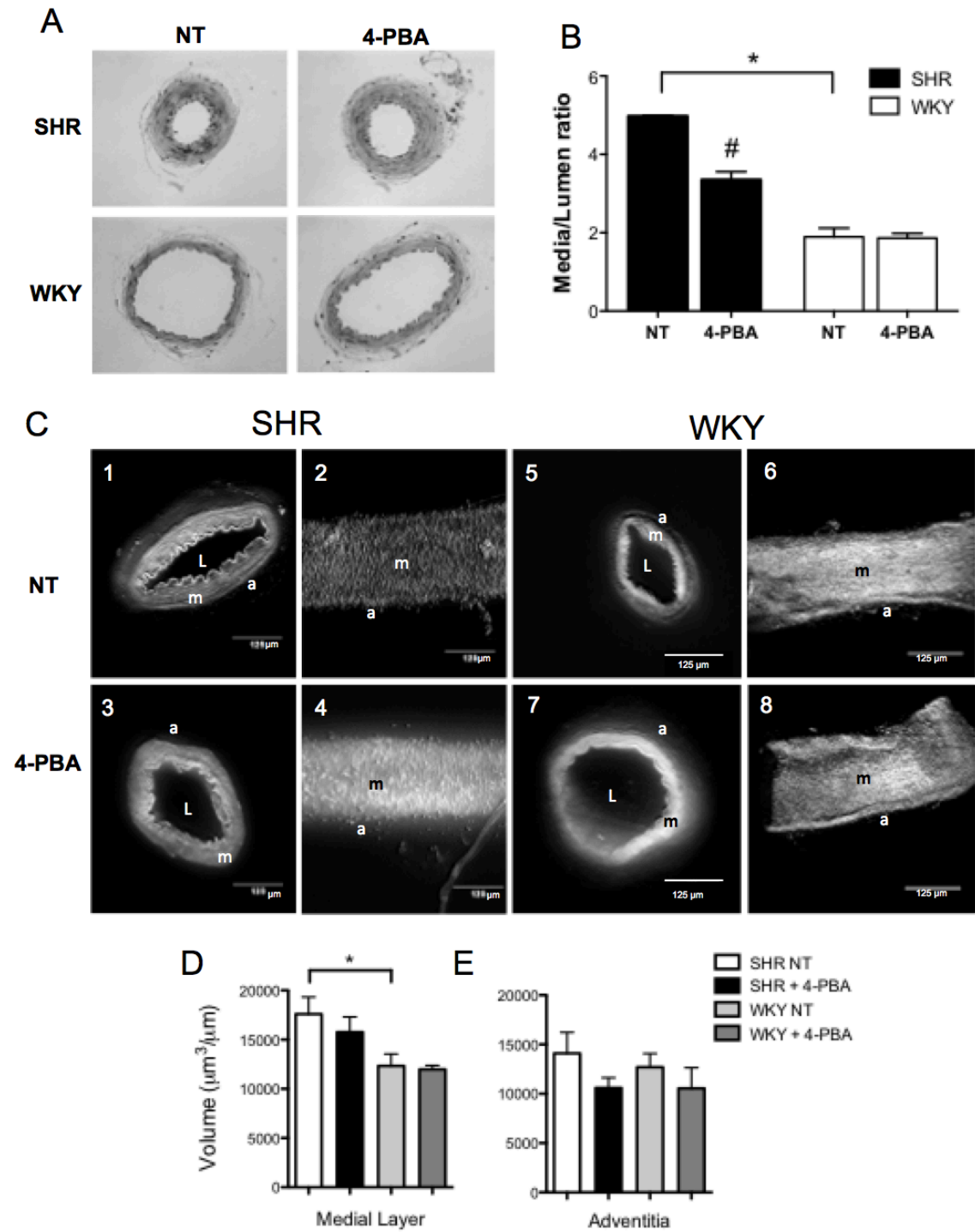


Figure 4. 4-PBA treatment reduces media-to-lumen ratio of mesenteric resistance arteries. (A) Non-treated and 4-PBA-treated mesenteric arteries were stained with Masson's Trichrome and imaged. (B) Media-to-lumen ratio was significantly increased in non-treated SHR mesenteric arteries compared with WKY vessels. Media-to-lumen ratio was significantly reduced in 4-PBA-treated SHR vessels compared with non-treated SHR mesenteric arteries. (C) 3-dimensional reconstructions of non-treated (Images 1 and 5) and 4-PBA-treated (Images 3 and 7) vessels are displayed. Whole artery reconstructions of non-treated (Images 2 and 6) and 4-PBA-treated (Images 4 and 8) vessels are also shown. L = lumen, m = media, a = adventitia. (D) While 4-PBA treatment had no effect on the medial layer volume, SHR rats demonstrated significantly higher medial volume compared with WKY rats. (E) No change was found in the adventitial layer volume with 4-PBA treatment. *, $P < 0.05$ vs. WKY NT; #, $P < 0.05$ vs. SHR NT.

Figure 5.

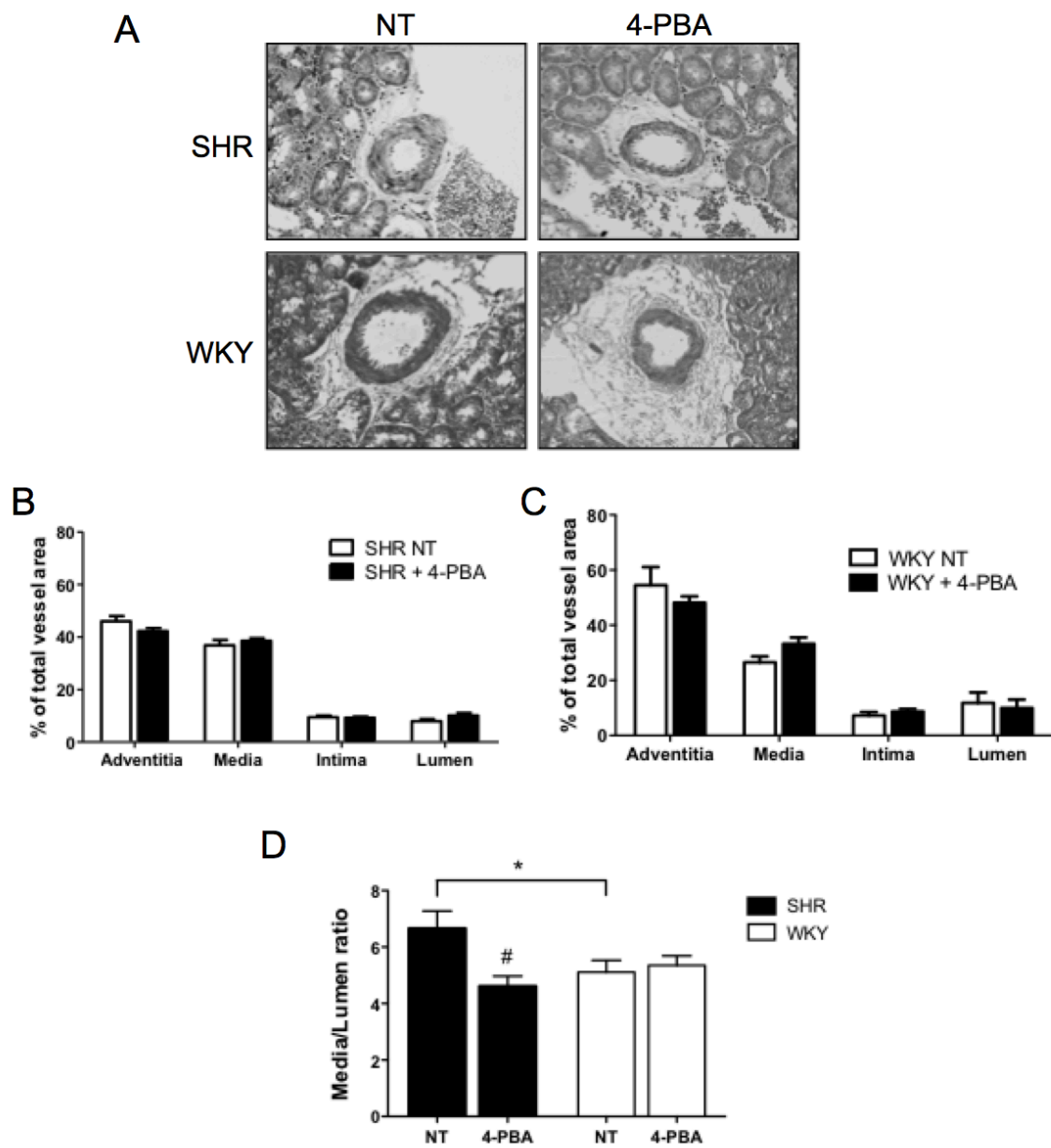


Figure 5. 4-PBA treatment reduced the media-to-lumen ratio in SHR arcuate arteries. (A) Non-treated and 4-PBA-treated kidneys were stained with Masson's Trichrome, and arcuate arteries were imaged. (B) Structural analysis shows no significant change in the proportion of adventitia, media, intima, or lumen between non-treated and 4-PBA-treated SHR arcuate arteries. (C) No structural changes were found in WKY arcuate arteries either. (D) Media-to-lumen ratio was significantly elevated in non-treated SHR arcuate arteries compared to WKY vessels. 4-PBA treatment significantly reduced media-to-lumen ratio in SHR vessels to a level similar to the WKY. *, $P < 0.05$ vs. WKY NT; #, $P < 0.05$ vs. SHR NT.

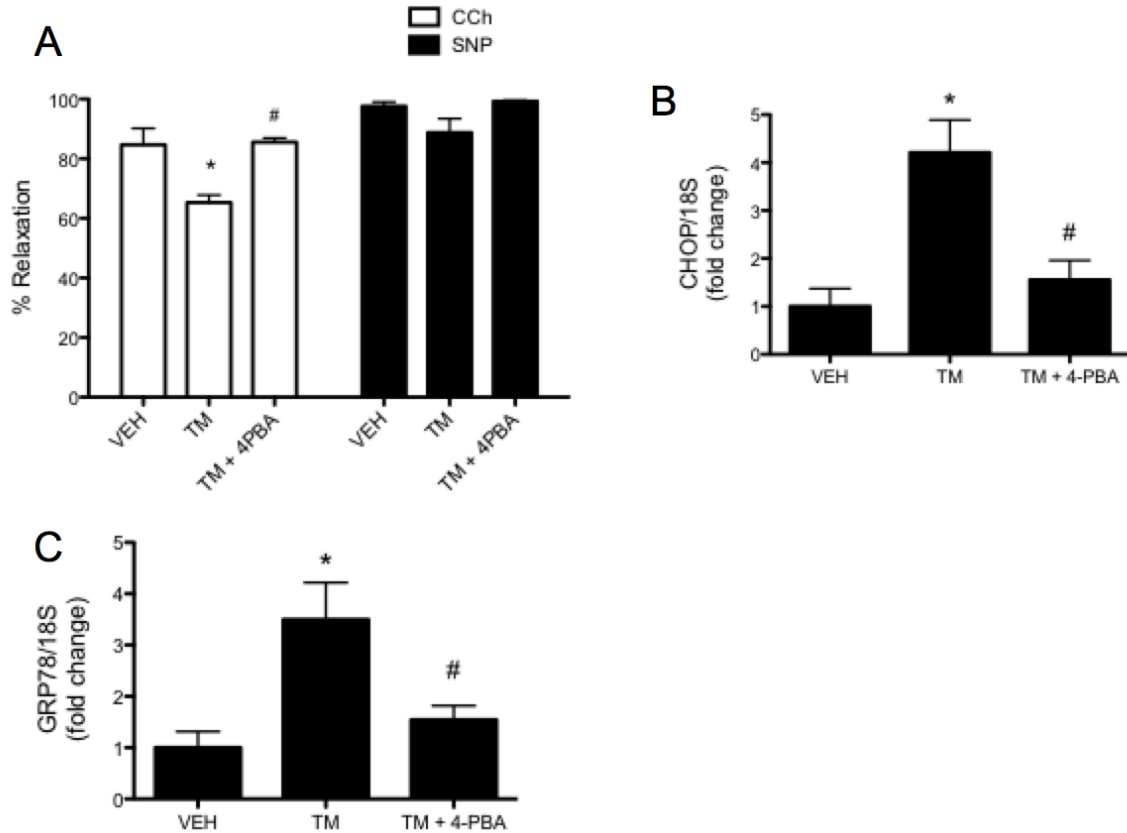


Figure 6. Tunicamycin-mediated ER stress decreases carbachol-induced vasodilation in WKY rat mesenteric arteries. (A) Carbachol (CCh)-induced vasodilation in SHR mesenteric arteries was reduced with TM treatment and recovered with 4-PBA. Sodium nitroprusside (SNP)-induced vasodilation in PHE-pre-contracted vessels revealed no difference between any of the treatments. (B) rt-PCR indicates a significant increase in CHOP mRNA levels with TM treatment; 4-PBA co-treatment prevented this effect. (C) TM-treatment increased GRP78 mRNA levels, while 4-PBA prevented this increase. *, $P < 0.05$ vs. VEH; #, $P < 0.05$ vs. TM.

Figure 7.

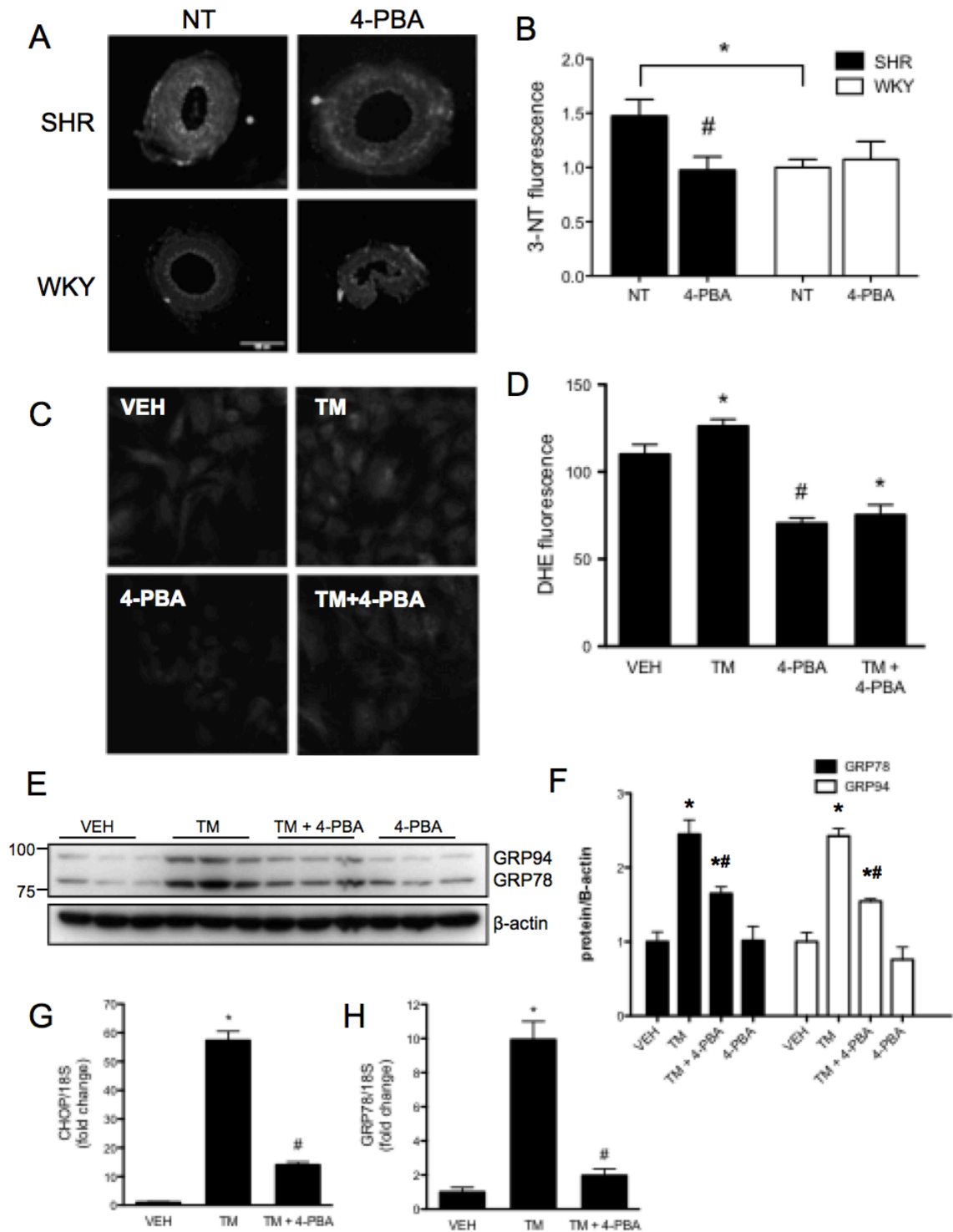


Figure 7. ER stress stimulates superoxide generation in vascular smooth muscle

cells. (A) Mesenteric arteries from untreated or 4-PBA-treated WKY and SHR animals were fluorescently stained for 3-nitrotyrosine (3-NT). (B) Analysis demonstrates that inhibiting ER stress with 4-PBA reduced 3-NT staining in SHR. 4-PBA had no effect on 3-NT staining in WKY rats, which had naturally lower levels of 3-NT generation compared with SHR. *, $P < 0.05$ vs. WKY NT; #, $P < 0.05$ vs. SHR NT. (C) Representative dihydroethidium (DHE) fluorescence micrographs show superoxide generation in cells treated with ER stress inducer tunicamycin (TM) with or without 4-PBA. (D) Analysis of DHE fluorescence shows TM increases superoxide generation, while 4-PBA prevents this increase. 4-PBA treatment alone decreases superoxide generation when compared with VEH. (E) Arterial smooth muscle cells were treated with vehicle (VEH; DMSO), TM, TM+4-PBA, or 4-PBA alone. (F) Densitometric analysis demonstrated a significant increase in ER stress markers GRP78 and GRP94 with TM treatment. 4-PBA was able to prevent increased GRP78 and GRP94 expression. (G) TM treatment increased CHOP mRNA levels, while 4-PBA prevented this increase. (H) GRP78 mRNA levels were also increased by TM treatment; 4-PBA prevented this effect. *, $P < 0.05$ vs. VEH; #, $P < 0.05$ vs. TM.

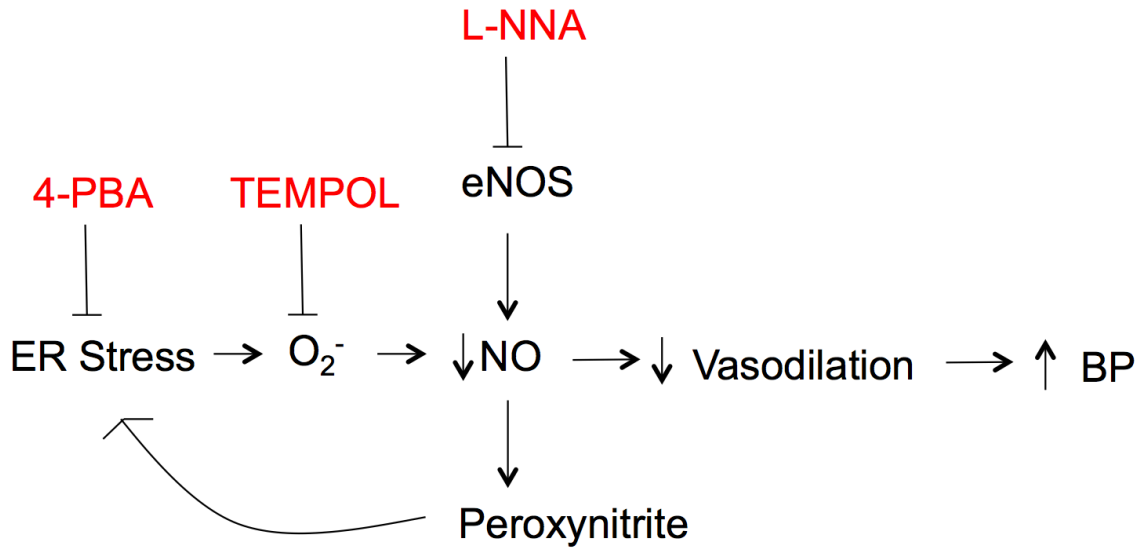


Figure 8. Proposed mechanism of ER stress-induced hypertension in the SHR. In accordance with our findings, ER stress causes superoxide generation in resistance vessels of the SHR, which decreases the bioavailability of nitric oxide (NO) in these vessels. Increased bioavailability of NO can generate peroxynitrite, causing further ER stress. NO is produced via eNOS, which can be inhibited by L-NNA leading to reduced NO. Decreased NO leads to reduced endothelial-dependent vasodilation. This in turn increases total peripheral resistance contributing to an increased blood pressure (BP) and hypertension in the SHR. Reducing superoxide generation, by inhibiting protein misfolding with 4-PBA or scavenging superoxide with TEMPOL increases NO bioavailability leading to improved vasodilation and ultimately decreased blood pressure in the SHR.

CHAPTER 5

Endoplasmic reticulum stress inhibition limits the progression of chronic kidney disease in the Dahl salt-sensitive rat

Victoria Yum, Rachel E. Carlisle, Chao Lu, Elise Brimble, Jasmine Chahal, Chandak Upagupta, Kjetil Ask, and Jeffrey G. Dickhout.

American Journal of Physiology Renal Physiology (2016). 312; F230-F244.
Doi: 10.1152/ajprenal.00119.2016

© Copyright by *The American Physiological Society*

Chapter link:

Preserving the myogenic response through ER stress inhibition protects from renal damage and delays CKD progression, while lowering blood pressure alone does not. ER stress can lead to activation of the UPR, and is associated with many forms of kidney disease (Dickhout & Krepinsky, 2009). In fact, the UPR is activated in nephrons of animals and humans with proteinuric nephropathy (Lindenmeyer et al., 2008). As mentioned in chapters 3 and 4, treatment with the LWCC 4-PBA can prevent ER stress-mediated renal damage by inhibiting the UPR, and contractility studies indicate that inhibiting ER stress with 4-PBA can improve endothelial-dependent relaxation in mesenteric resistance arteries. When maintained on a high salt diet, the Dahl salt-sensitive rat displays proteinuria, renal interstitial fibrosis, cardiac hypertrophy, cardiac fibrosis, and activation of the local renal and cardiac renin-angiotensin-aldosterone system (Mori et al., 2008). Integrating Brown Norway chromosome 13 into the genomic DNA of Dahl salt-sensitive rats prevents kidney disease in these animals (Cowley et al., 2001). This prevents the rats from developing elevated blood pressure, indicating that resolving chronic kidney injury reduces hypertension in the DSS rat (Cowley et al., 2001; Mattson et al., 2008). This manuscript establishes that preserving the myogenic response, and not simply lowering blood pressure, is essential to preventing hypertensive CKD. Additionally, inhibiting ER stress with a LWCC can preserve the myogenic response. Preservation of the myogenic response protects the glomerular filtration barrier, and thus, prevents proteinuria. Lowering blood pressure, without inhibiting ER stress, worsens proteinuria, protein cast formation, and renal interstitial fibrosis.

Author's contribution:

R.E. Carlisle, V. Yum, and J.G. Dickhout designed the study. R.E. Carlisle, V. Yum, and C. Lu conducted the animal studies and collected tissues. R.E. Carlisle and V. Yum analysed tissues and performed related quantifications. R.E. Carlisle, J. Chahal, and C. Upagupta performed cell culture experiments, and related analyses. R.E. Carlisle, V. Yum, C. Lu, and E. Brimble assembled the results, and generated the figures in the manuscript. R.E. Carlisle and V. Yum wrote the manuscript. R.E. Carlisle and E. Brimble revised the manuscript. R.E. Carlisle, V. Yum, K. Ask, and J.G. Dickhout reviewed and edited the manuscript. All authors approved of the final submission.

Running title: 4-PBA reduces proteinuria

Endoplasmic reticulum stress inhibition limits the progression of chronic kidney disease in the Dahl salt-sensitive rat

Victoria Yum¹, Rachel E. Carlisle¹, Chao Lu¹, Elise Brimble¹, Jasmine Chahal¹, Chandak Upagupta¹, Kjetil Ask² and Jeffrey G. Dickhout¹.

¹Department of Medicine, Division of Nephrology, McMaster University and St. Joseph's Healthcare Hamilton, Hamilton, Ontario, Canada.

²Department of Medicine, Division of Respiriology, McMaster University, St. Joseph's Healthcare Hamilton, Hamilton, Ontario, Canada

Address correspondence to:

Jeffrey G. Dickhout, PhD

Department of Medicine, Division of Nephrology

McMaster University and St. Joseph's Healthcare Hamilton

50 Charlton Avenue East

Hamilton, Ontario, Canada, L8N 4A6

Phone: 905-522-1155 ext. 35334

Fax: 905-540-6589

Email: jdickhou@stjosham.on.ca

Key words: 4-phenylbutyric acid, endoplasmic reticulum stress, myogenic response, proteinuria, salt-sensitive hypertension

ABSTRACT

Proteinuria is one of the primary risk factors for the progression of chronic kidney disease (CKD), and has been implicated in the induction of endoplasmic reticulum (ER) stress. We hypothesized that the suppression of ER stress with a low molecular weight chemical chaperone, 4-phenylbutyric acid (4-PBA), would reduce the severity of CKD and proteinuria in the Dahl salt-sensitive (SS) hypertensive rat. To induce hypertension and CKD, 12-week old male rats were placed on a high salt (HS) diet for 4-weeks with or without 4-PBA treatment. We assessed blood pressure and markers of CKD, including proteinuria, albuminuria, and renal pathology. Further, we determined if HS feeding resulted in an impaired myogenic response, subsequent to ER stress. 4-PBA treatment reduced salt-induced hypertension, proteinuria and albuminuria, and preserved myogenic constriction. Further, renal pathology was reduced with 4-PBA treatment, as indicated by lowered expression of pro-fibrotic markers and fewer intratubular protein casts. In addition, ER stress in the glomerulus was reduced, and the integrity of the glomerular filtration barrier was preserved. These results suggest that 4-PBA treatment protects against proteinuria in the SS rat by preserving the myogenic response, and by preventing ER stress, which led to a breakdown in the glomerular filtration barrier. As such, alleviating ER stress serves as a viable therapeutic strategy to preserve kidney function and to delay the progression of CKD in the animal model under study.

INTRODUCTION

The progression of chronic kidney disease (CKD) culminates in end-stage renal disease (ESRD), which requires renal replacement therapy. In spite of the numerous risk factors that predispose individuals to CKD, there is a predictable manner in which the disease progresses. Affected individuals develop renal interstitial fibrosis, nephron loss, and tubular atrophy, resulting in a reduction in the filtration capacity of the kidney (52). Although the etiology of CKD is varied, proteinuria has been consistently identified as one of the most significant risk factors for progressive severity (32). With an incidence of 11% in the United States and a growing prevalence, addressing the healthcare burden of CKD represents a major public health initiative (15).

To protect the kidney from changes in systemic blood pressure and to maintain renal blood flow autoregulation, two mechanisms are known: tubuloglomerular feedback and the myogenic response (40, 62). Transgenic animal models of hypertension and/or CKD demonstrate a correlation between renal disease and an impaired myogenic response (17, 55, 58, 63-65). These reports indicate a strong association between an altered myogenic response and kidney disease, independent of hypertensive status. Impaired myogenic constriction can lead to glomerular hyperfiltration and subsequent renal pathology, including proteinuria (6, 7, 31). Excessive levels of protein in the nephron can form protein casts within the tubules, causing further damage, such as tubule obstruction and fibrosis (4, 5, 24, 68).

Proteinuria has been implicated in the induction of endoplasmic reticulum (ER) stress (33, 41, 46, 56). ER stress occurs when the amount of unfolded proteins surpasses the folding capabilities of the ER. As a result, several protective pathways are initiated to

preserve cellular function; if insufficient, apoptosis ensues (19). In cultured proximal tubule cells, albumin overload induced ER stress marker overexpression; similar results were observed in animal models of proteinuric kidney disease (18, 47, 56). Furthermore, ER stress markers were elevated in kidney biopsies from patients with proteinuric nephropathy (3, 51).

The Dahl salt-sensitive (SS) rat model develops proteinuria and CKD in response to high salt (HS) feeding. Consomic SS rats with normotensive Brown Norway chromosome 13 intergressed into their genome were used as a control; these SS-BN13 rats are normotensive and do not develop salt-induced renal damage (16). The Brenner hypothesis asserts that glomerular hyperfiltration and increased intraglomerular capillary pressure cause renal damage, such as that induced by renal mass reduction experiments (6, 7). In context of this study, loss of myogenic constriction in preglomerular vessels would also result in increased intraglomerular pressure. We hypothesized that inhibiting ER stress with the chemical chaperone 4-phenylbutyric acid (4-PBA) would preserve renal blood flow autoregulation and prevent proteinuric kidney damage. To explore this hypothesis, features of CKD were assessed, including proteinuria and fibrosis. Our results suggest a mechanism through which ER stress-mediated impairments in myogenic constriction is a contributor to the pathogenesis of proteinuric CKD in the SS rat model of CKD, independent of hypertensive status.

METHODS

In vitro studies

Immortalized human proximal tubule (HK-2) cells were grown to confluence and treated for 18 h with vehicle (DMSO) thapsigargin (TG; 200 nM), or TG with 4-PBA (1 mM). Cells were lysed and underwent Western blotting for the amino acid sequence KDEL found in the ER stress marker GRP94. Western blotting was performed, as previously described (8). HK-2 cells were treated with vehicle, TG, or TG combined with varying doses of 4-PBA (0.01 mM-10 mM). Cells were stained with thioflavin T (5 μ M) for 15 mins at 37°C. Stained cells were then fixed with 4% paraformaldehyde, and mounted on microscope slides. Images were taken at 40X magnification using an Olympus IX81 Nipkow scanning disc confocal microscope, and analysis was performed using Metamorph image analysis software. Protein aggregation was quantified by measuring the fluorescence intensity within a specified region normalized to the background. HK-2 cells were treated with various ER stress inducers, including tunicamycin (TM; 1 μ g/ml), TG (200 nM), and A23187 (10 μ M) for 24 h. Cell death caused by these ER stress inducers has been shown to be minimal (20). Cells were subsequently fixed with 4% paraformaldehyde and stained for β -catenin (Cell Signaling; #2677).

Animal study

Male Dahl salt-sensitive (SS), Dahl salt-sensitive consomic Brown Norway chromosome 13 (SS-BN13) rats, and Sprague-Dawley rats (Charles River) were maintained at St Joseph's Healthcare Hamilton Animal Facility. 12-week old SS and SS-

BN13 animals were placed on either a normal salt (NS; 0.4% NaCl; AIN-76A, Research Diets, New Brunswick, NJ) or a high salt (HS; 8% NaCl) diet for 4 weeks. 4-phenylbutyric acid (4-PBA; 1 g/kg/day) was added to the drinking water one week prior to HS feeding and continued until sacrifice. 4-PBA-treated water was changed every 3 days, based on animal weight, and water consumption. Hydralazine (15 mg/kg/day) and nifedipine (25 mg/kg/day) were prepared in edible gelatin cubes and placed in cages daily, starting one week prior to HS feeding.

Tail cuff plethysmography (Kent Scientific, CODA system) was used to indirectly measure blood pressure (27). Blood pressure was also measured directly through carotid artery cannulation. 24-hour urine samples were collected and analyzed for total protein and albumin excretion at weeks 0, 1, and 3. At the end of the study period, animals were sacrificed by exsanguination. Blood was collected for analysis of blood urea nitrogen (BUN) and plasma creatinine levels. Kidneys were perfused with Hank's basic salt solution (HBSS) to clear blood. A segment of the arcuate artery of the left kidney was removed to perform vascular studies. Samples of the right kidney were removed and fixed in 4% buffered paraformaldehyde and processed for paraffin embedding. All animal work was done in accordance with the McMaster University Animal Research Ethics Board guidelines.

Urinalysis

Urine protein concentration was analyzed by Core Laboratories at St Joseph's Healthcare Hamilton and 24 hour protein excretion was then calculated using 24 hour urine volume collected in metabolic cages. Albumin was analyzed using a rat albumin

enzyme-linked immunosorbent assay (ELISA) kit and following manufacturer's directions (Bethyl Laboratory, Texas, USA). Briefly, 96-well plates were coated with primary antibody diluted in coating buffer overnight and blocked for 1 hour. Diluted samples (1:1000 - 1:500 000) were incubated in wells for one hour and then incubated with horseradish peroxidase (HRP) detection antibody. After washing the wells, tetramethylbenzidine (TMB) substrate solution (Sigma) was placed in each well and the reaction was stopped with 0.18 M H₂SO₄. Plates were then read at 450 nm with a plate reader (Molecular Devices Spectra Max Plus384 Absorbance Microplate Reader).

Vascular studies

Renal arcuate arteries were dissected from surrounding kidney tissue. Vessels were transferred to a dual vessel chamber containing 37°C HBSS and mounted in blind-sac method, as previously described (21). A subset of vessels were treated for 6 hours with tunicamycin (TM; 1 µg/mL) in the presence or absence of 4-PBA (1 mM). The chamber was connected to a PS-200 system to pressurize the vessel with a servo controller and peristaltic pump. Vessel lumen diameter was recorded continuously with a video dimension analyzer (Living Systems Instrumentation, Burlington, VT). Vessels were imaged and recorded with a Leica WILD M3C microscope and Hitachi KP-113 CCD. After equilibrating the vessels for 60 min at 40 mmHg of pressure, lumen-diameter curves were generated by using step-wise increases in intraluminal pressure from 80 to 180 mmHg (5 min each). Changes in lumen diameter were calculated as the difference between the lumen diameter at each pressure point and the lumen diameter at 80 mmHg.

Tissue staining and analysis

Periodic acid-Schiff (PAS)-stained kidney sections were imaged using a BX41 Olympus microscope with an Olympus DP70 camera, and protein casts were quantified (16). Immunohistochemical staining for α - smooth muscle actin (α -SMA) and picrosirius red (PSR) was performed by Core Laboratories at McMaster University. Immunohistochemical (IHC) staining for GRP78 (Santa Cruz; sc-1050) was performed on kidney sections, as previously (44). IHC staining for CHOP (Santa Cruz; sc-575) was performed, as previously (43), in conjunction with PAS staining. α -SMA staining was quantified using MetaMorph software (Version 7.7.3.0) by calculating area density of stained regions. PSR-stained newly deposited collagen was imaged using polarized light microscopy, which allows collagen fibres to appear bright and non-collagen elements to appear dark (59). Briefly, a polarizer and analyzer were used on the microscope during image capture. The polarizer and analyzer eliminate light, causing the dark background. Due to the repeated pattern of collagen, light is diffracted; the birefringent property of collagen combined with the use of the polarizer and analyzer cause the collagen to appear green, red, or yellow, against a dark background. Quantification was performed by measuring area density of collagen birefringence. Area density of GRP78 staining was quantified using Image-Pro Plus (Media Cybernetics, Version 5.1). Transmission electron microscopy (TEM) was used to assess glomerular ultrastructure. Tissues were fixed, embedded in plastic, and stained as previously described (22). The rough ER of glomerular podocytes was assessed using TEM, where images in the perinuclear region from podocytes were acquired at 50 000X. Thirty or more ER segments were measured in each animal group. The rough ER structure was selected with the free-hand selection tool

in ImageJ software (NIH; Bethesda, MD), recording the area and perimeter of the ER segment. Area to perimeter ratio was used to indicate rough ER dilation, since there is an increase in rough ER area as rough ER dilation occurs (66).

qRT-PCR

RNA was extracted from arcuate arteries using the RNeasy mini kit (Qiagen, Toronto, Canada), as per the manufacturer's instructions. cDNA was prepared using the SuperScript VILO cDNA Synthesis Kit (Life Technologies, Burlington, Canada). Forward (F) and reverse (R) primers are as follows: GRP78: (F) 5-CTG GGT ACA TTT GAT CTG ACT GG-3 and (R) 5-GCA TCC TGG TGG CTT TCC AGC CAT TC-3; CHOP: (F) 5-AGC TGG AAG CCT GGT ATG AG-3 and (R) 5-GAC CAC TCT GTT TCC GTT TC-3; 18S: (F) 5-GTT GGT TTT CGG AAC TGA GGC-3 and (R) 5-GTC GGC ATC GTT TAT GGT CG-3. Amplification was measured using SYBR green (Life Technologies) on a Vii7 Real-Time PCR System (Life Technologies).

Statistical analysis

Quantitative results are expressed as the mean \pm standard error of the mean, and were analyzed using ANOVA with Bonferroni correction. Significant differences were recognized at the 95% level. Linear regression analysis was performed in GraphPad Prism (Version 5.0a), using 95% confidence intervals to identify significant differences between slopes.

RESULTS

To determine the efficacy of 4-PBA inhibiting ER stress in the kidney, misfolded proteins were measured in proximal tubule cells. Proximal tubule cells were treated with TG in the presence or absence of 4-PBA, and subsequently underwent Western blotting for GRP94 (Figure 1A). Quantification demonstrates that TG induced ER stress, as demonstrated by increased GRP94 expression; 4-PBA prevented TG-induced ER stress (Figure 1B). Increased thioflavin T staining determined that TG treatment induced protein aggregation in these cells. Co-treatment with 4-PBA dose-dependently reduced ER stress-mediated protein aggregation, demonstrating the effectiveness of 4-PBA in inhibiting ER stress (Figure 1C and D). 4-PBA prevents ER stress-mediated β -catenin (green; arrows) translocation to the nucleus, preserving cell-cell interactions (Figure 1E).

Blood pressure is lowered with 4-PBA treatment

To determine the effect of ER stress inhibition on blood pressure, HS-fed rats were treated with 4-PBA (Table 1). HS feeding increased systolic (SBP) and diastolic blood pressure (DBP) in both SS-BN13 and SS rats. 4-PBA treatment significantly reduced SBP in SS-BN13 and SS rats, and DBP in SS-BN13 rats. BUN and serum creatinine levels were unchanged after 4 weeks of HS feeding.

4-PBA prevents salt-induced proteinuria and albuminuria

To assess kidney injury, 24-hour total urinary protein and albumin excretion was analyzed. No significant differences were observed in SS-BN13 animals. HS-fed SS rats demonstrated a significant increase in proteinuria; this effect was prevented with 4-PBA

treatment (Figure 2A). Similar statistical differences were observed with albumin excretion (Figure 2B). The progression of proteinuria and albuminuria was analyzed over the course of three weeks using linear regression. In SS-BN13 animals, there were no significant differences in the slopes of proteinuria (Figure 2C) or albuminuria (Figure 2D) between treatment groups. In SS rats, HS diet significantly increased the rate of proteinuria development; treatment with 4-PBA did not significantly reduce the slope (Figure 2E). HS feeding increased the slope of albuminuria; treatment with 4-PBA significantly reduced the slope to that approximating NS diet (Figure 2F).

ER stress inhibition preserves the myogenic response

Renal arcuate arteries were used to examine myogenic constriction in response to HS feeding and to determine the involvement of ER stress. Myogenic constriction is demonstrated by an active reduction in lumen diameter with increased intraluminal pressure (Figure 3A). The lumen diameter significantly increased in response to intraluminal pressure in HS-fed SS rats; the myogenic response was preserved with 4-PBA treatment (Figure 3B). A significant increase in ER stress marker (GRP78 and CHOP) mRNA expression was found in arcuate arteries from HS-fed SS rats. 4-PBA treatment protected against HS-induced expression of ER stress markers (Figure 3C). To determine the role of ER stress in myogenic constriction, arcuate arteries from Sprague-Dawley rats were treated with the ER stress inducer, TM, or co-treated with 4-PBA. TM-induced ER stress attenuated the myogenic response, similar to HS-fed SS rats. Co-treatment with 4-PBA partially preserved myogenic constriction (Figure 3D). Similar to

the HS-fed SS rats, 4-PBA co-treatment inhibited TM-induced GRP78 and CHOP mRNA upregulation in arcuate arteries (Figure 3E).

4-PBA prevents ER stress-mediated renal injury

As ER stress inhibition prevented increased albuminuria, which is a marker of glomerular impairment (14), ER stress induction was examined in SS rat glomeruli. Staining for GRP78 demonstrates low levels of the protein are present in the cortex of the kidney of SS rats, independent of salt consumption (Figure 4A). Quantification of GRP78 staining determined that ER stress was induced in the glomeruli of HS-fed SS rats. Further, glomerular GRP78 expression was significantly lower in rats treated with 4-PBA (Figure 4B). Kidneys were IHC stained for CHOP and co-stained with PAS. Staining demonstrates CHOP expression (arrows) in cells of damaged areas in the cortex of the kidney, including tubules containing protein casts of all rats and glomeruli of HS-fed rats (Figure 4C).

To examine the effects of ER stress inhibition on the integrity of the glomerular filtration barrier (GFB), transmission electron microscopy was used to assess cortical ultrastructure. No discernible differences in the GFB, podocytes, or proximal tubules were seen between treatment groups of SS-BN13 rats (Figure 4D). The GFB of the HS-fed SS animals demonstrated podocyte effacement and basement membrane expansion. Further, the podocytic rough ER was dilated; these effects were prevented by 4-PBA treatment. Proximal tubules were imaged to determine if there was any dilation of the rough ER; however, no difference was found in the proximal tubules between groups (Figure 4E). Area to perimeter ratio of podocytic rough ER was measured in SS rats. The

ratio was larger in HS-fed rats, confirming the presence of rough ER dilation and, thus, ER stress (Figure 4F).

4-PBA prevents protein cast formation and fibrosis

To determine the effect of 4-PBA treatment on renal pathology, kidney sections were imaged to observe renal protein casts, which were primarily located in enlarged tubules within the medulla (Figure 5A). HS-fed SS rats developed significantly greater protein cast area density compared to NS-fed rats. This increase was prevented with 4-PBA treatment (Figure 5B).

To examine the effect of ER stress inhibition on renal interstitial fibrosis, kidneys were stained for α -SMA, a marker of myofibroblasts (Figure 6A). HS-fed SS rats exhibited a significantly greater expression of α -SMA, indicating development of interstitial fibrosis; reduced α -SMA expression was observed with 4-PBA treatment (Figure 6B). PSR stain was used to examine fibrillar collagen deposition, another marker of fibrosis (38). Staining was predominantly located in areas surrounding damage in both cortex and medulla (Figure 7A). HS-fed SS rats developed significantly more collagen deposition compared to NS-fed animals. Inhibiting ER stress with 4-PBA significantly reduced collagen deposition in the kidney (Figure 7B).

Reducing blood pressure alone does not prevent renal damage

To determine whether the renoprotective effects of 4-PBA were due to ER stress inhibition or secondary effects of blood pressure lowering induced by 4-PBA treatment, HS-fed SS rats were treated with a vasodilators, hydralazine or nifedipine. Both

hydralazine treatment and nifedipine treatment lowered SBP and DBP to a level comparable with 4-PBA (Figure 8A). Hydralazine treatment did not reduce proteinuria or albuminuria, despite its ability to lower blood pressure. Similar results were found with nifedipine treatment, supporting a role for ER stress-mediated renal injury (Figure 8B). To examine renal pathology, kidneys were stained with PAS (Figure 8C) and α -SMA (Figure 8D). Unlike with 4-PBA treatment, hydralazine and nifedipine did not reduce protein cast formation (Figure 8E) or renal interstitial fibrosis, as demonstrated with α -SMA staining (Figure 8F). Masson's trichrome, an additional measure of fibrosis, demonstrated reduced collagen deposition (blue stain) with 4-PBA treatment compared with untreated HS-fed SS animals. However, lowering blood pressure with hydralazine or nifedipine did not reduce collagen deposition (Figure 8G).

DISCUSSION

The current study describes the ability of 4-PBA, an ER stress inhibitor, to reduce chronic renal injury by modifying associated features, including proteinuria. Our findings suggest that 4-PBA treatment protects against proteinuria in the SS rat by preserving myogenic constriction, and by reducing protein misfolding in the podocytes. 4-PBA is an ER stress inhibitor, which functions by helping to fold proteins in the ER, thereby preventing the aggregation of misfolded proteins in the cell (Figure 1C). However, 4-PBA has additional effects beyond its action as a chemical chaperone. It is a weak histone deacetylase inhibitor and an ammonia scavenger used in the treatment of urea cycle disorders (8).

Hypertension is a significant predictor of the development of ESRD (36). In this study, inhibiting ER stress with 4-PBA lowered salt-induced elevations in SBP and DBP to the same degree as the vasodilators, hydralazine and nifedipine. ER stress has been previously implicated in the pathogenesis of hypertension. In a C57BL/6 mouse model, TM treatment significantly elevated SBP and DBP; inhibiting ER stress with 4-PBA co-treatment restored normotensive levels (45). A similar result was observed in angiotensin II-induced hypertension (45). In spontaneously hypertensive rats, inhibiting ER stress with 4-PBA or TUDCA lowered SBP and DBP. The authors provide some evidence that this effect is mediated through inhibition of contractility of smooth muscle cells in the vasculature (10, 61). Whereas the referenced studies implicate ER stress in hypertension of various origins, our model has identified an additional role for ER stress in the progression of proteinuric kidney disease.

Several reports have identified proteinuria as a significant independent risk factor for the progression of ESRD, with even small changes to baseline impacting severity (2, 35, 36). A recent analysis of a diverse North American population found proteinuria to be the most significant predictor for the development of ESRD (32). Successive elevations in the level of proteinuria were associated with corresponding increases in risk (32). In the current study, we assessed whether mitigating ER stress influenced proteinuria levels in a salt-sensitive model of hypertensive CKD. Treatment with 4-PBA significantly reduced levels of proteinuria and albuminuria that developed over the course of 3 weeks on a HS diet. A similar effect was observed when assessing the rate of progression of proteinuria and albuminuria levels, suggesting that reversing ER stress prevents glomerular hyperfiltration. In support, a human CKD patient treated with 4-PBA developed

progressive reduction of proteinuria (25). Several reports have implicated proteinuria in the induction of ER stress (33, 41, 46, 56). Elevated levels of several ER stress response genes were detected in kidney biopsies derived from patients with diabetic nephropathy involving proteinuria (46). Reticulon-1A, which mediates ER stress and apoptosis, is upregulated in various forms of CKD in mice and humans (26); further, knockout of this protein prevents proteinuria-mediated tubulointerstitial injury (26, 67). Additionally, transgenic animal models that develop proteinuria show ER stress-mediated podocyte damage (11, 33, 34). Preserving the structural integrity of the podocyte is essential for maintaining the selectivity of the GFB. In support, individuals with diabetic nephropathy have altered podocyte function; this may result from glomerular hyperfiltration and, thereby, worsen kidney pathology (50, 53). Protecting podocytes from injury due to unfavourable hemodynamics may be essential to slow the progression of proteinuria and, thus, CKD (57).

To explore the role of podocyte integrity in CKD, we assessed the ability of the arcuate artery to protect the GFB through myogenic constriction, and the effect of salt loading on pre-glomerular vessel function. In SS rats, a HS diet disrupted the myogenic response and induced ER stress in arcuate arteries. These effects were prevented with 4-PBA treatment. Similar results were found in non-hypertensive arcuate arteries treated with TM, confirming that altered myogenic contractility can be produced by ER stress. We propose a mechanism through which HS feeding may be linked to ER stress and proteinuria through impaired myogenic constriction, which in turn results in barotrauma to the GFB. Large conductance Ca^{2+} -activated K^+ channels (BK_{Ca}) and L-type Ca^{2+} channels are thought to play a role in myogenic constriction (28, 29, 42). Myogenic

constriction is inhibited by the L-type Ca^{2+} channel blocker, nifedipine (13), demonstrating dependence of the myogenic response on L-type Ca^{2+} channels. In conditions of ER stress, the folding and delivery of this channel to the plasma membrane would be inhibited, much like we have demonstrated the folding and delivery of the epithelial junctional protein, β -catenin, is inhibited (Figure 1E). In support, ER stress has been associated with blood vessel dysfunction, particularly endothelial-dependent relaxation (10) and agonist-mediated constriction (39, 61).

4-PBA's ability to protect against albuminuria and to preserve myogenic activity provides evidence that the chaperone plays a role in maintaining glomerular function. In response to HS feeding, ER stress was induced in the glomerulus. This coincided with disruption to the GFB and dilated podocytic rough ER, a feature that is indicative of protein misfolding (30, 60). Treatment with 4-PBA prevented ultrastructural changes. While ultrastructural changes were not found in the proximal tubules, the ER stress marker, GRP78, was present. This suggests that GRP78 is natively expressed in these cells in order to provide the necessary function of protein folding. Additional evidence for ER stress-mediated glomerular dysfunction was identified in a rat model of 5/6 renal nephrectomy, where protein accumulated in the podocytes as a result of increased intraglomerular protein passage. This corresponded with podocyte injury and an increase in $\text{TGF}\beta 1$ activity, providing a mechanism through which glomerulosclerosis may develop (1). Preserving the integrity of podocytic ultrastructure not only maintains glomerular function but also prevents further CKD-associated renal damage, like fibrosis. Further, simulating a myogenic response using a servo-controlled pump in HS-fed SS rats protects the kidney from renal interstitial fibrosis and protein cast formation (54).

Interstitial fibrosis is a contributing factor to renal injury and dysfunction in CKD, for which proteinuria is thought to be an instigating factor (23). TGF β 1 has been implicated in renal disease as a mediator of renal fibrosis through the induction of tubular cell apoptosis, and the progressive deposition of extracellular matrix components (48). Our model of salt-induced CKD demonstrated several features of renal interstitial fibrosis, including α -SMA and collagen deposition; accumulation of both markers was decreased with 4-PBA treatment. We have previously shown that ER stress directly induces a profibrotic response in human proximal tubule cells. Inhibiting protein translation preserved epithelial integrity and prevented expression of profibrotic markers (9). Other reports have further implicated ER stress in the pathogenesis of fibrosis. In a unilateral ureteral obstruction mouse model, ER stress contributed to renal tubule cell apoptosis and fibrosis (12). ER stress, specifically ATF4 expression, induces lipocalin-2, which mediates cell death, leading to tubular fibrosis (25). Furthermore, treatment with a chemical chaperone significantly reduced the activity of TGF β 1 in angiotensin II-induced murine hypertension (39), as well as tubulointerstitial fibrosis in mice with proteinuric CKD (25). In this angiotensin II-induced hypertension model, ER stress inhibition led to a subsequent reduction of cardiac hypertrophy and fibrosis, supporting a role for ER stress in TGF β 1 activity (39). We have observed a similar role for ER stress in TGF β 1-mediated renal fibrosis in cultured proximal tubule cells (unpublished data).

The Brenner hypothesis states that reduced renal mass or reduced nephron number increases intraglomerular pressure, leading to glomerular hyperfiltration in the remaining nephrons (6, 7). Thus, it has been suggested that reversing hypertension can slow the

progression of CKD (49). This is clearly shown in many clinical trials of CKD patients (37). However, preservation of renal blood flow autoregulation through maintenance of the myogenic response may also prevent increased intraglomerular pressure and slow CKD progression. To determine whether 4-PBA's protective effect derives from its ability to restore normotensive levels or preserve the myogenic response, other blood pressure lowering agents that inhibit myogenic constriction were used to lower blood pressure to the same degree as 4-PBA. SS rats were treated with oral dosing of hydralazine or nifedipine that are vasodilators that inhibit myogenic constriction. Although SBP and DBP were normalized, no reversal was observed in proteinuria, protein cast formation, or renal interstitial fibrosis. This suggests that lowering blood pressure alone is insufficient to prevent glomerular hyperfiltration and ensuing renal damage; further, the functionality of the myogenic response plays a significant role in protecting the kidney, independent of hypertensive status. As such, prevention of ER stress serves as a viable therapeutic strategy to preserve kidney function and to delay the progression of CKD.

ACKNOWLEDGMENTS

None.

SOURCES OF FUNDING

This work was supported by research grants to Jeffrey G. Dickhout from the Canadian Institutes of Health Research (OSO-115895 and MOP-133484). Financial support from St. Joseph's Healthcare Hamilton is also acknowledged. Jeffrey G. Dickhout also acknowledges salary support from St. Joseph's Healthcare Hamilton. Support from the Division of Nephrology in the Department of Medicine at McMaster University is acknowledged. Dr. Dickhout also holds a Kidney foundation of Canada, Krescent New Investigator award. This work was partially funded by scholarship awards, Father Sean O'Sullivan Research Studentship Award and Ontario Graduate Scholarship, granted to Rachel E. Carlisle.

DISCLOSURES

None.

REFERENCES

1. Abbate M, Zoja C, Morigi M, et al. Transforming growth factor-beta1 is up-regulated by podocytes in response to excess intraglomerular passage of proteins: a central pathway in progressive glomerulosclerosis. *Am J Pathol.* 2002;161(6):2179-93.
2. Astor BC, Matsushita K, Gansevoort RT, et al. Lower estimated glomerular filtration rate and higher albuminuria are associated with mortality and end-stage renal disease. A collaborative meta-analysis of kidney disease population cohorts. *Kidney Int.* 2011;79(12):1331-40.
3. Bek MF, Bayer M, Muller B, et al. Expression and function of C/EBP homology protein (GADD153) in podocytes. *Am J Pathol.* 2006;168(1):20-32.
4. Bertani T, Cutillo F, Zoja C, Brogгинi M, Remuzzi G. Tubulo-interstitial lesions mediate renal damage in adriamycin glomerulopathy. *Kidney Int.* 1986;30(4):488-96.
5. Bertani T, Rocchi G, Sacchi G, Mecca G, Remuzzi G. Adriamycin-induced glomerulosclerosis in the rat. *Am J Kidney Dis.* 1986;7(1):12-9.
6. Brenner BM, Lawler EV, Mackenzie HS. The hyperfiltration theory: a paradigm shift in nephrology. *Kidney Int.* 1996;49(6):1774-7.
7. Brenner BM, Meyer TW, Hostetter TH. Dietary protein intake and the progressive nature of kidney disease: the role of hemodynamically mediated glomerular injury in the pathogenesis of progressive glomerular sclerosis in aging, renal ablation, and intrinsic renal disease. *N Engl J Med.* 1982;307(11):652-9.
8. Carlisle RE, Brimble E, Werner KE, et al. 4-Phenylbutyrate inhibits tunicamycin-induced acute kidney injury via CHOP/GADD153 repression. *PLoS One.* 2014;9(1):e84663.
9. Carlisle RE, Heffernan A, Brimble E, et al. TDAG51 mediates epithelial-to-mesenchymal transition in human proximal tubular epithelium. *Am J Physiol Renal Physiol.* 2012;303(3):F467-81.
10. Carlisle RE, Werner KE, Yum V, et al. Endoplasmic reticulum stress inhibition reduces hypertension through the preservation of resistance blood vessel structure and function. *J Hypertens.* 2016.
11. Chen YM, Zhou Y, Go G, Marmorstein JT, Kikkawa Y, Miner JH. Laminin beta2 gene missense mutation produces endoplasmic reticulum stress in podocytes. *J Am Soc Nephrol.* 2013;24(8):1223-33.

12. Chiang CK, Hsu SP, Wu CT, et al. Endoplasmic reticulum stress implicated in the development of renal fibrosis. *Mol Med*. 2011;17(11-12):1295-305.
13. Coats P, Johnston F, MacDonald J, McMurray JJ, Hillier C. Signalling mechanisms underlying the myogenic response in human subcutaneous resistance arteries. *Cardiovasc Res*. 2001;49(4):828-37.
14. Cohen-Bucay A, Viswanathan G. Urinary markers of glomerular injury in diabetic nephropathy. *Int J Nephrol*. 2012;2012:146987.
15. Coresh J, Selvin E, Stevens LA, et al. Prevalence of chronic kidney disease in the United States. *JAMA*. 2007;298(17):2038-47.
16. Cowley AW, Jr., Roman RJ, Kaldunski ML, et al. Brown Norway chromosome 13 confers protection from high salt to consomic Dahl S rat. *Hypertension*. 2001;37(2 Pt 2):456-61.
17. Cupples WA, Braam B. Assessment of renal autoregulation. *Am J Physiol Renal Physiol*. 2007;292(4):F1105-23.
18. Cybulsky AV, Takano T, Papillon J, Bijian K. Role of the endoplasmic reticulum unfolded protein response in glomerular epithelial cell injury. *J Biol Chem*. 2005;280(26):24396-403.
19. Dickhout JG, Carlisle RE, Austin RC. Interrelationship between cardiac hypertrophy, heart failure, and chronic kidney disease: endoplasmic reticulum stress as a mediator of pathogenesis. *Circ Res*. 2011;108(5):629-42.
20. Dickhout JG, Chahal J, Matthews A, Carlisle RE, Tat V, Naiel S. Endoplasmic reticulum stress causes epithelial cell disjunction. *Journal of Pharmacological Reports*. 2016;1(1):5.
21. Dickhout JG, Lee RM. Structural and functional analysis of small arteries from young spontaneously hypertensive rats. *Hypertension*. 1997;29(3):781-9.
22. Dickhout JG, Lhotak S, Hilditch BA, et al. Induction of the unfolded protein response after monocyte to macrophage differentiation augments cell survival in early atherosclerotic lesions. *FASEB J*. 2011;25(2):576-89.
23. Eddy AA. Proteinuria and interstitial injury. *Nephrol Dial Transplant*. 2004;19(2):277-81.
24. Eddy AA, Kim H, Lopez-Guisa J, Oda T, Soloway PD. Interstitial fibrosis in mice with overload proteinuria: deficiency of TIMP-1 is not protective. *Kidney Int*. 2000;58(2):618-28.

25. El Karoui K, Viau A, Dellis O, et al. Endoplasmic reticulum stress drives proteinuria-induced kidney lesions via Lipocalin 2. *Nat Commun.* 2016;7:10330.
26. Fan Y, Xiao W, Li Z, et al. RTN1 mediates progression of kidney disease by inducing ER stress. *Nat Commun.* 2015;6:7841.
27. Feng M, Whitesall S, Zhang Y, Beibel M, D'Alecy L, DiPetrillo K. Validation of volume-pressure recording tail-cuff blood pressure measurements. *Am J Hypertens.* 2008;21(12):1288-91.
28. Gebremedhin D, Lange AR, Narayanan J, Aebly MR, Jacobs ER, Harder DR. Cat cerebral arterial smooth muscle cells express cytochrome P450 4A2 enzyme and produce the vasoconstrictor 20-HETE which enhances L-type Ca²⁺ current. *J Physiol.* 1998;507 (Pt 3):771-81.
29. Harder DR, Narayanan J, Gebremedhin D. Pressure-induced myogenic tone and role of 20-HETE in mediating autoregulation of cerebral blood flow. *Am J Physiol Heart Circ Physiol.* 2011;300(5):H1557-65.
30. Hartley T, Siva M, Lai E, Teodoro T, Zhang L, Volchuk A. Endoplasmic reticulum stress response in an INS-1 pancreatic beta-cell line with inducible expression of a folding-deficient proinsulin. *BMC Cell Biol.* 2010;11:59.
31. Hostetter TH, Olson JL, Rennke HG, Venkatachalam MA, Brenner BM. Hyperfiltration in remnant nephrons: a potentially adverse response to renal ablation. *Am J Physiol.* 1981;241(1):F85-93.
32. Hsu CY, Iribarren C, McCulloch CE, Darbinian J, Go AS. Risk factors for end-stage renal disease: 25-year follow-up. *Arch Intern Med.* 2009;169(4):342-50.
33. Inagi R, Nangaku M, Onogi H, et al. Involvement of endoplasmic reticulum (ER) stress in podocyte injury induced by excessive protein accumulation. *Kidney Int.* 2005;68(6):2639-50.
34. Inagi R, Nangaku M, Usuda N, et al. Novel serpinopathy in rat kidney and pancreas induced by overexpression of meginin. *J Am Soc Nephrol.* 2005;16(5):1339-49.
35. Iseki K, Ikemiya Y, Iseki C, Takishita S. Proteinuria and the risk of developing end-stage renal disease. *Kidney Int.* 2003;63(4):1468-74.
36. Ishani A, Grandits GA, Grimm RH, et al. Association of single measurements of dipstick proteinuria, estimated glomerular filtration rate, and hematocrit with 25-year incidence of end-stage renal disease in the multiple risk factor intervention trial. *J Am Soc Nephrol.* 2006;17(5):1444-52.

37. Jafar TH, Stark PC, Schmid CH, et al. Progression of chronic kidney disease: the role of blood pressure control, proteinuria, and angiotensin-converting enzyme inhibition: a patient-level meta-analysis. *Ann Intern Med.* 2003;139(4):244-52.
38. Junqueira LC, Bignolas G, Brentani RR. Picrosirius staining plus polarization microscopy, a specific method for collagen detection in tissue sections. *Histochem J.* 1979;11(4):447-55.
39. Kassan M, Galan M, Partyka M, et al. Endoplasmic reticulum stress is involved in cardiac damage and vascular endothelial dysfunction in hypertensive mice. *Arterioscler Thromb Vasc Biol.* 2012;32(7):1652-61.
40. Khavandi K, Greenstein AS, Sonoyama K, et al. Myogenic tone and small artery remodelling: insight into diabetic nephropathy. *Nephrol Dial Transplant.* 2009;24(2):361-9.
41. Kimura K, Jin H, Ogawa M, Aoe T. Dysfunction of the ER chaperone BiP accelerates the renal tubular injury. *Biochem Biophys Res Commun.* 2008;366(4):1048-53.
42. Lange A, Gebremedhin D, Narayanan J, Harder D. 20-Hydroxyeicosatetraenoic acid-induced vasoconstriction and inhibition of potassium current in cerebral vascular smooth muscle is dependent on activation of protein kinase C. *J Biol Chem.* 1997;272(43):27345-52.
43. Lhotak S, Sood S, Brimble E, et al. ER stress contributes to renal proximal tubule injury by increasing SREBP-2-mediated lipid accumulation and apoptotic cell death. *Am J Physiol Renal Physiol.* 2012;303(2):F266-78.
44. Lhotak S, Zhou J, Austin RC. Immunohistochemical detection of the unfolded protein response in atherosclerotic plaques. *Methods Enzymol.* 2011;489:23-46.
45. Liang B, Wang S, Wang Q, et al. Aberrant endoplasmic reticulum stress in vascular smooth muscle increases vascular contractility and blood pressure in mice deficient of AMP-activated protein kinase-alpha2 in vivo. *Arterioscler Thromb Vasc Biol.* 2013;33(3):595-604.
46. Lindenmeyer MT, Rastaldi MP, Ikehata M, et al. Proteinuria and hyperglycemia induce endoplasmic reticulum stress. *J Am Soc Nephrol.* 2008;19(11):2225-36.
47. Liu G, Sun Y, Li Z, et al. Apoptosis induced by endoplasmic reticulum stress involved in diabetic kidney disease. *Biochem Biophys Res Commun.* 2008;370(4):651-6.
48. Loeffler I, Wolf G. Transforming growth factor-beta and the progression of renal disease. *Nephrol Dial Transplant.* 2014;29 Suppl 1:i37-i45.

49. Lv J, Ehteshami P, Sarnak MJ, et al. Effects of intensive blood pressure lowering on the progression of chronic kidney disease: a systematic review and meta-analysis. *CMAJ*. 2013;185(11):949-57.
50. Magee GM, Bilous RW, Cardwell CR, Hunter SJ, Kee F, Fogarty DG. Is hyperfiltration associated with the future risk of developing diabetic nephropathy? A meta-analysis. *Diabetologia*. 2009;52(4):691-7.
51. Markan S, Kohli HS, Joshi K, et al. Up regulation of the GRP-78 and GADD-153 and down regulation of Bcl-2 proteins in primary glomerular diseases: a possible involvement of the ER stress pathway in glomerulonephritis. *Mol Cell Biochem*. 2009;324(1-2):131-8.
52. Metcalfe W. How does early chronic kidney disease progress? A background paper prepared for the UK Consensus Conference on early chronic kidney disease. *Nephrol Dial Transplant*. 2007;22 Suppl 9:ix26-30.
53. Mogensen C. Early glomerular hyperfiltration in insulin-dependent diabetics and late nephropathy. *Scandinavian journal of clinical & laboratory investigation*. 1986;46(3):201-6.
54. Mori T, Polichnowski A, Glocka P, et al. High perfusion pressure accelerates renal injury in salt-sensitive hypertension. *J Am Soc Nephrol*. 2008;19(8):1472-82.
55. New DI, Chesser AM, Raftery MJ, Yaqoob MM. The myogenic response in uremic hypertension. *Kidney Int*. 2003;63(2):642-6.
56. Ohse T, Inagi R, Tanaka T, et al. Albumin induces endoplasmic reticulum stress and apoptosis in renal proximal tubular cells. *Kidney Int*. 2006;70(8):1447-55.
57. Pagtalunan ME, Miller PL, Jumping-Eagle S, et al. Podocyte loss and progressive glomerular injury in type II diabetes. *J Clin Invest*. 1997;99(2):342-8.
58. Ren Y, D'Ambrosio MA, Liu R, Pagano PJ, Garvin JL, Carretero OA. Enhanced myogenic response in the afferent arteriole of spontaneously hypertensive rats. *Am J Physiol Heart Circ Physiol*. 2010;298(6):H1769-75.
59. Sadoun E, Reed MJ. Impaired angiogenesis in aging is associated with alterations in vessel density, matrix composition, inflammatory response, and growth factor expression. *J Histochem Cytochem*. 2003;51(9):1119-30.
60. Schonthal AH. Endoplasmic reticulum stress: its role in disease and novel prospects for therapy. *Scientifica (Cairo)*. 2012;2012:857516.
61. Spitler KM, Matsumoto T, Webb RC. Suppression of endoplasmic reticulum stress improves endothelium-dependent contractile responses in aorta of the

- spontaneously hypertensive rat. *Am J Physiol Heart Circ Physiol*. 2013;305(3):H344-53.
62. Takenaka T, Forster H, De Micheli A, Epstein M. Impaired myogenic responsiveness of renal microvessels in Dahl salt-sensitive rats. *Circ Res*. 1992;71(2):471-80.
 63. Van Dokkum RP, Alonso-Galicia M, Provoost AP, Jacob HJ, Roman RJ. Impaired autoregulation of renal blood flow in the fawn-hooded rat. *Am J Physiol*. 1999;276(1 Pt 2):R189-96.
 64. van Dokkum RP, Sun CW, Provoost AP, Jacob HJ, Roman RJ. Altered renal hemodynamics and impaired myogenic responses in the fawn-hooded rat. *Am J Physiol*. 1999;276(3 Pt 2):R855-63.
 65. Verseput GH, Braam B, Provoost AP, Koomans HA. Tubuloglomerular feedback and prolonged ACE-inhibitor treatment in the hypertensive fawn-hooded rat. *Nephrol Dial Transplant*. 1998;13(4):893-9.
 66. Wiest DL, Burkhardt JK, Hester S, Hortsch M, Meyer DI, Argon Y. Membrane biogenesis during B cell differentiation: most endoplasmic reticulum proteins are expressed coordinately. *J Cell Biol*. 1990;110(5):1501-11.
 67. Xiao W, Fan Y, Wang N, Chuang PY, Lee K, He JC. Knockdown of RTN1A attenuates ER stress and kidney injury in albumin overload-induced nephropathy. *Am J Physiol Renal Physiol*. 2016;310(5):F409-15.
 68. Zandi-Nejad K, Eddy AA, Glassock RJ, Brenner BM. Why is proteinuria an ominous biomarker of progressive kidney disease? *Kidney Int Suppl*. 2004(92):S76-89.

Figure 1.

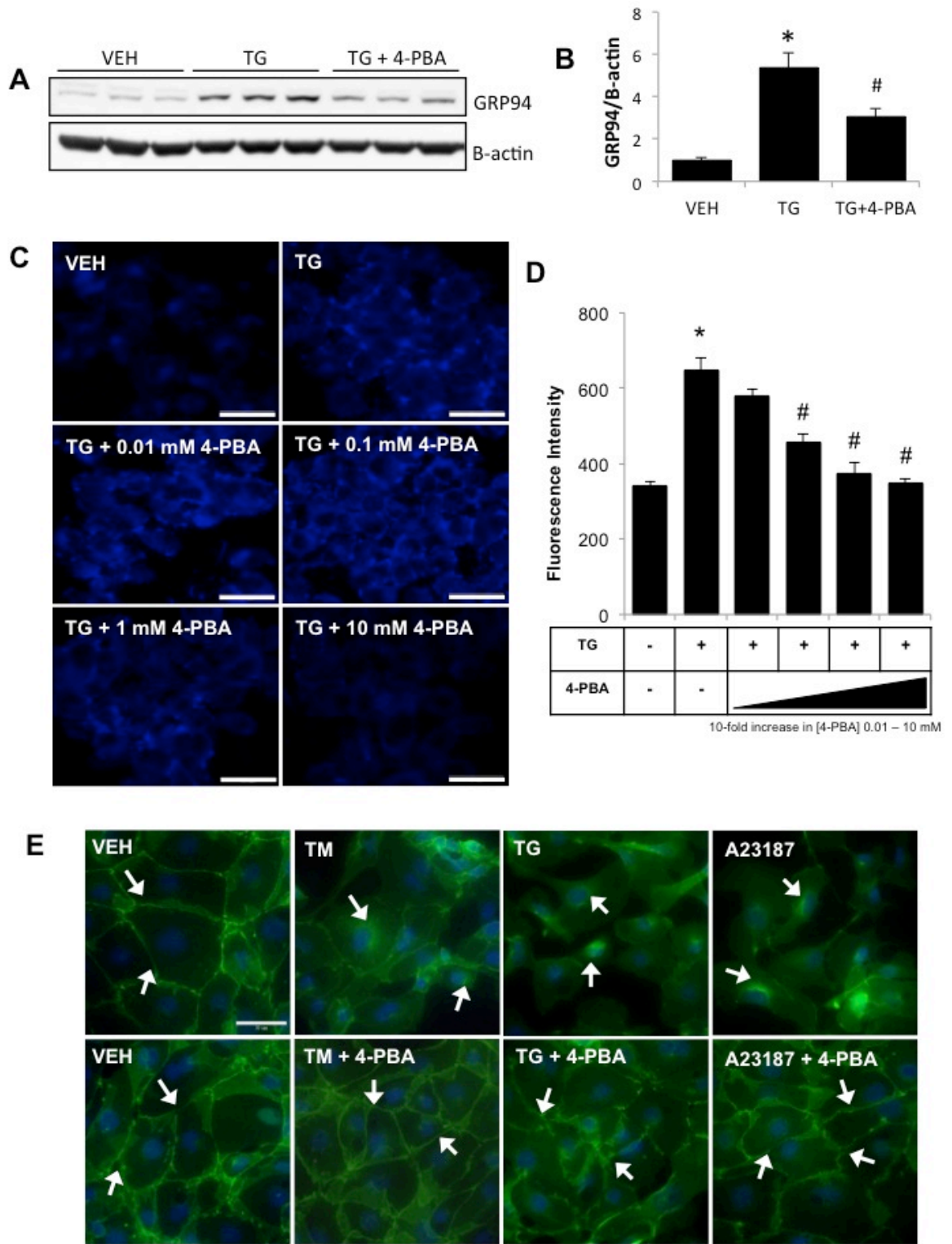


Figure 1. 4-PBA treatment inhibits thapsigargin-induced accumulation of misfolded proteins in HK-2 cells. (A) HK-2 cells were treated with vehicle (VEH; DMSO), thapsigargin (TG), or TG with 4-PBA for 18 h. (B) Western blotting demonstrates an increase in the ER stress marker GRP94 in response to TG treatment, which was prevented with 4-PBA co-treatment. β -actin was used as a loading control. (C) HK-2 cells were treated with TG in the presence or absence of increasing doses of 4-PBA (0.01 mM, 0.1 mM, 1 mM, 10 mM) for 24 h; thioflavin T staining shows protein aggregation (blue). (D) Quantification demonstrates that increasing doses of 4-PBA prevented TG-induced accumulation of misfolded proteins. (E) HK-2 cells were treated with ER stress inducers, tunicamycin (TM; 1 μ g/ml), TG, or A23187 (10 μ M) in the presence or absence of 4-PBA for 24 h. Staining for β -catenin (green, arrows) indicates ER stress inhibition prevents translocation of β -catenin to the perinuclear region and preserves cell-cell interaction. *, $p < 0.05$ vs VEH; #, $p < 0.05$ vs TG; bar=50 μ m.

Figure 2.

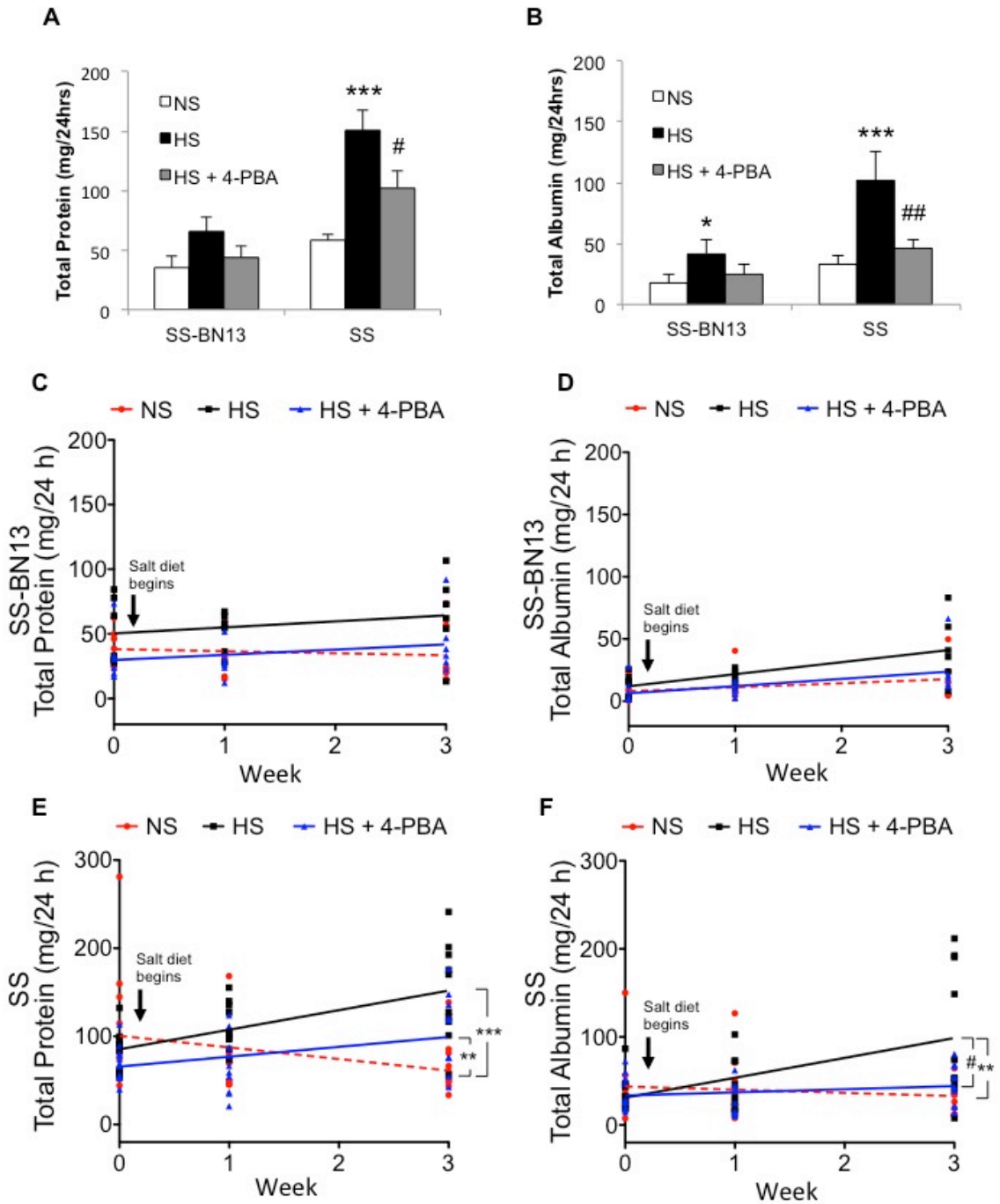


Figure 2. 4-PBA prevents increased proteinuria and albuminuria. At 3 weeks, 24 h total protein (A) and albumin (B) were significantly elevated in high salt (HS)-fed SS rats, whereas 4-PBA treatment inhibited these responses. HS diet also increased albumin excretion in SS-BN13 animals; no other significant differences were observed. When progression of (C) proteinuria and (D) albuminuria was assessed through regression analysis, no significant differences were observed in SS-BN13 animals. However, HS diet significantly induced (E) proteinuria and (F) albuminuria in SS rats. Co-treatment with 4-PBA significantly reduced proteinuria and albuminuria in SS rats. ***, $p < 0.001$ vs NS; **, $p < 0.01$ vs NS; *, $p < 0.05$ vs NS; ###, $p < 0.01$ vs HS; #, $p < 0.05$ vs HS.

Figure 3.

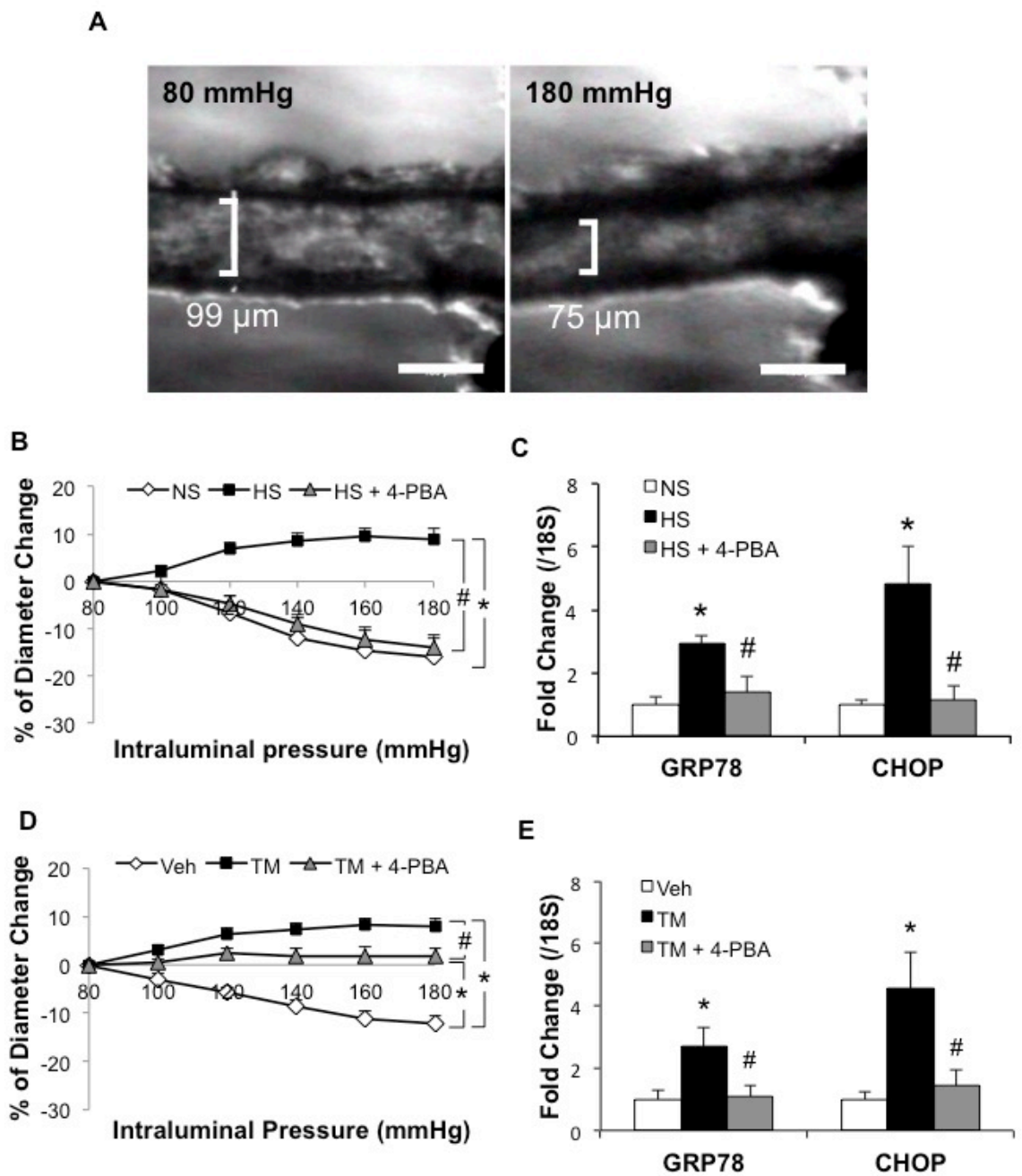


Figure 3. 4-PBA treatment preserves myogenic constriction in the arcuate artery through modulation of ER stress. (A) Percent of lumen diameter constriction in response to increasing luminal pressure depicts myogenic response in the arcuate artery. Bar=100 μm . (B) Myogenic constriction is absent in Dahl salt-sensitive (SS) rats fed a high salt (HS) diet; treatment with 4-PBA prevents this effect. *, $p < 0.05$ vs normal salt (NS); #, $p < 0.05$ vs HS. (C) mRNA expression of ER stress markers GRP78 and CHOP is significantly elevated in arcuate arteries isolated from HS-fed SS rats. Treatment with 4-PBA prevented this upregulation. (D) *Ex vivo* Sprague-Dawley (SD) arcuate arteries treated with tunicamycin (TM) showed absent myogenic constriction; co-treatment with 4-PBA partially restored the myogenic response. *, $p < 0.05$ vs Veh; #, $p < 0.05$ vs TM. (E) mRNA expression of GRP78 and CHOP in *ex-vivo* SD arcuate arteries was significantly increased in response to TM treatment. Co-treatment with 4-PBA significantly reduced ER stress marker expression. *, $p < 0.05$ vs Veh; #, $p < 0.05$ vs TM.

Figure 4 (1/3).

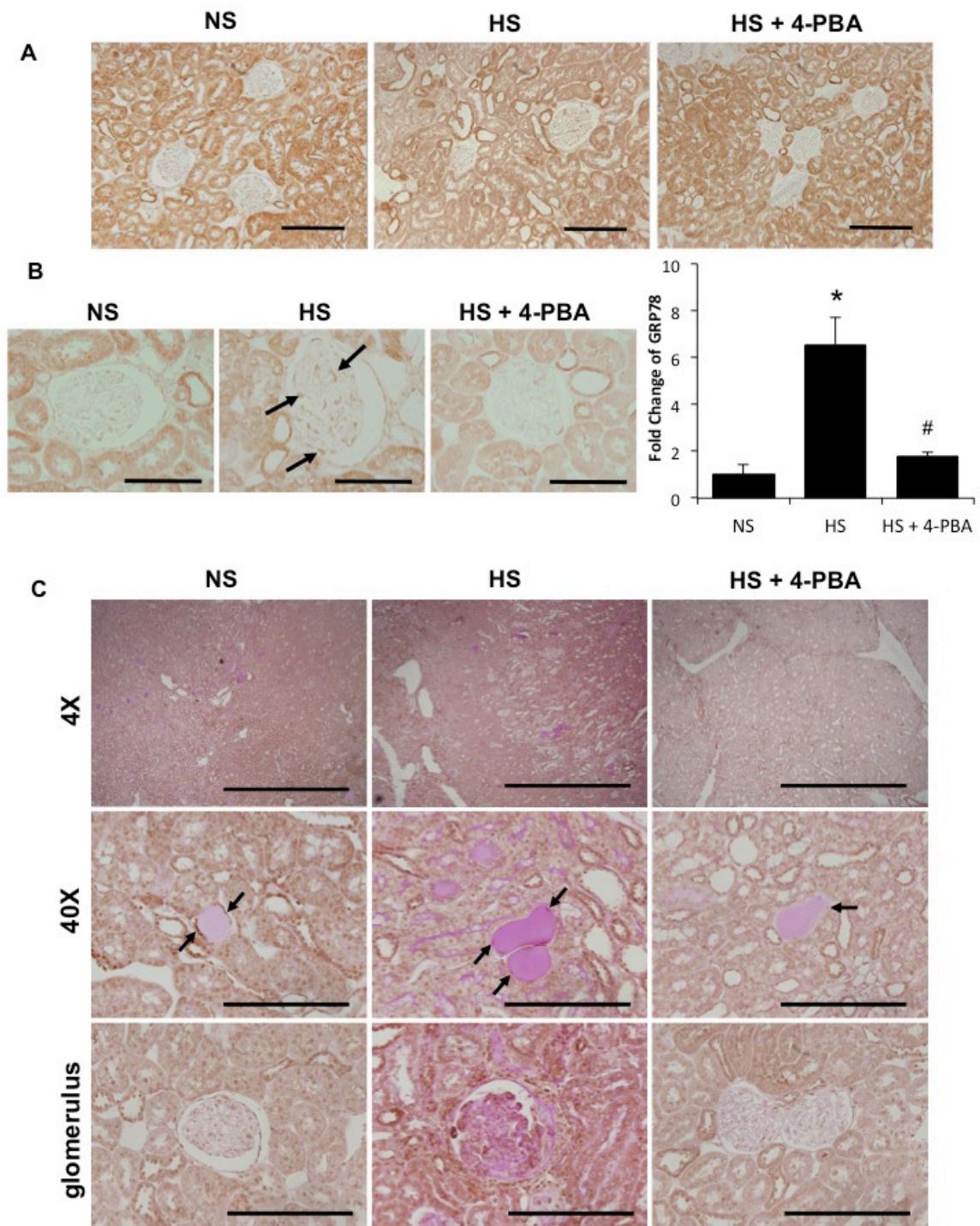


Figure 4 (2/3).

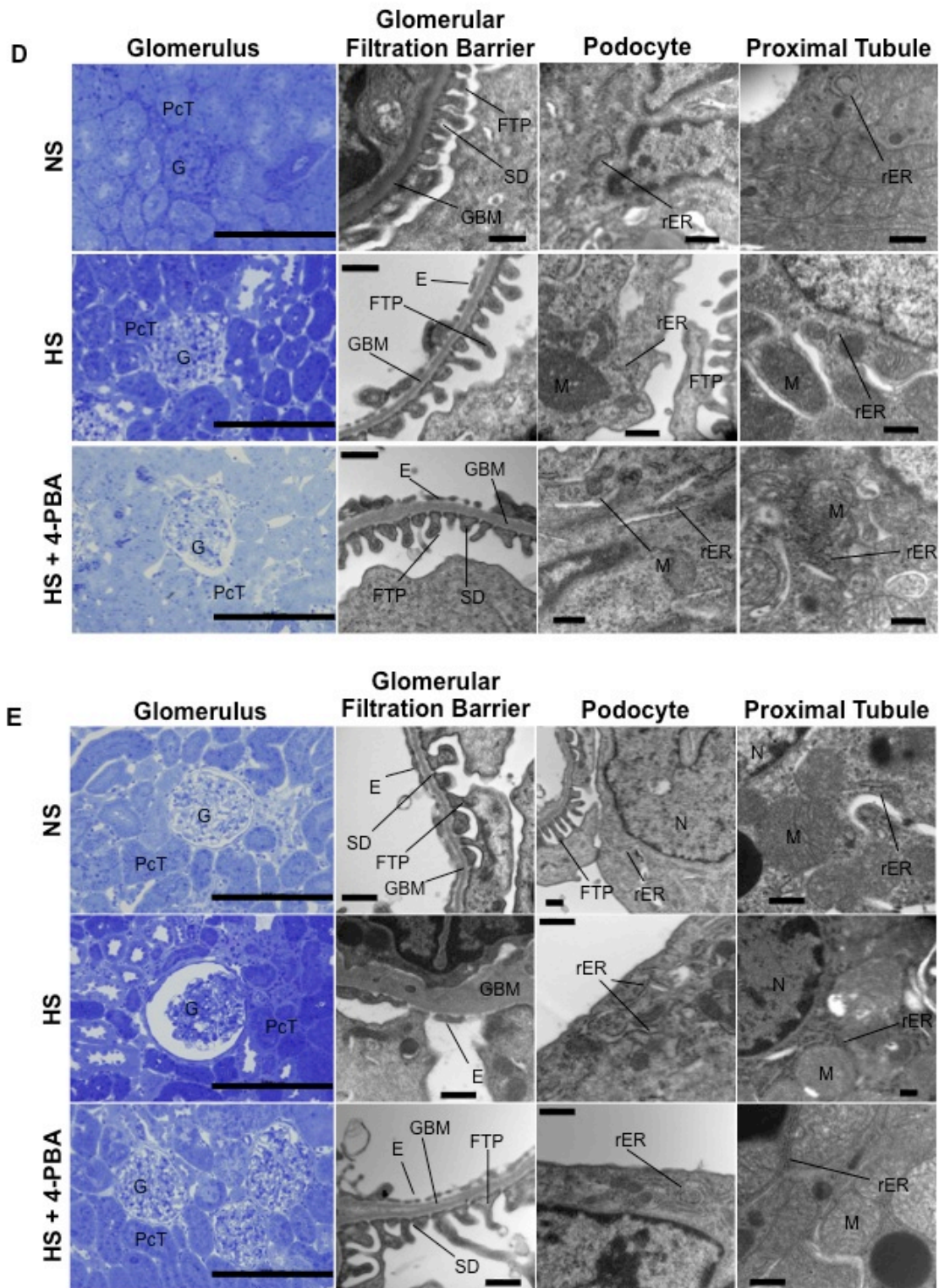


Figure 4 (3/3).

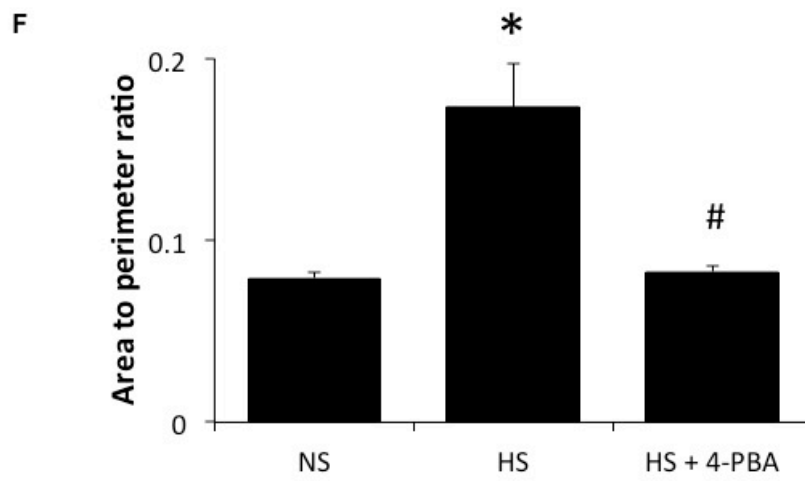


Figure 4. 4-PBA treatment inhibits ER stress and protects the glomerular filtration barrier. (A) Low magnification images of GRP78-stained kidneys demonstrate native staining in the proximal tubules of Dahl salt-sensitive (SS) rats, independent of salt feeding. Bar=200 μ m. (B) High salt (HS)-fed SS rats demonstrated a significant increase in glomerular GRP78 staining (arrows); this effect was inhibited with 4-PBA treatment. *, $p < 0.05$ vs normal salt (NS); #, $p < 0.05$ vs HS; bar=100 μ m. (C) CHOP and periodic acid-Schiff-stained kidneys demonstrate CHOP staining (arrows) surrounding protein casts, as well as in sclerosed glomeruli. 4X bar=2 mm; 40X bar=200 μ m. (D) Toluidine blue-stained kidney sections show glomerular ultrastructure of SS-BN13 rats. Transmission electron microscopy (TEM) found no significant damage to the glomerular filtration barrier (GFB) or podocytic rough endoplasmic reticulum (ER) in SS-BN13 rats. (E) HS-fed SS rats showed dilation of the Bowman's capsule; this effect was prevented with 4-PBA treatment. Treatment with 4-PBA prevented salt-induced disruption of the GFB and dilation of rough ER in SS rats [endothelial cells (E), foot process (FTP), glomerular basement membrane (GBM), glomerulus (G), mitochondria (M), nucleus (N), proximal convoluted tubule (PcT) rough endoplasmic reticulum (rER), and slit diaphragm (SD)]. Light microscopy bar=200 μ m; TEM bar=500 nm. (F) Area to perimeter ratio of podocytic rough ER is significantly higher in HS-fed SS rats; 4-PBA-treated rats did not demonstrate rough ER dilation. *, $p < 0.05$ vs NS; #, $p < 0.05$ vs HS.

Figure 5.

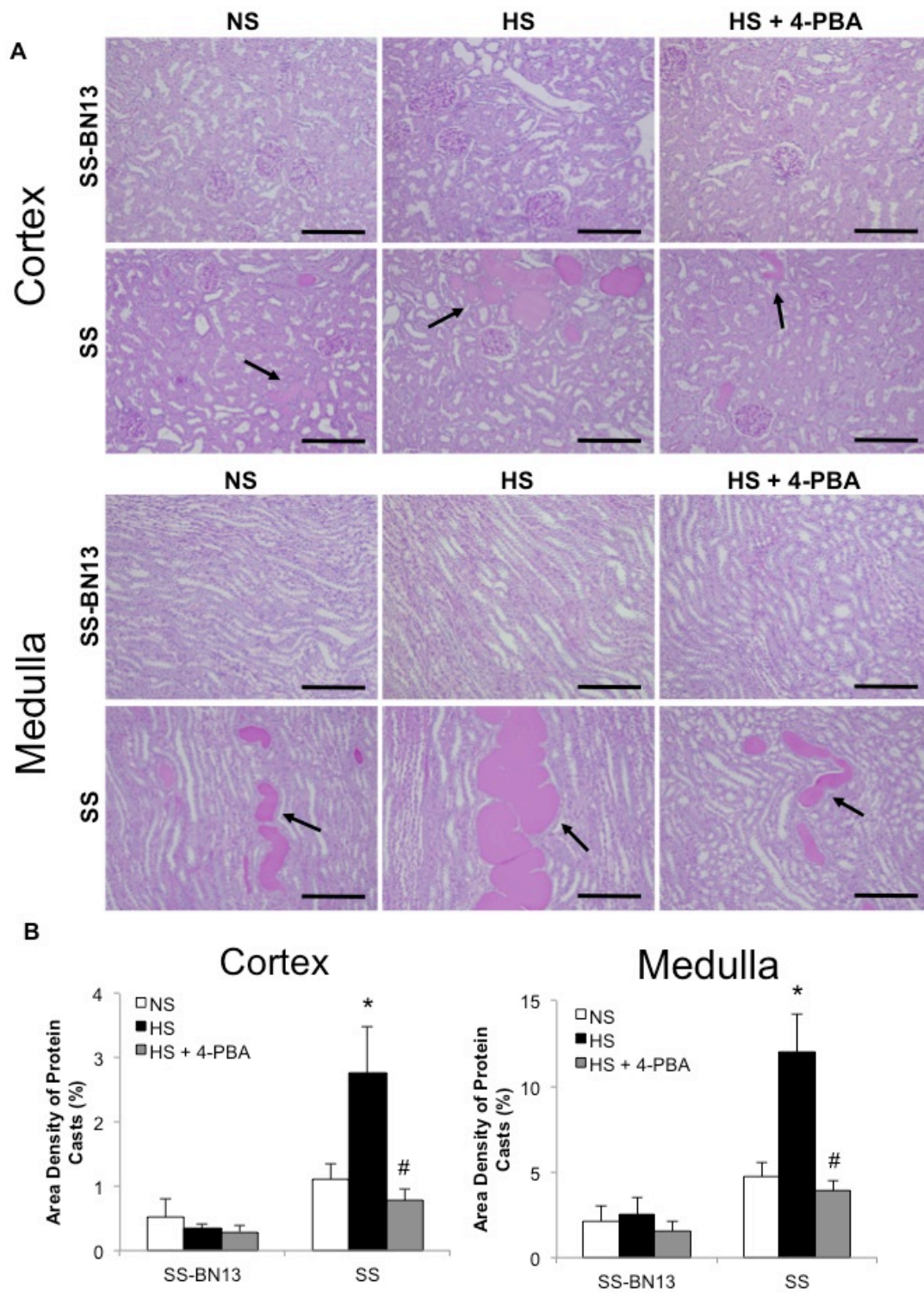


Figure 5. 4-PBA prevents intratubular protein cast formation. (A) Kidney sections from SS-BN13 and Dahl salt-sensitive (SS) rats were Periodic acid-Schiff-stained to observe intratubular protein casts (arrows) in the renal cortex and medulla. Bar=200 μ m. (B) Quantification showed a significant increase of area density of protein casts in cortex and medulla of high salt (HS)-fed SS rats; the effect was reversed with 4-PBA treatment. No changes were observed in SS-BN13 animals in response to HS diet or co-treatment with 4-PBA. *, $p < 0.05$ vs normal salt (NS); #, $p < 0.05$ vs HS.

Figure 6.

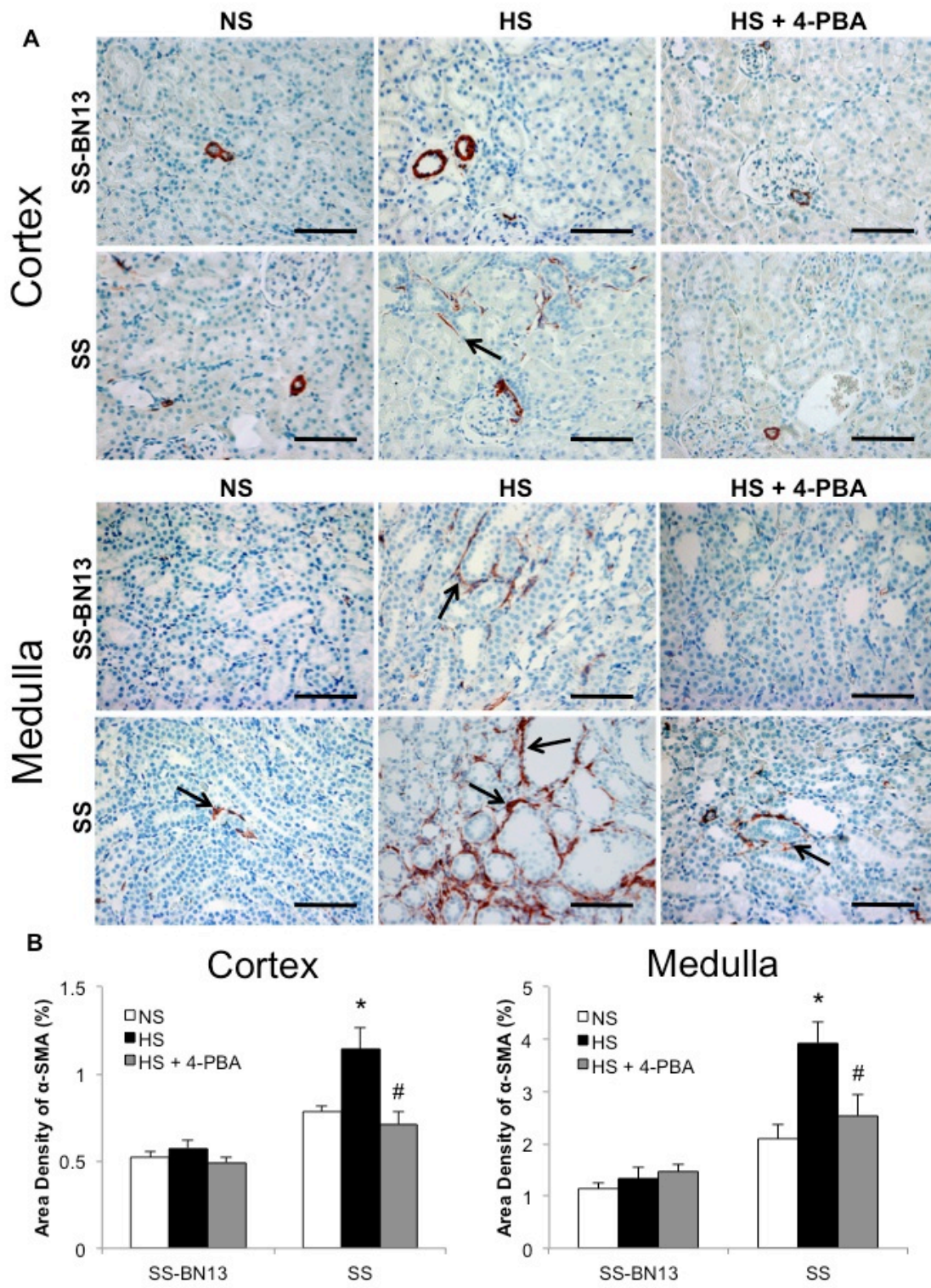


Figure 6. 4-PBA prevents salt-induced renal interstitial fibrosis. (A) Kidney sections from SS-BN13 and Dahl salt-sensitive (SS) rats were stained for α -smooth muscle actin (α -SMA; arrows). Bar=200 μ m. (B) Quantification of α -SMA in the renal cortex and medulla of SS rats showed significant increases in expression due to high salt (HS) diet. Treatment with 4-PBA prevented salt-induced interstitial fibrosis in these animals. No changes were observed in SS-BN13 animals in response to HS diet or co-treatment with 4-PBA. *, $p < 0.05$ vs normal salt (NS); #, $p < 0.05$ vs HS.

Figure 7.

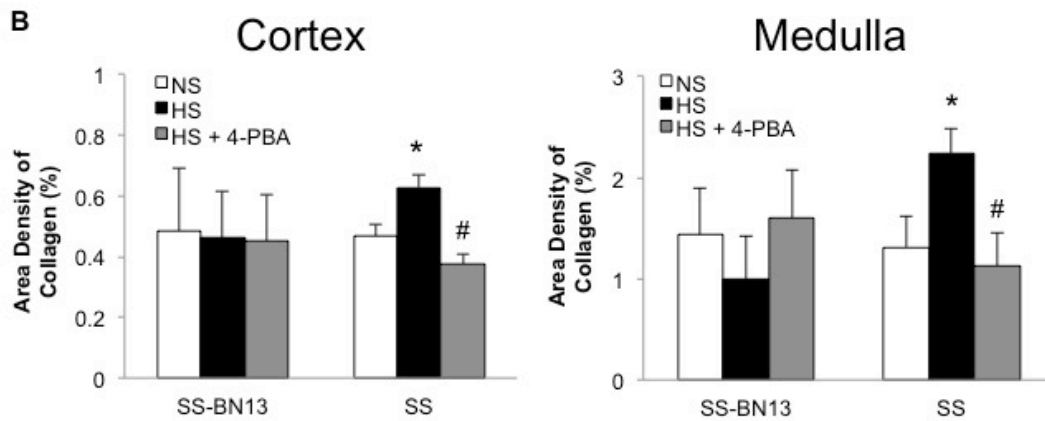
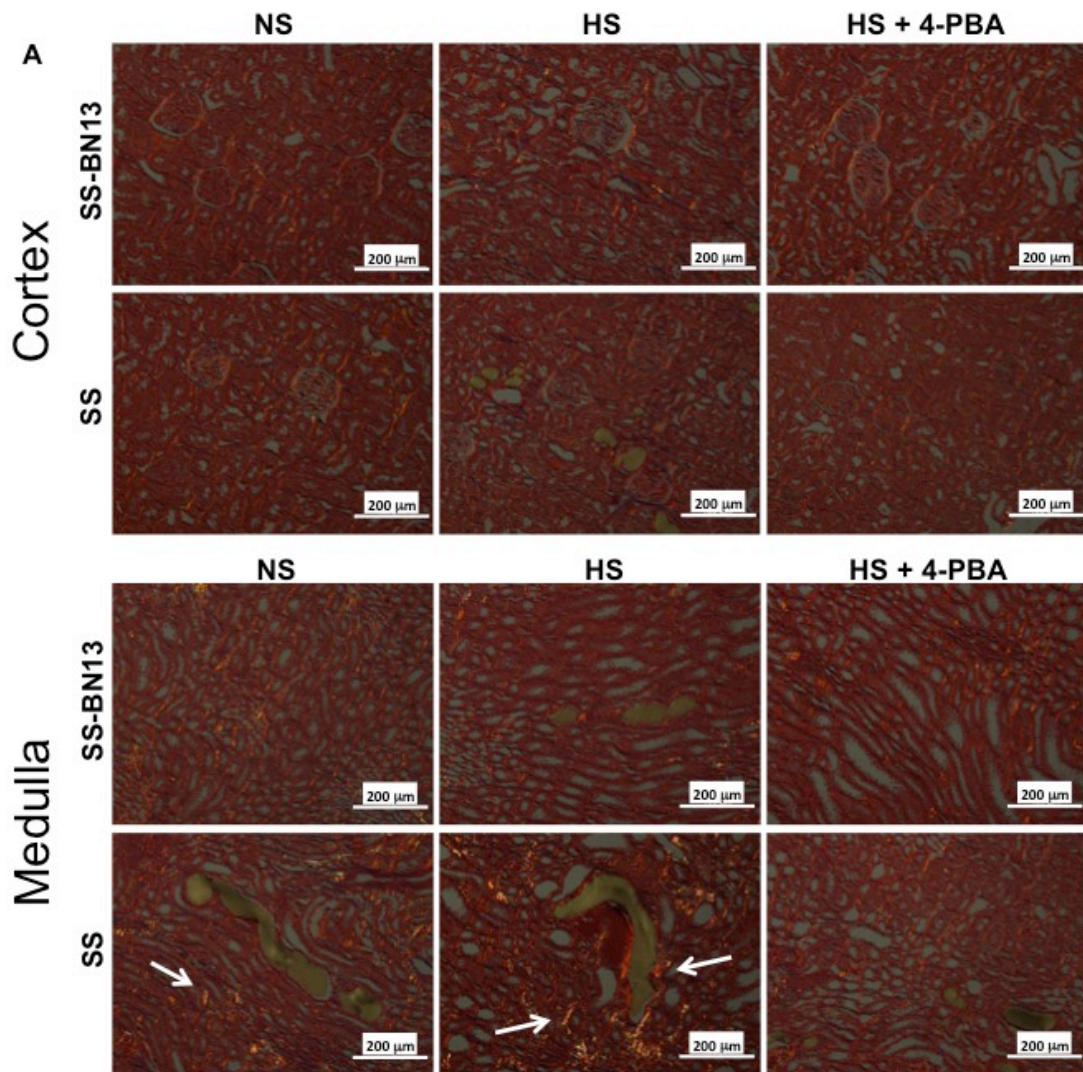
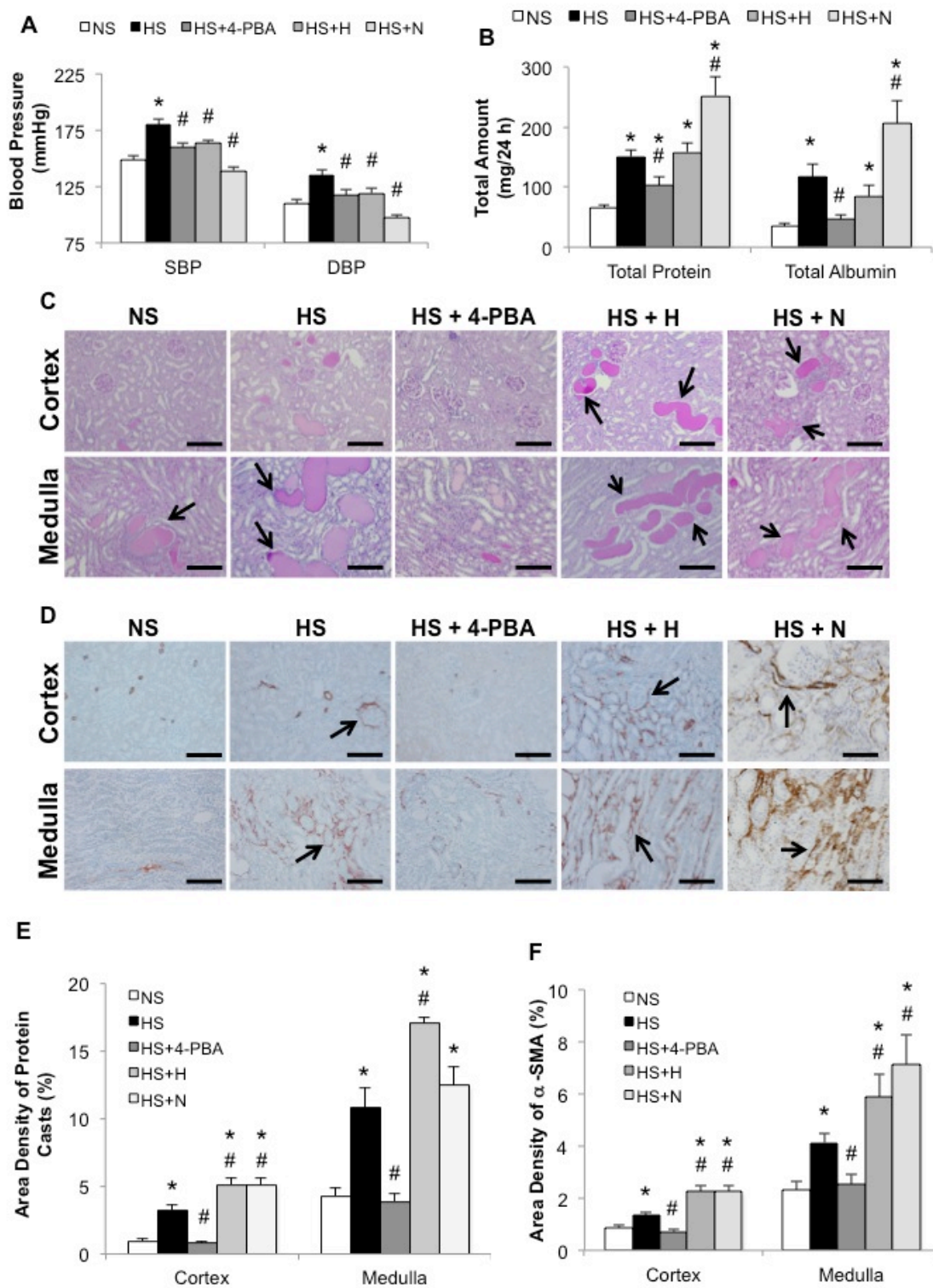


Figure 7. 4-PBA prevents salt-induced renal collagen deposition. (A) Picrosirius red staining was performed on kidney sections from SS-BN13 and Dahl salt-sensitive (SS) rats to illustrate collagen deposition in renal cortex and medulla (arrows). Bar=200 μ m. (B) Quantification of collagen demonstrates increased deposition in high salt (HS)-fed SS rats; this effect was significantly inhibited in response to 4-PBA treatment. No significant changes were observed in SS-BN13 animals in response to HS diet or co-treatment with 4-PBA. *, $p < 0.05$ vs normal salt (NS); #, $p < 0.05$ vs HS.

Figure 8.



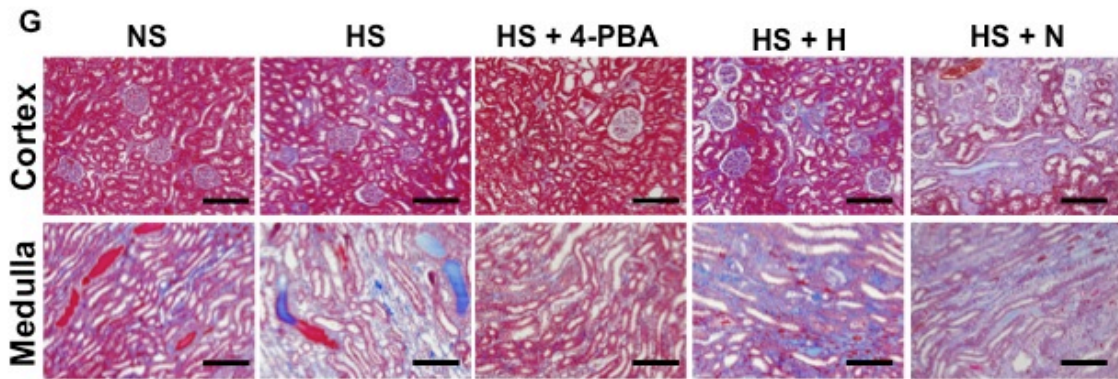


Figure 8. 4-PBA treatment prevents proteinuria, albuminuria, and renal pathology, independent of blood pressure effects. (A) The vasodilators hydralazine (HS+H) and nifedipine (HS+N) lowered systolic and diastolic blood pressures to the same extent as 4-PBA (HS+PBA) in high salt (HS)-fed Dahl salt-sensitive (SS) rats. (B) Whereas proteinuria and albuminuria were lowered in 4-PBA-treated HS-fed SS rats, this effect was not observed in hydralazine- or nifedipine-treated animals. (C) Kidneys were stained with periodic acid-Schiff stain to examine intratubular protein cast formation. (D) To examine renal fibrosis, kidneys were stained for α -smooth muscle actin (SMA). (E) Both hydralazine and nifedipine worsened intratubular protein cast formation (arrows) in the cortex of the kidney when compared with HS-fed rats. Hydralazine treatment also worsened protein cast formation in the medulla, while nifedipine treatment demonstrates results similar to HS feeding. (F) HS+H and HS+N rats developed significantly worse cortical and medullary interstitial fibrosis (arrows). (G) Masson's trichrome staining found more collagen staining (blue) in HS, HS+H, and HS+N animals. Blue collagen staining appears to be lessened in HS-fed rats treated with 4-PBA. *, $p < 0.05$ vs NS; #, $p < 0.05$ vs HS; bar=200 μm .

Table 1. Blood pressure, blood urea nitrogen, and plasma creatinine levels before and after salt feeding with 4-phenylbutyric acid treatment

Rat Groups	SBP, mmHg	DBP, mmHg	BUN, mmol/L	Creatinine, μmol/L
SS-BN13 (pre-treatment) (n=18)	135.3 ± 2.6	91.8 ± 2.6	————	————
SS-BN13 (0.4% NaCl) (n=6)	131.5 ± 3.1	92.0 ± 1.8	6.5 ± 0.32	23.8 ± 2.1
SS-BN13 (8% NaCl) (n=6)	149.4 ± 2.6 *	101.6 ± 3.2 *	6.3 ± 0.25	23.5 ± 1.3
SS-BN13 (8% NaCl + 4-PBA) (n=6)	130.7 ± 4.1 #	89.0 ± 4.4 #	8.0 ± 0.84	22.8 ± 1.9
SS (pre-treatment) (n=30)	147.4 ± 2.3	101.2 ± 2.9	————	————
SS (0.4% NaCl) (n=10)	150.8 ± 4.0	108.8 ± 3.9	6.5 ± 0.34	25.5 ± 2.1
SS (8% NaCl) (n=10)	174.7 ± 5.5 *	128.0 ± 6.6 *	7.2 ± 0.46	25 ± 2.2
SS (8% NaCl + 4-PBA) (n=10)	159.1 ± 4.1 #	117.0 ± 5.4	7.8 ± 0.77	21.2 ± 1.5

*, p < 0.05 vs 0.4% NaCl; #, p < 0.05 vs 8% NaCl

CHAPTER 6

Discussion and future directions

6.1 DISCUSSION

ER stress plays a significant role in the development of CKD, including hypertensive nephrosclerosis, and thus maintaining proteostasis within renal cells is important in preventing renal damage. This thesis demonstrates that ER stress can cause renal epithelial tubular cell disjunction with associated β -catenin nuclear translocation (chapter 2), renal damage and tubular cell apoptosis (chapter 3), endothelial dysfunction (chapter 4), and hypertensive nephrosclerosis (chapter 5), and that inhibiting ER stress limits these outcomes. Inhibiting a specific UPR pathway, such as with salubrinal-mediated PERK inhibition in chapter 2, may be effective, but does not attenuate the accumulation of misfolded proteins in the ER or activation of the other UPR pathways. In contrast, LWCCs can be used to encourage proper protein folding, inhibit activation of the three UPR pathways, and prevent subsequent ER stress-mediated end organ damage.

6.1.1 ER stress initiates EMT and the development of renal interstitial fibrosis

Renal tubular epithelial cells undergo ER stress in certain conditions, preventing proteins in the ER from folding correctly and functioning properly within the cell. Chapter 2 illustrates how renal epithelial cells undergoing ER stress transform their phenotype to a mesenchymal-like cell, causing cellular disjunction and altering the structure of the cytoskeleton. EMT occurs in three circumstances: embryogenesis (type 1), organ fibrosis (type 2), and cancer progression and metastasis (type 3). Organ fibrosis is induced in situations of chronic injury, and is primarily mediated by fibroblasts and myofibroblasts (Cannito et al., 2010).

Renal interstitial fibrosis is characterized by an accumulation of extracellular matrix components in the interstitium, and the most common animal model used to study fibrosis involves UUO. This is because the model achieves progressive renal fibrosis without any exogenous toxins that may have additional effects on the kidney. UUO induces TGF- β signalling, and subsequent activation of Smad2/3 (Fu et al., 2006). The renal tubules become dilated, flattened, and atrophic; inflammatory cells infiltrate the kidney; and extracellular matrix components aggregate in the interstitium (Yang et al., 2010). UUO-mediated ER stress is primarily found in renal tubular cells (Fan et al., 2015; Liu et al., 2015), and may be partially the result of ischemia (Chevalier et al., 2009). ER stress induces apoptosis in the tubules (Liu et al., 2015; Yoneda et al., 2001), which can be inhibited with genetic knockout of the ER stress-inducible gene *Mkk3* (Ma et al., 2007). Genetic knockout of another ER stress-inducible and pro-fibrotic protein, Smad3, prevents apoptosis, inflammation, and fibrosis (Inazaki et al., 2004; Tanjore et al., 2013). Cellular apoptosis can lead to atubular glomeruli and tubular atrophy, while interstitial macrophages release cytokines that induce fibroblast proliferation and activation (Chevalier et al., 2009). While ER stress-mediated apoptosis and inflammation are critical in the progression of fibrosis, loss of cell-cell adhesions may also play a significant role in the development of renal interstitial fibrosis.

Junctional proteins, such as E-cadherin and β -catenin, are essential for kidney function, as they help preserve epithelial cell polarity. However, during ER stress, β -catenin dissociates from E-cadherin and the actin cytoskeleton, and translocates to the cytoplasm. The loss of organized cell-cell junctions is caused by β -catenin being retained in the ER and being unable to deliver E-cadherin to the cell membrane (Dickhout et al.,

2016). In support, similar results were found in thyroid epithelial cells (Ulianich et al., 2008), as well as in type II alveolar epithelial cells (Tanjore et al., 2011) treated with ER stress inducers.

The ER stress protein TDAG51 is critical to the progression of TGF- β -mediated fibrosis, as demonstrated in chapter 2. TDAG51 acts as a translational regulator and can be induced by ER stress, with preliminary research indicating both the PERK and IRE1 pathways, but not ATF6, play a role in TDAG51 expression (Supplementary figure 1 – Appendix 2). Further, a model of hypertensive CKD has demonstrated reduced renal interstitial fibrosis in TDAG51 knockout mice (Supplementary figure 2 – Appendix 2). TDAG51 contains a pleckstrin homology-like domain, in addition to proline-glutamine and proline-histidine repeat sequences (Nagai, 2016). Proteins that contain proline-glutamine and proline-histidine repeats are responsible for transcription regulation (Park et al., 1996) and/or apoptosis (Gomes et al., 1999), while proteins containing a pleckstrin homology domain tend to play a role in cytoskeletal organization (Haslam et al., 1993; Ingley & Hemmings, 1994). In support, chapter 2 demonstrates that TDAG51 expression induces apoptosis and contributes to cytoskeletal organization.

While the destruction of epithelial cell-cell junctions results in increased tubular permeability, the source of fibroblasts in the renal interstitium is still unclear and somewhat controversial (Galichon et al., 2013; Zeisberg & Duffield, 2010). Epithelial cells undergoing EMT do not appear to contribute a significant number of fibroblasts by migration into the interstitium to cause fibrosis (LeBleu et al., 2013); however, it should be noted that EMT, the transition from an epithelial to mesenchymal cell phenotype, is a process that does not necessarily involve cell migration. Thus, evidence that precludes

epithelial cell migration to the interstitium does not preclude a role for EMT in renal interstitial fibrosis. A verifiable mechanism through which EMT may result in renal interstitial fibrosis is through the reduction of epithelial junctions, and resulting increase in tubular permeability (Lovisa et al., 2015).

6.1.2 4-PBA is renoprotective through direct ER stress inhibiting effects in the kidney

ER stress is associated with a number of renal diseases, including ischemia-mediated acute kidney injury (Montie et al., 2005; Yang et al., 2014), genetic forms of renal disease (Yang et al., 2013), and proteinuric nephropathies (Cunard & Sharma, 2011; Lindenmeyer et al., 2008). Chapter 3 demonstrates that pharmacologically inhibiting ER stress using the LWCC 4-PBA, at a dose of 1 g/kg/day, can protect the kidney from ER stress-mediated structural damage. Tunicamycin, which has nephrotoxic effects, was used to induce ER stress-mediated acute kidney injury in mice. 4-PBA treatment directly inhibited ER stress in the kidney, and thus reduced damage. 4-PBA also has renoprotective effects in other models of kidney injury, including preventing podocytic apoptosis in a model of diabetic nephropathy (Cao et al., 2016) and protecting against renal dysfunction in mutant mouse models of proteinuric nephropathy (El Karoui et al., 2016). As mentioned, 4-PBA prevents protein aggregation through the interaction of its hydrophobic regions with the exposed hydrophobic regions of misfolded proteins (Cortez & Sim, 2014; Mimori et al., 2013). The maintenance of proteostasis, as accomplished through 4-PBA preventing protein aggregation, inhibits activation of the UPR and subsequent upregulation of injurious proteins, such as CHOP.

In addition to being an ER stress inhibitor, 4-PBA also possesses HDACi properties (Miller et al., 2011). HDACis prevent histone deacetylation, but can also prevent deacetylation of spliced XBP1 (Wang et al., 2011). Spliced XBP1 is a highly active transcription factor downstream from IRE1 in the UPR that may prevent apoptosis through the upregulation of protein folding chaperones (Hosoi et al., 2012). This suggests that 4-PBA may inhibit ER stress by directly folding proteins, as well as increasing transcription of additional protein folding chaperones. Interestingly, compounds with similar molecular structures to 4-PBA demonstrated that protection against tunicamycin-mediated neuronal cell death was due to its protein folding properties (Mimori et al., 2013).

To provide sufficient end organ protection, a LWCC must maintain a selective and localized response, while also being highly effective. A comparison between prominent LWCCs, 4-PBA, DHA, TUDCA, glycerol, and trehalose determined the potency and efficacy of the drugs (Upagupta et al., 2017). Of these LWCCs, 4-PBA is most effective at reducing ER stress, while DHA is most potent. Structurally, 4-PBA and DHA share common features, including a long unsaturated hydrocarbon with a hydrophobic region on one end, and a hydrophilic region on the other end. It is believed that the length of the hydrophobic region is responsible for the potency of the LWCC (Upagupta et al., 2017). As such, it is justifiable to speculate that hydrophobic LWCCs (4-PBA, DHA, and TUDCA) are more effective and potent than osmolyte LWCCs (glycerol, trehalose). Despite differences in potency and efficacy, both hydrophobic and osmolyte LWCCs have been shown to be protective against end organ damage, including renal damage. TUDCA, which prevents protein aggregation in renal tubular epithelial cells with ER

stress (Upagupta et al., 2017; Zhang et al., 2016), also reduces albuminuria, renal interstitial fibrosis, mesangial matrix expansion, and tubular apoptosis in diabetic nephropathy (Zhang et al., 2016). Further, TUDCA protects against ischemia-mediated structural damage and apoptosis caused by ER stress-inducible caspase-9 (Cheung et al., 2006; Gupta et al., 2012), as well as fibrotic cytokines, inflammatory cytokines, and reactive oxygen species in aldosterone-induced renal damage (Guo et al., 2016). While DHA is primarily associated with neuroprotection (Begum et al., 2013; Belayev et al., 2009), and can inhibit ER stress-mediated inflammation in traumatic brain injury (Harvey et al., 2015), it also has renoprotective effects. DHA can increase lifespan and protect from renal disease in short-lived lupus-prone mice. Further, it inhibits the pro-inflammatory cytokine interleukin-18, which is increased in lipopolysaccharide-induced kidney disease (Halade et al., 2010). Orally delivered, trehalose has demonstrated some renoprotective effects in mice with diabetic nephropathy (Lin et al., 2016), in addition to having neuroprotective effects (Liu et al., 2005). Intramuscular injection of the LWCC glycerol can actually induce renal injury, effectively causing rhabdomyolysis. Injection induces the breakdown of striated muscle fibres and subsequent release of myoglobin into the bloodstream, which causes damage to the kidney. There is some evidence of ER stress induction in rhabdomyolysis (Zhao et al., 2016). However, aerosolized glycerol is able to prevent fibrosis and inflammation in asthmatic lungs of mice (Makhija et al., 2014), suggesting delivery method may play a significant role in whether the effects of LWCCs are protective or injurious. It should be noted that studies have demonstrated effective use of 4-PBA when delivered via intraperitoneal injection as a protective measure against ER

stress-mediated damage in organs other than the kidney (Inden et al., 2007; Luo et al., 2015).

6.1.3 Inhibiting ER stress prevents endothelial dysfunction and subsequent hypertension

The pathogenesis of hypertension is incompletely understood, primarily due to the numerous factors that can affect the disorder. However, ER stress has been implicated in the development of hypertension. In fact, a tunicamycin mouse model has demonstrated that ER stress induction causes hypertension; inhibiting ER stress with 4-PBA prevented increases in blood pressure (Liang et al., 2013). Similar results were found in angiotensin II-treated mice (Kassan et al., 2012; Liang et al., 2013), angiotensin II/deoxycorticosterone acetate/salt-treated mice (Mohammed-Ali et al., 2017), and genetically hypertensive rats (Spitler et al., 2013). Evidence suggests this effect is the result of inhibited contractility of vascular smooth muscle cells (Spitler et al., 2013), with hypertensive animals demonstrating ER stress induction in resistance vessels (Kassan et al., 2012). Chapter 4 demonstrates that orally delivered 4-PBA can prevent structural vessel alterations and inhibit ER stress in resistance vessels in an animal model of essential hypertension. It was determined that ER stress decreases nitric oxide bioavailability, and thus endothelial-dependent vasodilation.

There are a number of factors that are responsible for endothelial-dependent vasodilation in non-hypertensive resistance arteries, including nitric oxide, endothelium-derived hyperpolarizing factors, and prostacyclin. However, hypertensive vessels respond primarily to nitric oxide, with attenuated endothelium-derived hyperpolarizing factors and

prostacyclin, as demonstrated in SHR_s (Bussemaker et al., 2003; Fujii et al., 1992; Mantelli et al., 1995; Mori et al., 2006), as well as hypertensive Sprague Dawley rats (Kang et al., 2007). ER stress causes endothelial dysfunction through reduced endothelial nitric oxide synthase activity, and thus impaired vasodilation and increased vasoconstriction. 4-PBA can act directly on the hypertensive vessels to reduce ER stress, and reverse vessel dysfunction. The superoxide dismutase mimetic TEMPOL is also able to restore endothelium-dependent vasodilation, and lower blood pressure (Schnackenberg et al., 1998). These data suggest a hypertensive mechanism involving superoxide and nitric oxide reacting to form peroxynitrite, reducing nitric oxide bioavailability (Chen et al., 2007; Schnackenberg et al., 1998). Interestingly, Sprague Dawley rats infused with angiotensin II demonstrated reduced blood pressure with TEMPOL treatment, indicating a role for oxidative stress in angiotensin II-mediated hypertension (Nishiyama et al., 2001).

Angiotensin II infusion-mediated hypertension induces ER stress in conduit and resistance vessels, causing endothelial dysfunction, increased aortic TGF- β activity, and reduced endothelial nitric oxide synthase. These effects are inhibited with LWCCs, 4-PBA and TUDCA, suggesting protein misfolding is the cause of pathology (Kassan et al., 2012). ER stress is a known inducer of oxidative stress (Bhandary et al., 2012), and peroxynitrite, a product of oxidative stress, can exacerbate ER stress (Dickhout et al., 2005). These data are in agreement with our finding that treatment with an ER stress inhibitor prevents superoxide formation. Interestingly, macrovascular endothelial dysfunction appears to be the result of increased TGF- β activity, while microvascular endothelial dysfunction is due to excessive oxidative stress (Kassan et al., 2012). Further,

endothelium-derived contractile factors that cause increased peripheral resistance in hypertension are inhibited with LWCC treatment. LWCCs inhibit ER stress in the aorta, as well as normalize cyclooxygenase expression and reactive oxygen species production, both of which are increased with ER stress (Spitler et al., 2013). Direct administration of angiotensin II to the subfornical organ of the brain induces hypertension, as well as ER stress in the brain. Both hypertension and ER stress are inhibited with LWCC treatment or supplementation of GRP78 (Young et al., 2012). While 4-PBA treatment can lower blood pressure through preserving blood vessel structure and function, lowering blood pressure alone may not have a significant effect on protecting the kidney in conditions of hypertensive nephrosclerosis.

6.1.4 Preserving the myogenic response through ER stress inhibition, and not simply lowering blood pressure, can protect against glomerular hyperfiltration

Hypertensive nephrosclerosis is characterized by high blood pressure and injury to the small blood vessels, glomeruli, tubules, and interstitium of the kidney. It has become evident that arterial stiffening with increased pulse pressure, and loss of renal autoregulation are the primary mechanisms of damage (Hill, 2008), both of which can be caused by ER stress (Choi et al., 2016; Spitler & Webb, 2014). Chapter 5 establishes that inhibiting ER stress with 4-PBA can reduce hypertensive nephrosclerosis more effectively than lowering blood pressure alone. This is likely due to the preservation of blood vessel structure and function, which protects the myogenic response from becoming dysregulated and resulting in glomerular hyperfiltration. In support, we have

demonstrated that lowering blood pressure alone, using vasodilators, does not protect the kidney, and can actually worsen renal damage.

Studies have demonstrated that vasodilators, such as the calcium channel blocker nifedipine, prevent myogenic constriction in various resistance arteries (Coats et al., 2001; Delaey & Van de Voorde, 2000). The impaired myogenic response prevents constriction of the afferent arteriole, resulting in glomerular hyperfiltration. Renal tubular epithelial cells exposed to fluid shear stress, such as that caused by hyperfiltration, undergo phenotypic alterations, losing epithelial markers but not gaining mesenchymal ones (Maggiorani et al., 2015). This suggests disjunction between tubular epithelial cells that do not necessarily undergo EMT, but may induce pro-fibrotic signalling. In support, *in vitro* data demonstrate increased TGF- β expression in renal proximal tubular epithelial cells exposed to fluid shear stress (Kunnen et al., 2017). Preventing fluid shear stress or glomerular hyperfiltration can likely protect renal cells from undergoing injury and the development of nephrosclerosis.

Preservation of renal autoregulation can protect against glomerular hyperfiltration and subsequent renal damage. As previously discussed, glomerular hyperfiltration is caused by afferent arteriole vasodilation; chapter 4 demonstrates that resistance vessel dysregulation, such as that found in impaired myogenic constriction, can be due to ER stress and endothelial dysfunction. Further, myogenic impairment precedes renal injury in the Fawn-Hooded Hypertensive rat, likely through impairment of stretch-induced mechanotransduction. Other factors involved in myogenic constriction include activation of the calmodulin/myosin light chain kinase pathway, MAPKs, and metabolites of arachidonic acid, such as 20-HETE (Ochodnický et al., 2010). In support, inhibiting ER

stress has been shown to prevent activation of the myosin light chain kinase pathway (Liang et al., 2013) and the MAPK pathway (Shi et al., 2015). Further, DSS rats lack 20-HETE, shown in Dahl salt-resistant rats to be critical to afferent arteriole myogenic response and ATP-mediated constriction (Ren et al., 2014). Chapter 5 establishes that myogenic constriction is impaired in response to direct administration of an ER stress inducer, which can be prevented with 4-PBA.

Hyperfiltration is associated with podocyte injury or loss; the low number of functional podocytes is demonstrated by foot process effacement and a bare glomerular basement membrane without properly functioning slit diaphragms. Mechanical stretch, a product of glomerular hyperfiltration, activates a localized angiotensin system with increased podocytic angiotensin II receptors (Durvasula et al., 2004). Mouse podocytes treated with angiotensin II develop ER stress, which can be inhibited with an angiotensin II receptor blocker (ARB) (Ha et al., 2015). Further, angiotensin II treatment induces podocytic apoptosis, which can also be inhibited with an ARB (Fukami et al., 2013), as well as podocytic EMT (Bai et al., 2017). Podocytes treated with TGF- β also undergo EMT, demonstrating loss of podocytic epithelial markers (P-cadherin, zonula occludens-1, and nephrin), while increasing expression of the intermediate filament desmin (Li et al., 2008). This may be of particular interest, as chapter 2 demonstrates that ER stress can increase expression of TGF- β . When taken together, these data suggest that glomerular hyperfiltration may induce damage to the podocytes and slit diaphragm through angiotensin II-mediated ER stress, and subsequent apoptosis and EMT. Further studies are required to elucidate the role of ER stress in this pathology, and the capacity of LWCCs to inhibit consequent renal injury.

6.2 FUTURE DIRECTIONS

In this thesis, the role of ER stress in the development of hypertensive CKD, and the use of 4-PBA to inhibit ER stress and subsequent injury in the kidney have been established. However, some questions remain unanswered and are discussed below.

6.2.1 Determination of the role TDAG51 plays in the development of EMT and fibrosis.

While it has been established that TDAG51 is induced by ER stress and plays a role in EMT and fibrosis, its function(s) and mechanism(s) have yet to be fully elucidated. Chapter 2 demonstrates that overexpression of TDAG51 induces cell shape change and apoptosis, and that TDAG51 knockout prevents TGF- β -mediated fibrosis. Additionally, inhibiting ER stress with 4-PBA reduces interstitial damage and collagen deposition in a UUO model of fibrosis (Liu et al., 2016). As such, an interesting point of inquiry is the specific role of TDAG51 in fibrosis, and whether TDAG51 knockout can prevent EMT and fibrosis in the kidney. Further, as 4-PBA prevented ER stress-mediated fibrosis in a UUO model, it should be determined if this was due to inhibition of TDAG51 expression or an alternate mechanism.

6.2.2 Investigation of ER stress-mediated effects in podocytes in a model of glomerular hyperfiltration.

As angiotensin II induces hypertension, as well as ER stress and injury in podocytes, an intriguing area of future study is to investigate the effects of ARBs in an animal model of hypertensive nephrosclerosis, such as the DSS rat. The DSS rat is an excellent model

system for this study, as demonstrated in chapter 5 by: a) impaired myogenic response that causes glomerular hyperfiltration, b) podocyte injury and foot process effacement, c) dilated ER in the podocytes, indicative of ER stress, and d) prevention of these effects through ER stress inhibition. Further, ARBs have been shown to have renoprotective qualities in DSS rats, attenuating proteinuria, glomerular sclerosis, and renal interstitial fibrosis (Liang & Leenen, 2008; Nakaya et al., 2002; Oguchi et al., 2014). However, it is yet unclear if these renoprotective effects are dependent on blood pressure lowering, as results conflict on the antihypertensive effects of ARBs in DSS rats. Subcutaneous injection of ARBs reduced blood pressure and protected against vascular fibrosis in DSS rats from 5-9 weeks of age (Liang & Leenen, 2008), while ARBs delivered orally from 6-14 weeks of age did not (Oguchi et al., 2014). Further, ARBs have also been shown to prevent ER stress, apoptosis, and fibrosis in UUO kidneys (Chiang et al., 2011). This study could determine the contribution of angiotensin II inhibition and ER stress inhibition in protecting the kidney from glomerular hyperfiltration-mediated injury.

In addition to the examination of ARB effects on podocytes, another avenue of study could involve alternative LWCCs. As mentioned, hydrophobic LWCC with a long unsaturated hydrocarbon with hydrophobic and hydrophilic ends are likely the most potent. Molecules that fit this structural description, such as DHA, could be used to treat the DSS model of hypertensive nephrosclerosis. This would determine if other LWCCs can maintain proteostasis in the podocytes of the kidney, and if that will prevent glomerular hyperfiltration and subsequent nephron loss and renal damage.

6.2.3 Examination of renal function in a model of hypertensive nephrosclerosis.

A limitation of the current work is the lack of renal function measurement. As such, a pertinent avenue of investigation involves measuring renal function in a model of hypertensive nephrosclerosis treated with 4-PBA and/or another LWCC. While chapter 5 demonstrates that inhibiting ER stress is pivotal in the prevention of proteinuria, protein cast formation, and renal interstitial fibrosis, it is unclear whether proper renal function is maintained. As such, the DSS rat model is an excellent candidate for this study, as is treatment with 4-PBA, which has already been shown to have renoprotective effects in this model. Further, LWCCs protect against decline in renal function in other models of kidney disease (El Karoui et al., 2016; Wang et al., 2017). Renal function decline should be measured using GFR, as serum creatinine levels are not sensitive enough to accurately measure mild and moderate reductions in renal function (Cowley et al., 2013). Treatment with additional LWCCs of different chemical structures and mechanisms could provide an enhanced understanding of how ER stress inhibition protects against hypertensive nephrosclerosis.

6.3 CONCLUSIONS

The central aim of this thesis was to communicate that: (i) ER stress causes cellular injury and death, and can lead to hypertensive CKD, and (ii) the inhibition of ER stress can prevent the development of hypertensive nephrosclerosis. The findings of these studies could have implications for clinicians and researchers working with hypertensive nephrosclerosis. This thesis demonstrated that the ER stress protein TDAG51 plays a

critical role in TGF- β -mediated fibrosis. Further, 4-PBA directly inhibits renal damage by suppressing ER stress-induced apoptosis, and endothelial dysfunction-mediated hypertension by preserving nitric oxide bioavailability. Finally, this thesis determined that lowering blood pressure alone does not protect the kidney from glomerular hyperfiltration-mediated damage, but that lowering blood pressure with an ER stress inhibitor can be renoprotective. The findings of the preceding studies emphasize the need for determining the role ER stress plays in the development of hypertensive nephrosclerosis, and how vascular and renal injury can be prevented using LWCCs.

CHAPTER 7

References

- Amann, K., Nichols, C., Tornig, J., Schwarz, U., Zeier, M., Mall, G., & Ritz, E. (1996). Effect of ramipril, nifedipine, and moxonidine on glomerular morphology and podocyte structure in experimental renal failure. *Nephrol Dial Transplant*, *11*(6), 1003-1011.
- Arendshorst, W. J., & Beierwaltes, W. H. (1979). Renal and nephron hemodynamics in spontaneously hypertensive rats. *Am J Physiol*, *236*(3), F246-251.
- Bai, C., Liang, S., Wang, Y., & Jiao, B. (2017). Knocking down TCF8 inhibits high glucose- and angiotensin II-induced epithelial to mesenchymal transition in podocytes. *Biosci Trends*, *11*(1), 77-84.
- Bakris, G. L., & Ritz, E. (2009). The message for World Kidney Day 2009: hypertension and kidney disease: a marriage that should be prevented. *Kidney Int*, *75*(5), 449-452.
- Basseri, S., Lhotak, S., Sharma, A. M., & Austin, R. C. (2009). The chemical chaperone 4-phenylbutyrate inhibits adipogenesis by modulating the unfolded protein response. *J Lipid Res*, *50*(12), 2486-2501.
- Bassik, M. C., & Kampmann, M. (2011). Knocking out the door to tunicamycin entry. *Proc Natl Acad Sci U S A*, *108*(29), 11731-11732.
- Begum, G., Harvey, L., Dixon, C. E., & Sun, D. (2013). ER stress and effects of DHA as an ER stress inhibitor. *Transl Stroke Res*, *4*(6), 635-642.
- Beilin, L. J., & Puddey, I. B. (2006). Alcohol and hypertension: an update. *Hypertension*, *47*(6), 1035-1038.
- Belayev, L., Khoutorova, L., Atkins, K. D., & Bazan, N. G. (2009). Robust docosahexaenoic acid-mediated neuroprotection in a rat model of transient, focal cerebral ischemia. *Stroke*, *40*(9), 3121-3126.
- Bhandary, B., Marahatta, A., Kim, H. R., & Chae, H. J. (2012). An involvement of oxidative stress in endoplasmic reticulum stress and its associated diseases. *Int J Mol Sci*, *14*(1), 434-456.
- Bianchi, G., Fox, U., Di Francesco, G. F., Giovanetti, A. M., & Pagetti, D. (1974). Blood pressure changes produced by kidney cross-transplantation between spontaneously hypertensive rats and normotensive rats. *Clin Sci Mol Med*, *47*(5), 435-448.
- Bowman, T. S., Gaziano, J. M., Buring, J. E., & Sesso, H. D. (2007). A prospective study of cigarette smoking and risk of incident hypertension in women. *J Am Coll Cardiol*, *50*(21), 2085-2092.

- Boyce, M., Bryant, K. F., Jousse, C., Long, K., Harding, H. P., Scheuner, D., . . . Yuan, J. (2005). A selective inhibitor of eIF2 α dephosphorylation protects cells from ER stress. *Science*, *307*(5711), 935-939.
- Brenner, B. M., Lawler, E. V., & Mackenzie, H. S. (1996). The hyperfiltration theory: a paradigm shift in nephrology. *Kidney Int*, *49*(6), 1774-1777.
- Brenner, B. M., Meyer, T. W., & Hostetter, T. H. (1982). Dietary protein intake and the progressive nature of kidney disease: the role of hemodynamically mediated glomerular injury in the pathogenesis of progressive glomerular sclerosis in aging, renal ablation, and intrinsic renal disease. *N Engl J Med*, *307*(11), 652-659.
- Brostrom, M. A., Mourad, F., & Brostrom, C. O. (2001). Regulated expression of GRP78 during vasopressin-induced hypertrophy of heart-derived myocytes. *J Cell Biochem*, *83*(2), 204-217.
- Bryant, K. F., Macari, E. R., Malik, N., Boyce, M., Yuan, J., & Coen, D. M. (2008). ICP34.5-dependent and -independent activities of salubrinal in herpes simplex virus-1 infected cells. *Virology*, *379*(2), 197-204.
- Bucciantini, M., Giannoni, E., Chiti, F., Baroni, F., Formigli, L., Zurdo, J., . . . Stefani, M. (2002). Inherent toxicity of aggregates implies a common mechanism for protein misfolding diseases. *Nature*, *416*(6880), 507-511.
- Bussemaker, E., Popp, R., Fisslthaler, B., Larson, C. M., Fleming, I., Busse, R., & Brandes, R. P. (2003). Aged spontaneously hypertensive rats exhibit a selective loss of EDHF-mediated relaxation in the renal artery. *Hypertension*, *42*(4), 562-568.
- Campese, V. M. (1994). Salt sensitivity in hypertension. Renal and cardiovascular implications. *Hypertension*, *23*(4), 531-550.
- Cannito, S., Novo, E., di Bonzo, L. V., Busletta, C., Colombatto, S., & Parola, M. (2010). Epithelial-mesenchymal transition: from molecular mechanisms, redox regulation to implications in human health and disease. *Antioxid Redox Signal*, *12*(12), 1383-1430.
- Cao, A. L., Wang, L., Chen, X., Wang, Y. M., Guo, H. J., Chu, S., . . . Peng, W. (2016). Ursodeoxycholic acid and 4-phenylbutyrate prevent endoplasmic reticulum stress-induced podocyte apoptosis in diabetic nephropathy. *Lab Invest*, *96*(6), 610-622.
- Carducci, M. A., Nelson, J. B., Chan-Tack, K. M., Ayyagari, S. R., Sweatt, W. H., Campbell, P. A., . . . Simons, J. W. (1996). Phenylbutyrate induces apoptosis in human prostate cancer and is more potent than phenylacetate. *Clin Cancer Res*, *2*(2), 379-387.

- Carlisle, R. E., Brimble, E., Werner, K. E., Cruz, G. L., Ask, K., Ingram, A. J., & Dickhout, J. G. (2014). 4-Phenylbutyrate inhibits tunicamycin-induced acute kidney injury via CHOP/GADD153 repression. *PLoS One*, *9*(1), e84663.
- Carretero, O. A., & Oparil, S. (2000). Essential hypertension. Part I: definition and etiology. *Circulation*, *101*(3), 329-335.
- Carroll, M. F., & Temte, J. L. (2000). Proteinuria in adults: a diagnostic approach. *Am Fam Physician*, *62*(6), 1333-1340.
- Chen, X., Patel, K., Connors, S. G., Mendonca, M., Welch, W. J., & Wilcox, C. S. (2007). Acute antihypertensive action of Tempol in the spontaneously hypertensive rat. *Am J Physiol Heart Circ Physiol*, *293*(6), H3246-3253.
- Chen, Y. T., Stewart, D. B., & Nelson, W. J. (1999). Coupling assembly of the E-cadherin/beta-catenin complex to efficient endoplasmic reticulum exit and basal-lateral membrane targeting of E-cadherin in polarized MDCK cells. *J Cell Biol*, *144*(4), 687-699.
- Cheung, H. H., Lynn Kelly, N., Liston, P., & Korneluk, R. G. (2006). Involvement of caspase-2 and caspase-9 in endoplasmic reticulum stress-induced apoptosis: a role for the IAPs. *Exp Cell Res*, *312*(12), 2347-2357.
- Chevalier, R. L., Forbes, M. S., & Thornhill, B. A. (2009). Ureteral obstruction as a model of renal interstitial fibrosis and obstructive nephropathy. *Kidney Int*, *75*(11), 1145-1152.
- Chiang, C. K., Hsu, S. P., Wu, C. T., Huang, J. W., Cheng, H. T., Chang, Y. W., . . . Liu, S. H. (2011). Endoplasmic reticulum stress implicated in the development of renal fibrosis. *Mol Med*, *17*(11-12), 1295-1305.
- Choi, S. K., Lim, M., Byeon, S. H., & Lee, Y. H. (2016). Inhibition of endoplasmic reticulum stress improves coronary artery function in the spontaneously hypertensive rats. *Sci Rep*, *6*, 31925.
- Coats, P., Johnston, F., MacDonald, J., McMurray, J. J., & Hillier, C. (2001). Signalling mechanisms underlying the myogenic response in human subcutaneous resistance arteries. *Cardiovasc Res*, *49*(4), 828-837.
- Collins, A. F., Pearson, H. A., Giardina, P., McDonagh, K. T., Brusilow, S. W., & Dover, G. J. (1995). Oral sodium phenylbutyrate therapy in homozygous beta thalassemia: a clinical trial. *Blood*, *85*(1), 43-49.
- Conrad, C. H., Brooks, W. W., Hayes, J. A., Sen, S., Robinson, K. G., & Bing, O. H. (1995). Myocardial fibrosis and stiffness with hypertrophy and heart failure in the spontaneously hypertensive rat. *Circulation*, *91*(1), 161-170.

- Cortez, L., & Sim, V. (2014). The therapeutic potential of chemical chaperones in protein folding diseases. *Prion*, 8(2).
- Cowley, A. W., Jr., & Roman, R. J. (1996). The role of the kidney in hypertension. *JAMA*, 275(20), 1581-1589.
- Cowley, A. W., Roman, R. J., Kaldunski, M. L., Dumas, P., Dickhout, J. G., Greene, A. S., & Jacob, H. J. (2001). Brown Norway chromosome 13 confers protection from high salt to consomic Dahl S rat. *Hypertension*, 37(2 Pt 2), 456-461.
- Cowley, A. W., Ryan, R. P., Kurth, T., Skelton, M. M., Schock-Kusch, D., & Gretz, N. (2013). Progression of glomerular filtration rate reduction determined in conscious Dahl salt-sensitive hypertensive rats. *Hypertension*, 62(1), 85-90.
- Cunard, R., & Sharma, K. (2011). The endoplasmic reticulum stress response and diabetic kidney disease. *Am J Physiol Renal Physiol*, 300(5), F1054-F1061.
- De Miguel, C., Das, S., Lund, H., & Mattson, D. L. (2010). T lymphocytes mediate hypertension and kidney damage in Dahl salt-sensitive rats. *Am J Physiol Regul Integr Comp Physiol*, 298(4), R1136-1142.
- Delaey, C., & Van de Voorde, J. (2000). Pressure-induced myogenic responses in isolated bovine retinal arteries. *Invest Ophthalmol Vis Sci*, 41(7), 1871-1875.
- Dhaun, N., Macintyre, I. M., Melville, V., Lilitkarntakul, P., Johnston, N. R., Goddard, J., & Webb, D. J. (2009). Blood pressure-independent reduction in proteinuria and arterial stiffness after acute endothelin-a receptor antagonism in chronic kidney disease. *Hypertension*, 54(1), 113-119.
- Dickhout, J. G., Carlisle, R. E., & Austin, R. C. (2011). Interrelationship between cardiac hypertrophy, heart failure, and chronic kidney disease: endoplasmic reticulum stress as a mediator of pathogenesis. *Circ Res*, 108(5), 629-642.
- Dickhout, J. G., Chahal, J., Matthews, A., Carlisle, R. E., Tat, V., & Naiel, S. (2016). Endoplasmic reticulum stress causes epithelial cell disjunction. *Journal of Pharmacological Reports*, 1(1), 5.
- Dickhout, J. G., Hossain, G. S., Pozza, L. M., Zhou, J., Lhotak, S., & Austin, R. C. (2005). Peroxynitrite causes endoplasmic reticulum stress and apoptosis in human vascular endothelium: implications in atherogenesis. *Arterioscler Thromb Vasc Biol*, 25(12), 2623-2629.
- Dickhout, J. G., & Krepinsky, J. C. (2009). Endoplasmic reticulum stress and renal disease. *Antioxid Redox Signal*, 11(9), 2341-2352.
- Dickhout, J. G., & Lee, R. M. (1997). Structural and functional analysis of small arteries from young spontaneously hypertensive rats. *Hypertension*, 29(3), 781-789.

- Durvasula, R. V., Petermann, A. T., Hiromura, K., Blonski, M., Pippin, J., Mundel, P., . . . Shankland, S. J. (2004). Activation of a local tissue angiotensin system in podocytes by mechanical strain. *Kidney Int*, *65*(1), 30-39.
- Dyer, E. S., Paulsen, M. T., Markwart, S. M., Goh, M., Livant, D. L., & Ljungman, M. (2002). Phenylbutyrate inhibits the invasive properties of prostate and breast cancer cell lines in the sea urchin embryo basement membrane invasion assay. *Int J Cancer*, *101*(5), 496-499.
- El Karoui, K., Viau, A., Dellis, O., Bagattin, A., Nguyen, C., Baron, W., . . . Terzi, F. (2016). Endoplasmic reticulum stress drives proteinuria-induced kidney lesions via Lipocalin 2. *Nat Commun*, *7*, 10330.
- El-Nahas, A. M. (2003). Plasticity of kidney cells: role in kidney remodeling and scarring. *Kidney Int*, *64*(5), 1553-1563.
- Engin, F., & Hotamisligil, G. S. (2010). Restoring endoplasmic reticulum function by chemical chaperones: an emerging therapeutic approach for metabolic diseases. *Diabetes Obes Metab*, *12 Suppl 2*, 108-115.
- Enomoto, A., Takeda, M., Tojo, A., Sekine, T., Cha, S. H., Khamdang, S., . . . Niwa, T. (2002). Role of organic anion transporters in the tubular transport of indoxyl sulfate and the induction of its nephrotoxicity. *J Am Soc Nephrol*, *13*(7), 1711-1720.
- Fan, Y., Xiao, W., Li, Z., Li, X., Chuang, P. Y., Jim, B., . . . He, J. C. (2015). RTN1 mediates progression of kidney disease by inducing ER stress. *Nat Commun*, *6*, 7841.
- Farris, A. B., & Colvin, R. B. (2012). Renal interstitial fibrosis: mechanisms and evaluation. *Curr Opin Nephrol Hypertens*, *21*(3), 289-300.
- Feld, L. G., Van Liew, J. B., Brentjens, J. R., & Boylan, J. W. (1981). Renal lesions and proteinuria in the spontaneously hypertensive rat made normotensive by treatment. *Kidney Int*, *20*(5), 606-614.
- Fraser, S. D., Roderick, P. J., & Taal, M. W. (2016). Where now for proteinuria testing in chronic kidney disease?: Good evidence can clarify a potentially confusing message. *Br J Gen Pract*, *66*(645), 215-217.
- Fu, P., Liu, F., Su, S., Wang, W., Huang, X. R., Entman, M. L., . . . Lan, H. Y. (2006). Signaling mechanism of renal fibrosis in unilateral ureteral obstructive kidney disease in ROCK1 knockout mice. *J Am Soc Nephrol*, *17*(11), 3105-3114.
- Fujii, K., Tominaga, M., Ohmori, S., Kobayashi, K., Koga, T., Takata, Y., & Fujishima, M. (1992). Decreased endothelium-dependent hyperpolarization to acetylcholine

- in smooth muscle of the mesenteric artery of spontaneously hypertensive rats. *Circ Res*, 70(4), 660-669.
- Fukami, K., Yamagishi, S., Kaifu, K., Matsui, T., Kaida, Y., Ueda, S., . . . Okuda, S. (2013). Telmisartan inhibits AGE-induced podocyte damage and detachment. *Microvasc Res*, 88, 79-83.
- Galichon, P., Finianos, S., & Hertig, A. (2013). EMT-MET in renal disease: Should we curb our enthusiasm? *Cancer Lett*, 341, 24-29.
- Gething, M. J., & Sambrook, J. (1992). Protein folding in the cell. *Nature*, 355(6355), 33-45.
- Gomes, I., Xiong, W., Miki, T., & Rosner, M. R. (1999). A proline- and glutamine-rich protein promotes apoptosis in neuronal cells. *J Neurochem*, 73(2), 612-622.
- Greka, A., & Mundel, P. (2012). Cell biology and pathology of podocytes. *Annu Rev Physiol*, 74, 299-323.
- Guo, H., Li, H., Ling, L., Gu, Y., & Ding, W. (2016). Endoplasmic Reticulum Chaperon Tauroursodeoxycholic Acid Attenuates Aldosterone-Infused Renal Injury. *Mediators Inflamm*, 2016, 4387031.
- Gupta, S., Li, S., Abedin, M. J., Noppakun, K., Wang, L., Kaur, T., . . . Steer, C. J. (2012). Prevention of acute kidney injury by tauroursodeoxycholic acid in rat and cell culture models. *PLoS One*, 7(11), e48950.
- Ha, T. S., Park, H. Y., Seong, S. B., & Ahn, H. Y. (2015). Angiotensin II induces endoplasmic reticulum stress in podocyte, which would be further augmented by PI3-kinase inhibition. *Clin Hypertens*, 21, 13.
- Halade, G. V., Rahman, M. M., Bhattacharya, A., Barnes, J. L., Chandrasekar, B., & Fernandes, G. (2010). Docosahexaenoic acid-enriched fish oil attenuates kidney disease and prolongs median and maximal life span of autoimmune lupus-prone mice. *J Immunol*, 184(9), 5280-5286.
- Harvey, L. D., Yin, Y., Attarwala, I. Y., Begum, G., Deng, J., Yan, H. Q., . . . Sun, D. (2015). Administration of DHA Reduces Endoplasmic Reticulum Stress-Associated Inflammation and Alters Microglial or Macrophage Activation in Traumatic Brain Injury. *ASN Neuro*, 7(6).
- Haslam, R. J., Koide, H. B., & Hemmings, B. A. (1993). Pleckstrin domain homology. *Nature*, 363(6427), 309-310.
- Hayakawa, K., Nakajima, S., Hiramatsu, N., Okamura, M., Huang, T., Saito, Y., . . . Kitamura, M. (2010). ER stress depresses NF-kappaB activation in mesangial

- cells through preferential induction of C/EBP beta. *J Am Soc Nephrol*, 21(1), 73-81.
- Helal, I., Fick-Brosnahan, G. M., Reed-Gitomer, B., & Schrier, R. W. (2012). Glomerular hyperfiltration: definitions, mechanisms and clinical implications. *Nat Rev Nephrol*, 8(5), 293-300.
- Higgins, D. F., Kimura, K., Bernhardt, W. M., Shrimanker, N., Akai, Y., Hohenstein, B., . . . Haase, V. H. (2007). Hypoxia promotes fibrogenesis in vivo via HIF-1 stimulation of epithelial-to-mesenchymal transition. *J Clin Invest*, 117(12), 3810-3820.
- Hill, G. S. (2008). Hypertensive nephrosclerosis. *Curr Opin Nephrol Hypertens*, 17(3), 266-270.
- Hill, N. R., Fatoba, S. T., Oke, J. L., Hirst, J. A., O'Callaghan, C. A., Lasserson, D. S., & Hobbs, F. D. (2016). Global Prevalence of Chronic Kidney Disease - A Systematic Review and Meta-Analysis. *PLoS One*, 11(7), e0158765.
- Hodeify, R., Megyesi, J., Tarcsafalvi, A., Mustafa, H. I., Hti Lar Seng, N. S., & Price, P. M. (2013). Gender differences control the susceptibility to ER stress-induced acute kidney injury. *Am J Physiol Renal Physiol*, 304(7), F875-882.
- Hoffmann, S., Podlich, D., Hahnel, B., Kriz, W., & Gretz, N. (2004). Angiotensin II type 1 receptor overexpression in podocytes induces glomerulosclerosis in transgenic rats. *J Am Soc Nephrol*, 15(6), 1475-1487.
- Hosoi, T., Korematsu, K., Horie, N., Suezawa, T., Okuma, Y., Nomura, Y., & Ozawa, K. (2012). Inhibition of casein kinase 2 modulates XBP1-GRP78 arm of unfolded protein responses in cultured glial cells. *PLoS One*, 7(6), e40144.
- Hossain, G. S., van Thienen, J. V., Werstuck, G. H., Zhou, J., Sood, S. K., Dickhout, J. G., . . . Austin, R. C. (2003). TDAG51 is induced by homocysteine, promotes detachment-mediated programmed cell death, and contributes to the development of atherosclerosis in hyperhomocysteinemia. *J Biol Chem*, 278(32), 30317-30327.
- Huang, L., Zhang, R., Wu, J., Chen, J., Grosjean, F., Satlin, L. H., . . . Zheng, F. (2011). Increased susceptibility to acute kidney injury due to endoplasmic reticulum stress in mice lacking tumor necrosis factor-alpha and its receptor 1. *Kidney Int*, 79(6), 613-623.
- Humphreys, B. D., Lin, S.-L., Kobayashi, A., Hudson, T. E., Nowlin, B. T., Bonventre, J. V., . . . Duffield, J. S. (2010). Fate tracing reveals the pericyte and not epithelial origin of myofibroblasts in kidney fibrosis. *Am J Pathol*, 176(1), 85-97.

- Hye Khan, M. A., Neckar, J., Manthati, V., Errabelli, R., Pavlov, T. S., Staruschenko, A., . . . Imig, J. D. (2013). Orally active epoxyeicosatrienoic acid analog attenuates kidney injury in hypertensive Dahl salt-sensitive rat. *Hypertension*, *62*(5), 905-913.
- Inazaki, K., Kanamaru, Y., Kojima, Y., Sueyoshi, N., Okumura, K., Kaneko, K., . . . Nakao, A. (2004). Smad3 deficiency attenuates renal fibrosis, inflammation, and apoptosis after unilateral ureteral obstruction. *Kidney Int*, *66*(2), 597-604.
- Inden, M., Kitamura, Y., Takeuchi, H., Yanagida, T., Takata, K., Kobayashi, Y., . . . Shimohama, S. (2007). Neurodegeneration of mouse nigrostriatal dopaminergic system induced by repeated oral administration of rotenone is prevented by 4-phenylbutyrate, a chemical chaperone. *J Neurochem*, *101*(6), 1491-1504.
- Ingle, E., & Hemmings, B. A. (1994). Pleckstrin homology (PH) domains in signal transduction. *J Cell Biochem*, *56*(4), 436-443.
- Intengan, H. D., & Schiffrin, E. L. (2000). Structure and mechanical properties of resistance arteries in hypertension: role of adhesion molecules and extracellular matrix determinants. *Hypertension*, *36*(3), 312-318.
- Iwano, M., Plieth, D., Danoff, T. M., Xue, C., Okada, H., & Neilson, E. G. (2002). Evidence that fibroblasts derive from epithelium during tissue fibrosis. *J Clin Invest*, *110*(3), 341-350.
- Jatoi, N. A., Jerrard-Dunne, P., Feely, J., & Mahmud, A. (2007). Impact of smoking and smoking cessation on arterial stiffness and aortic wave reflection in hypertension. *Hypertension*, *49*(5), 981-985.
- Kang, K. T., Sullivan, J. C., Sasser, J. M., Imig, J. D., & Pollock, J. S. (2007). Novel nitric oxide synthase--dependent mechanism of vasorelaxation in small arteries from hypertensive rats. *Hypertension*, *49*(4), 893-901.
- Kassan, M., Galan, M., Partyka, M., Saifudeen, Z., Henrion, D., Trebak, M., & Matrougui, K. (2012). Endoplasmic reticulum stress is involved in cardiac damage and vascular endothelial dysfunction in hypertensive mice. *Arterioscler Thromb Vasc Biol*, *32*(7), 1652-1661.
- Kawakami, T., Inagi, R., Wada, T., Tanaka, T., Fujita, T., & Nangaku, M. (2010). Indoxyl sulfate inhibits proliferation of human proximal tubular cells via endoplasmic reticulum stress. *Am J Physiol Renal Physiol*, *299*(3), F568-F576.
- Kim, S. R., Kim, D. I., Kang, M. R., Lee, K. S., Park, S. Y., Jeong, J. S., & Lee, Y. C. (2013). Endoplasmic reticulum stress influences bronchial asthma pathogenesis by modulating nuclear factor kappaB activation. *J Allergy Clin Immunol*, *132*(6), 1397-1408.

- Kimball, S. R. (1999). Eukaryotic initiation factor eIF2. *Int J Biochem Cell Biol*, 31(1), 25-29.
- Kimura, G., & Brenner, B. M. (1997). Implications of the linear pressure-natriuresis relationship and importance of sodium sensitivity in hypertension. *J Hypertens*, 15(10), 1055-1061.
- Kinugasa, F., Noto, T., Matsuoka, H., Urano, Y., Sudo, Y., Takakura, S., & Mutoh, S. (2010). Prevention of renal interstitial fibrosis via histone deacetylase inhibition in rats with unilateral ureteral obstruction. *Transpl Immunol*, 23(1-2), 18-23.
- Kunnen, S. J., Leonhard, W. N., Semeins, C., Hawinkels, L., Poelma, C., Ten Dijke, P., . . . Peters, D. J. M. (2017). Fluid shear stress-induced TGF-beta/ALK5 signaling in renal epithelial cells is modulated by MEK1/2. *Cell Mol Life Sci*, 74(12), 2283-2298.
- LeBleu, V. S., Taduri, G., O'Connell, J., Teng, Y., Cooke, V. G., Woda, C., . . . Kalluri, R. (2013). Origin and function of myofibroblasts in kidney fibrosis. *Nat Med*, 19(8), 1047-1053.
- Lee, A. S. (2001). The glucose-regulated proteins: stress induction and clinical applications. *Trends Biochem Sci*, 26(8), 504-510.
- Levey, A. S., Bosch, J. P., Lewis, J. B., Greene, T., Rogers, N., & Roth, D. (1999). A more accurate method to estimate glomerular filtration rate from serum creatinine: a new prediction equation. Modification of Diet in Renal Disease Study Group. *Ann Intern Med*, 130(6), 461-470.
- Levey, A. S., & Coresh, J. (2012). Chronic kidney disease. *Lancet*, 379(9811), 165-180.
- Li, Y., Kang, Y. S., Dai, C., Kiss, L. P., Wen, X., & Liu, Y. (2008). Epithelial-to-mesenchymal transition is a potential pathway leading to podocyte dysfunction and proteinuria. *Am J Pathol*, 172(2), 299-308.
- Liang, B., & Leenen, F. H. (2008). Prevention of salt-induced hypertension and fibrosis by AT1-receptor blockers in Dahl S rats. *J Cardiovasc Pharmacol*, 51(5), 457-466.
- Liang, B., Wang, S., Wang, Q., Zhang, W., Viollet, B., Zhu, Y., & Zou, M. H. (2013). Aberrant endoplasmic reticulum stress in vascular smooth muscle increases vascular contractility and blood pressure in mice deficient of AMP-activated protein kinase-alpha2 in vivo. *Arterioscler Thromb Vasc Biol*, 33(3), 595-604.
- Lin, C. F., Kuo, Y. T., Chen, T. Y., & Chien, C. T. (2016). Quercetin-Rich Guava (*Psidium guajava*) Juice in Combination with Trehalose Reduces Autophagy,

Apoptosis and Pyroptosis Formation in the Kidney and Pancreas of Type II Diabetic Rats. *Molecules*, 21(3), 334.

- Lindenmeyer, M. T., Rastaldi, M. P., Ikehata, M., Neusser, M. A., Kretzler, M., Cohen, C. D., & Schlondorff, D. (2008). Proteinuria and hyperglycemia induce endoplasmic reticulum stress. *J Am Soc Nephrol*, 19(11), 2225-2236.
- Liu, Q. F., Ye, J. M., Deng, Z. Y., Yu, L. X., Sun, Q., & Li, S. S. (2015). Ameliorating effect of Klotho on endoplasmic reticulum stress and renal fibrosis induced by unilateral ureteral obstruction. *Iran J Kidney Dis*, 9(4), 291-297.
- Liu, R., Barkhordarian, H., Emadi, S., Park, C. B., & Sierks, M. R. (2005). Trehalose differentially inhibits aggregation and neurotoxicity of beta-amyloid 40 and 42. *Neurobiol Dis*, 20(1), 74-81.
- Liu, S. H., Yang, C. C., Chan, D. C., Wu, C. T., Chen, L. P., Huang, J. W., . . . Chiang, C. K. (2016). Chemical chaperon 4-phenylbutyrate protects against the endoplasmic reticulum stress-mediated renal fibrosis in vivo and in vitro. *Oncotarget*, 7(16), 22116-22127.
- Liu, Y. (2010). New insights into epithelial-mesenchymal transition in kidney fibrosis. *J Am Soc Nephrol*, 21(2), 212-222.
- Loffing, J., Moyer, B. D., Reynolds, D., & Stanton, B. A. (1999). PBA increases CFTR expression but at high doses inhibits Cl(-) secretion in Calu-3 airway epithelial cells. *Am J Physiol*, 277(4 Pt 1), L700-708.
- Lovisa, S., LeBleu, V. S., Tampe, B., Sugimoto, H., Vадnagara, K., Carstens, J. L., . . . Kalluri, R. (2015). Epithelial-to-mesenchymal transition induces cell cycle arrest and parenchymal damage in renal fibrosis. *Nat Med*, 21(9), 998-1009.
- Luo, T., Chen, B., & Wang, X. (2015). 4-PBA prevents pressure overload-induced myocardial hypertrophy and interstitial fibrosis by attenuating endoplasmic reticulum stress. *Chem Biol Interact*, 242, 99-106.
- Ma, F. Y., Tesch, G. H., Flavell, R. A., Davis, R. J., & Nikolic-Paterson, D. J. (2007). MKK3-p38 signaling promotes apoptosis and the early inflammatory response in the obstructed mouse kidney. *Am J Physiol Renal Physiol*, 293(5), F1556-1563.
- Maggiorani, D., Dissard, R., Belloy, M., Saulnier-Blache, J. S., Casemayou, A., Ducasse, L., . . . Buffin-Meyer, B. (2015). Shear Stress-Induced Alteration of Epithelial Organization in Human Renal Tubular Cells. *PLoS One*, 10(7), e0131416.
- Makhija, L., Krishnan, V., Rehman, R., Chakraborty, S., Maity, S., Mabalirajan, U., . . . Agrawal, A. (2014). Chemical chaperones mitigate experimental asthma by

- attenuating endoplasmic reticulum stress. *Am J Respir Cell Mol Biol*, 50(5), 923-931.
- Mantelli, L., Amerini, S., & Ledda, F. (1995). Roles of nitric oxide and endothelium-derived hyperpolarizing factor in vasorelaxant effect of acetylcholine as influenced by aging and hypertension. *J Cardiovasc Pharmacol*, 25(4), 595-602.
- Marciniak, S. J., Yun, C. Y., Oyadomari, S., Novoa, I., Zhang, Y., Jungreis, R., . . . Ron, D. (2004). CHOP induces death by promoting protein synthesis and oxidation in the stressed endoplasmic reticulum. *Genes Dev*, 18(24), 3066-3077.
- Maschio, G., Alberti, D., Janin, G., Locatelli, F., Mann, J. F., Motolese, M., . . . Zucchelli, P. (1996). Effect of the angiotensin-converting-enzyme inhibitor benazepril on the progression of chronic renal insufficiency. The Angiotensin-Converting-Enzyme Inhibition in Progressive Renal Insufficiency Study Group. *N Engl J Med*, 334(15), 939-945.
- Matsusaka, T., Asano, T., Niimura, F., Kinomura, M., Shimizu, A., Shintani, A., . . . Ichikawa, I. (2010). Angiotensin receptor blocker protection against podocyte-induced sclerosis is podocyte angiotensin II type 1 receptor-independent. *Hypertension*, 55(4), 967-973.
- Mattson, D. L., Dwinell, M. R., Greene, A. S., Kwitek, A. E., Roman, R. J., Jacob, H. J., & Cowley, A. W., Jr. (2008). Chromosome substitution reveals the genetic basis of Dahl salt-sensitive hypertension and renal disease. *Am J Physiol Renal Physiol*, 295(3), F837-842.
- Metcalf, W. (2007). How does early chronic kidney disease progress? A background paper prepared for the UK Consensus Conference on early chronic kidney disease. *Nephrol Dial Transplant*, 22 Suppl 9, ix26-30.
- Meyer, T. W., & Hostetter, T. H. (2007). Uremia. *N Engl J Med*, 357(13), 1316-1325.
- Miller, A. C., Cohen, S., Stewart, M., Rivas, R., & Lison, P. (2011). Radioprotection by the histone deacetylase inhibitor phenylbutyrate. *Radiat Environ Biophys*, 50(4), 585-596.
- Mimori, S., Ohtaka, H., Koshikawa, Y., Kawada, K., Kaneko, M., Okuma, Y., . . . Hamana, H. (2013). 4-Phenylbutyric acid protects against neuronal cell death by primarily acting as a chemical chaperone rather than histone deacetylase inhibitor. *Bioorg Med Chem Lett*, 23(21), 6015-6018.
- Mimori, S., Okuma, Y., Kaneko, M., Kawada, K., Hosoi, T., Ozawa, K., . . . Hamana, H. (2012). Protective effects of 4-phenylbutyrate derivatives on the neuronal cell death and endoplasmic reticulum stress. *Biol Pharm Bull*, 35(1), 84-90.

- Minamino, T., & Kitakaze, M. (2010). ER stress in cardiovascular disease. *J Mol Cell Cardiol*, 48(6), 1105-1110.
- Mohammed-Ali, Z., Lu, C., Marway, M. K., Carlisle, R. E., Ask, K., Lukic, D., . . . Dickhout, J. G. (2017). Endoplasmic reticulum stress inhibition attenuates hypertensive chronic kidney disease through reduction in proteinuria. *Sci Rep*, 7, 41572.
- Montie, H. L., Kayali, F., Haezebrouck, A. J., Rossi, N. F., & Degracia, D. J. (2005). Renal ischemia and reperfusion activates the eIF 2 alpha kinase PERK. *Biochim Biophys Acta*, 1741(3), 314-324.
- Moreno, J. A., Halliday, M., Molloy, C., Radford, H., Verity, N., Axten, J. M., . . . Mallucci, G. R. (2013). Oral treatment targeting the unfolded protein response prevents neurodegeneration and clinical disease in prion-infected mice. *Sci Transl Med*, 5(206), 206ra138.
- Mori, T., Polichnowski, A., Glocka, P., Kaldunski, M., Ohsaki, Y., Liang, M., & Cowley, A. W., Jr. (2008). High perfusion pressure accelerates renal injury in salt-sensitive hypertension. *J Am Soc Nephrol*, 19(8), 1472-1482.
- Mori, Y., Ohyanagi, M., Koida, S., Ueda, A., Ishiko, K., & Iwasaki, T. (2006). Effects of endothelium-derived hyperpolarizing factor and nitric oxide on endothelial function in femoral resistance arteries of spontaneously hypertensive rats. *Hypertens Res*, 29(3), 187-195.
- Nagai, M. A. (2016). Pleckstrin homology-like domain, family A, member 1 (PHLDA1) and cancer. *Biomed Rep*, 4(3), 275-281.
- Nakaya, H., Sasamura, H., Mifune, M., Shimizu-Hirota, R., Kuroda, M., Hayashi, M., & Saruta, T. (2002). Prepubertal treatment with angiotensin receptor blocker causes partial attenuation of hypertension and renal damage in adult Dahl salt-sensitive rats. *Nephron*, 91(4), 710-718.
- Nguyen, N. T., Magno, C. P., Lane, K. T., Hinojosa, M. W., & Lane, J. S. (2008). Association of hypertension, diabetes, dyslipidemia, and metabolic syndrome with obesity: findings from the National Health and Nutrition Examination Survey, 1999 to 2004. *J Am Coll Surg*, 207(6), 928-934.
- Niederreiter, L., & Kaser, A. (2011). Endoplasmic reticulum stress and inflammatory bowel disease. *Acta Gastroenterol Belg*, 74(2), 330-333.
- Niki, T., Rombouts, K., De Bleser, P., De Smet, K., Rogiers, V., Schuppan, D., . . . Geerts, A. (1999). A histone deacetylase inhibitor, trichostatin A, suppresses myofibroblastic differentiation of rat hepatic stellate cells in primary culture. *Hepatology*, 29(3), 858-867.

- Nishiyama, A., Fukui, T., Fujisawa, Y., Rahman, M., Tian, R. X., Kimura, S., & Abe, Y. (2001). Systemic and regional hemodynamic responses to tempol in angiotensin II-infused hypertensive rats. *Hypertension*, *37*(1), 77-83.
- O'Bryan, G. T., & Hostetter, T. H. (1997). The renal hemodynamic basis of diabetic nephropathy. *Semin Nephrol*, *17*(2), 93-100.
- Ochodnický, P., Henning, R. H., Buikema, H. J., de Zeeuw, D., Provoost, A. P., & van Dokkum, R. P. (2010). Renal vascular dysfunction precedes the development of renal damage in the hypertensive Fawn-Hooded rat. *Am J Physiol Renal Physiol*, *298*(3), F625-633.
- Ofstad, J., & Iversen, B. M. (2005). Glomerular and tubular damage in normotensive and hypertensive rats. *Am J Physiol Renal Physiol*, *288*(4), F665-672.
- Oguchi, H., Sasamura, H., Shinoda, K., Morita, S., Kono, H., Nakagawa, K., . . . Itoh, H. (2014). Renal arteriolar injury by salt intake contributes to salt memory for the development of hypertension. *Hypertension*, *64*(4), 784-791.
- Okamoto, K., & Aoki, K. (1963). Development of a strain of spontaneously hypertensive rats. *Jpn Circ J*, *27*, 282-293.
- Oparil, S., Zaman, M. A., & Calhoun, D. A. (2003). Pathogenesis of hypertension. *Ann Intern Med*, *139*(9), 761-776.
- Oyadomari, S., & Mori, M. (2004). Roles of CHOP/GADD153 in endoplasmic reticulum stress. *Cell Death Differ*, *11*(4), 381-389.
- Palatini, P. (2012). Glomerular hyperfiltration: a marker of early renal damage in pre-diabetes and pre-hypertension. *Nephrol Dial Transplant*, *27*(5), 1708-1714.
- Pallet, N., Bouvier, N., Bendjallah, A., Rabant, M., Flinois, J. P., Hertig, A., . . . Anglicheau, D. (2008). Cyclosporine-induced endoplasmic reticulum stress triggers tubular phenotypic changes and death. *Am J Transplant*, *8*(11), 2283-2296.
- Papandreou, I., Denko, N. C., Olson, M., Van Melckebeke, H., Lust, S., Tam, A., . . . Koong, A. C. (2011). Identification of an Irelalpha endonuclease specific inhibitor with cytotoxic activity against human multiple myeloma. *Blood*, *117*(4), 1311-1314.
- Park, C. G., Lee, S. Y., Kandala, G., Lee, S. Y., & Choi, Y. (1996). A novel gene product that couples TCR signaling to Fas(CD95) expression in activation-induced cell death. *Immunity*, *4*(6), 583-591.
- Perlmutter, D. H. (2002). Chemical chaperones: a pharmacological strategy for disorders of protein folding and trafficking. *Pediatr Res*, *52*(6), 832-836.

- Pescatello, L. S., Franklin, B. A., Fagard, R., Farquhar, W. B., Kelley, G. A., Ray, C. A., & American College of Sports, M. (2004). American College of Sports Medicine position stand. Exercise and hypertension. *Med Sci Sports Exerc*, *36*(3), 533-553.
- Peti-Peterdi, J., & Harris, R. C. (2010). Macula densa sensing and signaling mechanisms of renin release. *J Am Soc Nephrol*, *21*(7), 1093-1096.
- Phuphanich, S., Baker, S. D., Grossman, S. A., Carson, K. A., Gilbert, M. R., Fisher, J. D., & Carducci, M. A. (2005). Oral sodium phenylbutyrate in patients with recurrent malignant gliomas: a dose escalation and pharmacologic study. *Neuro Oncol*, *7*(2), 177-182.
- Prunotto, M., Compagnone, A., Bruschi, M., Candiano, G., Colombatto, S., Bandino, A., . . . Ghiggeri, G. (2010). Endocellular polyamine availability modulates epithelial-to-mesenchymal transition and unfolded protein response in MDCK cells. *Lab Invest*, *90*(6), 929-939.
- Quan, S., & Bardwell, J. C. (2012). Chaperone discovery. *Bioessays*, *34*(11), 973-981.
- Rapp, J. P., & Dene, H. (1985). Development and characteristics of inbred strains of Dahl salt-sensitive and salt-resistant rats. *Hypertension*, *7*(3 Pt 1), 340-349.
- Reckelhoff, J. F., Zhang, H., & Granger, J. P. (1997). Decline in renal hemodynamic function in aging SHR: role of androgens. *Hypertension*, *30*(3 Pt 2), 677-681.
- Ren, Y., D'Ambrosio, M. A., Garvin, J. L., Peterson, E. L., & Carretero, O. A. (2014). Mechanism of impaired afferent arteriole myogenic response in Dahl salt-sensitive rats: role of 20-HETE. *Am J Physiol Renal Physiol*, *307*(5), F533-538.
- Rishikof, D. C., Ricupero, D. A., Liu, H., & Goldstein, R. H. (2004). Phenylbutyrate decreases type I collagen production in human lung fibroblasts. *J Cell Biochem*, *91*(4), 740-748.
- Ritz, E., & Orth, S. R. (1999). Nephropathy in patients with type 2 diabetes mellitus. *N Engl J Med*, *341*(15), 1127-1133.
- Rombouts, K., Niki, T., Greenwel, P., Vandermonde, A., Wielant, A., Hellemans, K., . . . Geerts, A. (2002). Trichostatin A, a histone deacetylase inhibitor, suppresses collagen synthesis and prevents TGF-beta(1)-induced fibrogenesis in skin fibroblasts. *Exp Cell Res*, *278*(2), 184-197.
- Ryan, M. J., Johnson, G., Kirk, J., Fuerstenberg, S. M., Zager, R. A., & Torok-Storb, B. (1994). HK-2: an immortalized proximal tubule epithelial cell line from normal adult human kidney. *Kidney Int*, *45*(1), 48-57.
- Sacks, F. M., Svetkey, L. P., Vollmer, W. M., Appel, L. J., Bray, G. A., Harsha, D., . . . Group, D. A.-S. C. R. (2001). Effects on blood pressure of reduced dietary sodium

- and the Dietary Approaches to Stop Hypertension (DASH) diet. DASH-Sodium Collaborative Research Group. *N Engl J Med*, 344(1), 3-10.
- Sakai, N., Wada, T., Yokoyama, H., Lipp, M., Ueha, S., Matsushima, K., & Kaneko, S. (2006). Secondary lymphoid tissue chemokine (SLC/CCL21)/CCR7 signaling regulates fibrocytes in renal fibrosis. *Proc Natl Acad Sci U S A*, 103(38), 14098-14103.
- Saw, S., Kale, S. L., & Arora, N. (2012). Serine protease inhibitor attenuates ovalbumin induced inflammation in mouse model of allergic airway disease. *PLoS One*, 7(7), e41107.
- Schnackenberg, C. G., Welch, W. J., & Wilcox, C. S. (1998). Normalization of blood pressure and renal vascular resistance in SHR with a membrane-permeable superoxide dismutase mimetic: role of nitric oxide. *Hypertension*, 32(1), 59-64.
- Schröder, M., & Kaufman, R. J. (2005). ER stress and the unfolded protein response. *Mutat Res*, 569(1-2), 29-63.
- Shi, J., Jiang, Q., Ding, X., Xu, W., Wang, D. W., & Chen, M. (2015). The ER stress-mediated mitochondrial apoptotic pathway and MAPKs modulate tachypacing-induced apoptosis in HL-1 atrial myocytes. *PLoS One*, 10(2), e0117567.
- Simonds, S. E., & Cowley, M. A. (2013). Hypertension in obesity: is leptin the culprit? *Trends Neurosci*, 36(2), 121-132.
- Spitler, K. M., Matsumoto, T., & Webb, R. C. (2013). Suppression of endoplasmic reticulum stress improves endothelium-dependent contractile responses in aorta of the spontaneously hypertensive rat. *Am J Physiol Heart Circ Physiol*, 305(3), H344-353.
- Spitler, K. M., & Webb, R. C. (2014). Endoplasmic reticulum stress contributes to aortic stiffening via proapoptotic and fibrotic signaling mechanisms. *Hypertension*, 63(3), e40-e45.
- Sprague Dawley outbred rat. (2017). *Research Models and Services*.
- Stevens, L. A., Coresh, J., Greene, T., & Levey, A. S. (2006). Assessing kidney function--measured and estimated glomerular filtration rate. *N Engl J Med*, 354(23), 2473-2483.
- Tanaka, M., Machida, Y., Niu, S., Ikeda, T., Jana, N. R., Doi, H., . . . Nukina, N. (2004). Trehalose alleviates polyglutamine-mediated pathology in a mouse model of Huntington disease. *Nat Med*, 10(2), 148-154.
- Tanjore, H., Cheng, D.-S., Degryse, A. L., Zoz, D. F., Abdolrasulnia, R., Lawson, W. E., & Blackwell, T. S. (2011). Alveolar epithelial cells undergo epithelial-to-

- mesenchymal transition in response to endoplasmic reticulum stress. *J Biol Chem*, 286(35), 30972-30980.
- Tanjore, H., Lawson, W. E., & Blackwell, T. S. (2013). Endoplasmic reticulum stress as a pro-fibrotic stimulus. *Biochim Biophys Acta*, 1832(7), 940-947.
- Tissue Expression of PHDLA1. (2017). Retrieved from <http://www.proteinatlas.org/ENSG00000139289-PHLDA1/tissue/primary+data>
- Ulianich, L., Garbi, C., Treglia, A. S., Punzi, D., Miele, C., Raciti, G. A., . . . Jeso, B. D. (2008). ER stress is associated with dedifferentiation and an epithelial-to-mesenchymal transition-like phenotype in PC C13 thyroid cells. *J Cell Sci*, 121(Pt 4), 477-486.
- Umareddy, I., Pluquet, O., Wang, Q. Y., Vasudevan, S. G., Chevet, E., & Gu, F. (2007). Dengue virus serotype infection specifies the activation of the unfolded protein response. *Virology*, 4, 91.
- Upagupta, C., Carlisle, R. E., & Dickhout, J. G. (2017). Analysis of the potency of various low molecular weight chemical chaperones to prevent protein aggregation. *Biochem Biophys Res Commun*, 486(1), 163-170.
- Wang, F. M., Chen, Y. J., & Ouyang, H. J. (2011). Regulation of unfolded protein response modulator XBP1s by acetylation and deacetylation. *Biochem J*, 433(1), 245-252.
- Wang, X. Z., Lawson, B., Brewer, J. W., Zinszner, H., Sanjay, A., Mi, L. J., . . . Ron, D. (1996). Signals from the stressed endoplasmic reticulum induce C/EBP-homologous protein (CHOP/GADD153). *Mol Cell Biol*, 16(8), 4273-4280.
- Wang, Z., do Carmo, J. M., Aberdein, N., Zhou, X., Williams, J. M., da Silva, A. A., & Hall, J. E. (2017). Synergistic Interaction of Hypertension and Diabetes in Promoting Kidney Injury and the Role of Endoplasmic Reticulum Stress. *Hypertension*, 69(5), 879-891.
- Wright, G., Noiret, L., Damink, S. W. M. O., & Jalan, R. (2011). Interorgan ammonia metabolism in liver failure: the basis of current and future therapies. *Liver Int*, 31(2), 163-175.
- Wu, J., Kraja, A. T., Oberman, A., Lewis, C. E., Ellison, R. C., Arnett, D. K., . . . Rao, D. C. (2005). A summary of the effects of antihypertensive medications on measured blood pressure. *Am J Hypertens*, 18(7), 935-942.
- Wu, J., Zhang, R., Torreggiani, M., Ting, A., Xiong, H., Striker, G. E., . . . Zheng, F. (2010a). Induction of diabetes in aged C57B6 mice results in severe nephropathy:

- an association with oxidative stress, endoplasmic reticulum stress, and inflammation. *Am J Pathol*, 176(5), 2163-2176.
- Wu, X., He, Y., Jing, Y., Li, K., & Zhang, J. (2010b). Albumin overload induces apoptosis in renal tubular epithelial cells through a CHOP-dependent pathway. *OMICS*, 14(1), 61-73.
- Xiao, C., Giacca, A., & Lewis, G. F. (2011). Sodium phenylbutyrate, a drug with known capacity to reduce endoplasmic reticulum stress, partially alleviates lipid-induced insulin resistance and beta-cell dysfunction in humans. *Diabetes*, 60(3), 918-924.
- Yam, G. H., Gaplovska-Kysela, K., Zuber, C., & Roth, J. (2007). Sodium 4-phenylbutyrate acts as a chemical chaperone on misfolded myocilin to rescue cells from endoplasmic reticulum stress and apoptosis. *Invest Ophthalmol Vis Sci*, 48(4), 1683-1690.
- Yang, H. C., Zuo, Y., & Fogo, A. B. (2010). Models of chronic kidney disease. *Drug Discov Today Dis Models*, 7(1-2), 13-19.
- Yang, J., Zheng, W., Wang, Q., Lara, C., Hussein, S., & Chen, X. Z. (2013). Translational up-regulation of polycystic kidney disease protein PKD2 by endoplasmic reticulum stress. *FASEB J*, 27(12), 4998-5009.
- Yang, J. R., Yao, F. H., Zhang, J. G., Ji, Z. Y., Li, K. L., Zhan, J., . . . He, Y. N. (2014). Ischemia-reperfusion induces renal tubule pyroptosis via the CHOP-caspase-11 pathway. *Am J Physiol Renal Physiol*, 306(1), F75-84.
- Yao, M., Chen, H., & Yan, J. (2015). Thermodynamics of force-dependent folding and unfolding of small protein and nucleic acid structures. *Integr Biol (Camb)*, 7(10), 1154-1160.
- Yoneda, T., Imaizumi, K., Oono, K., Yui, D., Gomi, F., Katayama, T., & Tohyama, M. (2001). Activation of caspase-12, an endoplasmic reticulum (ER) resident caspase, through tumor necrosis factor receptor-associated factor 2-dependent mechanism in response to the ER stress. *J Biol Chem*, 276(17), 13935-13940.
- Yoshikawa, M., Hishikawa, K., Marumo, T., & Fujita, T. (2007). Inhibition of histone deacetylase activity suppresses epithelial-to-mesenchymal transition induced by TGF-beta1 in human renal epithelial cells. *J Am Soc Nephrol*, 18(1), 58-65.
- Young, C. N., Cao, X., Guraju, M. R., Pierce, J. P., Morgan, D. A., Wang, G., . . . Davisson, R. L. (2012). ER stress in the brain subfornical organ mediates angiotensin-dependent hypertension. *J Clin Invest*, 122(11), 3960-3964.

- Yu, H. C., Burrell, L. M., Black, M. J., Wu, L. L., Dilley, R. J., Cooper, M. E., & Johnston, C. I. (1998). Salt induces myocardial and renal fibrosis in normotensive and hypertensive rats. *Circulation*, *98*(23), 2621-2628.
- Zeisberg, E. M., Potenta, S. E., Sugimoto, H., Zeisberg, M., & Kalluri, R. (2008). Fibroblasts in kidney fibrosis emerge via endothelial-to-mesenchymal transition. *J Am Soc Nephrol*, *19*(12), 2282-2287.
- Zeisberg, M., & Duffield, J. S. (2010). Resolved: EMT produces fibroblasts in the kidney. *J Am Soc Nephrol*, *21*(8), 1247-1253.
- Zhang, J., Fan, Y., Zeng, C., He, L., & Wang, N. (2016). Tauroursodeoxycholic Acid Attenuates Renal Tubular Injury in a Mouse Model of Type 2 Diabetes. *Nutrients*, *8*(10).
- Zhao, W., Huang, X., Zhang, L., Yang, X., Wang, L., Chen, Y., . . . Wu, G. (2016). Penethylidine Hydrochloride Pretreatment Ameliorates Rhabdomyolysis-Induced AKI by Activating the Nrf2/HO-1 Pathway and Alleviating Endoplasmic Reticulum Stress in Rats. *PLoS One*, *11*(3), e0151158.

APPENDICES

APPENDIX 1 – Copyright permissions

American Physiology Society

Copyright permission policy:

<http://www.the-aps.org/mm/Publications/Info-For-Authors/Copyright>

These guidelines apply to the reuse of articles, figures, charts, and photos in the *American Journal of Physiology Renal Physiology*.

Posting of the accepted or final version of articles or parts of articles is restricted and subject to the following conditions: APS permits whole published articles to be reproduced without charge in dissertations and posted to thesis repositories. Full citation is required.

PLOS ONE

Copyright permission policy:

<https://www.plos.org/license>

PLOS ONE is an open access journal.

PLOS applies the Creative Commons Attribution license to works we publish. Under this license, authors retain ownership of the copyright for their content, but they allow anyone to download, reuse, reprint, modify, distribute and/or copy the content as long as the original authors and source are cited.

Royal College of General Practitioners

Permission has been granted by the Royal College of General Practitioners for the reuse of a figure from “Where now for proteinuria testing in chronic kidney disease? Good evidence can clarify a potentially confusing message” in the *British Journal of General Practice*. Further information can be found on page 257.

Wolters Kluwer

Copyright permission policy:

http://journals.lww.com/jhypertension/_layouts/15/1033/oaks.journals/rightsandpermissions.aspx

These guidelines apply to the reuse of articles, figures, charts, and photos in the *Journal of Hypertension*.

Please note that when requesting to use a full article in a thesis, permission is not granted for the final published article to be used. Only the final peer-reviewed article may be used. You do not need a permission license to use your final peer-reviewed manuscript.

Wolters Kluwer has granted permission to reuse two excerpts and one figure from “Interrelationship between cardiac hypertrophy, heart failure, and chronic kidney disease: endoplasmic reticulum stress as a mediator of pathogenesis” in *Circulation Research*. A copy of this license can be found on page 259.

Elsevier

Copyright permission policy:

<https://www.elsevier.com/about/our-business/policies/copyright/permissions>

These guidelines apply to the reuse of articles, figures, charts, and photos in *Biochemical and Biophysical Research Communications* and the *Journal of Pharmacological Reports*.

As a general rule, permission should be sought from the rights holder to reproduce any substantial part of a copyrighted work. This includes any text, illustrations, charts, tables, photographs, or other material from previously published sources. Authors can include their articles in full or in part in a thesis or dissertation for non-commercial purposes.

Elsevier has granted permission to reproduce an excerpt from “Animal models of kidney disease” in *Animal Models for the Study of Human Disease*. A copy of this permission can be found on page 262.

6/29/2017

Copyright Clearance Center



Confirmation Number: 11653042
Order Date: 06/28/2017

Customer Information

Customer: Rachel Carlisle
Account Number: 3001162801
Organization: Rachel Carlisle
Email: carlsre@mcmaster.ca
Phone: +1 (289) 808-5934
Payment Method: Invoice

This is not an invoice**Order Details**

The British journal of general practice : the journal of the Royal College of General Practitioners

Billing Status: N/A

Order detail ID: 70587722	Permission Status: Granted
ISSN: 1478-5242	Permission type: Republish or display content
Publication Type: e-Journal	Type of use: Republish in a thesis/dissertation
Volume:	Order License Id: 4137770849864
Issue:	
Start page:	Requestor type: Not-for-profit entity
Publisher: ROYAL COLLEGE OF GENERAL PRACTITIONERS	Format: Print, Electronic
Author/Editor: Royal College of General Practitioners	Portion: chart/graph/table/figure
	Number of charts/graphs/tables/figures: 1
	Title or numeric reference of the portion(s): British Journal of General Practice
	Title of the article or chapter the portion is from: Where now for proteinuria testing in chronic kidney disease? Good evidence can clarify a potentially confusing message
	Editor of portion(s): N/A
	Author of portion(s): SDS Fraser, PJ Roderick, MW Taal
	Volume of serial or monograph: 66
	Page range of portion: 216
	Publication date of portion: April 2016
	Rights for: Main product
	Duration of use: Life of current edition
	Creation of copies for the disabled: no
	With minor editing privileges: no
	For distribution to: Canada

<https://www.copyright.com/printOrder.do?id=11653042>

1/2

6/29/2017

Copyright Clearance Center

In the following language(s)	Original language of publication
With incidental promotional use	no
Lifetime unit quantity of new product	Up to 499
Made available in the following markets	education/professional
The requesting person/organization	Rachel Carlisle
Order reference number	
Author/Editor	Rachel Carlisle
The standard identifier of New Work	N/A
Title of New Work	Inhibiting protein aggregation prevents the development of hypertensive nephrosclerosis
Publisher of New Work	McMaster University
Expected publication date	Aug 2017
Estimated size (pages)	250

Note: This item was invoiced separately through our **RightsLink service**. [More info](#)

\$ 0.00

Total order items: 1

Order Total: \$0.00

[About Us](#) | [Privacy Policy](#) | [Terms & Conditions](#) | [Pay an Invoice](#)

Copyright 2017 Copyright Clearance Center



This permission letter is issued as of 27 June 2017 by Wolters Kluwer, a corporation organized under the laws of the State of New York and having as one of its principal offices a location at Two Commerce Square 2001 Market Street Philadelphia, PA 19103 USA (referred to in this Agreement as "LICENSOR") for (Referred to in this agreement as "LICENSEE") listed below:

LICENSEE

Rachel Carlisle
50 Charlton Ave East
Hamilton, ON
Canada
L8N 4A6

CONTENT

Wolters Kluwer Content:	Dickhout JG, Carlisle RE, Austin RC, Kitakaze M. "Interrelationship between cardiac hypertrophy, heart failure, and chronic kidney disease: endoplasmic reticulum stress as a mediator of pathogenesis." <i>Circulation Research</i> . 2011;108:629-642.
Material Used:	<ul style="list-style-type: none"> • 2 excerpts: "Synthesis of proteins through the endoplasmic reticulum" and "Progression of chronic kidney disease through ER stress." • Figure 1
Request Number:	501279720 (501279708)
Invoice Number:	D6358229

PERMISSION OF THE ABOVE CONTENT IS RESTRICTED TO:

1. Purpose of the reuse:	Thesis/Disseration
2. Format:	Print and Electronic (Institutional Repository only)
3. New Reuse:	"Inhibiting protein aggregation prevents the development of hypertensive nephrosclerosis."
4. Requestor Type:	Academic
5. Additional Permissions:	Permission is granted for reuse of the 2 excerpts listed above as gratis. The fee provided below is for permission to use Figure 1.

ROYALTIES

6. The LICENSEE shall pay to the LICENSOR the following for this permission request: **\$75.00 USD**
7. Any monies due from the LICENSEE to the LICENSOR shall be paid as follows: **Bank Details Below**

Bank Address: Bank of America Account # 5800956913 Wolters Kluwer Health 135 S. LaSalle Street Chicago, IL 60603	Routing and Codes: ACH/EFT/EDI - ABA Routing # 071000039 Domestic Wire Transfers - ABA Routing #026009593 International Wire Transfers - Swift Code BOFAUS3NXXX Tax ID: 13-2932696
--	--

WARRANTIES AND OBLIGATIONS

- 9) LICENSOR further represents and warrants that, to the best of its knowledge and belief, LICENSEE's contemplated use of the Content as represented to LICENSOR does not infringe any valid rights to any third party.

BREACH

- 10) If LICENSEE fails to comply with any provisions of this agreement, LICENSOR may serve written notice of breach of LICENSEE and, unless such breach is fully cured within fifteen (15) days from the receipt of notice by LICENSEE, LICENSOR may thereupon, at its option, serve notice of cancellation on LICENSEE, whereupon this Agreement shall immediately terminate.

TERM

11)

- a) Permission is granted for a **one time use only**. Rights herein do not apply to future reproductions, editions, revisions, or other derivative works. This Permission shall be effective as of the date of execution by the Parties for the maximum period of **12 months** which will end on 27 June 2018 and should be renewed after the term expires unless the permission is for the reuse in a journal or a book. In such cases the validity of this agreement should be the life of the book edition/journal issue.
- b) A credit line will be prominently placed and include: **For books** – the author(s), title of book, edition, copyright holder, year of publication; **For journals** – the author(s), titles of article, title of journal, volume number, issue number and inclusive pages and website URL to the journal page. Where a learned society holds the copyright, the details of that society must be included in the credit line and Wolters Kluwer should be shown as the Publisher.
- c) The requestor warrants that the material shall not be used in any manner which may be considered derogatory to the title, content, or authors of the material, or to Wolters Kluwer.
- d) You hereby indemnify and hold harmless Wolters Kluwer and their respective officers, directors, employees and agents, from and against any and all claims, costs, proceeding or demands arising out of your unauthorized use of the Licensed Material.
- e) Permission granted is non-exclusive, and is valid throughout the world in the English language and the languages specified in your original request.
- f) Wolters Kluwer cannot supply the requestor with the original artwork, electronic files or a "clean copy."
- g) Permission is valid if the borrowed material is original to a Wolters Kluwer imprints (Lippincott Williams & Wilkins, Lippincott-Raven Publishers, Williams & Wilkins, Lea & Febiger, Harwal, Rapid Science, Little Brown & Company, Harper & Row Medical, American Journal of Nursing Co, and Urban & Schwarzenberg - English Language, Raven Press, Paul Hoeber, Springhouse, Ovid).
- h) If you opt not to use the material requested above, please notify Wolters Kluwer within 90 days of the original invoice date.
- i) This permission does not apply to images/tables/content that are credited to publications other than Wolters Kluwer or its Societies. For images credited to non-Wolters Kluwer books or journals, you will need to obtain permission from the source referenced in the figure or table legend or credit line before making any use of the image(s), table(s) or other content.
- j) With the exception of text size or color, no Wolters Kluwer material is permitted to be modified or adapted without publisher approval.
- k) Adaptations are protected by copyright, so if you would like to reuse material that we have adapted from another source, you will need not only our permission, but the permission of the right holder of the original material. The adaptation should be credited as follows: Adapted with permission from Wolters Kluwer: Book author, title, year of publication or Journal name, article author, title, reference citation, year of publication. Please note that modifications are permitted on occasional basis only and permissions requests must be sought by Wolters Kluwer.
- l) While you may exercise the rights licensed immediately upon issuance of the license at the end of the licensing process for the transaction, provided that you have disclosed complete and accurate details of your proposal use, no license is finally effective unless and until full payment is received from you (by the publisher). If full payment is not received on a timely basis, then any license preliminarily granted shall be deemed automatically revoked and shall be void as if never granted. Further, in the event that you breach any of these terms and conditions or any of other Wolters Kluwer's billing and payment terms and conditions, the license is automatically revoked and shall be void as if never granted. Use of materials as described in a revoked license, as well as any use of the materials beyond the scope of an unrevoked license, may constitute copyright infringement and publisher reserves the right to take any and all action to protect its copyright in the materials.
- m) If the permission fee for the requested use of our material has been waived in this instance, please be advised that future requests for Wolters Kluwer materials may incur a fee.
- n) For STM Signatories Only: Any permission granted for a particular edition will apply also to subsequent editions and for editions in other languages, provided such editions are for the work as a whole in situ and does not involve the separate exploitation of the permitted illustrations or excerpts. Please view: [STM Permissions Guidelines](#)

- o) For Journals Only:
- i) Please note that articles in the ahead-of-print stage of publication can be cited and the content may be re-used by including the date of access and the unique DOI number. Any final changes in manuscripts will be made at the time of print publication and will be reflected in the final electronic version of the issue. **Disclaimer:** Articles appearing in the Published Ahead-of-Print section have been peer-reviewed and accepted for publication in the relevant journal and posted online before print publication. Articles appearing as publish ahead-of-print may contain statements, opinions, and information that have errors in facts, figures, or interpretation. Accordingly, Wolters Kluwer, the editors and authors and their respective employees are not responsible or liable for the use of any such inaccurate or misleading data, opinion or information contained in the articles in this section.
 - ii) Where a journal is being published by a learned society, the details of that society must be included in the credit line.
 - (1) The following statement needs to be added when reprinting the material in Open Access journals only: “promotional and commercial use of the material in print, digital or mobile device format is prohibited without the permission from the publisher Wolters Kluwer. Please contact healthpermissions@wolterskluwer.com for further information.”
 - (2) Exceptions: In case **Diseases of the Colon & Rectum, Plastic Reconstructive Surgery, The Green Journal, Critical Care Medicine, Pediatric Critical Care Medicine, the American Heart Association Publications and the American Academy of Neurology** the following guideline applies: no drug/trade name or logo can be included in the same page as the material re-used.
 - iii) If granted permissions to republish a full text article in another language, Wolters Kluwer should be sent a copy of the translated PDF. Please include disclaimer below on all translated copies:
 - (a) ***Wolters Kluwer and its Societies take no responsibility for the accuracy of the translation from the published English original and are not liable for any errors which may occur.***
 - iv) Reuse of full text articles in English is prohibited.

MISCELLANEOUS

- 12) **Assignment:** License conveyed hereunder by the LICENSOR shall not be assigned or granted in any manner conveyed to any third party by the LICENSEE without the consent in writing to the LICENSOR.
- 13) **Governing Law:** The laws of The State of New York shall govern interpretation of this Agreement and all rights and liabilities arising hereunder.
- 14) **Unlawful:** If any provision of this Agreement shall be found unlawful or otherwise legally unenforceable, all other conditions and provisions of this Agreement shall remain in full force and effect.

AS WITNESS THE HAND AND SEALS OF THE PARTIES HERETO:



27 June 2017

Representative Signature Date
 Andrew Richardson
 Wolters Kluwer VP of Business Development – Health Learning Research & Practice Division




Dear Rachel Carlisle

We hereby grant you permission to reproduce the material detailed below at no charge **in your thesis, in print and on MacSphere** and subject to the following conditions:

1. If any part of the material to be used (for example, figures) has appeared in our publication with credit or acknowledgement to another source, permission must also be sought from that source. If such permission is not obtained then that material may not be included in your publication/copies.
2. Suitable acknowledgment to the source must be made, either as a footnote or in a reference list at the end of your publication, as follows:

"This article was published in Publication title, Vol number, Author(s), Title of article, Page Nos, Copyright Elsevier (or appropriate Society name) (Year)."
3. Your thesis may be submitted to your institution in either print or electronic form.
4. Reproduction of this material is confined to the purpose for which permission is hereby given.
5. This permission is granted for non-exclusive world **English** rights only. For other languages please reapply separately for each one required. Permission excludes use in an electronic form other than as specified above. Should you have a specific electronic project in mind please reapply for permission.
6. This includes permission for the Library and Archives of Canada to supply single copies, on demand, of the complete thesis. Should your thesis be published commercially, please reapply for permission.

Yours sincerely



Jennifer Jones
Permissions Specialist

Elsevier Limited, a company registered in England and Wales with company number 1982084, whose registered office is The Boulevard, Langford Lane, Kidlington, Oxford, OX5 1GB, United Kingdom.

Title: Ms Rachel Carlisle

Institute/company: McMaster University
Address: 50 Charlton Ave East
Post/Zip Code: L8N 4A6
City: Hamilton
State/Territory: Ontario
Country: Canada
Telephone: 2898085934
Email: carlisre@mcmaster.ca

Type of Publication: Book

Book Title: Animal models for the study of human disease
Book ISBN: 978-0-12-809468-6
Book Author: Zahraa Mohammed-Ali, Rachel E. Carlisle, Samera Nademi, Jeffrey G. Dickhout
Book Year: 2017
Book Pages: 379 to 416
Book Chapter number: 16
Book Chapter title: Animal models of kidney disease

I would like to use: Excerpt(s)

Quantity of material:

Excerpts: 265

Are you the author of the Elsevier material? Yes

If not, is the Elsevier author involved? Yes

If yes, please provide details of how the Elsevier author is involved: I am the author, but despite choosing "yes" for that question, I also had to answer this question. So... the Elsevier author is involved with my project, because the author is me.

In what format will you use the material? Print and Electronic

Will you be translating the material? No

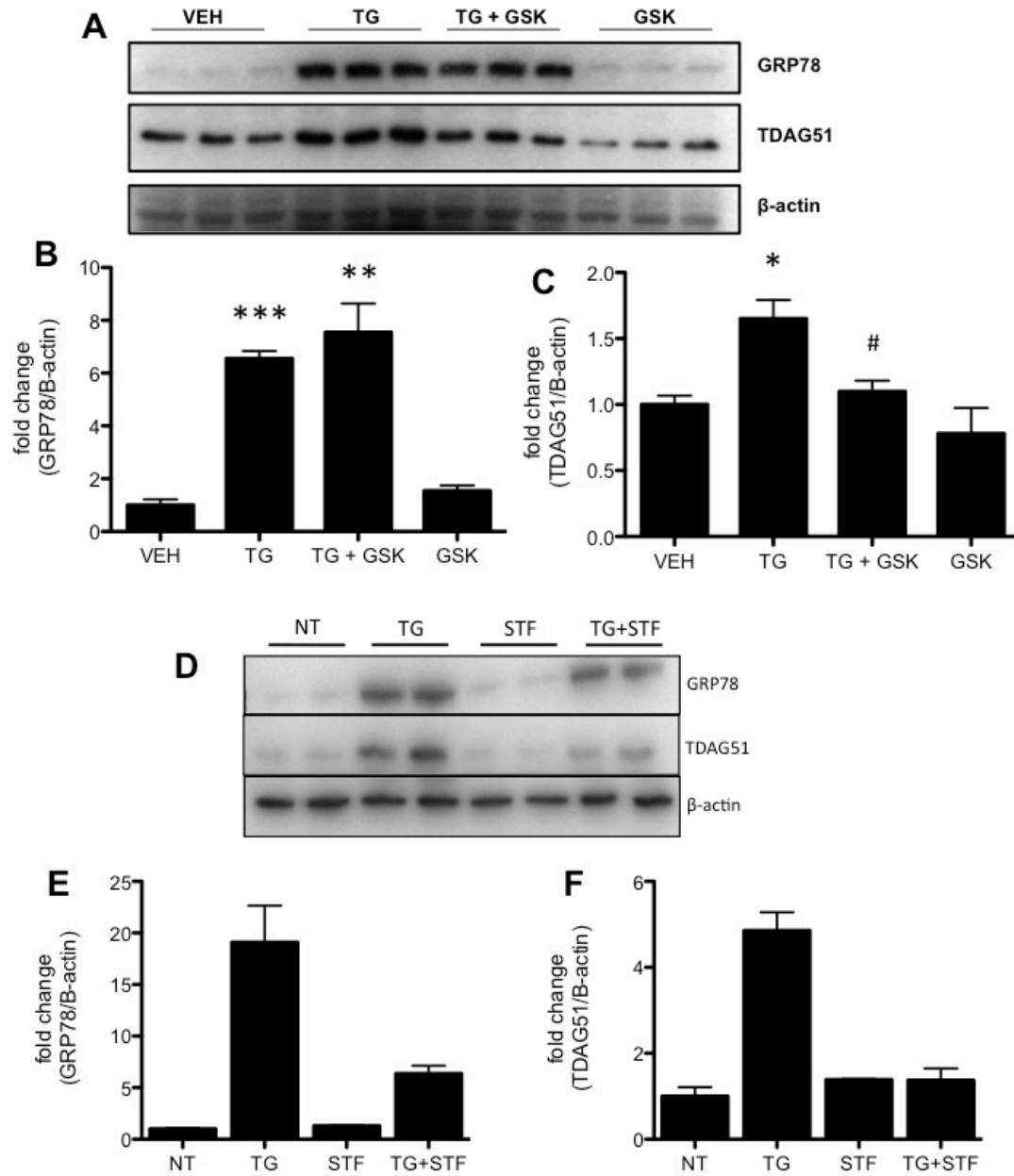
If yes, specify language:

Information about proposed use: Reuse in a thesis/dissertation

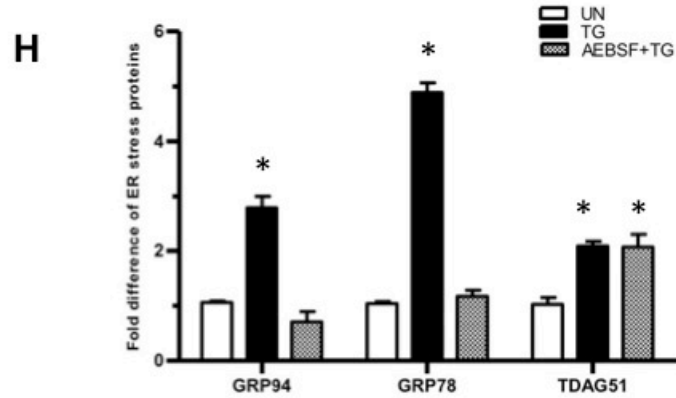
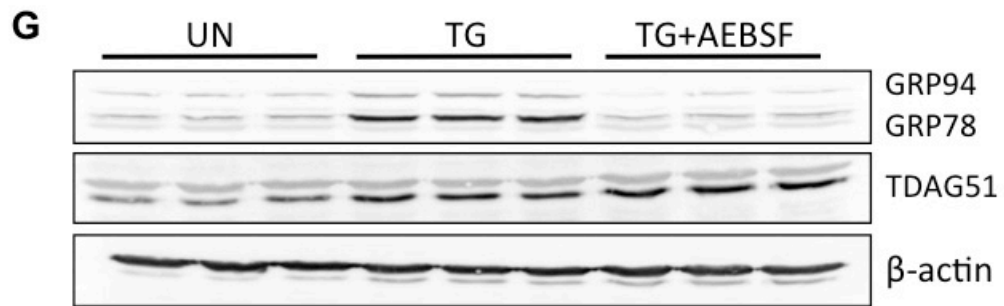
Proposed use text: McMaster University requires grant of an irrevocable, non-exclusive license to McMaster University and to Library and Archives Canada to reproduce the material as part of the thesis

Additional Comments / Information:

APPENDIX 2 – Supplementary figure 1 (1/2).

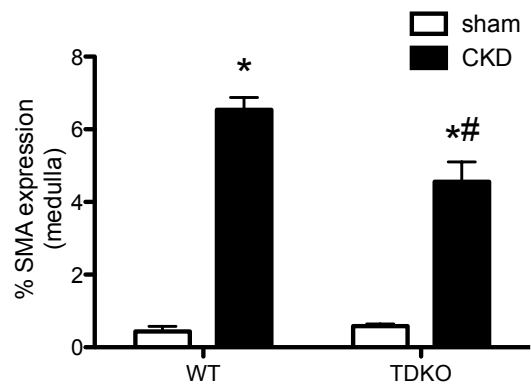
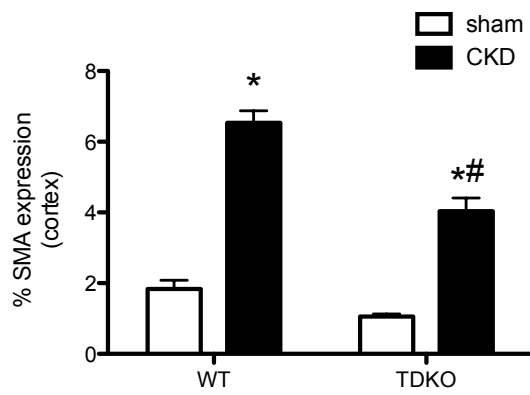
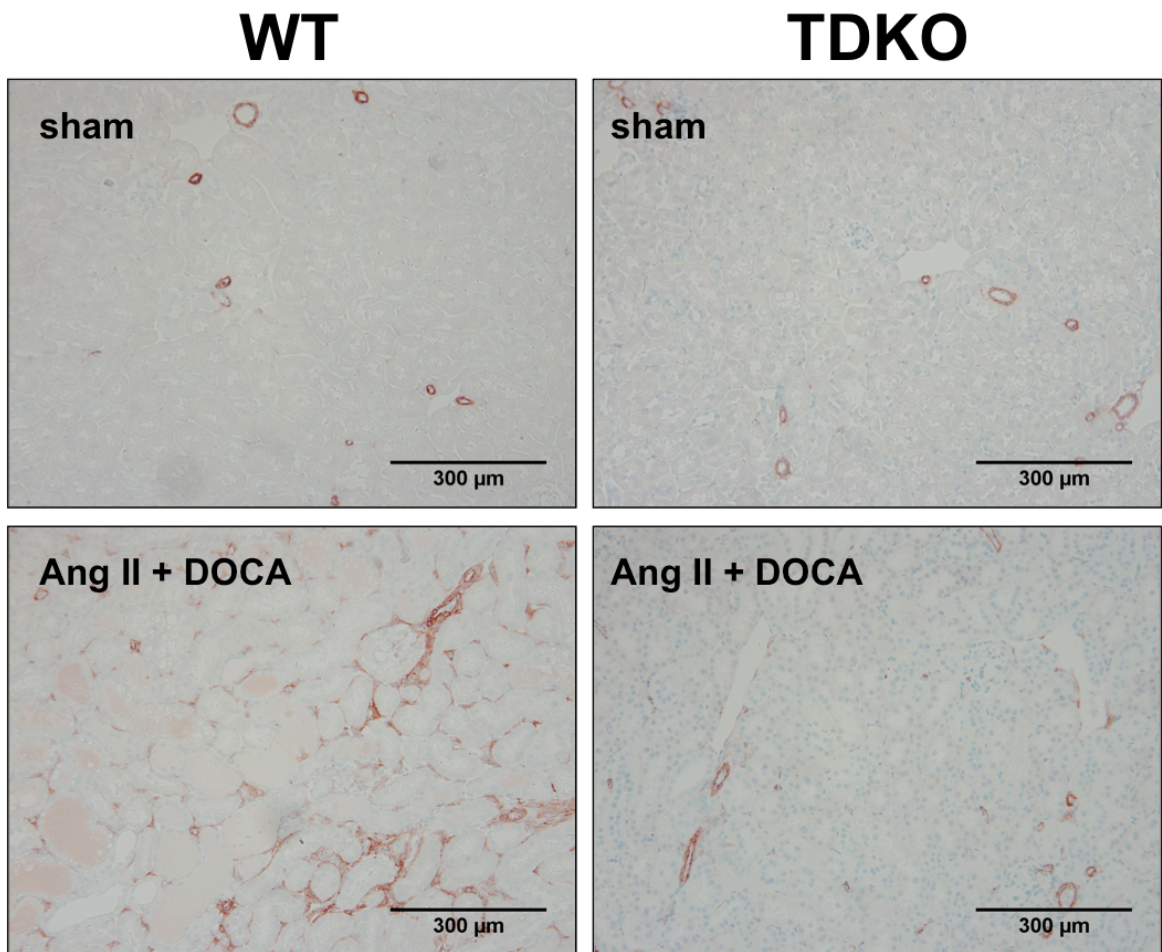


Supplementary figure 1 (2/2).



Supplementary figure 1. TDAG51 is upregulated in the PERK and IRE1 pathways of the unfolded protein response, but not the ATF6 pathway. Human proximal tubular epithelial (HK-2) cells were treated with the ER stress inducer thapsigargin (TG) in the presence or absence of an inhibitor of an unfolded protein response pathway, and subsequently underwent western blotting and quantification. (A) Cells were treated with TG with or without the PERK phosphorylation inhibitor GSK-2606414 (GSK). Quantification demonstrates increased GRP78 (B) and CHOP (C) in response to TG treatment. GSK inhibited CHOP expression. (D) Cells were treated with TG with or without the IRE1 inhibitor STF-083010 (STF). STF reduced GRP78 (E) and TDAG51 (F) expression. (G) Cells were treated with TG in the presence or absence of the ATF6 inhibitor AEBSF. (H) Expression of ER stress markers GRP78 and GRP94 were reduced with AEBSF, while TDAG51 was not (unpublished data).

Supplementary figure 2.



Supplementary figure 2. TDAG51 knockout reduces renal interstitial fibrosis in a model of chronic kidney disease. Wild type (WT) and TDAG51 knockout (TDKO) mice were randomly allocated into two groups: 1) ‘sham’, sham surgery, normal drinking water, or 2) ‘AngII + DOCA’, subcutaneously-implanted angiotensin II infusion pump and deoxycorticosterone acetate (DOCA) pellet, 1% NaCl drinking water. This model proceeded for three weeks, after which the mice were sacrificed. Kidneys were harvested at sacrifice, and fixed, embedded, sectioned, and stained for α -smooth muscle actin (SMA). Quantification demonstrates reduced α -SMA expression in TDKO mice compared with WT mice in both the cortex and medulla of the kidney (unpublished data).
*, $P < 0.05$ vs sham; #, $P < 0.05$ vs WT.